MEASUREMENT and CONTROL in FOOD PROCESSING

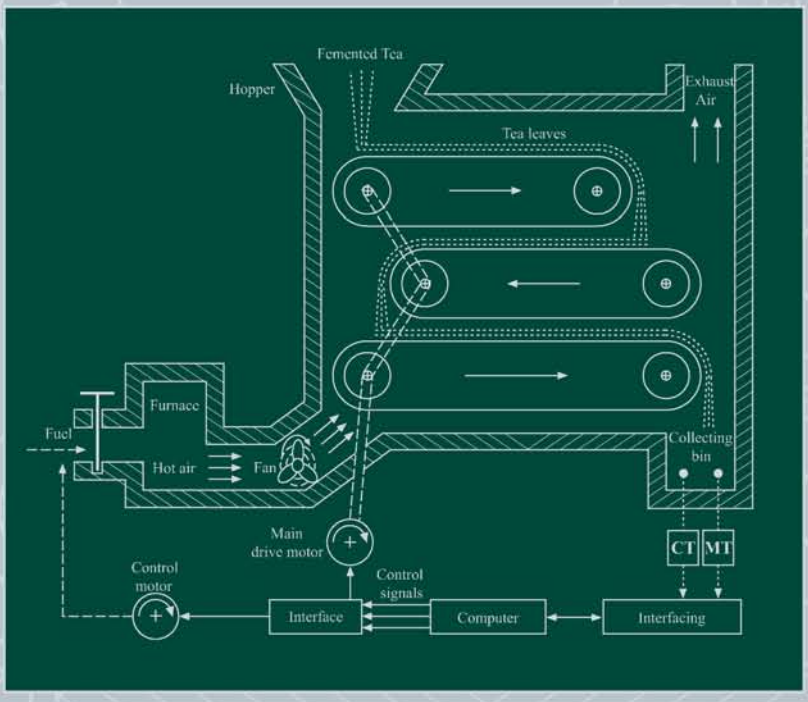

Manabendra Bhuyan, Ph.D.

CRC Taylor & Francis
Taylor & Francis Group

MEASUREMENT and CONTROL in FOOD PROCESSING

MEASUREMENT and CONTROL in FOOD PROCESSING

Manabendra Bhuyan, Ph.D.

Taylor & Francis
Taylor & Francis Group
Boca Raton London New York

CRC is an imprint of the Taylor & Francis Group,
an informa business

Published in 2007 by
CRC Press
Taylor & Francis Group
6000 Broken Sound Parkway NW, Suite 300
Boca Raton, FL 33487-2742

Printed in the United States of America on acid-free paper
10 9 8 7 6 5 4 3 2 1

International Standard Book Number-10: 0-8493-7244-5 (Hardcover)
International Standard Book Number-13: 978-0-8493-7244-5 (Hardcover)
Library of Congress Card Number 2006001546

Library of Congress Cataloging-in-Publication Data

Bhuyan, Manabendra.
Measurement and control in food processing / Manabendra Bhuyan.
p. cm.
Includes bibliographical references and index.
ISBN-13: 978-0-8493-7244-5 (alk. paper)
ISBN-10: 0-8493-7244-5 (alk. paper)
1. Food industry and trade. I. Title.

TP370.B49 2006
664'.02--dc22 2006001546

informa
Taylor & Francis Group
is the Academic Division of Informa plc.

Visit the Taylor & Francis Web site at
http://www.taylorandfrancis.com

and the CRC Press Web site at
http://www.crcpress.com

Foreword

Maintenance of the quality of processed food is a matter of concern for both food manufacturers and customers. If a product does not meet the established specifications, then it has to be sold at a loss, destroyed, or reworked. Therefore, quality control in food processing has become an integral part of the food processing industry. By the end of the 20th century, the food processing industry gradually adopted automated process control technologies and left behind traditional inspection methods for ensuring food quality and safety. Food quality and safety activities shifted from human inspection of individual pieces to automated, statistically driven monitoring systems for improved quality control. The new approach monitors key control points in the process to make sure that the finished products will meet the specifications. These changes were possible due to the advantages of computers, microchips, and sensor technology.

From the smallest baker to the largest snack manufacturer, food processing has many operations elements in common. From receiving raw materials to the finished product involving blending, the entire period of processing, removing defects, value addition, checking weight, and packaging, measurement and control devices have important roles to play. Therefore, it is essential that the detecting systems are properly calibrated and users understand the limitations of the systems.

Although different instruments or devices were used for several decades for measurement and control parameters during food processing, there have been tremendous changes in these instruments due to advancement in related areas. The measurement devices have become more accurate and efficient, less power consuming, smaller in size, easier to operate, and also cheaper in many instances. Detection systems and control mechanisms will continue to be developed and improved. During the last 10 years sophistication of scanning technology has improved many times over. Currently, biosensors are attracting a great deal of interest.

There exists much literature in the area, but it has not been compiled in one place. The author has made an attempt to compile all the available information and present it in a comprehensive manner. This book is divided into five major chapters covering various aspects of measurement and control in food processing. Apart from describing the principles and their applications, suitable examples, problems, and their solutions are also provided wherever applicable.

This book will be useful for food scientists, instrumentation engineers, transducer manufacturers, and food processing engineers. This is basically a reference book, but can also be a textbook for food science and technology courses being offered in different colleges and universities at the graduate level.

I feel honored to have been asked to write the foreword for such an important book. I would like to congratulate Dr. M. Bhuyan, the author, for his dedication and wholehearted effort to present the book in this form. He has made a valuable contribution to food science and technology.

Professor P. C. Deka
Vice-Chancellor
Tezpur University, India

Preface

The beginning of my research in instrumentation and control in the tea industry dates back to the early 1990s, when I first recognized the need for appropriate literature on the subject. I still remember when I had to jostle through dozens of tables of contents and indexes looking for discussions of a suitable converter for measuring process parameters in the tea industry. I also remember how much of my valuable time was devoted to designing a circuit for lack of proper literature. The feeling of need at that time translated into the idea for this book now.

During the last few decades, many innovations came to the world of instrumentation and control in food processing, and in spite of a significant amount of literature distributed in various places, common texts are still far less than expected. *Measurement and Control in Food Processing* is an attempt to make food scientists aware of various means of food-related measurements and controls, help instrumentation engineers and transducer manufacturers design instruments and control schemes suitable for food-processing environments, make food engineers attentive to the applicability of instrumentation and control to enhance quality and productivity, and more importantly, educate students of food science or food technology courses on methods and techniques of measurements and control in food processing.

The advent of super-specializations in food processing has caused confusion about who actually handles measurement and control in food processing. A food-processing engineer may not know how to design a controller circuit, but at the same time an instrumentation engineer may not know what complex flavor components emanate from a cup of tea. It is not difficult to establish coordination between these two areas of knowledge. During my long experience in food-related instrumentation and control, I have encountered such problems and realized that there should not be a sharp line between these two forms of expertise. This motivated me to address the problems faced by food-processing engineers in quantifying food-related parameters and their control from the angles both of food processing and instrumentation.

The book is divided into five major chapters, beginning with an illustrated introduction to food processing measurement and control in chapter 1. Chapter 2, a cornerstone for the book, is devoted to background materials about basic principles of transducers and controllers. Numerical problems are discussed in several sections so that readers can understand the applicability of food-processing devices. Readers who have already completed a course in instrumentation and control can skip this chapter or can read it to refresh their knowledge. Chapter 3 deals exclusively with measurement techniques for food processing, covering a significant amount of food-related process

parameters. The chapter features the relevance and importance of process parameters in food-processing industries and discussion of measuring techniques, and specific applications in most recent developments have been enumerated. A number of texts from research publications have been included and several intelligent instrumentation techniques that have emerged in recent years have been presented. In chapter 4, topics on controllers and indicators for food-processing industries with a good deal of practical application have been presented. Recent nontraditional control schemes, such as fuzzy control, are also discussed in this chapter. Microcomputer-based process monitoring and control is a major issue today. The devices, standards, and procedures and suitable examples for process–computer interaction are presented in chapter 5.

The book is intended to respond well to the need of food engineers, instrumentation engineers, transducer manufacturers, researchers, teachers, and students of food science or food technology. Although the book looks like a reference work, it can also be a good textbook for a course in food science, food technology, or biosystems.

While the book is the result of my untiring efforts, there are many others who contributed to its development. I must thank Prof. P.C. Deka, Vice-chancellor, Tezpur University, India, for writing the foreword, where he has presented a valuable comment on the aim and scope of the book; and my M Tech students, A.G. Venkatesh, Mahanada Saharaia, Pawan Kumar Bhargav, and Riku Chutia, for helping me with the artwork and text. A special thanks to A.G. Venkatesh, who went to a lot of trouble with a major part of the artwork, sending it via email from the University of Manchester, and asking me to let him know "if there is anything more I can do." Thanks also to my research scholars, Kishana Ram Kashwan and Surajit Borah, who helped me to include some of the topics from their theses; to my colleagues, J.C. Dutta and P.P. Sahu, for their kind support during preparation of the manuscript; and to our office assistants, Dwipendra Ch. Das and Dibakar Nath, for their help.

I am grateful to the staff of Taylor & Francis Group for their professional guidance and advice during the preparation of the project proposal and the manuscript, particularly to Susan B. Lee, Amber Donley, Marsha Pronin, and the production team. I am also grateful to the reviewers (unknown) of my original book proposal.

I must thank my wife, Arihana (Nanti), who helped me indirectly in writing the book, particularly during the last few weeks before sending the manuscript to the publisher. I thank my daughter and son, Abhishruti (Pahi) and Abhinab (Pol), for their patience during the writing of this book.

Contents

This book is dedicated

to the fond memory of my mother Rupoprabha Bhuyan

and my father Ratnadhar Bhuyan

and to all those who die every day

from diseases related to inadequate diets

and lack of nutrients in foods

1

Introduction

CONTENTS

1.1 Food Processing Industries

Food processing is a vast sector of the industrial world. A major percentage of cereals, vegetables, and fruits are processed for human consumption and preservation for future use. In the United States, the combined activities of the agricultural, food processing, marketing functions, and supporting

industries generate about 20% of the gross national product and one fourth of the total workforce. According to a survey on current business, approximately 1.7 million people in the United States were directly employed in food manufacturing alone in 1991, not counting related businesses [1]. Food technology is the application of concepts generated by food science in processing, preservation, packaging, and distribution of safe and nutritious food.

At one time food manufacturers did not pay much attention to production of food by scientific methods as is done today. Due to the traditional pattern of the food industries, many food manufacturers still try to produce quality products with the old-fashioned approaches of measurement and control methods: touching, smelling, and visual inspection. However, considerable quality, efficiency, and energy are sacrificed in adopting these traditional techniques.

The desirable characteristics of a food product are mainly determined by its demand and usage. The quality control of processed food products has become a concern both for manufacturers and consumers. Therefore, quality control methods in food processing are required for the survival of the industry because of user consciousness about safe and healthy products. Apart from the important chemical and physical changes that can take place during different stages of manufacturing, the quality of raw materials is also an important factor. A good-quality food product cannot be processed from poor-quality raw materials. Apart from composition, uniformity of size, shape, color, and flavor have also become important in food processing.

The chemical aspect of food products is such an expansive field that it is not possible to cover in detail and it is outside the scope of this book. Hence a brief overview of a series of food processing industries is given in this chapter, with an emphasis on the use of instrumentation and control.

When food processing was in its early stages, not much attention was paid to relating quality to physical and chemical characteristics. However, as the demand for quality products gradually increased, analysis of the relation between chemical and physical characteristics started among food manufacturers. The following sections give an overview of some food manufacturing processes with the potential of measurement and control strategies.

1.1.1 Canned and Bottled Fruits and Vegetables

Only good raw materials can result in superior quality food products. Food specification defines ripeness of fruits by the maturity ratio, given by:

$$\frac{\text{Total solids, g/100ml}}{\text{Acidity (as citric), g/ml}}$$

This ratio changes rapidly during the ripening period and reaches an optimum value. This ratio can be different in different geographical regions;

for example, in the case of orange juice, this ratio is 8 in California and Israel, whereas South Africa requires a minimum value of 5.

Many similar terms have also been formulated to define the maturity of vegetables. A criterion for canning and freezing peas, for example, has been formulated on the basis of content of alcohol in insoluble solids, which is that percentage of the fresh weight insoluble in 80% of ethyl alcohol after boiling for 30 min. A tenderometer is a common instrument for determining this criterion.

In an unprocessed state, fruits and vegetables consist of an agglomeration of biochemical systems and their products, microorganisms such as yeast, molds, and bacteria. After processing and canning, the food should be in a stabilized condition and the dish should have the same taste as that of the fresh material. Application of heat during processing causes undesirable changes during storage due to enzyme loss and microorganism quality. To avoid this and to improve the quality, the canned products are treated in a blanching process. In this process, the free and intercellular gases from the tissues are removed, causing a greater vacuum in the can and shrinking the tissues for ease of handling and filling. However, in this process there is a considerable loss of soluble nutrients such as sugars, amino acids, and vitamins. An electronic blanching process might reduce this loss to a considerable extent.

Once the cans are filled with fruit, heat treatment is performed, removing gases from the fruit tissues. Thermal heating stabilizes the product by killing microorganisms. The pH value of the food is responsible for the microflora content in the can and the resistance to heat. Canned and bottled fruits and vegetables are generally divided into the following four basic groups based on their pH values:

1. Low-acid groups (pH of 5.3 and above); most vegetables
2. Medium low-acid groups (pH of 5.3–4.5); carrots
3. Medium-acid groups (pH of 4.5–3.7); tomatoes, pears, cherries, pineapples, and peaches
4. High-acid groups (pH of 3.7 and below); apples, plums, and berries

The process of thermal heating is performed with varying degrees of time and temperature levels. In the last two groups, heating is done at 212°F for a shorter period; but in low-acid and medium low-acid groups, high temperature is used for heating the product. The *temperature coefficient* is a number in bacteriology that dictates the increase or decrease of temperature in °F that causes an increase or decrease in number of bacterial spores by a factor of 10. Thus, for example, if heating sterilizes the product when the food item is heated at 258°F and kills 10 times more bacterial spores than heating at 240°F, the factor is 18. This factor generally varies from 15 to 22. There must be an optimum time and degree of heating for getting the best processing through sterilization. Thus, in production of canned fruits and vegetables, a correct correlation among the pH value, heating temperature, and heating duration will result in an optimum solution for quality control of the product.

1.1.1.1 Quality Control of Ingredients

The specifications of ingredient materials for best results are termed standards. The standards used by a manufacturer depend on the product in which the material is to be used and on the manufacturing process. There is no universally set standard for each material. Setting a standard for ingredient material requires vast experience in handling, and the manufacturer might set its own specifications. Nevertheless, some broad outlines can be given for dictating the specifications in the following categories:

- Identity: This is a precise definition of originality of the material. Only microscopic tests can determine these attributes.
- Purity and composition: The aspects of this standard can have the following factors:
  1. Chemical: This gives assay requirements such as percentage of moisture, fat, protein, antioxidants, additives, and so on.
  2. Physical: This specifies the requirements such as size, color, weight, viscosity, density, and so on.
- Microbiological: This refers to microbiological organisms responsible for health, safety significance, and sanitary conditions. Tests conducted to measure sanitary conditions are called filth tests.
- Packaging: This refers to the net weight and quantity of the packaging material.
- Storage: This standard depicts the conditions for cold storage outside the factory. Warehouse conditions such as temperature and relative humidity are major concerns of this category.

During the processes of cooking, canning, and sterilization and filling of fruits and vegetables, several process parameters must be measured and controlled, including the following:

1. pH, temperature, and timing during thermal heating of canned fruits and vegetables
2. Moisture content, fat, protein, antioxidants, pH, color, brix, and flavor of the product
3. Filling weight and filling temperature for canning
4. Temperature and humidity control during storage trials

1.1.2 Beer

Beer is an alcoholic beverage used worldwide. Considerable advances have been made during the last decades in the brewing industry in quality and maintaining uniformity.

The beer brewing process uses four principal ingredients: malts, hops, water, and yeast. Barley is converted into malt and combined with water to form a

mash. Fermentable sugar, maltose, is formed due to the presence of enzymes in the malt. Malt is prepared from barley corns in a process called malting. Chemical analysis, appearance, flavor, texture, and moisture content determine purity of malts. The sugar maltose is boiled in a kettle with the addition of hops. It is then strained, cooled, and sent to a fermenting vessel, where yeast is added. After a few days, alcohol is developed from the sugar and the resulting beer is filtered and drained to a storage reservoir and then pasteurized. Pasteurization is the heating process required to destroy pathogenic microorganisms. Controlled boiling of sugar maltose in the brew kettle is essential in brewing to prevent insipid color, excessive bitterness, cloudy appearance, and inconsistent taste of the final product. Moreover the efficiency of the process can be improved by maximizing heat transfer and evaporation [2].

The major parameters of beer that need measurement and control are the following:

1. Temperature during pasteurization and evaporation
2. Flow rate of product in various stages
3. Color matching against standard colors set by brewing conventions of various countries
4. Measurement of yeast cell counts and minerals
5. Turbidity of the solution
6. pH measurement of infected pitching yeast for its purification
7. Estimation of oxygen, nitrogen, and hydrogen in the head space of bottled beer

1.1.3 Ciders

Ciders are manufactured by fermentation of apple juice, which is a popular drink in many countries. Juice is extracted from disintegrated apple by applying hydraulic pressure on the pulp. Colloidal separation of juice from the pressed pulp is achieved by adding a pectin-degrading enzyme followed by a gelatin solution. Centrifugation and filtration of the gelatin solution removes the precipitate. Evaporation reduces the volume of juice for intermediate storage (see [3] for further details). Addition of sulfur dioxide or ascorbic acid to the juice causes fermentation and reduces the tendency of the product to become brown. Considerable attention should be given to the following quality factors for the unfermented and fermented products:

The unfermented juice

1. Specific gravity of the fruit juice
2. Total sugar content of the fruit juice
3. Total acidity (pH)
4. Tannin content
5. Pectin content

The fermented product

1. Specific gravity and viscosity
2. Alcohol content
3. Sugar content
4. Total acidity
5. Tannin content
6. Sulfur dioxide content

1.1.4 Soft Drinks

Soft drinks are refreshing, nonalcoholic beverages. Soft drinks can be categorized into the following groups:

1. Fruit drink or fruit juice
2. Soda water or any artificially carbonated water, either flavored or nonflavored
3. Ginger beer or any herbal or plant-based beverages

The ingredients of bottling syrup are: sugar, fruit juices, essences, citric or other permitted acids, artificial sweeteners, preservatives, colors, and emulsions for cloudy products. Bottling syrup is prepared by careful addition of all the ingredients in correct proportion and sequence. To control the quality of the syrup, chemical and physical tests must be carried out. The following parameters are responsible for the flavor of the syrup:

1. Percentage of soluble solids
2. Acidity (pH)
3. Sulfur dioxide and sodium benzonate content determination

1.1.4.1 Syrup Dosing and Filling

For high-speed bottling, a premix system is more popular in bottling plants. Here the syrup is mixed in correct proportion in a carbon dioxide pressurized mixing chamber. An exact proportion of water is combined, cooled, carbonated, and filled into the bottle. The flavored syrup content or capacity prior to filling can be measured by an online refractometer, and a control signal can be generated for adjusting the proportions of the ingredients.

1.1.4.1.1 On-Line Monitoring of the Qualities of Syrup

Brix, carbonation, and capacity of syrup must be graphically monitored for managerial and quality-control purposes. Graphical records of the essential quantities of syrup before bottling are powerful tools for statistical quality

control. Apart from quality control of syrup, the soft drink industry focuses much attention on the hygiene of processing and bottling to keep bacteriological infection to a permitted limit.

1.1.5 Sugar

Sugar is the cheapest kind of food item with a high calorie value per unit cost. Per capita consumption of sugar is considered an indicator of a country's standard of living. A number of plants contain sucrose, including: sugarcane, sugar beets, maple trees, certain palm trees, and sweet sorghum trees. Commercially, however, sugarcane and sugar beets are usually used for sugar extraction because they are major sources of sucrose. Sixty percent of the total sugar produced is obtained from sugarcane. The production of refined sugar from cane includes two stages:

1. The extraction of sugar juice from cane and its conversion into raw sugar.
2. The purification of raw sugar into refined sugar.

For extraction of the juice from cane, which contains 16% sugar, the cane is first passed through crushing rollers, then through squeezing rollers under high pressure and a spray of water. Milk of lime is added to the juice and heated, causing coagulation of the impurities, arresting suspended solids, and allowing sedimentation of the mud.

The clarified juice is then concentrated in multiple effect evaporators to a solid content of about 65% for removing water content. This process produces sugar crystals called *massecute* and a mother syrup. The raw sugar crystals are separated from the syrup in a centrifugal machine. The mother syrup is recycled to extract more raw sugar.

The refining of raw sugar is a comparatively complex process requiring skill and experience. The purpose of refining is to extract the maximum amount of pure sucrose. The refining process involves seven stages of operation.

1. Affination: for removal of outer syrup film from the crystal surface
2. Melting: to dissolve the affined raw sugar
3. Defecation: to remove impurities
4. Decolorization: to remove the reddish color of molasses
5. White sugar boiling: to crystallize the sugar
6. Granulation: to produce dry and free-flowing sugar
7. Recovery: to recycle the syrup left

This is the conventional sequence of operation in refining, but there can be variations in the defecation and decolorization processes.

Process parameter monitoring and control in the sugar industry is essential for manufacturing a product of uniform quality from raw materials of variable quantities. Two other important aspects of process control are minimizing fuel consumption and sugar loss. During processing, sucrose solutions are hydrolyzed, forming invert sugar and causing chemical loss. At low pH (e.g., 8), the inversion is slow but it is higher at high temperature. To estimate the chemical loss, therefore, measurement of pH and temperature are prime criteria.

Dry crystalline sucrose is noninverting but when it contains acids or some enzymes, the sucrose gets hydrolyzed. The invert sugar is hygroscopic; hence the moisture content of the crystalline sugar also contributes to further enhancing the process of formation of invert sugar. The ideal ratio of sugar to water content is 100:1. As the moisture content is very minimal, sources of error can contribute to the water content estimation. Therefore, sensitive and accurate methods of moisture content measurement have to be employed in this situation.

The appearance (hue) of the sugar is also a mark of its quality, influenced by the color and grain size. Therefore, detection of the color and grain size certainly helps in quality-control schemes in the sugar industry.

The sucrose content of the juice is also important. The most accurate method of sucrose content measurement is the polarization of raw sugar. Ash is a kind of impurity that can be present in the refined sugar. Although this impurity does not account for any hazard, estimation of ash is most frequently carried out both during processing and on the final refined sugar because it is a general indication of the degree of refining. The conductometry method is generally used for ash content determination in sugar.

1.1.6 Jams and Jellies

Jams are sugar pectin gels obtained from fruit juice. Jellies are different from jams in composition and texture. Strawberries, raspberries, black currants, red currants, guava, and pineapple are some of the fruits with high sugar content suitable for jam and jelly.

Generally fruit pulps are preserved for production in the off-season. The most common method of preservation is adding sulfur dioxide with the fruit pulp. The sulfur dioxide is added as a gas, 6% aqueous solution, or a solution of sodium meta bisulfate or calcium sulfate.

For jam preparation, fruit pulp and liquid pectin syrup are transported to boiling pans through pipes. They are mixed to get a pH value of 3.0 and the mixture is then boiled at about 105°C. During boiling, agents like yeast, molds, and other destroying enzymes are removed.

In jelly manufacturing, a mixture of sucrose and glucose syrup is boiled until solid content reaches 90%. The cooking is performed in open pan evaporators or vacuum pans. After cooking, it is cooled to between 98°C and

99°C, added with soaked gelatin. Finally, color and flavor are also added. The final product is stored in large slabs or molds.

Because pectin is the sole component of fruit juice, it cannot be destroyed during cooking. In many cases, fruit pulp contains a considerable amount of pectin-destroying enzymes. Therefore the pulp should be sufficiently cooked to release all of the enzymes. Even a small trace of enzyme left after cooking will hydrolyze the pectin, forming gelatinous masses. In view of this, detection of such natural enzymes in the fruit pulp and the cooked pulp is necessary.

Fruit pulps should contain uniform food content; it is therefore necessary to perform tests to detect the fruit concentration. Fruit concentration can be ascertained by measuring the percentage content of soluble solids by refractometer. Acidity and percentage of insoluble solids are also important parameters. For manufacturing jellies, the fruit pulp should contain high gelatin with an ideal Bloom strength of 250, a reading obtained from a Bloom gelometer. Measurement of pH must also be performed because gel content is dependent on it.

1.1.7 Black Tea

Tea is a high-value crop due to its high per capita consumption and demand. Production of black tea from green tea leaves involves certain well-defined processing stages determined by specific processing parameters. The quality of tea can be interpreted as the presence of desirable characteristics like flavor that pleases the sense of consumers, the briskness that refreshes, and the strength or pungency that determines how many cups of tea can be brewed from one kilogram of tea leaves. Production of tea involves the major processes of withering, rolling, fermenting, drying, and grading.

During withering, the moisture level of the freshly picked green tea leaves is reduced from around 77% to between 55% and 70% by circulating air using electrically operated fans. During very rainy or damp weather conditions, hot air is also used for withering. Therefore, the extent of withering (expressed in percentage of moisture content) is determined by the withering air flow, the relative humidity of the air, and the total time of withering.

The withered leaves are treated in the rolling process to damage the cell membranes. This is performed in rolling tables for manufacturing orthodox tea. For cut, tear, and curl (CTC) tea manufacturing, the withered tea leaves are cut in a CTC cutter or Rotorvane (a cutter machine). The important parameters that determine the quality of the processed tea in this stage are: the pressure of the roller, the sharpness of the CTC roller, the gap between the CTC rollers, and the temperature of the rolling room.

The rolled tea leaves are then sent to the fermenting stage, where they undergo the chemical changes determining their color, flavor, and strength. In this stage the rolled tea leaves are thinly spread in aluminum trays (tray fermentation) or on a clean floor (floor fermentation) until the color of the green leaves changes to dark copper. The most important parameters in this process responsible for

the quality of the tea are the ambient temperature and relative humidity of the fermenting room. The quality of the tea is developed in this stage primarily due to the formation of two enzymes: *thearubigin* (TR) and *theaflavin* (TF).

The fermented tea is dried to deactivate its enzymes and stop fermentation and to remove the moisture. This is achieved by passing hot air between 95°C and 145°C through the fermented tea in drying machines. The moisture in the final black tea is reduced to the range of 3% to 5%. The desired moisture content of the dried leaves can be achieved by maintaining the required feed rate of fermented leaves and the inlet temperature of the hot air. The manufactured black tea is then sorted into different grades or sizes using sorting machines. The different grades of tea are then weighed, packed in jute sacks or wooden boxes, and sealed so that the tea cannot absorb extra moisture from the outside environment. The packed tea boxes or packets are sent to tea warehouses for selling or auction. Black tea is currently available in evacuated small packets of 200 g, 500 g, and so on. Evacuation of the packet ensures that quality of the tea does not deteriorate.

The following parameters must be monitored and controlled to maintain the quality of black tea during manufacturing [3]:

Parameters that need monitoring

1. Moisture content of the green tea leaves, withered tea leaves, fermented tea leaves, and final black tea leaves
2. Relative humidity of air during withering and fermenting
3. Velocity of withering air
4. Percentage of withering
5. Temperature of air during withering and drying
6. Degree of fermentation, formation of color, flavor, and enzymes

Controllable parameters [4]

1. Withering on completeness of the process
2. Rolling time sequence and display timings
3. Relative humidity and temperature during fermentation
4. Overdrying and underdrying of tea during the drying process
5. Automated sorting of black tea

1.2 Introduction to Process Instrumentation and Control

There has been considerable development in the field of instrumentation in the last few decades. The reason for this rapid growth is that its principles

are based on multidisciplinary facts and the applications are also multidisciplinary in nature. As technology advances in different fields, instrumentation also advances technologically. There is always an increasing need for precise, efficient measurement schemes in industrial environments. Industrial control and automation are meaningless without a proper instrumentation scheme. Therefore, technological advancement requires advancement in both instrumentation and control. A judicious amalgamation of instrumentation and control can only contribute to the industrial needs for improving quality, increasing productivity, increasing efficiency, reducing manufacturing costs and material waste, saving energy, and so on.

1.2.1 An Industrial Process

An industrial process is a manufacturing unit in which a series of continuous or regularly occurring actions take place in a predetermined or planned manner to produce the desired product. The product changes from the raw material stage to the final product stage within a certain span of time. During this transition, there might be more than one form of physical or chemical change of property of the material. On the other hand, there can be addition or removal of materials in quantity. The physical and chemical changes that take place in the materials or components in an industrial process are mainly responsible for the quality of the final product. The causes of the physical and chemical changes are the variations of some parameters that get reflected in some other parameters. These parameters are called *process parameters* or *process variables.* It is evident that the process action mainly depends on the process variables, so careful attention to the process variables is very much essential to knowing the state of the process action. The process variables that indicate the correctness of the process action are the *process outputs* or *system outputs.* The process variables that can change the process action are the *process inputs* or *system inputs.* This concept of process input and output variables is explained by an example of a tea dryer illustrated by a block diagram in figure 1.1.

The industrial process of black tea manufacturing that takes place inside the tea dryer is a physical and chemical change of state of the fermented tea. In a chain type of dryer, fermented tea is fed through a hopper onto a moving chain conveyer, which circulates the tea at a constant speed from the top left side to the bottom right side of the dryer. Hot air is injected from the bottom left side to dry the tea.

Chemical change of the tea is a complex process that is difficult to model. If we consider only the physical change of drying of the tea in this process, fermented tea is the raw material and black tea is the product. The quality of the final product can be defined by the process output variables (controlled) such as grade, color, and moisture content. The feed rate, moisture content of the fermented tea, and the temperature of the hot air are the manipulated input variables. These variables have independent, direct influence on the output variables. However, not all input variables are always

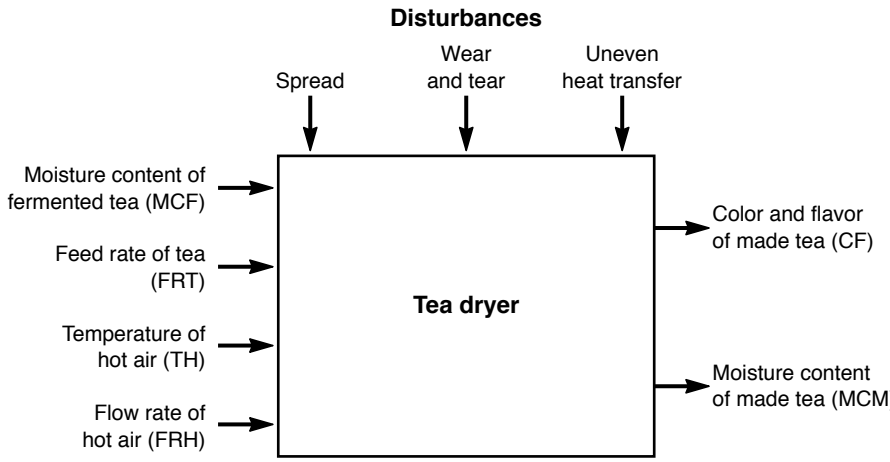

FIGURE 1.1
Block diagram of a tea dryer.

highly responsible for the quality of the product. For example, in a tea dryer, the density of the fermented tea does not have a direct influence or might have a low gain influence on the product quality.

At this point we can identify the flow rate of the black tea as productivity of the final product rather than defining it as quality. Not all process input or output variables affect the quality of the product. Some process output variables might not indicate the quality of the product in a process. The flow rate of the black tea is a similar kind of output variable. Therefore, sufficient process knowledge is required to identify the actual process outputs that represent the quality of the final product. Similarly, some input variables might not affect the quality of the product in a process. The block diagram in figure 1.2 represents the tea drying process, taking into account the cross-correlations between the input and output parameters.

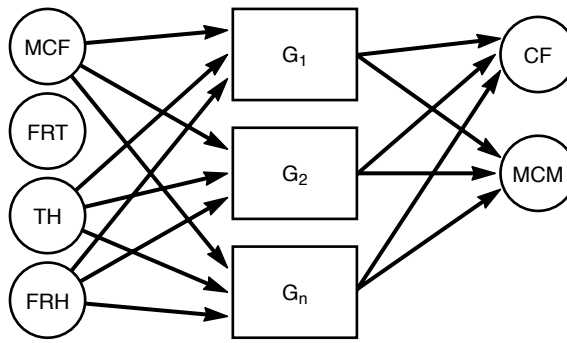

FIGURE 1.2
Illustration of cross-relations in dryer input–output variables. (Notations as per figure 1.1.)

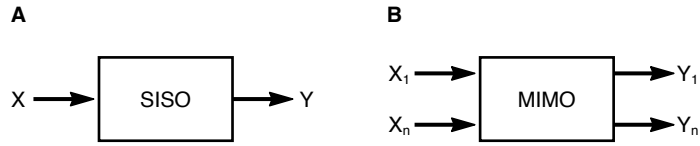

FIGURE 1.3
Models of process systems: (A) SISO model; (B) MIMO model.

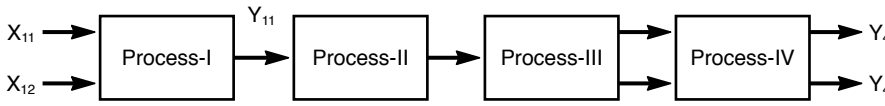

FIGURE 1.4
Block diagram of a multiprocess system.

A process can thus be represented by a system with manipulated input variables and controlled output process variables. The manipulated input variables control the quality of the final product and the controlled output variables carry the signature of the quality of the product.

A process can be classified on the basis of numbers of input and output variables. For example a system can be a single-input, single-output (SISO) or a multiple-input, multiple-output (MIMO) system (fig. 1.3). Most food processing generally consists of a combination of SISO and MIMO intermediate systems (fig. 1.4).

1.2.2 Process Parameters

Industrial processes to be handled by measurement and instrumentation can vary widely, from a simple oven at a biscuit factory to a complex brewing process. In this case, the parameters to be measured, controlled, or monitored can range from the temperature of the oven at the biscuit factory to the various process parameters of a brewing process, such as: temperature, pressure, flow rate, level, pH, color, flavor, volatile compounds, mineral content, and so on. Moreover, the parameters might have to be measured under different stringent conditions, like: high pressure, high temperature, noxious gaseous conditions, large-magnitude shocks and vibrations, corrosive environments, and so on. There can be a good number of combined subconditions of these situations, such as: temperature measurement of a fluid under high pressure, pressure measurement of a very corrosive fluid, vibration measurement of a machine under radioactive emission, and so on. The most important point in instrumentation under such conditions is to develop special sensors or to select the right equipment for error-free measurement of the process parameters of interest.

1.2.3 Batch and Continuous Processes

Production of a particular commodity involves well-defined multiple process operations in a predetermined sequence, procedure, and time. If the raw materials are treated in the stages of operations continuously with a single stream of product flow, the process is called a *continuous process.* If the product flow is discontinuous, meaning the raw materials or ingredients are treated with a time lag between stages, the process is called a *batch process.* However, it is difficult to have a purely batch process or a purely continuous one. Some batch processes demand continuous control of some variables and some continuous processes require some batch processing stages at the end of the schedule like batch sorting, batch packaging, and so forth.

In the past, most of the chemical and petroleum-based products were manufactured in batch mode. Later it was felt that if there is a large demand for single product and a system is inherently suited (physically or chemically), a continuous process is more efficient than a batch process. If these conditions are not fulfilled or the product does not become cost-effective to produce using continuous process machinery, batch mode continues to be quite popular. Apart from this inherent advantage, batch mode processes have other beneficial qualities, such as: processing flexibility, multiple uses of equipment, and higher safety in handling hazardous ingredients or products because of short processing duration. One added advantage of batch mode processing is easy controllability. A continuous mode process will have much more complex cross-correlation between process parameters than a batch mode process.

1.2.4 Process Instrumentation and Control

As defined earlier, a process carries out a single or a series of operations in a sequential manner leading toward a particular goal or object. The process is governed by the controlled variables, which is the desired output. A manipulated variable is a parameter that is varied by the controller to adjust the output to the desired quality or quantity. In a process, *control* is the technique of setting the outputs if there is deviation from the desired level; the manipulated input variables are adjusted to minimize the deviation. In a process, the causes of deviation of the output variables from a streamlined behavior can be either internal or external to the process. Irrespective of the reasons for the deviations, they are always categorized as *disturbances.* Some disturbances are regular in nature (deterministic) and can be predicted and compensated for within the system, but some cannot be predicted (stochastic). The effects of unpredictable disturbances can only be compensated for by a feedback control system.

In a closed-loop feedback control system, the difference between the output of the system and the set point or desirable input is used as a measure for the repair to be performed. The difference is called the *error,* which is used to adjust the controllable input variable. To understand a manual control

system, imagine the control of an electric heater by a human operator. The operator controls the temperature under a specific condition, for example, the maximum and minimum limits. The operator looks at the thermometer, and if the temperature is above the specified limit, he or she switches the power off and thereby decreases the temperature. When the temperature decreases below the minimum limit, the operator switches the power on and the temperature rises again. This is a manual control approach in which the human operator works as a controller.

In another situation, consider an electric oven temperature that is controlled within a certain limit using a simple thermal switch. When the temperature of the oven crosses the limit, the thermal switch disconnects electric power to the oven, working as a controlled switch. If the temperature drops below the limit, the thermal switch operates to continue the power supply to the oven, thereby increasing the temperature. The set point of the temperature limit is imposed on the thermal switch; that is, the thermal switch is adjusted as per the temperature limit. In this example the thermal switch works both as a sensor and feedback controller. This feedback controller is basically an on–off controller that simply switches the input to the system to on or off state when the output goes below or above the set point, respectively. Figure 1.5 shows the block diagram of a feedback control system and figure 1.6 shows the temperature controller. There are few other types of traditional controllers, such as proportional, derivative, and integral controllers that vary the input according to some function of the error signal. The

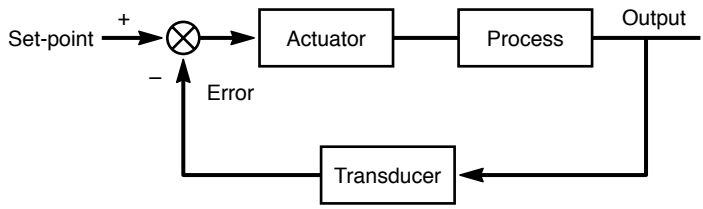

FIGURE 1.5
A feedback control system.

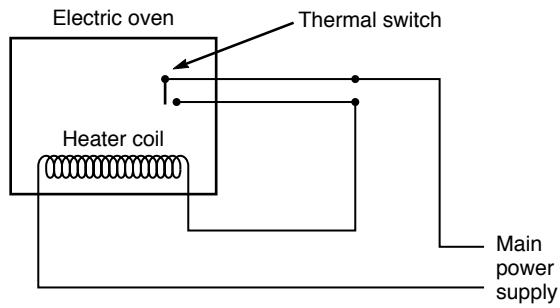

FIGURE 1.6
Schematic diagram of a temperature-controlled electric oven.

advantage of a feedback control system is that a deviation of the output from the set point can be minimized by proper controller design. The output of a process generally fluctuates or deviates from the quality limit due to disturbances or variations in the process parameters. If feedback control is adopted, such deviations can be eliminated or minimized easily.

In contrast to manual control, in automatic control, measurement and adjustment are made automatically and continuously. Manual control can be used in simple and linear processes in which disturbances are fewer, the process is not fast, and minimal monitoring is required. In situations in which process variables change too rapidly for the operator to take action, automatic control is compulsory. Thus in an alternative arrangement for the heater control example, the temperature can be measured by a suitable sensor, then the signal is processed and fed to a controller for adjusting the process input. A simple electronic circuit to follow simple control laws can be realized by the controller. For complex control schemes the controller is realized using a microprocessor or a personal computer.

In industry, controllers are generally used to perform a particular kind of control action or a combination of two or more actions. The type of control action produced is called the *control mode.* The selection of a particular kind of control action depends on the complexity of the control parameters for which it is required, behavior of the process variables, and cost effectiveness. The different modes of traditional control actions are as follows:

1. On–off or two-position control
2. Proportional control (P)
3. Proportional plus integral control (PI)
4. Proportional plus derivative (rate) control (PD)
5. Proportional plus integral plus derivative control (PID)

Traditional control schemes are not always successful in nonlinear, complex systems where advanced and intelligent control laws are found to be more convenient. Such controllers are discussed in chapter 5.

1.2.4.1 On–Off Control Action

An on–off controller is the simplest and most inexpensive of controllers. An on–off controller results in an output action, in only two states, depending on the level of the manipulated variable. Describing the control action with reference to a valve on a flow pipe, the control actions are**:** "the valve is fully open" and "the valve is fully closed." One state of the output is used when the manipulated variable is above the desired level (set point) and the other state is used when the manipulated variable is below the set point level.

Consider an on–off control action for a temperature-controlled batch retort used for closing and heat sterilization operation of cans to achieve microbiological stability in canning. As soon as the temperature crosses the set level,

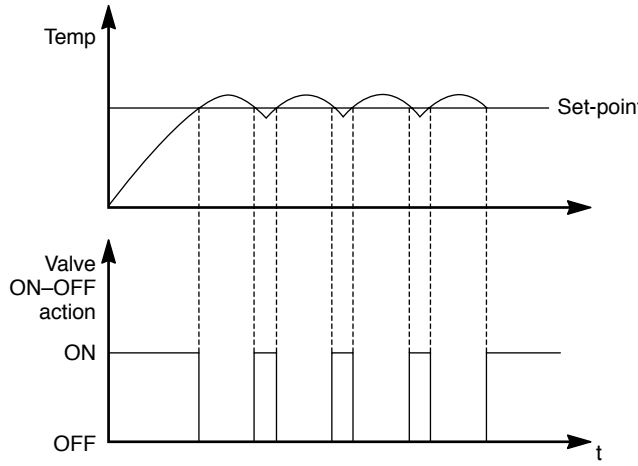

FIGURE 1.7
On–off control action of temperature controller.

the steam entry valve is turned off. This causes the temperature to come down to the set level because the valve is still in the off position. Cycling of temperature and switching of the valve, on and off, continues simultaneously, as shown in figure 1.7.

The range of temperature variation and the rate of switching are two very important features of an on–off controller. They are dependent on the process response and characteristics. The range of temperature variation determines the precision of the controller, and a high rate of switching causes mechanical disturbances to the final control elements like actuators, valves, relays, and so on. Therefore, a simple on–off controller causes output to cycle rapidly as temperature crosses the set point. To eliminate this disadvantage, an on–off differential gap is introduced to the control action. This function causes the heater to turn off when the temperature exceeds the set point by a certain amount, which is generally half the gap. The gap prevents the controller from cycling rapidly. Figure 1.8 shows the characteristics of an on–off temperature controller with a differential gap. The representation of the differential gap for an on–off controller is shown in figure 1.9. As the temperature gradually increases from level A and reaches B through F, the heater turns off, dropping to point C. The temperature continues up to D, and then decreases to point E, where the heater once again turns on. The temperature might slightly drop up to point G, then again reaches B through F, repeating the cycle. Incorporation of the differential gap in an on–off controller considerably reduces oscillations of the controlled output.

1.2.4.2 Proportional Control Action

In a proportional controller, the manipulated variable is proportionately adjusted according to the variation of the actual output from the desired

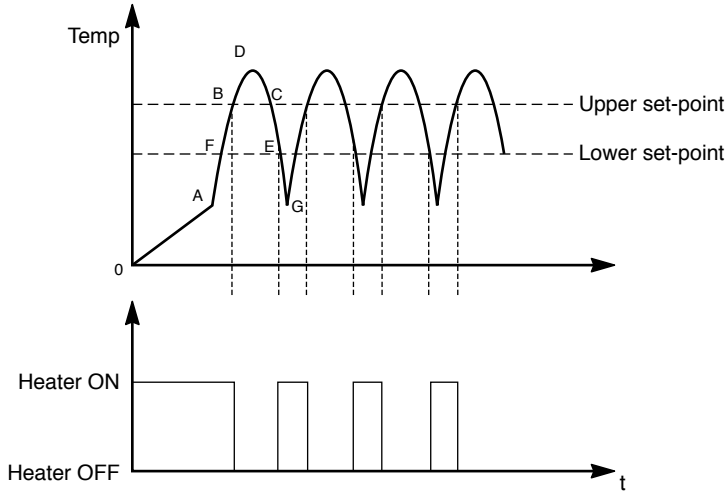

FIGURE 1.8
On–off control action of a temperature controller with a differential gap.

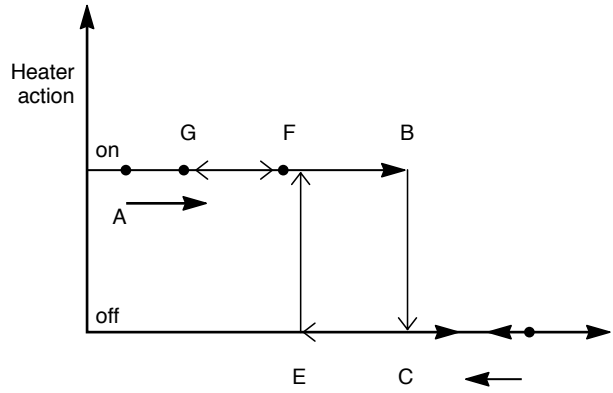

FIGURE 1.9
Representation of the control action due to the differential gap.

output. In the case of a temperature-controlled electric heater, the electrical power to the heater is adjusted proportionately to the deviation of temperature from the set level. The electrical voltage to the heater is decreased by an amount proportional to the temperature by which it exceeds the set level. The voltage is increased similarly when the temperature decreases from the set level. This brings the heater temperature to the set point level. The temperature range, over which the voltage is adjusted from 0% to 100%, is called the *proportional band*. This is normally expressed as a percentage of the operating range of the system and the set point is centered at 50%. In a proportional controller with a working span of 100°C, a 10% proportional

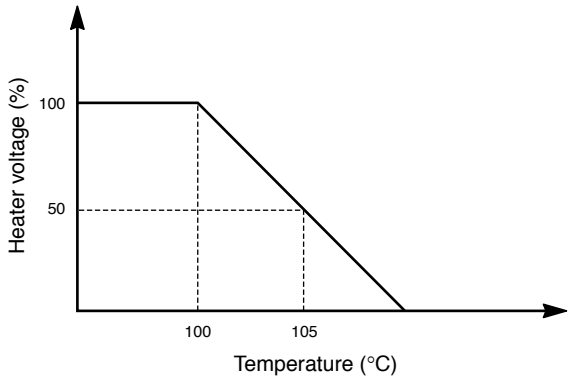

FIGURE 1.10
Transfer characteristic of a proportional controller.

band would be 10°C and the highest and lowest ranges of the band are 5°C away from the set point level. The transfer characteristic of a proportional controller is shown in figure 1.10. The figure illustrates that below 100°C, which is the lowest range of the proportional band, the heater power should be 100%. On the other hand, above the highest range of the proportional band (i.e., 110°C), the heater voltage should be zero. The voltage to be applied to the heater therefore can be determined from the characteristic graphically. The heater voltage is fixed at 50% at the set point level. There is every possibility that the proportional band might need to be adjusted as per the requirement of the process response and characteristics. Hence the proportional controller can have a wide band or narrow band of control. The transfer characteristics of wide band and narrow band proportional controllers are shown in figure 1.11.

In a narrow band proportional controller, a small change in temperature causes a large manipulated output. The performance of a proportional controller can be expressed in terms of the controller gain as

$$\text{Gain} = 100\% / \text{proportional band (percent)}.$$

Hence, the gain of a narrow band proportional controller is higher than that of a wide band controller. A proportional controller is suitable for a system where deviation of output is not large and is not sudden. A proportional controller can be incorporated in a closed-loop feedback control system illustrated in figure 1.12. The output signal is sensed by a sensor and amplified before comparison with the set point level. The error signal is positive when the output is below the set point level, negative when the output is above the set point, and zero when the output is adjusted to make it equal to the set point. The proportional output is 50% when the error signal is zero.

In practical situations, the heat input for attaining set point temperature never equals 50% of the maximum available. Therefore, the output temperature

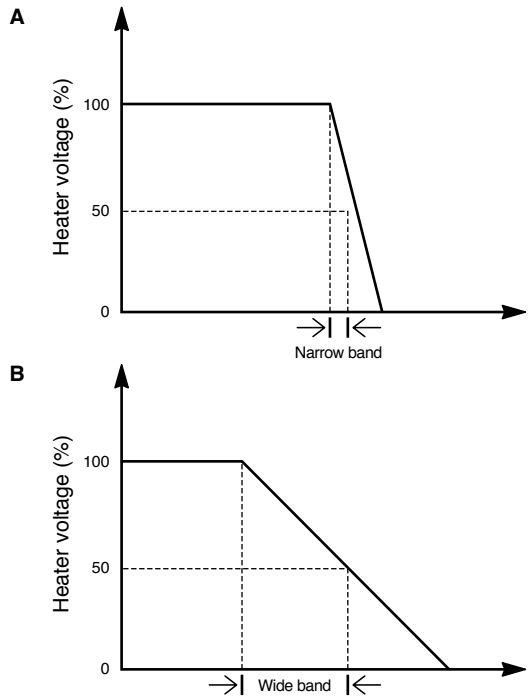

FIGURE 1.11
Transfer characteristic of (A) a narrow band and (B) a wide band proportional controller.

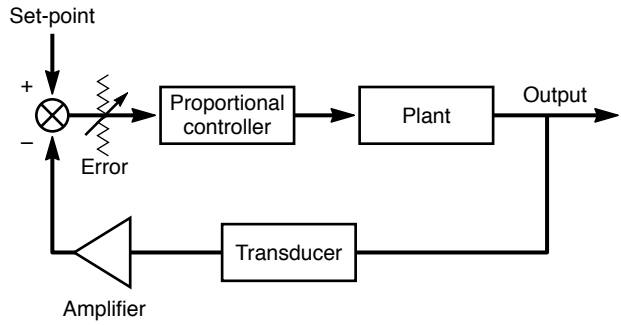

FIGURE 1.12
Block diagram of a proportional controller.

oscillates before coming to an equilibrium condition. The temperature difference between the stabilized and set point level is called the *offset*. The offset temperature value becomes less in a narrow band proportional controller.

For fine-tuning of a controller the offset must be removed. This can be done manually or automatically. Manual reset is a traditional method in which a potentiometer is used to nullify the offset electrically. The amount of proportional

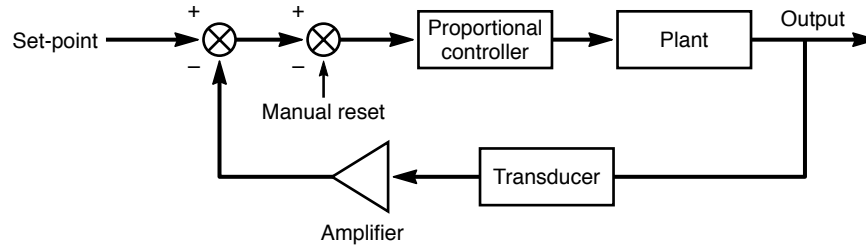

FIGURE 1.13
Block diagram of a proportional controller with manual reset.

band shifting is manually done, step by step, until the manipulated input to controller (process heat demand) conforms with the set point level of temperature. The manual reset proportional controller is shown in figure 1.13.

1.2.4.3 Proportional Plus Integral Control Action

An automatic reset proportional controller performs a reset operation with the help of an electronic integrator. The error is integrated and added with the error signal. Due to the integral term in the control law, a sudden change in deviation is tracked continuously, at a certain rate, determined by the reset rate (inverse of the integral time). Performance of a proportional controller is expressed by two terms: proportional gain and integral time constant. During integral time, equal parts of the output signal due to integral action advance as that of the output signal due to proportional action.

The block diagram and timing diagram of a proportional plus integral controller are shown in figure 1.14 and figure 1.15, respectively.

1.2.4.4 Derivative Control Action

Derivative control incorporates a term in the control law, which is first derivative of the error signal. It facilitates the shift of the proportional band either up or down to compensate for rapidly changing outputs. The controller tracks the set point level at a rate proportional to the rate of change of the error signal. If the output makes a sudden jump, the derivative action immediately brings

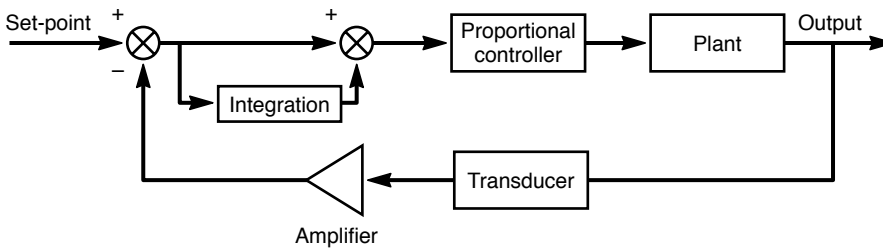

FIGURE 1.14
Block diagram of a proportional plus integral controller.

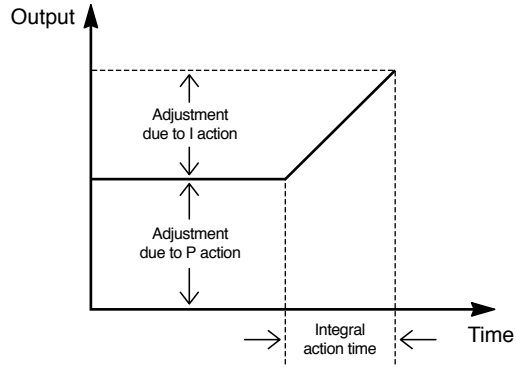

FIGURE 1.15
Typical characteristics of a PI controller.

the output toward the set point level. If the output changes gradually at a constant rate, the output tracks the set point at a similar rate to the proportional action. In this control action, a derivative time constant can also be defined in a similar manner. The derivative action does not have any limit of occurrence, unlike integral action. The derivative action can occur even outside the proportional band. The speed of correction is proportional to the amount of deviation, but this incorporates oscillations in the system output. The timing diagram of a proportional plus derivative control action is shown in figure 1.16.

1.2.4.5 PID Controller

Combination of these three modes of control action is advantageous for controlling complex processes. This mode of control is best suited for cases where the output fluctuations are large and sudden and the system has a lag. The block diagram of a proportional-integral-derivative controller (PID) controller is shown in figure 1.17.

1.2.5 Selection of Controller

Selection of a controller for a particular application requires attention to several factors. It has been found that the simplest controller that meets the requirement of the process is the best and least expensive. Although a better controller might be employed in a process that needs precise tuning of the output, a simple controller can be adequate in a process that permits a comparatively wide range of outputs.

Selection of a controller depends on the following factors:

1. Process response curve
2. Physical system analysis
3. Past experience
4. Experimental testing

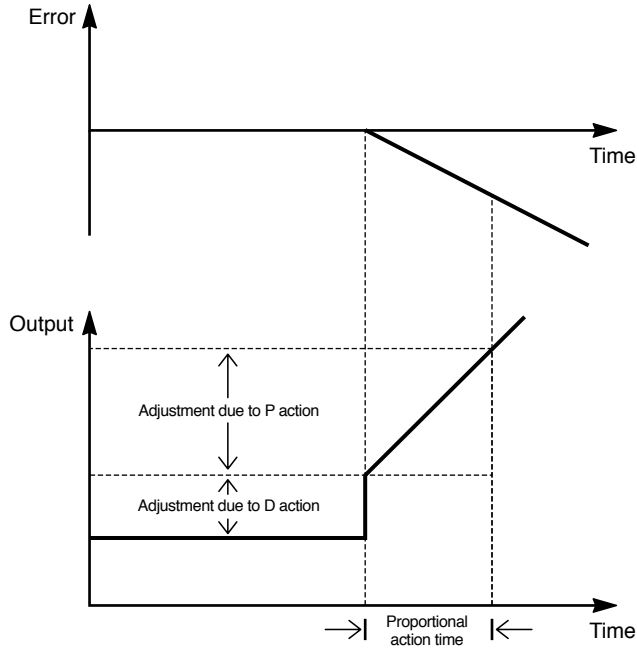

FIGURE 1.16
Typical characteristics of proportional plus derivative controller.

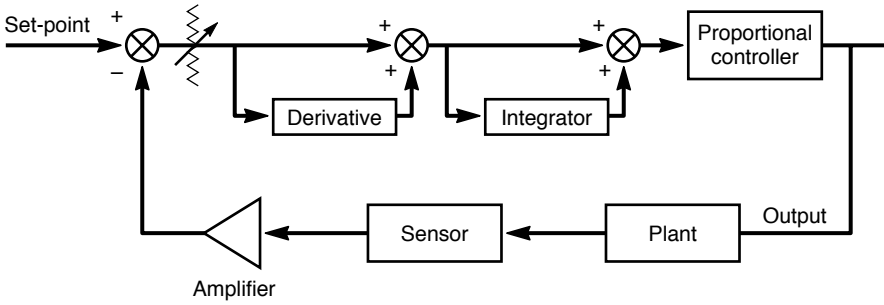

FIGURE 1.17
Block diagram of a PID controller.

A process response curve is a plot between the process outputs with time when a steady input is applied. The process response curve for a first-order thermal system is shown in figure 1.18. The essential characteristics of a thermal process response curve are the time constant and the rate of temperature increase. The controllability of a process depends on these two factors. If the curve becomes steeper, the controllability of the process becomes difficult. If the output temperature (T_p) starts increasing as soon as the input is applied, there is no propagation delay or dead time. This relates to the time constant (τ). Such a system is easy to control. In a more complicated situation,

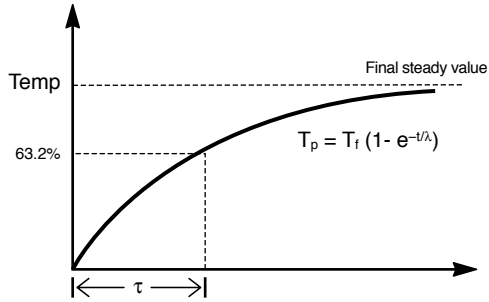

FIGURE 1.18
Response of a first-order thermal system.

when a heater is modified with thick metal plates, it introduces more time lag in the thermal system. This will introduce a second time constant, which results in a second-order system that is more difficult to control than a first-order system. The size of the process compared to the output requirement is also a major factor in selecting the controller. An oversized process does not give stable output, whereas an undersized one gives slow response. Analyzing controllability and process output stability requirements will help in selecting the controller. Thorough knowledge about the process response in the past is also an important clue. Experimental verification of the process response by computer simulation of the process is also a faithful method of selection of a controller. However there are obviously some guidelines for controller selection, as follows:

1. A proportional controller is used where:
   a. load analysis is insignificant.
   b. offset can be permitted.
   c. a narrow proportional band is permitted.
2. Integral control is used where:
   a. offset cannot be permitted.
   b. process has a lag.
3. Derivative control is used where:
   a. sudden and large deviation of output takes place.
   b. there are severe plant lags.

1.3 Conclusion

In the food industry, numerous approaches are involved in every step, from research to trade, where engineering techniques are mandatory. Our objective

is to help those practically involved with those engineering approaches to make food processing more scientific and engineered. There is confusion about who designs the food processing measurements and controls: a food scientist or an instrumentation engineer? What should a food science course cover? The definitions are misleading in the present day because behind the measurement and control of most food processing systems is the skill of both the food scientists and the engineers. In the broad perspective of food processing measurement and control, a food scientist is also an instrumentation engineer and vice versa.

The objective of this chapter is to inform food scientists as well as instrumentation engineers about the basics of engineering concepts of measurement and control and food processes, respectively.

This chapter presented a short description of the various food processing industries and the process parameters, as well as their importance in quality control. The basic structures of process input–output variables and basic principles of feedback control systems were also presented.

These basic concepts will be especially useful in understanding the various measurement and control techniques discussed in later chapters.

References

1. Potter, N. N., and Hotchkiss, J. H. 1995. *Food science* (5th ed). Gaithersburg, MD: Coultate TP.
2. Lewis, M. J. 1995. *Brewing*. New York: Chapman & Hall.
3. Ranken, M. D., and Kill, R. C. 1993. *Food industries manual* (23rd ed.). London: Blackie Academic & Professional.
4. Bhuyan, M. 1997. *An integrated PC based tea process monitoring and control system*, PhD thesis, Department of Electronics, Gauhati University, India.

Further Reading

1. Beckett, S. T. (Ed.). 1994. *Industrial chocolate manufacture and use* (2nd ed.). London: Blackie Academic & Professional.
2. Multon, J. L. (Ed.). 1996. *Quality control for foods and agricultural products*. New York: VCH Publishers.
3. Ogata, K. 1982. *Modern control engineering*. New Delhi: Prentice Hall.
4. Kuo, B. C. 1982. *Automatic control systems* (3rd ed.). New Delhi: Prentice Hall.
5. Johnson, C. D. 2000. *Process control instrumentation technology* (6th ed.). Upper Saddle River, NJ: Prentice Hall International.

2

Measuring and Controlling Devices

CONTENTS

2.1 Role of Transducers in Food Processing

Transducers and sensors are the basic input devices for industrial process measurement and control. In some industries automatic control devices are not adopted, either due to lack of necessity or lack of cost-effectiveness. In such situations, transducers might be used only for routine checks of various

process parameters such as oven temperature in a small-scale biscuit factory. In this case, obviously, a microprocessor or a computer-based automatic controller is not cost effective. Hence, observing the temperature of the oven by a thermocouple-based temperature indicator is sufficient. This implies that the measurement is taken manually so that the dough does not get overbaked or underbaked.

Strictly speaking, transducers are not very commonly used devices in electrical or electronic systems in industry. Transducers are used in systems only when some parameters of the system are to be quantified, measured, and observed. Some transducers are not of an electrical or electronic nature at all, like a mercury bulb thermometer used for measuring oven temperature. This instrument is not capable of generating an electrical signal to be applied to an electronic circuit. Such transducers are often used, but they are of no use in applications where automatic control is required. Therefore, by *transducer,* we mean here an electrical type of transducer, unless specifically mentioned otherwise.

Generally, a transducer is a device that converts a physical signal to a signal of convenient form for measurement. The convenient form of signal is most commonly an electrical voltage, current, or pulse frequency. The electrical voltage or current might need amplification, filtration, or linearization, which are performed by circuits known as signal processing circuits. Sometimes pulse or frequency signals need processing like wave shaping, modulation, and so on.

A wide range of physical parameters must be measured in industrial, laboratory, medical, space, and household equipment. The most common physical parameters that require transducers are temperature, pressure, and flow. Almost 90% of all the process parameters fall into these three categories. Other less common parameters that require transducers for measurement are position, displacement, velocity, acceleration, weight, force, density, and viscosity. Some other less common parameters are humidity, moisture content, pH, sound level, mixing ratio, turbidity, color, and flavor.

We have imagined that all the transducers used for measurement of these process parameters comprise a single unit that transduces the physical parameters straight to an electrical signal. However, this is not always true because many transducers need help from a primary sensing device to convert a physical signal to another convenient physical signal. In the second stage, the second physical signal is again converted to a proper electrical signal for measurement. In this type of transducer, the first stage is called a *primary transducer* and the second stage is called a *secondary transducer.* Mechanical devices like bourdon tube, bellows, diaphragms, springs, rings, and levers are some examples of primary sensors. These sensors are mostly elastic members that undergo some mechanical deformations or displacements when force, pressure, or load is applied to them. Some of the primary sensors alone represent a transducer where the parameter, in whatever form it is sensed, is used for the final application. Examples of such transducers are spindles, contacting members, pins, and fingers. This chapter covers the principles and areas of application of different transducers and controlling devices.

2.2 Classification of Transducers

The need for measurement of newer types of physical parameters is also a reason for the increasingly large number of transducers. Based on design principles and application, transducers are grouped into the following four different classes:

1. Self-generating type
2. Variable parameter type
3. Pulse or frequency generating type
4. Digital type

2.2.1 Self-Generating Type

Self-generating transducers are designed to generate an electrical signal in proportion to the input physical signal. In most cases self-generating nature of the transducer is an inherent property of the material used for the transducer. When the physical signal stimulates the material, a voltage is developed. Examples are piezoelectric crystals, thermocouples, pH electrodes, radioactive sensors, photocells, electrodynamics, electromagnetics, and eddy-current type. The voltage developed by almost all the self-generating transducers is of very low strength and cannot be directly used for displaying or actuating a control device. Voltage or current amplification is necessary before applying it to an indicator, recorder, or control device. Apart from voltage amplification, filtering of the signal to remove noise picked up also becomes necessary. Corruption of the signal by noise is a very common problem in the case of transducers generating weak signals. The advantage of a self-generating transducer is that it does not require an extra source of power for the transducer.

2.2.2 Variable Parameter Type

A majority of the transducers fall into this category. Unlike self-generating transducers, a variable parameter type transducer cannot develop a voltage of its own. Instead, an electrical parameter of the device changes in proportion to the physical variable applied. The change in electrical parameter can be categorized as one of the following:

1. Change in resistance or conductance
2. Change in capacitance
3. Change in magnetic properties

2.2.2.1 Change in Resistance or Conductance

The resistive property of a material is exploited in designing these transducers. When a physical variable is applied, the geometrical or molecular configuration of the material is changed, causing its resistance to change proportionately. The variation of resistance is converted to a variation of voltage, commonly using a resistive circuit. The circuit uses a separate voltage source for generation of the signal. Examples of resistive transducers and the physical variables that can be measured are as follows:

- Potentiometer: displacement, load, force
- Strain gauge: strain, pressure, load, torque
- Resistive thermometer: temperature, flow
- Thermistor: temperature
- Hygroscopic sensor: moisture content
- E-nose sensor: flavor, humidity

2.2.2.2 Change in Capacitance

In capacitive transducers, the capacitance of a capacitor is made to vary with the input physical variable. The change in capacitance can be obtained either by changing the dimensions of the capacitor or by changing the dielectric property of the material of the capacitor. In this way, capacitive transducers can measure various kinds of physical parameters. The variation of the capacitance is utilized in a capacitive measuring circuit, such as a capacitance AC bridge, an oscillator, an integrator circuit, and so on. Examples of capacitive transducers are as follows:

- Variable area capacitor: angular displacement
- Charging/discharging capacitor: rotational speed
- Variable dielectric capacitor: moisture content, humidity, density, liquid level

2.2.2.3 Change in Magnetic Properties

A magnetic transducer works on the principle that one or more of the following magnetic properties changes in accordance with the input physical variable: self-inductance, mutual inductance, reluctance, and so on. In most of the magnetic transducers, the inductance of a magnetic coil is altered either by varying the magnetic properties of the core material or by varying the air gap in the magnetic core. In both cases the permeability of the magnetic path changes, which in turn varies the inductance of the transducer.

Variable inductance transducers are mainly used for dynamic measurements such as pressure, displacement, acceleration, force, angular position,

and so on. Variation of the reluctance or inductance is converted to a representable voltage signal with the help of an excitation voltage applied to a circuit, which comprises the transducer. Examples of magnetic transducers are: single-core reluctance pressure sensors, linear variable differential transformers, rotational variable displacement transformers, electrodynamic rotary motion transducers, synchro-angle transmitters, noncontact proximity sensors, and magnetostrictive force transducers.

2.2.3 Pulse or Frequency Generating Types

A self-generating or variable parameter type of transducer generally outputs a signal that changes in magnitude proportionately to the physical variable. Some of the self-generating types of transducers produce a train of pulses, the frequency of which is proportional to the input physical variable. Therefore, the measuring circuit of this type of transducer is a pulse or frequency counter that determines the number of pulses during a specific time period. The frequency is finally calibrated in terms of the input physical signal. Examples of pulse or frequency generating transducers are: an optical disc type of rotational transducer, turbine flow meter, radioactive flow meter, shaft speed meter, pressure sensing oscillator, shaft position transducer, and capacitive controlled humidity sensing oscillator.

2.2.4 Digital Transducers

Digital transducers are more convenient for interfacing to microprocessor or computers. Digital transducers are designed to generate a digital signal proportional to the physical variable. Digital transducers have four distinct forms:

1. Direct digital encoding
2. Pulse, frequency, and time encoding
3. Analog-to-digital encoding
4. Analog-to-digital conversion

Except for direct digital encoding, any other analog and frequency generating transducer can be transformed into a digital transducer using an additional digital processing circuit.

With the increase in the importance and role of transducers, modern transducers are designed to perform special tasks apart from sensing. Such transducers generally measure some indirect parameters using intelligent techniques. The additional functions that have to be carried out by these transducers include: linearization, averaging, biasing to a particular operating range, relating to an indirect variable, and so on. Such transducers are called *intelligent transducers*. Examples of intelligent transducer functions are: relative humidity determination using thermal sensors, moisture release

measurement by a load cell weighing system, brix measurement by refractometer, and calorimetric estimation of enzymes. Intelligent transducers have gained importance recently in critical instrumentation environments. By this concept, transducers are classified as intelligent transducers and nonintelligent or dumb transducers.

2.3 Self-Generating Transducers

Some of these transducers are based on a certain quality or property of a material, stimulation of which by a physical variable makes the material electrically active. Another band of transducers adopts some other voltage generating principles like a turbine flow meter. Some types of self-generating transducers are discussed here.

2.3.1 Piezoelectric Transducers

There are certain materials in crystal form that generate voltage when a mechanical force or pressure is applied along the planes (mechanical axis) or surfaces of the crystal. The voltage generated can be collected with the help of two precision electrodes placed across two other surfaces (electrical axis). Piezoelectric crystals available in nature are quartz and tourmaline. Rochelle salt, barium titrates, and ammonium dihydrogen phosphate (ADP) are synthetic crystals, but they cannot withstand high mechanical stress.

The piezoelectric transducers are cut from a larger crystal in the direction of any of the electrical or mechanical axes that are perpendicular to the crystal or optical axis. The principle behind the development of a voltage across the electrical planes of a piezoelectric crystal is that, when a mechanical force F causes a deformation to the crystal (fig. 2.1), a charge Q is produced. The charge produced is given by:

$$Q = dF \tag{2.1}$$

where d is the charge sensitivity of the crystal. The crystal material is a dielectric, hence it behaves as a capacitor across the electrical planes. The capacitance is given by

$$C = \varepsilon w l/t \tag{2.2}$$

that is,

$$w l/t = C / \varepsilon \tag{2.3}$$

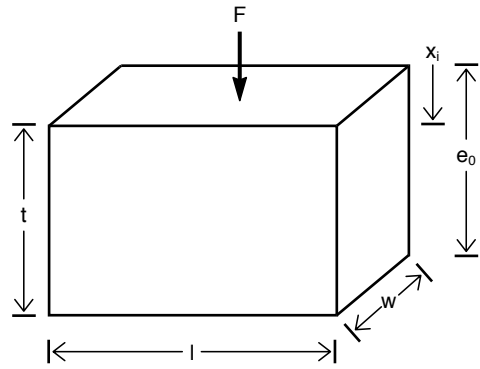

FIGURE 2.1
Mechanical stress applied to a piezoelectric crystal.

where

l = length of the crystal
w = width of the crystal
t = thickness of the crystal
ε = permittivity of the material
C = capacitance of the crystal

The charge developed in the crystal is also given by

$$Q = e_0 C \tag{2.4}$$

where e_0 is the voltage developed, that is, $e_0 = Q/C$. Making $Q = dF$ from equation 2.1

$$e_0 = dF/C \tag{2.5}$$

Another definition of the transducer is the voltage sensitivity, given by

$$\begin{aligned} g &= \text{Voltage gradient} / \text{Mechanical pressure} \\ &= \frac{e_0 / t}{F/wl} \end{aligned} \tag{2.6}$$

Using equation 2.3 and equation 2.5 the voltage sensitivity can be expressed as

$$g = \frac{e_0 C}{F\varepsilon} \tag{2.7}$$

Problem 2.1

A quartz crystal has a dimension of 2 mm × 2 mm × 1 mm. The crystal has the following properties: charge density, 2PC/N; Young modulus of elasticity, 8.6×10^{10} N/m; permittivity of the material, 40.6×10^{-12} F/m. The crystal is subjected to a strain of 10 μ strain. Calculate

(a) force applied
(b) charge developed
(c) voltage developed

SOLUTION

Given: Width = w = 2mm = 2×10^{-3} m
Length = l = 2mm = 2×10^{-3} m
Thickness = 1mm = 1×10^{-3} m
Charge density = $d = 2 \times 10^{-12}$ C/N
Permittivity = $\varepsilon = 40.6 \times 10^{-12}$ F/m

We know that stress developed (σ) = Young modulus (E) × strain (ε)

Hence $\sigma = 8.6 \times 10^{10} \times 10 \times 10^{-6}$
$= 8.6 \times 10^5$ N/m^2

The stress, $\sigma = F/A = F/wl$

(a) The force applied:
$F = \sigma \omega l$
$= 8.6 \times 10^5 \times 2 \times 2 \times 10^{-6}$
$= 3.44$ N

(b) The charge developed:
$Q = F/d$
$= 3.44 \times 2 \times 10^{-12}$
$= 6.88$ pC

(c) Voltage developed: $e_0 = Fg\, t/\omega l$
Voltage sensitivity: $g = d/\varepsilon = (2 \times 10^{-12})/(40.6 \times 10^{-12})$
$= 1/20.3$
Hence voltage developed (e_o)
$= (3.44 \times 1 \times 10^{-3})/(20.3 \times 2 \times 10^{-3} \times 2 \times 10^{-3})$
$= 42.36$ V

The equivalent circuit of a piezoelectric crystal is shown in figure 2.2. When the crystal is subjected to a sudden increase in force (a step input), a charge is stored in the capacitor. The capacitor eventually discharges exponentially and the charge leaks off through the finite leakage resistance R. The initial leakage rate is determined by the discharging time constant RC. The leakage resistance R can be as high as 10^8 MΩ in quartz crystal.

Due to the automatic discharging phenomenon, the quartz crystal can measure only relative pressure, sometimes denoted as pounds per square inch relative (Psir). It measures pressure relative to the initial transient level.

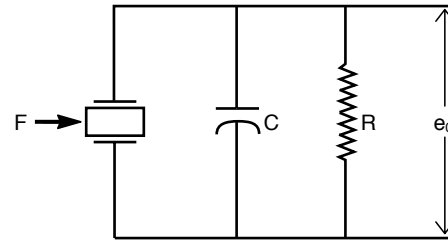

FIGURE 2.2
Equivalent circuit of piezoelectric crystal.

To limit the charge to leak off quickly, special amplifiers are used between the crystal and the recorder. These are voltage amplifiers with a charge converting capacitor at the input, or a charge amplifier with a capacitor in the feedback path. These special amplifiers are isolation amplifiers or vibration amplifiers. Modern piezoelectric transducers are equipped with built-in junction field effect transistors (JFET) or metal-oxide semiconductor field-effect transistors (MOSFET)-based isolation amplifier and signal conditioners. These transducers are called integrated circuit piezoelectric (ICP) transducers.

The outputs of piezoelectric crystals are normally corrupted by spurious noise signals caused by environmental effects such as temperature, moisture, and so on. To eliminate these effects, the transducers are designed with special compensating devices. In one type a built-in accelerometer cancels out the effect of motion from the output signals of the piezoelectric crystal.

Piezoelectric pressure sensors have several merits for dynamic pressure measurement. They are compact in size, lightweight, and robust. The operating frequency range covered is from almost DC to hundreds of kilohertz. Due to rugged construction, piezoelectric sensors are widely used in drastic environmental situations.

2.3.2 Thermocouples

It is the most common type of sensor used for temperature measurement, but in recent years thermocouples have been replaced by other temperature sensors like resistance temperature detectors (RTD), thermistors, semiconductors, and so on.

In 1821, Seebeck discovered that when two dissimilar metallic wires are joined together to form a junction and form a closed circuit (fig. 2.3) it causes electric current to flow in the circuit when the two end junctions are at two different temperatures. The current causes a small voltage developed across the circuit. The thermodeveloped electromagnetic frequency (EMF) is given by

$$e = K(T_a - T_b) \tag{2.8}$$

where K is the sensitivity of the thermocouple in V/°K and T_a and T_b are temperatures of the two junctions. A basic thermocouple device consists of two dissimilar metals A and B to form junction J_1, which is the measuring

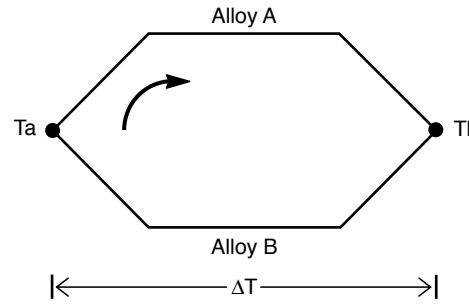

FIGURE 2.3
Seebeck thermo-EMF circuit.

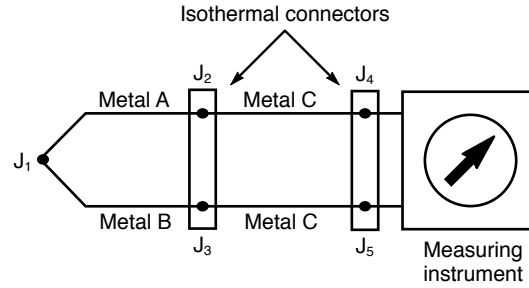

FIGURE 2.4
A practical thermocouple circuit.

junction. Two wires of material C are connected to the two metals A and B to form another two junctions J_2 and J_3 (fig. 2.4). The wires of metal C are used to transfer the EMF developed by the thermocouple to the measuring instrument, where it forms another two junctions J_4 and J_5. Junctions J_2 and J_3 are called *reference junctions,* and they must be kept at a known constant temperature. The additional junctions J_4 and J_5 should also be kept at constant temperature. Isothermal strips are used to connect junctions J_2, J_3, J_4, and J_5 to ensure constant temperature. When the measuring junction J_1 is at temperature T_m and the reference junctions (J_2 and J_3) are at temperature T_r, the EMF developed is given by this equation:

$$e_0 = K(T_m - T_r) \tag{2.9}$$

The output voltage e_0 will be proportional to the measuring junction temperature T_m only when the reference junction temperature T_r is at 0°C, so that

$$e_0 = KT_m \tag{2.10}$$

Earlier, to realize equation 2.10 in temperature indicators or controllers, the reference junction was kept inside an ice bath. However, in recent times reference junction compensation techniques are adopted where a correction EMF value with proper polarity is added to the observed EMF. The effect is same as keeping the reference junction at 0°C.

2.3.2.1 Thermocouple Materials

National and international standards committees have recommended a variety of thermocouple materials. Based on the materials used, thermocouples can be classified as:

1. Base material thermocouple
2. Rare material thermocouple

Base material thermocouples use pure metals and alloys of iron, copper, and nickel. These thermocouples are more sensitive, less expensive, and give a nearly linear output. The drawbacks of this type of thermocouples are their low melting point and deterioration due to oxidation. Rare material thermocouples are made of a combination of pure metals and alloys of platinum, tungsten, rhodium, and molybdenum. The main advantage of this type of thermocouple is its higher operating range. Table 2.1 shows some commonly used thermocouple materials and their important operating characteristics.

TABLE 2.1

Standard Thermocouples

Type	Materials[a]	Temperature Range(°C)	Accuracy (± °C)	Sensitivity (mV/°C)
E	Chromel/Constantan	–200–850	1.5	0.08
J	Iron/Constantan	–200–850	3.0	0.05
K	Chromel/Alumel	–200–1100	3.0	0.04
R	Platinum/rhodium (13%)	0–1400	2.0	0.012
S	Platinum/rhodium (10%)	0–1400	2.0	0.01
T	Copper/Constantan	–250–400	2.0	0.05

[a] First material is more positive when the hot junction temperature is more than the reference junction temperature.

Note: Constantan, Chromel, and Alumel are registered trade names of alloys.

Problem 2.2

A Chromel/Alumel thermocouple is assumed to have a nearly linear operating range up to 1100°C with an EMF of 45.15 mV at this temperature. The thermocouple is exposed to a temperature of 840°C. The cold junction temperature is estimated to be 25°C. Calculate the voltage measured without reference junction compensation.

SOLUTION

Given these data:

Output voltage = 45.15 mV at temperature 1100°C

The measuring junction temperature = T_m = 840°C

The cold junction temperature = T_r = 25°C

The sensitivity of the thermocouple:

$$K = 45.15\ \text{mV}/(1100 - 25)^\circ\text{C}$$
$$= 0.042\ \text{mV}/^\circ\text{C}$$
$$= 42\mu\text{V}/^\circ\text{C}$$

The EMF indicated by the measuring instrument

$$e_0 = K(T_m - T_r)$$
$$= 0.042 \times (840 - 25)$$
$$= 34.23\ \text{mV}$$

2.3.2.1.1 Amplification

The output voltage of thermocouple is very small, typically 10 mV to 50 mV or even lees. A direct temperature readout device with a thermocouple needs amplification of the voltage by a factor of 100 or so. In most cases an instrumentation amplifier is more suitable for thermocouple signal amplification. Apart from amplification, noise reduction measures might be required. Commonly used methods for noise reduction are:

1. Use of twisted thermocouple wire from measuring junction to reference junction
2. Grounding the measuring junction through the cable sheath
3. Use of an amplifier with a high common mode rejection ratio (CMRR)

2.3.2.2 Reference Junction Compensation

Practical realization of equation 2.10 needs a compensation component of voltage equivalent to KT_r, which is added to the thermocouple output voltage. With the advent of semiconductor thermal sensors, compensation circuits can be easily incorporated in the readout device. The semiconductor sensor senses the reference temperature T_r and produces an equivalent voltage depending on the type of thermocouple used and added with the output voltage using an op-amp summing amplifier. The addition operation of the compensation component can be done by software in case of computer-based measurement systems.

2.3.2.3 Thermocouple Installations

A bare thermocouple is not recommended because the junction and wires could get damaged due to mechanical shock, pressure, chemical reaction, and other factors. Therefore thermocouple wires are always installed with sheaths or placed inside thermo-wells (fig. 2.5). However sheaths or thermowells impose a temperature gradient along the length of the sheath. This error can be minimized by using long and small diameter wires, by using sheath material of higher thermal conductivity, and by ensuring a high degree of heat transfer between the medium and thermocouple. A high value of heat transfer improves the response of the sensor by reducing the lag.

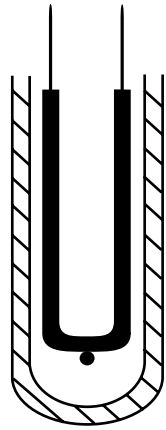

FIGURE 2.5
A sheathed thermocouple.

The following thermocouple sheath materials are commonly used:

1. Metals: Inconel 600 (maximum air temperature of 1150°C); stainless steel (maximum air temperature of 1150°C)
2. Ceramic: Silicon carbide, Frystan, alumina, and various types of porcelains
3. Molybdenum: Maximum operating temperature of 2205°C
4. Tantalum: Maximum operating temperature of 2482°C

2.3.2.4 Thermocouple Wire Insulators

To protect the two thermocouple wires from contacting each other and from direct heating, ceramic insulator sleeves are used. They are available in various sizes and shapes. Figure 2.6 shows some thermocouple wire insulators.

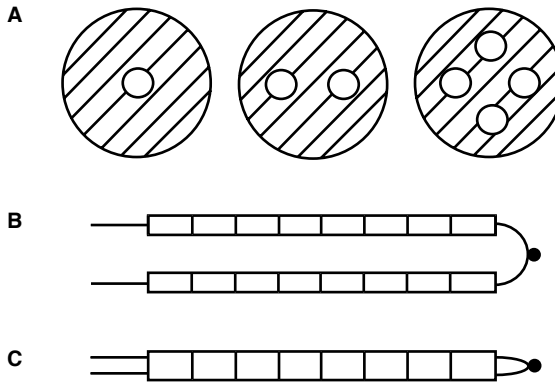

FIGURE 2.6
Thermocouple wires and insulators: (A) cross-sectional view of insulators; (B) single hole insulator; (C) double hole insulator.

2.3.3 Photoelectric Transducers

Light is a very common source of energy used in measurement and instrumentation. With the help of photo-electric transducers the intensity of light is measured either to determine one or more of the following:

1. Intensity of a beam of light in the visible range
2. Chemical or mechanical property of a material by absorbing light
3. Other physical quantity related to interruption of a light beam

There are three types of photoelectric transducers: photo-emissive, photoconductive, and photovoltaic. Out of these three types, only the photovoltaic type is a self-generating type; the other two transducers are variable parameter type.

2.3.3.1 Photo-Emissive Transducer

Certain photo-emissive agents, by the process of removal of surface electrons, release electrons when they are exposed to a beam of light. These materials are called *photo-emissive materials*. In a photo-emissive transducer, a photo-emissive cathode that is kept at a negative potential releases electrons when a beam of light falls on it. The electrons are collected at an anode and so a current flows in the circuit (fig. 2.7). The cathode is placed in an evacuated or glass tube filled with inert gas. The current flowing through the load

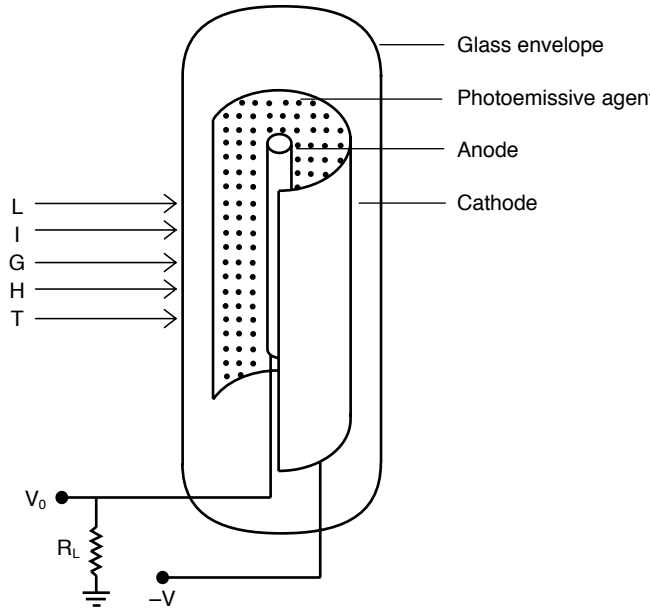

FIGURE 2.7
Photoemissive cell.

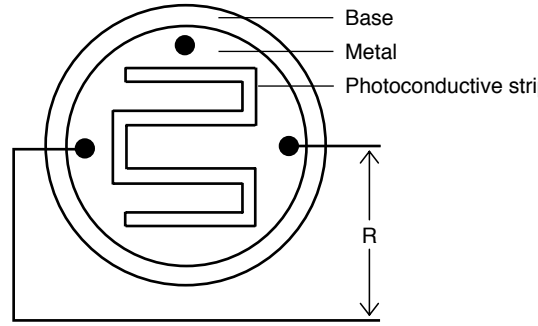

FIGURE 2.8
A photoconductive cell.

resistance is found to be proportional to the intensity of the light incident on the cathode. The most commonly used cathode material is silver. Silver is oxidized and a thin layer of cesium is applied to it. To increase the sensitivity of these devices, photo multiplier tubes are used. In these tubes, due to secondary emission and electron multiplication, an overall increase in electron flow is obtained. Luminous sensitivities of such devices range from 1A/lumen to more than 2,000A/lumen. Anode current ranges typically from 100 μA to a maximum of 1A.

2.3.3.2 Photoconductive Cell

Photoconductive transducers are made up of semiconductor materials like cadmium sulphide, cadmium selenide deposited in a zigzag pattern, a thin layer of germanium, lead sulfide, and so on; deposited over an insulating base like ceramic. The assembly is enclosed in a metal case with a glass window for the ray to pass through. The electrical conductivity of the layer is measured between two electrodes placed on two ends of the layer. When a beam of light falls on the layer, its resistance decreases considerably. The variation of the resistance due to change in light intensity is measured by a simple voltage dividing circuit or the commonly used Wheatstone bridge circuit. These transducers are very compact, rugged in construction, and highly sensitive. Photocells of this type are commercially available in different sizes ($\frac{1}{8}$ in. to 1 in. in diameter). Figure 2.8 shows the layout of such a photocell.

Different photoconductive materials possess different time constants and spectral bands. For example, CdS has a time constant of 100 ms and works in the spectral band of 0.47 to 0.71 μm. For practical use, a cell is rated in dark resistance and power dissipation. Most devices have a typical dark resistance value varying from hundreds of ohms to several megaohms and power dissipation of 50 mW to 500mW.

Problem 2.3

A photoconductive cell is used to display completeness of fermentation in a tea fermentation process as shown in figure 2.9. A relay should be operated

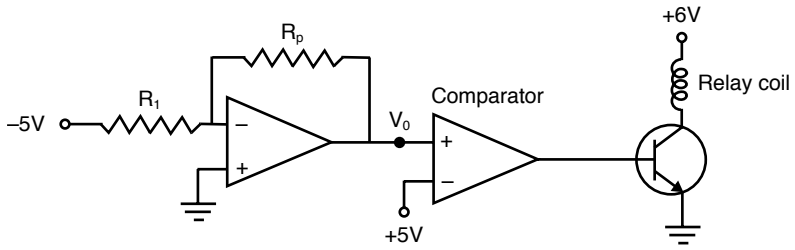

FIGURE 2.9
Relay circuit.

when there is a transition of tea color from green to coppery red. The resistance of the cell changes accordingly from 1 kΩ to 10.21 kΩ. Find the value of the resistance R_1.

SOLUTION
In the circuit the cell is connected to the feedback of op-amp as R_p and with –5 V as constant input voltage to the inverting terminal through R_1. The cell resistance at transition of tea color from green to coppery red is 10.21 kΩ. Therefore

$$R_p = 10.21 \text{ k}\Omega.$$

The comparator reference voltage is +5 V, so we can make the output voltage as +5 V to trigger the comparator so that the transistor switches on the relay.

From the equation of output voltage

$$V_0 = -V_i(R_p/R_1)$$
$$V_0 = -(-5)\ (10.21)/R_1 = 5 \text{ V}$$

This gives $R_1 = 10.21$ kΩ.

2.3.3.3 Photovoltaic Cell

Photovoltaic cells are made of gold-doped silicon (Si) or selenium (Se) materials. These cells supply an electrical current when connected to a load circuit. For sensing of radiation, these solar cells are devised by diffusing a layer of almost –0.5μ n-type material into a thin slice of single crystal p-type silicon of about 2 cm^2. When photons strike the p-layer, electrons in the n-layer cause conduction electrons and holes absorb them. The depletion zone potential of the p–n junction causes a potential difference across the cell. The solar cells conserve the radiant energy in the form of electrical power. The total electrical power conserved into the cell is proportional to the quantum of radiant energy.

In addition to the use of photovoltaic cells as radiant energy sensors, they are also used as solar cells for conserving sunlight as potential energy in a nonconventional form of energy. An op-amp amplifier can be used to interface the cell to a readout device. The spectral bands on Si- and Se-based cells are 0.44 μm to 0.62 μm, respectively. One disadvantage of photovoltaic cells is that their resistance changes with radiant light frequency.

2.3.3.4 Photodiode and Phototransistor

A photodiode (fig. 2.10) is a semiconductor diode used in reverse biased condition. When the reverse biased diode is subjected to direct illumination, a direct current flows almost in direct proportion to the light intensity. The main advantage of the photodiode is its fast response. Due to its good frequency response, it can be used faithfully for sensing light fluctuating at high frequency.

The phototransistor is more sensitive than a photodiode (by as much as 100 times) but its response is slow. In an NPN device, light falling on the central region produces electron hole pairs, reducing the barrier potential across the junctions. This results in more flow of current compared to the photodiode. Hence it is much more sensitive than a photodiode. Figure 2.11 shows the layout of a phototransistor.

2.3.4 Magneto-Electric Transducer

Magneto-electric transducers are also called induction-generator type transducers. These transducers work on the principle of generation of a voltage

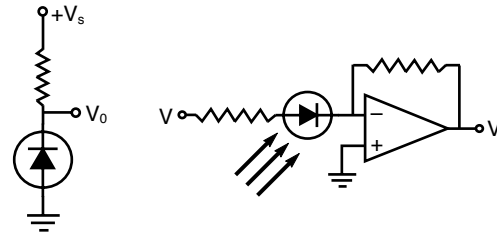

FIGURE 2.10
A photodiode circuit.

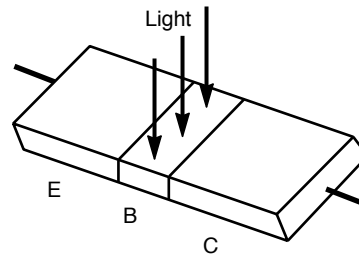

FIGURE 2.11
NPN junction phototransistor.

by electromagnetic induction. From the basic principle of the law, the induced EMF is given by

$$E = -L\frac{d\phi}{dt} \tag{2.11}$$

where L is the self-inductance of the coil and $d\phi/dt$ is the rate of change of flux linkage with the coil. When a conductor moves in a magnetic field, the voltage induced is given by

$$e = Blv \times 10^{-8} Volt \tag{2.12}$$

where B is the flux density (wb/cm^2), l is the length of the conductor (cm), and v is the velocity (cm/sec) of the conductor. The voltage developed in a coil is proportional to the strength of the magnetic field, total number of conductors, and velocity of the coil. Based on these design principles, the following magneto-electric transducers are available:

1. Angular velocity electrodynamic transducer
2. Linear velocity electromagnetic transducer
3. Pulse generator type transducer

2.3.4.1 Electrodynamic Transducer

In this transducer, conductors are wound on a ferromagnetic material to form a coil, which is allowed to rotate in the annular space between a permanent magnet and soft iron core (fig. 2.12). The voltage induced in the coil is tapped using carbon brushes or slip rings. This type of transducer is used for angular displacement and velocity measurements.

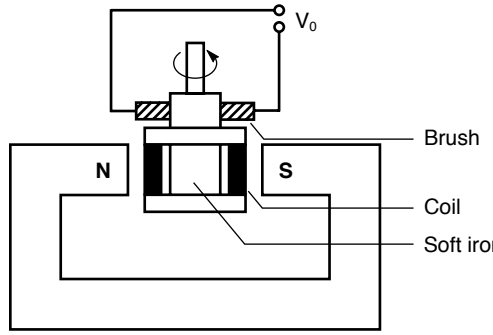

FIGURE 2.12
Electrodynamic transducer.

2.3.4.2 Electromagnetic Transducer

In an electromagnetic transducer a translation motion is used as the input to the transducer for generating the electric voltage. In one form (fig. 2.13A) of the transducer, a coil is wound on a nonmagnetic former that is allowed to move to and fro in the annular space of a permanent magnet. The rate of change of magnetic flux, cut by the conductors of the coil, is proportional to the transnational speed and the voltage induced in the coil. It is also proportional to the motion.

In another form (fig. 2.13B), a coil is wound on a permanent magnet and an object made of a ferromagnetic material is allowed to move at a certain velocity. The motion causes the object to change the air gap; the magnetic flux linked with the coil also changes at the same rate as that of the velocity of the object. Hence, the voltage induced indicates the transnational motion of the object.

Magnetoelectric transducers are mainly used to measure rotational speed of machines like motors, turbines and so on. When used as a rotational speed sensor, it is called a *tacho-generator*. Tacho-generators are especially useful as feedback elements of a positional control system.

Apart from direct use of revolutions per minute (RPM) measurement, these transducers are also used for liquid flow and vibration measurement.

2.3.4.3 Pulse Generator Type

In a pulse generating type of transducer, a rotor is driven by a mechanical force produced either by flow or by any other motion (fig. 2.14). The outer

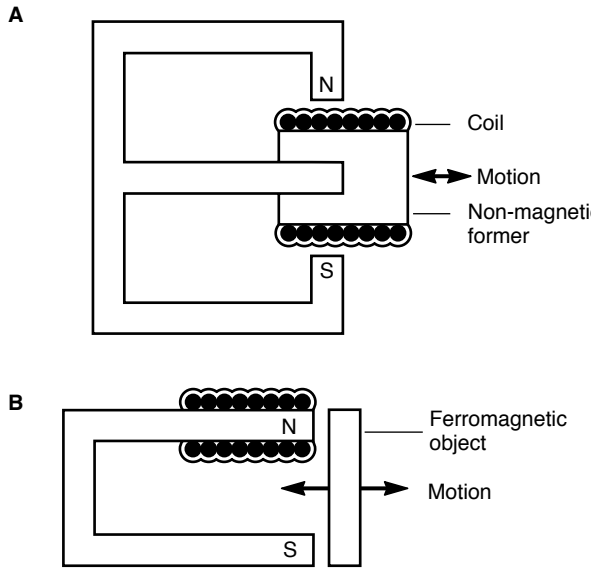

FIGURE 2.13
Electromagnetic transducers: (A) moving coil type; (B) moving object type.

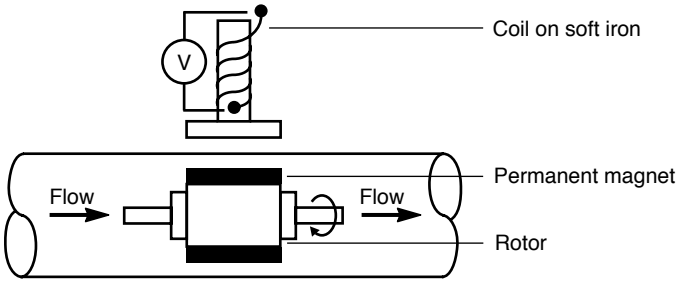

FIGURE 2.14
Pulse generating type of transducer.

periphery of the rotor is a strong permanent magnet and at the outside of the housing near the rotor, a coil wound on a soft iron is placed. The coil should be wound with a large number of turns (i.e., high inductance) so that sufficient EMF can be developed in it. When the rotor rotates, flux from the permanent magnet links with the coil only when the permanent magnet approaches the coil. The voltage induced in the coil is a train of pulses with frequency that is proportional to the speed of revolution of the rotor. Measurement of the pulse frequency gives a measure of the RPM of the rotor; figure 2.15 shows the type of pulse generated in this kind of transducer.

Figure 2.15A shows that four pulses are generated within a specific time, whereas figure 2.15B shows that eight pulses are generated during the same time span when the rotor speed is increased by two times in the second case.

2.3.5 Radioactive Transducer

Radioactive transducers are based on the absorption pattern or depth of penetration of radioactive rays in a medium. Radioactive rays are liberated by radio-isotopes like 60Co, 137Cs, 192Ir, and so on. The radioactive rays liberated by a radio-isotope are α, β, γ, and neutron radiations. The basic characteristics of radioactive rays for use as a source in instrumentation are the following:

1. Penetrating power
2. Half life
3. Half distance

2.3.5.1 Penetrating Power

The penetrating power of α radiation is the lowest of all types of radioactive radiations, which is about 11 cm in air and 0.1 mm in fabric. It is easily absorbed by a sheet of writing paper and an aluminum foil of 0.006 cm thickness. Penetration of β radiation is higher than α radiation due to its

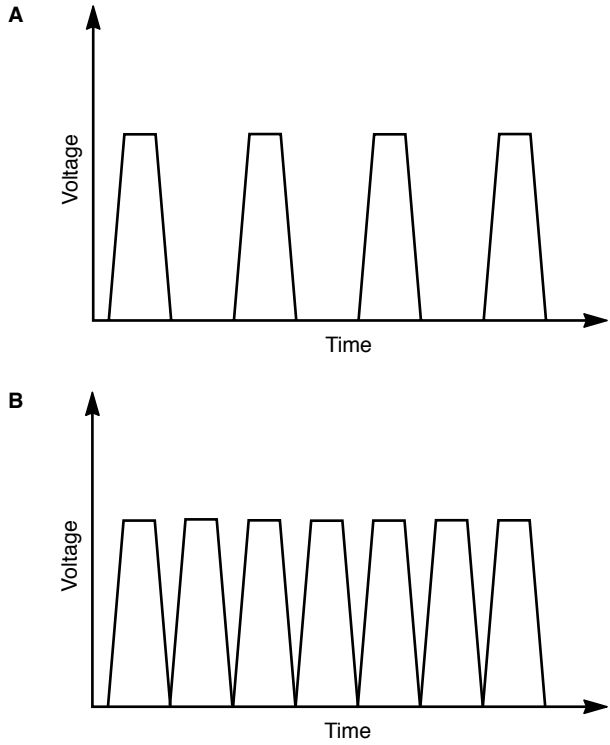

FIGURE 2.15
(A) Pulse waveform for a rotor speed n. (B) Pulse waveform for a rotor speed 2n.

smaller mass. It can travel up to 10 m in air and 10 to 12 mm in fabric, and it can be stopped by an aluminum layer of 5 mm to 6 mm and a lead sheet of 1 mm thickness. The γ radiation is electromagnetic radiation similar to X-rays, having the highest penetrating power. The γ radiation can travel through several inches of lead. When radiation travels through a medium its absorption in the medium can be expressed by

$$I = I_0 e^{-\mu_L d} \tag{2.13}$$

where I = strength of radiation after absorption
I_0 = strength of radiation before absorption
μ_L = linear absorption coefficient of the medium
$= \rho\mu_m$
where ρ = density of the medium
μ_m = mass absorption coefficient of the medium
d = distance traveled in the medium

The unit of radioactivity or strength of radiation is the Curie (C).

The absorption coefficients depend on several qualities of the medium, such as density, compactness, moisture content, impurities present, and so on. Hence, these factors or any other parameter affecting these factors can be measured based on this absorption principle of the radioactive rays. Two important properties of radioactive materials for instrumentation are half life and half distance.

2.3.5.2 Half Life

The radio-isotopes always try to disintegrate continuously to a more stable state. The time taken by the radio-isotope to fall to half of its strength is known as its *half life*. The half life of a radio isotope is given by

$$t_{half} = 0.693 / \lambda \tag{2.14}$$

where λ = decay constant.

The half life of radioactive sources varies from days to months and even years. For the use of instrumentation, the half life of a source should be high. This does not require frequent recalibration of the detector. In all radioactive sources, the date of activation and half life are written on them by the manufacturer.

2.3.5.3 Half Distance

Half distance of sources depends on the source energy level as well as the material of the medium. It is defined as the thickness of the medium that will allow only half the value of the source's intensity entering the medium. This gives a guideline for selecting a source depending on the thickness of the medium. Table 2.2 shows the comparison of a few radioactive sources used in instrumentation.

TABLE 2.2

Common Radio-Isotopes

Isotopes	Maximum Penetrating Power (mm)	Half Life	Relative Cost
60 Co	150	5.25 years	1.5
137 Cs	190	30.0 years	2.0
192 Ir	80	74.4 days	1.0
170 In	20	127 days	2.0

A basic radioactive instrumentation scheme for detecting physical parameters requires the following components:

1. Radioactive source
2. Radioactive detector

3. Electronic processing unit
4. Indicator or recorder

A diagram of such a basic radioactive instrumentation scheme is shown in figure 2.16. The radioactive rays are allowed to pass through the test medium, which moderates some of the radiation and so decreases the strength of the radiation. The resulting radiation at the output is detected by a radiation detector. A radiation detector is a device that converts the incident radiation to a proportional electrical signal, detecting the intensity degradation due to absorption. The following various kinds of suitable radiation detectors are available for use with specific applications:

1. Geiger Muller counter
2. Scintillation counter
3. Ionization chamber
4. Proportional counter
5. Semiconductor counter

The electrical signal obtained from a radiation detector is conditioned by an electronic processing unit and the processed signal is displayed by an indicator or recorder.

Two different methods are adopted for testing a medium using radioactive radiation: the direct transmission method and the back-scattering method. The direct transmission method is used when there is enough room to place the detector at the other side of the test medium (fig. 2.17). Hence, the source and the detector are placed on the two sides of the test medium. When the other side of the test medium is inaccessible or not enough room is available to place the detector, the back-scattering method is preferable. In this method, a very thin metallic foil placed at the back of the test medium is used as a reflecting surface (fig. 2.18). After passing through the medium, the radiation gets reflected back through the medium to the detector. Radioactive transducers are widely used for industrial applications due to their high accuracy,

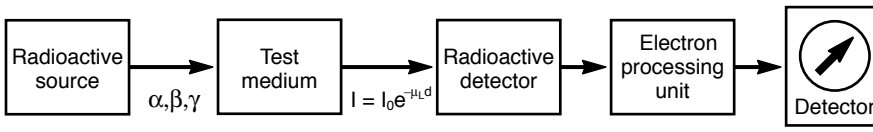

FIGURE 2.16
A basic radioactive instrumentation scheme.

FIGURE 2.17
Direct transmission method of measurement.

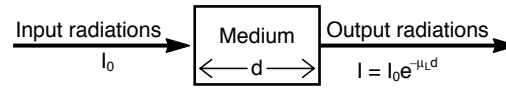

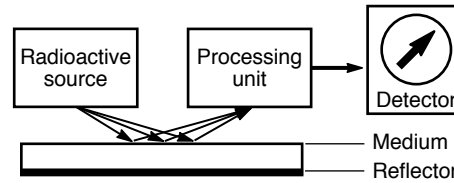

FIGURE 2.18
Back-scattering method of measurement.

high sensitivity, and low noise. The following are some different applications of radio-isotopic instrumentation:

1. Thickness measurement of solids
2. Density measurement of liquids
3. Crack, internal void, and compactness measurement
4. Flow measurement of liquids
5. Level measurement of liquids
6. Moisture content measurement of solids

2.4 Variable Parameter Type

Transducers that fall under the variable parameter type are resistive, inductive, and capacitive transducers. One of the most common features of these transducers is that they cannot generate a voltage of their own and so a separate power supply is needed to make the transducer active. There is great flexibility in augmenting the measuring circuit of these transducers according to some predetermined factors. There is not a fixed pattern of the complete transducer for different applications. Different values of sensitivity, accuracy, resolution, and so on can be obtained by proper design of the measuring circuit in different applications.

2.4.1 Resistive Transducer

The resistive property of a material in the form of a wire or foil is exploited in this type of transducer. Variation of the resistance of a wire of uniform cross-section and resistance can be obtained by changing physical conditions of the wire like temperature, displacement, stress and strain, moisture content, and so on. The variation of resistance of the wire can be expressed as

$$R = \rho L / A \tag{2.15}$$

where ρ is the resistivity of the material (Ω.cm), L is the length of the wire (cm), and A is the cross-sectional area of the wire (cm^2). The resistance R can

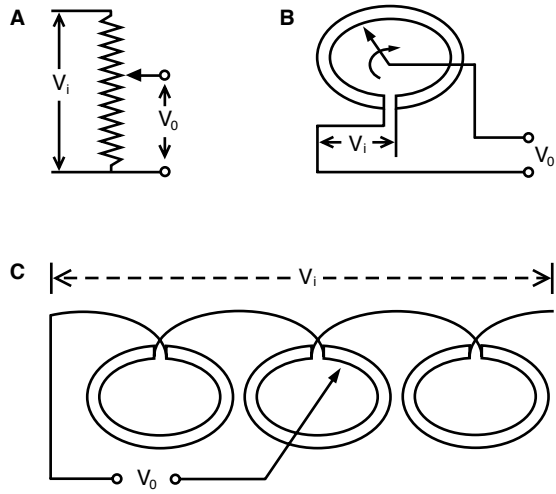

FIGURE 2.19
Potentiometers: (A) translational; (B) rotational; (C) helical.

be changed by changing any one of ρ, *L*, or *A*. In most resistive transducers, the variation in resistance takes place due to only one of these parameters at a time. All three quantities are very rarely varied in the same transducer. Some of the commonly used transducers are explained in the following sections.

2.4.1.1 Potentiometer

The potentiometer is one of the simplest resistive transducers used for measurement of translational or rotational displacement. In its simplest form, it consists of a potentiometer wire or a conducting strip with a movable contact attached to a clamp, called a slider or wiper. The contact motion can be translational, rotational, or helical. The translational resistive elements are straight devices, the full stroke length of which can range from 2 mm to 0.5 m. The rotational devices are circular in shape with a maximum angular displacement of 310° to 360°. Helical potentiometers (helipot) are multiturn rotational devices used for measurement of helical motion. Figure 2.19 shows different forms of potentiometers. For a translational potentiometer the output voltage e_0 can be calculated as

$$e_0 = input\ voltage \times \frac{resistance\ at\ the\ output}{total\ resistance\ of\ the\ P.M.}$$
$$e_0 = e_i \times \frac{(R_p X_i / X_t)}{R_p} = e_i \times \frac{X_i}{X_t} \tag{2.16}$$

where e_i = input DC excitation voltage
R_p = total resistance of the potentiometer

X_i = input displacement, cm
X_t = total potentiometer length, cm

The sensitivity of the device is given by

$$S = e_0 / X_i = e_i / X_t \quad (V/cm) \tag{2.17}$$

Hence, the sensitivity of a potentiometer can be increased by using a higher excitation voltage. The power dissipation capacity of a potentiometer is an important factor in designing it for a particular input voltage. Due to current flowing through the potentiometer, heat is developed that is proportional to the power dissipated, given by

$$P = e_i^2 \,/\, R_p \tag{2.18}$$

The input voltage is, therefore

$$e_i = \sqrt{PR_p} \tag{2.19}$$

For durability of the potentiometer, the power dissipation should be as low as possible. From equation 2.18, to minimize power dissipation of the input voltage should be small and resistance should be high. However, it is observed from equation 2.16 that reduction of input voltage will result a lower sensitivity. Therefore, a compromise between these two factors has to be made.

2.4.1.1.1 Materials

The following are the different types of potentiometer materials generally in use:

1. Wire wound. These potentiometers are made of some resistive wires wound over a nonmagnetic former. The materials used are alloys of nickel (i.e., chromium, nickel-copper) or some other precision resistive elements. These materials can carry comparatively large currents at high temperatures. Their resistance temperature coefficient is usually small, on the order of $20 \times 10^{-6}\ \Omega/\Omega/°C$.
2. Cermets potentiometer. It uses precious metal particles fused into a ceramic base. The fused metal particles act as a resistive element. The main advantages of such materials are their high power ratings and moderate temperature coefficient (from 100×10^{-6} to 200×10^{-6} $\Omega/\Omega/°C$).
3. Hot-molded carbon potentiometer. The resistive element of this potentiometer is fabricated by molding together a mixture of carbon and thermosetting plastic binder.

4. Carbon film potentiometer. In this potentiometer, the resistive element is a thin film of carbon deposited on a nonconducting base. Its main advantage is low cost but its temperature coefficient is high ($1{,}000 \times 10^{-6}\ \Omega/\Omega/°C$).

2.4.1.1.2 Advantages

1. The transducer is inexpensive, very simple to operate, and requires simple circuits.
2. The potentiometer is useful to measure large displacements.
3. The sensitivity is sufficiently high and therefore does not require an amplifier before driving control equipments.
4. The frequency response is good.

2.4.1.1.3 Disadvantages

1. The potentiometer requires a large torque or force to move the wiper.
2. Because the sliding contact is a moving part, it frequently gets misaligned, develops contact resistance, wears out, and produces noise.

2.4.1.2 Resistance Strain Gauge

Strain gauge is a resistive transducer that works on the principle of variation of resistance of a resistive element due to application of mechanical force or load. When a resistive element is subjected to a mechanical force, a mechanical stress (force/area) is developed along the element. If the element is elastic in nature, it undergoes mechanical strain (elongation or compression per unit length). Due to the deformation or dimensional change, the resistance of the element changes directly proportional to the cause of the strain (i.e., the applied mechanical force, pressure, motion, etc.). When the resistive element of a strain gauge is subjected to a mechanical stress, dimensional changes take place; that is, length increases and cross-sectional area decreases. A compressive stress causes a reverse dimensional change. This property of the material is called the *piezo-resistive effect*. The effect that changes resistance can be described by the following equations.

The resistance of a wire conductor is given by

$$R = \rho L / A$$

where ρ = the specific resistance of the material (Ω.m)
L = length of the conductor (m)
A = the cross-sectional area of the conductor (m^2)
= CD^2, C is a constant and D is the diameter (m)

Hence, we can write that

$$R = \rho L / CD^2$$

If the conductor is stretched or compressed, its resistance will change due to change in length and cross-sectional area and due to the piezo-resistance effect. Differentiation on R gives

$$dR = \frac{CD^2(Ld\rho + \rho dL) + \rho L 2C\, D\, dD}{(CD^2)^2}$$

$$dR / R = \frac{(1/CD^2)\left[(Ld\rho + \rho dL) + 2\rho L\, dD / D\right]}{\rho L / CD^2}$$

$$dR / R = \frac{dL}{L} + 2\frac{dD}{D} + \frac{d\rho}{\rho}$$

Dividing the equation by (dL/L) gives

$$\frac{(dR/R)}{(dL/L)} = 1 + 2v + \frac{(d\rho/\rho)}{(dL/L)} \tag{2.20}$$

where v is the Poisson's ratio of the material of the wire. The term

$$\frac{(dR/R)}{(dL/L)} = \lambda \tag{2.21}$$

is called the gauge factor of the strain gauge. The gauge factor of a strain gauge is a measure of its sensitivity. For most of the strain gauges the gauge factor is about 2.0 and for nickel its value can vary from –12 to +6.

Resistance strain gauges are classified into two basic forms: unbonded and bonded.

2.4.1.2.1 Unbonded Strain Gauges

An unbonded resistance strain gauge is made of a set of resistive wires of about 25μ in diameter stretched between two supports. The wires are stretched between two structures, one fixed and the other movable. Figure 2.20 shows such an unbonded strain gauge. The wires are stretched prior to application of strain to avoid sag and vibration. When the movable plate is displaced, the wires will be under tensile strain, causing a change in resistance. A displacement on the order of 50μ can cause a considerable strain in the wires. The four wires are connected to a Wheatstone bridge circuit that results in unbalanced output voltage. Unbonded strain gauges are suitable for measurement of very small displacements.

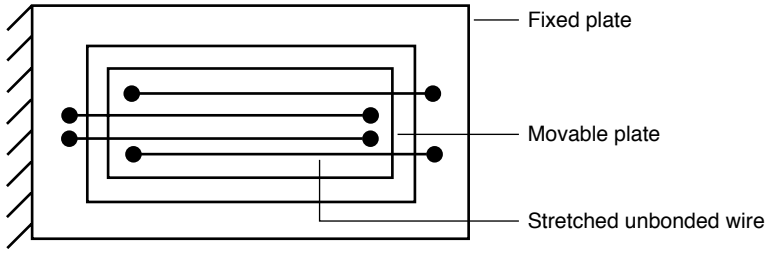

FIGURE 2.20
Unbonded strain gauge.

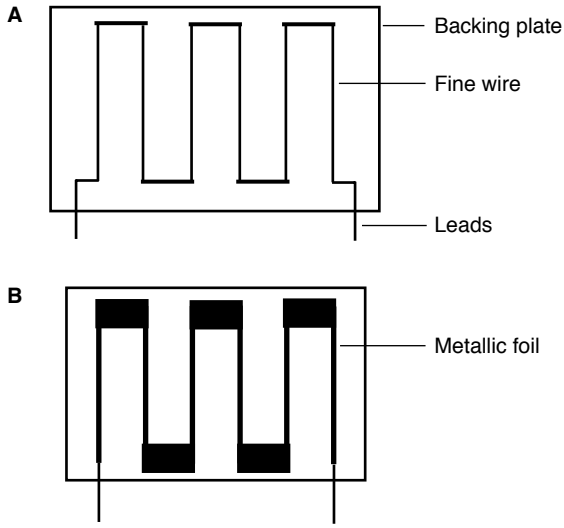

FIGURE 2.21
Bonded strain gauges: (A) wire gauge; (B) foil gauge.

2.4.1.2.2 Bonded Strain Gauges

Bonded strain gauges are very fine resistive wire elements (about 25μ in diameter) or very thin metallic foils printed or etched on a backing plate (usually paper) in a zigzag or looped pattern as shown in figure 2.21. The wire or the foil is covered by a protective material like a thin sheet of paper, bakelite, or Teflon. The backing plate is bonded to the surface of the test material using an appropriate bonding or cementing material. Once the gauge is bonded to the surface, it becomes a part of the surface and strain is uniformly transferred to the gauge.

When a material is under stress, strain is developed in two directions: the principal strain (ε_x) in the longitudinal axis and the transverse strain (ε_y) in the transverse axis. The transverse strain is given by

$$\varepsilon_y = -v\varepsilon_x \tag{2.22}$$

where ν is the Poisson's ratio. A strain gauge is always mounted on a surface with the longitudinal wire elements in the direction of the principal strain. Hence, a strain gauge picks up the principal strain with highest sensitivity in this direction. Because the end loops of the grid are in the direction of the transverse strain, the gauge picks up the transverse strain that results an error in the measurement. To make the gauge insensitive to this transverse strain, two methods are adopted. In one method the end loops are made of materials insensitive to strain like copper or gold (fig. 2.21A). In the other method the cross-sectional area of the end loops is made considerably larger than that of the longitudinal wire elements (fig. 2.21B). This reduces the transverse strain developed in the end loops of the strain gauge. Strain gauges are manufactured in various configurations based on different applications such as these:

1. Grid type
2. Rossette type
3. Torque type
4. Helical type

Looping down the strain wire in the insulated base in a back and forth manner (fig. 2.21A and fig. 2.21B) results in a grid type strain gauge. When the axis of the strain in a plane is not exactly known, it is difficult to bond the gauge in proper orientation for sensing the maximum strain developed. In such situations several grid gauges are placed as shown in figure 2.22. It shows a three-element rosette gauge in which the angle between any two longitudinal gauge axes is 45°.

Torque and helical gauges are used in special applications. Torque type gauges (fig. 2.23) have resistive element laid at an angle of 45° to the gauge

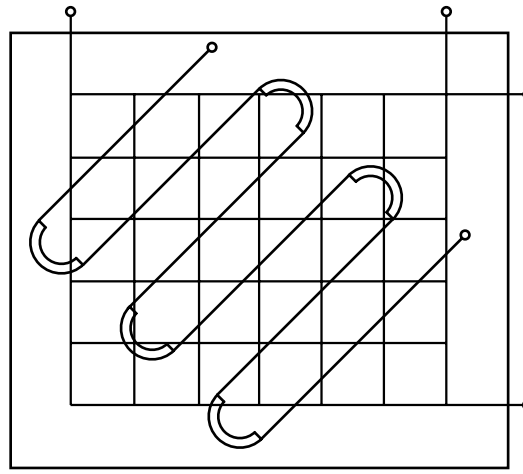

FIGURE 2.22
Rossette type strain gauge.

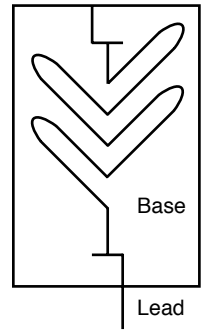

FIGURE 2.23
Torque gauge.

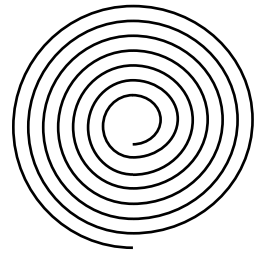

FIGURE 2.24
Helical gauge.

axis. This gauge is used to measure torque in a rotating shaft where a maximum strain is developed along the direction of 45° to the shaft axis. Helical gauges are used to pick up radial as well as circumferential strain developed in a diaphragm used for pressure measurement (fig. 2.24).

2.4.1.2.3 Ratings of Metallic Strain Gauges

The gauge factor of most of the metallic gauges falls in the range of 2.0 to 2.1. Foil and wire gauges are made from nichrome, Constantan (Ni and Cu), Isoelastic (Ni, Cr, and Mo), nickel, and platinum.

The resistance of strain gauges should be as high as possible to minimize other interfering factors. Typical values of wire gauge resistances are 120 Ω, 350 Ω, and 1,000 Ω; and 50 Ω and 1,000 Ω for foil gauges. The diameter of the wires used in the strain gauges is typically 25μ. This restricts its maximum current carrying capacity to the order of 30 mA.

2.4.1.2.4 Semiconductor Strain Gauges

Semiconductor strain gauges are used when a higher sensitivity is needed. Therefore, these strain gauges possess a higher gauge factor. Unlike metallic gauges, in semiconductor strain gauges the variation of resistance on application of strain is mainly due to variation of resistively. Germanium and silicon are two commonly used semiconductor materials. The sensitivity of such gauges depends on the degree of doping.

Semiconductor strain gauges are manufactured in wafer or filament forms, with a thickness of 0.05 mm, bonded to suitable insulating substrate material such as Teflon. The gauge factor of semiconductor strain gauges is 130 ± 10% for a gauge of 350 Ω, 1 in. long, 1/2 in. wide, and 0.005 in. thick. The operating range is ± 3,000 microstrain and the power consumption is only 0.1 W. The resolution is about 0.01 microstrain. The main advantages of semiconductor strain gauges are higher sensitivity, higher resolution, low hysteresis, higher frequency response, and small size.

2.4.1.2.5 Measuring Circuit

Signal conditioning circuits for strain gauges should eliminate two effects: First, the small change in resistance should be effectively converted to a change in voltage. Second, because the strain gauge is a resistive element, any deviation of gauge resistance due to change in temperature should be properly compensated. A full Wheatstone bridge configuration takes care of the first effect where four strain gauges of similar ratings are connected to the four branches of the bridge with proper strain polarity as shown in figure 2.25. The direction of the arrow of the resistors in the bridge circuit indicates the polarity of the strain developed. Let the unstrained normal resistances of the gauges be

$$R_1 = R_2 = R_3 = R_4$$

and the strained resistances of the gauge be

$$R_\varepsilon = R\left(1 \pm \frac{\Delta R}{R}\right)$$

where ΔR = small change in resistance due to application of strain ε.

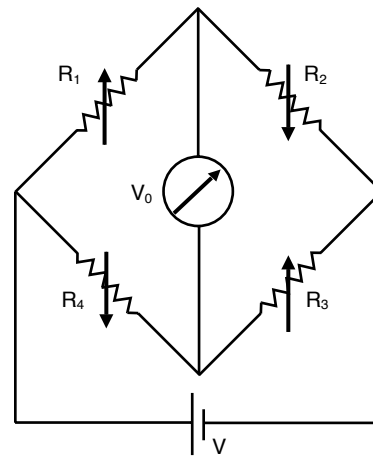

FIGURE 2.25
A Wheatstone bridge measuring circuit.

The unbalanced output voltage can be determined as

$$\begin{aligned} V_0 &= V\left[\frac{R+\Delta R}{(R+\Delta R)+(R-\Delta R)} - \frac{R-\Delta R}{(R+\Delta R)+(R-\Delta R)}\right] \\ &= V\left[\frac{R+\Delta R}{2R} - \frac{R-\Delta R}{2R}\right] \\ &= V\left[\frac{R+\Delta R-R+\Delta R}{2R}\right] \\ &= V\left[\frac{\Delta R}{R}\right] \end{aligned} \tag{2.23}$$

From eq. 2.21 $V_0 = V\lambda\varepsilon$

However if different resistance variations are considered for each gauge, the output voltage equation take the form

$$V_0 = \frac{V\lambda}{4}[\varepsilon_2 + \varepsilon_4 - \varepsilon_1 - \varepsilon_3] \tag{2.24}$$

where the individual strains picked up by the gauges are

$$\lambda\varepsilon_1 = \frac{\Delta R_1}{R_1},\ \lambda\varepsilon_2 = \frac{\Delta R_2}{R_2},\ \lambda\varepsilon_3 = \frac{\Delta R_3}{R_3} \text{ and } \lambda\varepsilon_4 = \frac{\Delta R_4}{R_4}$$

In most of the cases, four identical gauges are employed to get an output voltage by equation 2.23.

2.4.1.3 Diaphragm Pressure Sensor

Diaphragm pressure sensors are made up of two elements:

- A thin metallic diaphragm to sense and convert pressure to deflection
- Strain gauges bonded to the diaphragm to pick up strain developed in radial and tangential directions

It uses a metal diaphragm with good spring characteristics. The diaphragm is clamped to the periphery of the connecting pipe with screws and nuts as shown in figure 2.26. When the diaphragm is subjected to a pressure *P*, it undergoes a deflection given by the equation

$$P = \frac{16Et^4}{3r^4(1-v^2)}\left[(y/t) + 0.488(y/t)^3\right] \tag{2.25}$$

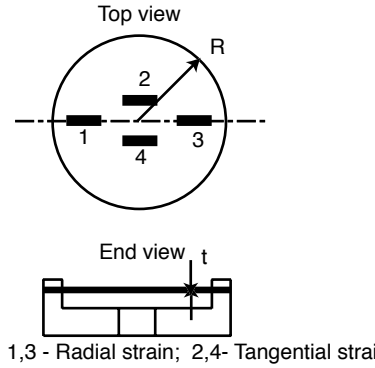

FIGURE 2.26
A diaphragm pressure sensor bonded with four strain gauges.

where P = pressure difference across diaphragm
E = modulus of elasticity of the material
t = thickness of the diaphragm
y = deflection of the diaphragm
v = Poisson's ratio
r = radius of diaphragm to clamped edge

For a small deflection, this equation is fairly linear, but sensitivity of the diaphragm becomes very small. Strain developed in two directions of the diaphragm, as follows:

1. A radial and tensile strain with maximum value at the outer periphery of the diaphragm
2. A tangential and compressive strain that is maximum at the center

These strains are picked up by two pairs of strain gauges as shown in figure 2.25. Strain gauges 1 and 3 sense the radial strain (tensile) and gauges 2 and 4 sense the tangential strain (compressive). The radial and tangential stresses are given by the equation

$$s_r = \frac{3pr^2\nu}{8t^2}\left[\left(\frac{1}{\nu}+1\right)-\left(\frac{3}{\nu}+1\right)(r_r / r)^2\right] \tag{2.26}$$

$$s_t = \frac{3pr^2\nu}{8t^2}\left[\left(\frac{1}{\nu}+1\right)-\left(\frac{3}{\nu}+3\right)(r_t / r)^2\right] \tag{2.27}$$

where r_r and r_t are the radii at which the corresponding radial and tangential gauges are bonded. A strain gauge experiences both radial and transverse strain, so the actual strain developed is

$$\varepsilon_r = (s_r - v\, s_t) / E \tag{2.28}$$

$$\varepsilon_t = (s_t - v\, s_r) / E \tag{2.29}$$

The four active strain gauges are configured in a full bridge configuration (fig. 2.26) so that the output becomes high and it additionally provides temperature compensation.

Problem 2.4

The pressure in the injecting pipe of a cold-drink bottling plant is measured by a diaphragm pressure sensor (fig. 2.25) with the following specifications:

Resistance of each gauge = 120 Ω, gauge factor = 2

Radius of the diaphragm (r) is 7 cm, radius of the position of the tangential gauges (r_t) is 1 cm, radius of the position of the radial gauges (r_r) is 6 cm, thickness of the diaphragm is 1 mm. Assume Young modulus of elasticity for the diaphragm material E = 2.07×10^5 N/mm^2 and Poisson's ratio = 0.25. Determine the radial and tangential strain developed in all four strain gauges if the pressure applied is 1 Pa.

SOLUTION

Given: R = 120 Ω, λ = 2.0

ν = 0.25

r = 7 cm = 0.07 m

p = 1 Pa

For r_r = 6 cm and putting the values of P, r, t, and ν in equation 2.26

$$s_r = \frac{(3)(1)(0.07)^2(0.25)}{8(0.001)^2}\left[(1/(0.25)+1) - (3/(0.25)+1)(0.06/0.07)^2\right]$$

$$= -2090\, N/m^2$$

Again

for r_t = 1 cm and putting the values of P, r, t, and ν in equation 2.27 the tangential stress

$$s_t = \frac{(3)(1)(0.07)^2(0.25)}{8(0.001)^2}\left[(1/(0.25)+1) - (3/(0.25)+1)(0.01/0.07)^2\right]$$

$$= 2175\, N/m^2$$

The tangential and radial strains can be calculated by using equation 2.28 and equation 2.29

$$\varepsilon_r = (s_r - \nu s_t) / E$$
$$= (-2090 - 2175 \times 0.25) / (2.07 \times 10^5)$$
$$= -1272 \times 10^5 = \varepsilon_1 = \varepsilon_3$$

and

$$\varepsilon_t = (s_t - \nu s_r) / E$$
$$= (2175 + 2090 \times 0.25) / (2.07 \times 10^5)$$
$$= 1303 \times 10^5 = \varepsilon_2 = \varepsilon_4$$

2.4.1.4 Load Cell

Load is an important parameter describing the mechanical force applied on a body. Measurement of load using a load cell gives an indication of some quality attribute of materials in the hopper or conveyor in a manufacturing unit. Force (F) and load (W) can be related by an equation as

$$F = Wg \tag{2.30}$$

where g is acceleration due to gravity.

2.4.1.4.1 Strain Gauge Based Load Cells

The principle of elastic deformation of a transmitting member due to application of load or force and the measurement of the deformation is utilized in this type of sensor. Various types of mechanical devices used for sensing load through development of strain are shown in figure 2.27. Every section of the mechanical load sensor undergoes relative linear displacement, which causes a strain. This strain is a measure of the load transmitted by the resistive strain gauges. The strain is measured by using four strain gauges configured in a bridge circuit arrangement. The strain gauges are bonded to the surface of the mechanical sensor, which senses tensile and compressive strain developed. The output voltage developed is amplified and calibrated to directly indicate the load or force. Forces as high as 10 tons or more can be measured by properly designing the mechanical sensor.

2.4.1.5 Resistance Temperature Detectors

It is a well-known fact that resistance of a metal element changes with temperature. This principle is used in resistance temperature detectors (RTDs). The change in resistance due to temperature variation is given by

$$R_t = R_0(1 + \alpha \Delta T) \tag{2.31}$$

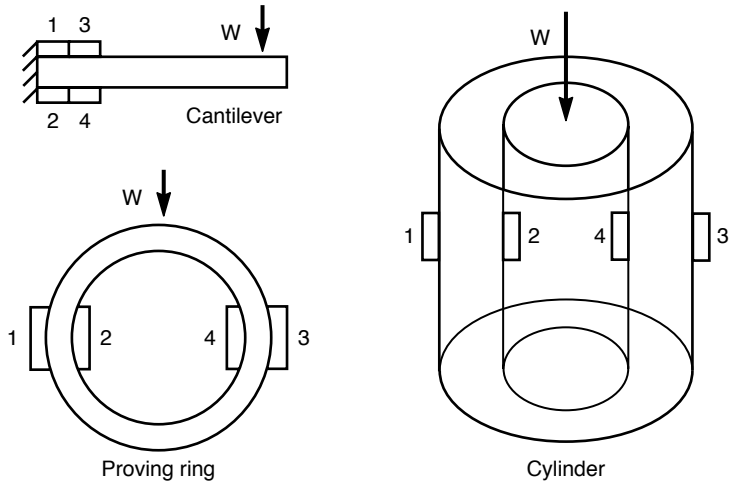

FIGURE 2.27
Load sensors.

where α is a positive resistance temperature coefficient. The metals used for making resistance thermometers are generally platinum (–190°C to 660°C), copper (–150°C to 250°C), and nickel (0°C to 325°C). The operating temperature ranges of these metals are observed to be not very high, so these elements are suitable for low temperature measurements only. The value of α for platinum is on the order of 0.004/°C and that of nickel is 0.005/°C. The requisite characteristics of these materials are as follows:

1. High temperature coefficients for higher sensitivity
2. High sensitivity for compactness
3. Good linearity for ease of calibration
4. Resistance to contamination for reliability

For a low temperature range, two other materials are found to be suitable: a gold–silver alloy for temperatures below 127°K and phosphor–bronze alloy for temperatures below 7°K. These alloys possess sensitivity about 55 times that of the ordinary metals.

2.4.1.5.1 Construction

A resistance wire with a diameter ranging from 0.002 cm to 0.06 cm is generally used, but a 0.01 cm diameter is most common. The wire is bifilarly wound on a nonconducting former or framework of mica-cross, ceramic flat, or round arbors. For surface temperature measurement a grid etched on an insulated surface is used. Figure 2.28 shows different constructions of RTDs. The resistance thermometers have a resistance of between 0.1 ohm and a few hundred ohms.

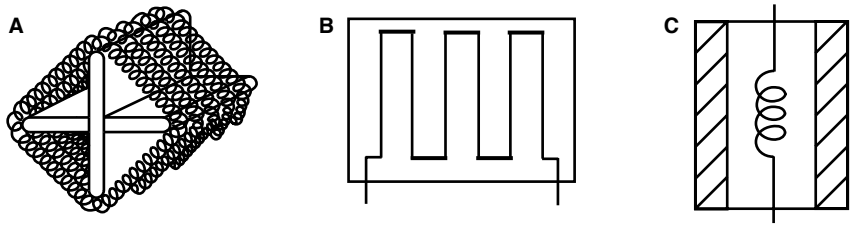

FIGURE 2.28
Resistive temperature sensors: (A) Mica cross; (B) Ceramic flat; (C) Round arbor

The resistance thermometer is protected from mechanical and environmental hazards by covering it with a protective tube of glass, quartz, porcelain, or other material.

An RTD is a very sensitive transducer to give an accuracy to 0.0001°C. The resistance of RTD is typically on the order of 0.1 ohm to few kilo ohms. The variation in resistance due to temperature is converted to a proportionate voltage signal by a Wheatstone bridge circuit as shown in figure 2.25. In figure 2.25, R_4 is the resistance of the sensing element of the thermometer with its mounting and connecting accessories; and R_1, R_2, and R_3 are three fixed resistors, the resistances of which are not affected by temperature. Before the measurement is started, the bridge is balanced to establish the following condition:

$$R_1/R_2 = R_3/R_4 \tag{2.32}$$

when the current through the meter is zero. When the sensor is subjected to variation in temperature, R_s changes from $(R_4 + \Delta R)$ making the bridge unbalanced; therefore, current flows through the meter. The meter current gives an indication of the variation in temperature. Advantages of resistance thermometers include accuracy, suitability for remote indication, fast response, less error, and stability.

Problem 2.5

An RTD with $\alpha = 0.005/°C$, $R_S = 300\ \Omega$ at 25°C is connected in a bridge circuit with $R_1 = R_2 = R_3 = 300\ \Omega$. The supply voltage to the bridge is 5 V and the RTD is used to measure temperature of chocolate during tempering. Find the output voltage of the circuit if the temperature of chocolate is 75°C (fig. 2.29).

SOLUTION
Given
R_0 (25°C) = 300 Ω
Change in temperature = ΔT = (75 − 25) = 50°C
Resistance temperature coefficient = α = 0.005/°C
Bridge supply voltage = 5 V

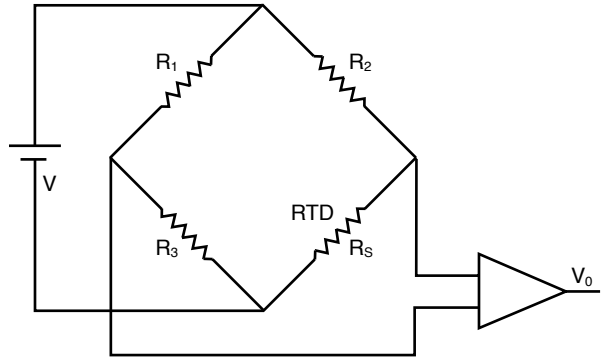

FIGURE 2.29
RTD measuring circuit.

The resistance of the RTD at 75°C (from equation 2.31)

$$R_s\,(75°C) = 300[1 + 0.005(50)]$$
$$= 375\ \Omega$$

The output voltage from the bridge circuit

$$V_0 = 5\left[\frac{300}{300+300} - \frac{300}{300+375}\right] Volt$$
$$= 278\,\text{mV}$$

2.4.1.6 Thermistors

Thermistors are semiconductor materials with negative temperature resistance coefficients; that is, their resistance decreases as temperature increases. The resistance of thermistors at room temperature usually ranges from 100 ohms to 10 mega ohms. They are so sensitive to temperature that a 1°C increase can decrease resistance at room temperature by 6%. The working ranges of thermistors are typically 100°C to 300°C. The resistance temperature characteristic of a thermistor is shown in figure 2.30. The equation relating the resistance and absolute temperature of a thermistor is given by

$$R_t = R_0 e^{(\frac{1}{T} - \frac{1}{T_0})\beta} \tag{2.33}$$

where R_t = resistance at T°K
R_0 = resistance at T_0°K
β = thermistor constant; its common value lies around 4000°K

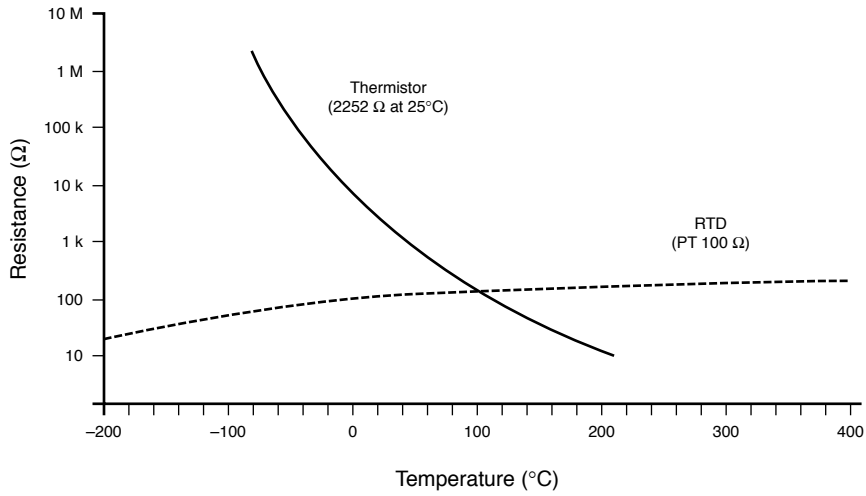

FIGURE 2.30
Resistance-temperature characteristic of a thermistor compared to RTD.

2.4.1.6.1 Materials

Most commonly used thermistor materials are oxides of metals like copper, iron, zinc, aluminum, and so on. These oxides or their sulfides or silicates are milled and mixed in appropriate proportions, pressed into desired shapes with binders, and finally sintered to get the thermistors.

2.4.1.6.2 Standard Forms

The most commonly manufactured forms of thermistor are beads, disc, washer, and rod types. Beads are made by forming small ellipsoids of thermistors on two parallel fine wires about 0.01 in. apart embedded tightly at high temperature. A protective cell of glass is generally used to house the beads. The bead can be evacuated or filled with a gas. The resistance of a bead of size 0.006 in. to 0.1 in. can be on the order of 300 ohms to 100 mega ohms.

Thermistor materials are subjected to high pressure for making discs. These round pieces are sintered and the two flat surfaces are silvered. Their sizes are normally 0.1 in. to 1 in. in diameter and 0.02 in. to 0.5 in. in thickness. In discs a hole is provided at the center to get a washer type form so that it can be mounted with screws and nuts. Normal sizes of washers are 0.75 in. in diameter. Different forms of thermistors are shown in figure 2.31.

2.4.1.6.3 Nonlinearity and Its Compensation

The nonlinear characteristic of a thermistor is disadvantageous for calibration and measurement. The nonlinearity can be overcome to some extent by

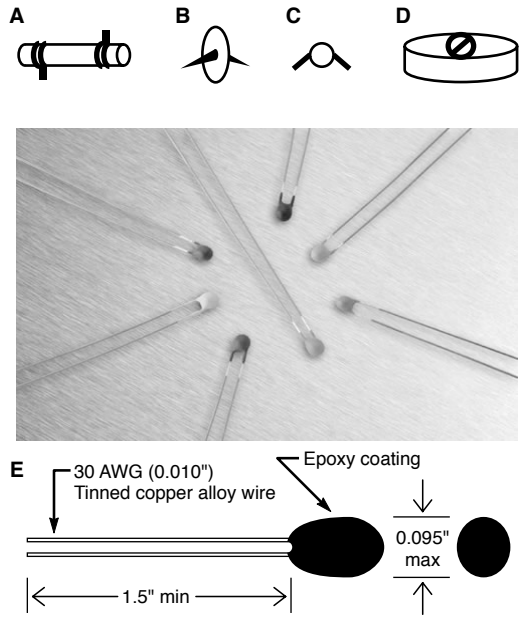

FIGURE 2.31
Forms of thermisters: (A) rod; (B) disc; (C) bead; (D) washer; (E) commercial ultra precision thermistors. (*E: Reprinted with permission from U.S. Sensor Corporation, USA*)

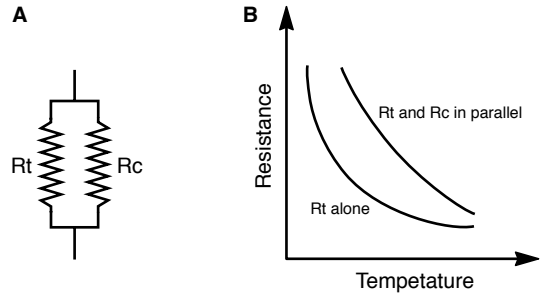

FIGURE 2.32
(A) Circuit for nonlinearity compensation. (B) Characteristics for compensated and uncompensated thermistor.

connecting a low resistance (R_c) parallel to the thermistor resistance (R_t). Figure 2.32 shows the circuit and the graph for nonlinearity compensation. The equivalent resistance of the compensated thermistor is given by

$$R_{eq} = (R_t R_c) / (R_t + R_c) \tag{2.34}$$

Rate of variation of compensated resistance with respect to temperature is

$$\frac{dR_{eq}}{dT} = \frac{dR_t}{dT} \cdot \frac{R_c^2}{(R_c + R_t)^2}$$

From this equation it is evident that

$$\frac{dR_{eq}}{dT} < \frac{dR_t}{dT} \tag{2.35}$$

It shows that although linearity of a thermistor is compensated by the additional resistor, the sensitivity is reduced. Thermistors with linearity as high as 0.2% over the temperature range of 0°C to 100°C are also available. Typical sensitivity values of thermistors are on the order of 3mV/°C at 200°C.

Thermistors are more popular as a device in limiter and regulator circuits, time delays, and temperature compensations than for absolute temperature measurement. The power dissipation constant of thermistors is typically 1mW/°C in free air. This parameter is important to estimate error produced due to self-heating.

Advantages of thermistors are as follows:

1. Compactness and low cost
2. Good response and good sensitivity
3. Negligible contact and lead resistance error due to higher resistance value of the thermistor

Disadvantages include the following:

1. Nonlinear characteristics
2. Low operating range
3. Error due to self-heating

2.4.1.7 Semiconductor Temperature Sensors

Thermal semiconductor sensors are suitable for sensing ambient temperature in the range of –55 to 155°C. A typical IC sensor develops a voltage or current signal proportional to absolute temperature. Accordingly, two types of IC sensors are commercially available: the voltage proportional to absolute temperature (VPTAT) and current proportional to absolute temperature (IPTAT). The connection diagram of a popular VPTAT, IC LM335, is shown in figure 2.33.

When properly calibrated the IC gives an output voltage of 2.98 V at 25°C and a variation of 10 mV/°C. A similar arrangement of an IC AD590, which is an IPTAT, is shown in figure 2.34. AD590 gives a sensitivity of 1 mV/°C, which is 10 times smaller than that of LM335. The main advantages of IC

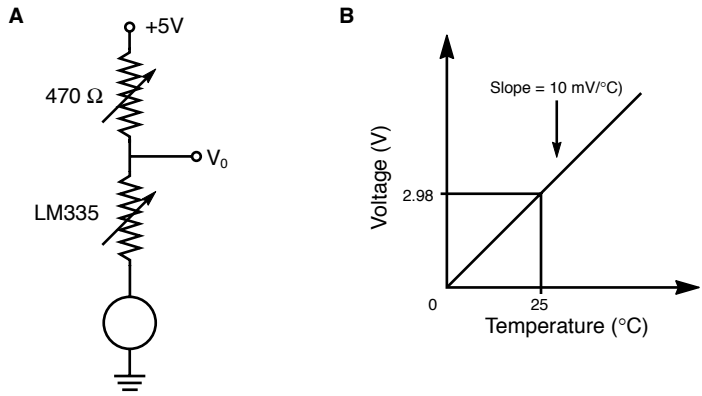

FIGURE 2.33
VPTAT: (A) connection diagram; (B) Temp-Volt characteristic.

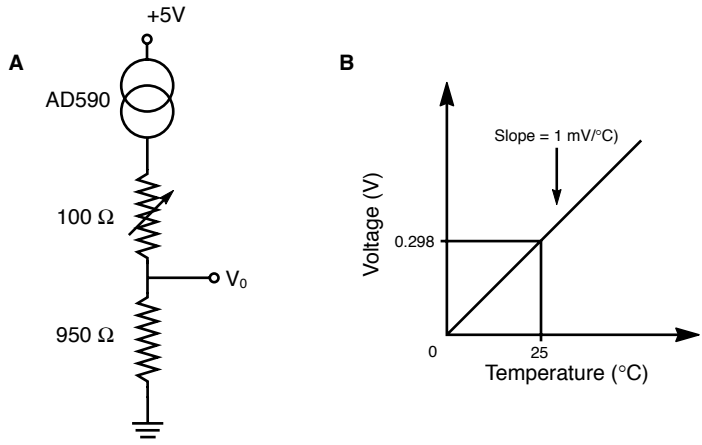

FIGURE 2.34
IPTAT: (A) connection diagram; (B) Temp-Volt characteristic.

thermal sensors are their small size, low cost, fast response, high linearity, and low output impedance. On the other hand the limitations are low operating range, need for offset reduction, and higher amplification.

Problem 2.6

An IC LM335 is used to measure the temperature of a food preservation room that is controlled at a temperature of –4°C. Find the (a) output voltage of the sensor, (b) offset voltage (V) to be nullified, and (c) amplification factor for getting 10 V at 100°C (fig. 2.35).

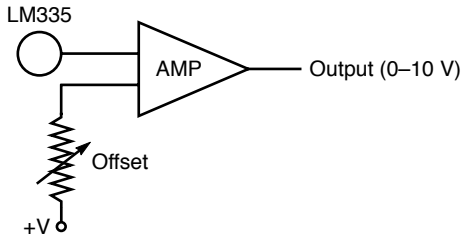

FIGURE 2.35
LM335 with the amplifier circuit.

SOLUTION
Given values
We know that the sensitivity of LM335 sensor = 10mV/°C
Calibrated output voltage at 25°C = 2.98 V
Difference of output voltage between 25°C and –4°C

$$= (25 - (-4)) \times \text{sensitivity}$$
$$= (25 + 4) \times 10 \text{ mV/°C}$$
$$= 290 \text{ mV}$$

(a) The sensor output voltage at –4°C = (2.98 – 0.290) V = 2.69 V
(b) The sensor output voltage at 0°C = 2.98 – (25 × 10) = 2.98 – 0.25
= 2.73 V

Hence, the offset voltage to be nullified is 2.73V
(c) The sensor output voltage at 100°C

$$= 2.73 + (100 \times 10) \text{ mV}$$
$$= 2.73 + 1.0 \text{ V}$$
$$= 3.73 \text{ V}$$

After nullifying the offset voltage, the differential input voltage to the amplifier at 100°C

$$= (3.73 - 2.73) \text{ V}$$
$$= 1.00 \text{ V}$$

The required amplified voltage at 100°C = 10 V
Hence, the amplification factor = 10 V/1.00 V

$$= 10$$

2.4.1.8 Hot Wire Anemometer

The hot wire anemometer is a resistive transducer used for measurement of flow of gas or liquid through a pipe. The basic principle and setup of the hot wire anemometer is that a resistive wire is placed across the flow stream and a constant current is allowed to flow through it (fig. 2.36). The heat

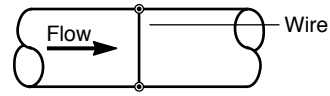

FIGURE 2.36
Setup of a hot wire anemometer in a pipe flow.

developed in the wire is dissipated into its surrounding when the velocity of the fluid changes; the amount of heat dissipated will also change. This heat loss changes the resistance of the wire. If the current supplied to the wire is kept constant, the change in resistance can be taken as a measure of the change in flow. This gives a constant current hot wire anemometer.

The resistive element is made of a platinum wire with a diameter of 0.0005 to 0.03 cm and a length of 0.1 to 1 cm. The diameter of the wire should be kept small to experience less fluid pressure. The length of the wire should be half of the pipe diameter and is placed at the center of the pipe with supports.

The variation in resistance of the wire due to change in fluid velocity is detected by a Wheatstone bridge circuit. Contamination is a major problem of the hot wire anemometer. Another drawback is that when the current is kept at large value and fluid velocity drops by a large amount suddenly, the wire might burn out.

2.4.1.9 Resistive Humidity Sensors

Humidity has been measured using various mechanical devices for a long time, but electrical resistance type humidity sensors are more popular than mechanical types because in electrical types the signal can be transmitted and recorded by electronic devices. This type of humidity sensor is based on variation of resistance of resistive wires on a nonconductive backing material, as shown in figure 2.37A.

The space between the two wire electrodes is filled with a hygroscopic compound like lithium chloride, phosphoric acid, calcium chloride, zinc chloride, or tin-tetrachloride. When the sensor is exposed to air containing water particles, the hygroscopic material absorbs water and the overall resistance between the two wire electrodes decreases. The change in resistance is on the order of 10 MΩ to 10 KΩ. This variation in resistance can be converted to a voltage by inserting the sensor in a resistive network or a Wheatstone bridge circuit as shown in figure 2.37B and figure 2.37C.

2.4.2 Inductive Transducers

Inductive transducers constitute a major part of the transducer family, mostly for displacement and proximity measurement. Inductive transducers can be broadly classified into two main types: self-generation and variable inductance.

In the self-generating type, a relative motion between a conductor and a magnetic field is converted to an induced voltage.

In a variable inductance transducer, the physical displacement is utilized to vary the self-inductance or mutual inductance of a coil. The inductance

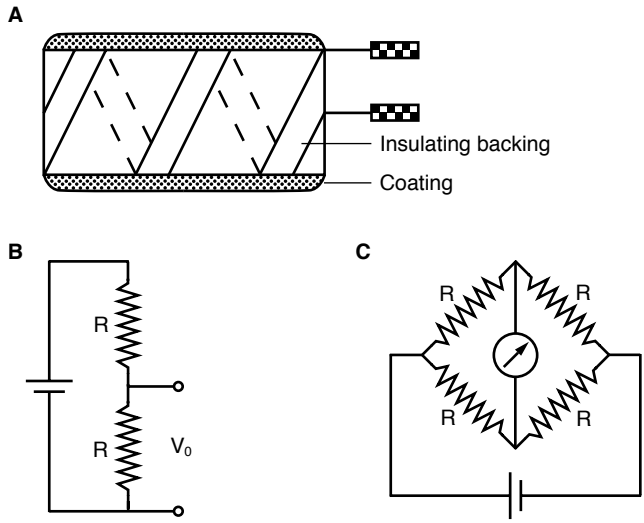

FIGURE 2.37
(A) Resistive humidity sensor. (B) Potentiometric circuit. (C) Bridge circuit.

of a coil can be changed by changing the following parameters by the displacement to be measured:

1. Number of turns of the coil
2. Length of the coil
3. Permeability of the core of the coil

2.4.2.1 Variable Inductance Type

The inductance of a coil of two different forms (as shown in fig. 2.38) can be changed by changing the number of turns.

2.4.2.1.1 Change in Permeability

A coil is wound over a ferromagnetic former into which an iron core can be inserted using a nonmagnetic handle (fig. 2.39). When the iron core is displaced inside the former, the total permeability of the magnetic circuit

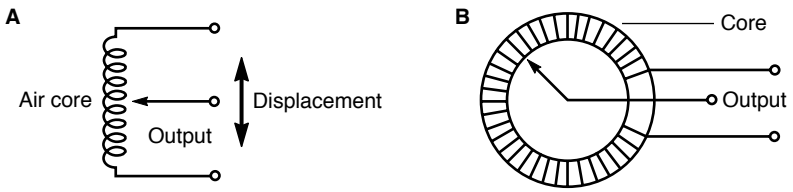

FIGURE 2.38
(A) Translational transducer. (B) Rotational transducer.

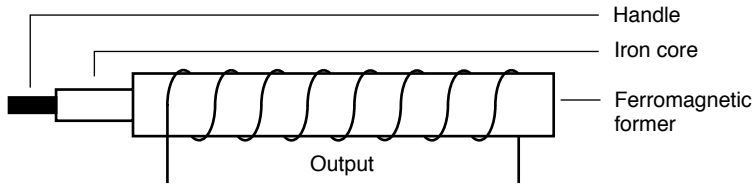

FIGURE 2.39
Variable permeability type sensor.

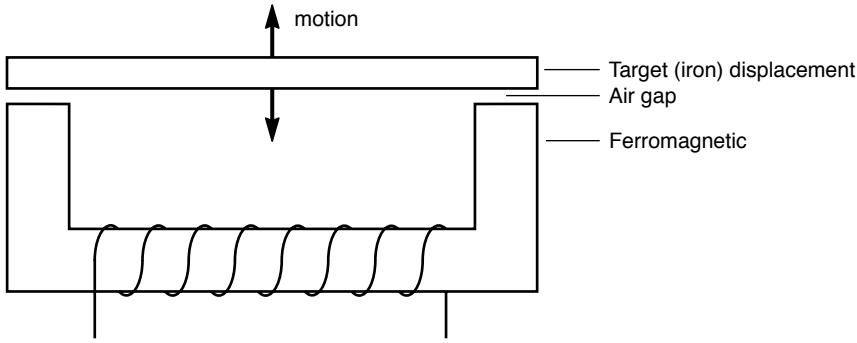

FIGURE 2.40
Variable reluctance type sensor.

increases and when the core is taken out the permeability decreases proportionately. Hence, the self-inductance of the coil changes with the displacement of the core.

2.4.2.2 Variable Reluctance Type Sensors

The reluctance of a magnetic circuit can be varied with displacement of a target with respect to a ferromagnetic core, as shown in figure 2.40.

The self-inductance of the coil is given by

$$L = N^2 / (R_i + R_g) \tag{2.36}$$

where N = number of turns
R_i = reluctance of iron path of the coil
R_g = reluctance of air gap

Practically the reluctance of the iron path can be neglected compared to the air gap; therefore

$$L = N^2 / R_g \tag{2.37}$$

The reluctance of the air gap is given by

$$R_g = l_g / \mu_0 A_g \tag{2.38}$$

where l_g = length of the air gap
μ_0 = absolute permeability
and A_g = area of flux path through air

Because permeability and area of flux path are constants, R_g is proportional to length of the air gap (l_g) and self-inductance (L) is inversely proportional to the length of the air gap. Therefore, as the target approaches the ferromagnetic coil, the air gap decreases and the self-inductance increases proportionately.

2.4.2.2.1 Voltage Generating Type

These are electromagnetic transducers designed to develop alternating voltage proportional to velocity or displacement of some moving object. One arrangement of this transducer is shown in figure 2.41.

2.4.2.2.2 Differential Voltage Transducer

A differential transducer works on the principle of a variable reluctance transducer. It consists of a coil having three windings—one primary and two identical secondary windings—as shown in figure 2.42. The two secondary windings are spaced symmetrically with respect to the primary coil. The coils are wound over a nonmagnetic former. A ferromagnetic core made of cast iron is inserted into the coil former with the help of a nonmagnetic handle. When the core is placed at the central location of the coil, the mutual inductances M_1 and M_2 between the primary and secondary windings (Sy_1 and Sy_2) become equal. M_1 and M_2 vary linearly as the core moves inside the coil; that is, M_1 decreases and M_2 increases when the core moves toward the right and similarly M_2 decreases and M_1 increases when the core moves toward the left.

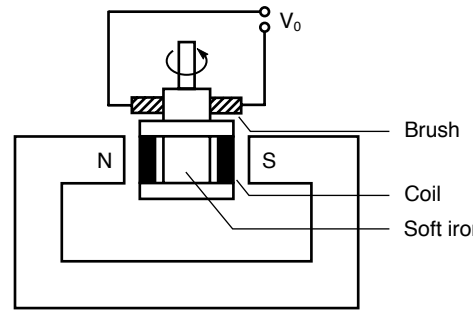

FIGURE 2.41
Electrodynamic transducer.

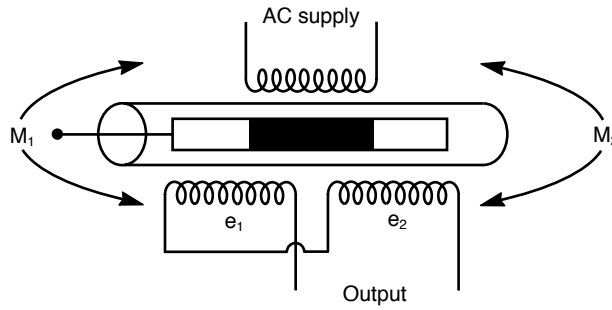

FIGURE 2.42
Transformer circuit of LVDT.

When the primary is supplied with an AC voltage (50 Hz–20 KHz), AC voltages are induced in the two secondary windings given by the equation

$$e_1 = M_1 \frac{di}{dt} \text{ and } e_2 = M_2 \frac{di}{dt} \tag{2.39}$$

where i is the current in the primary winding.
When the core moves toward the right, $e_2 > e_1$
and when the core moves toward the left, $e_1 > e_2$.

Because the two secondary windings are connected in phase opposition, the output voltage e_0 is given by

$$|e_0| = |e_1 - e_2| \tag{2.40}$$

Hence, the output voltage is a modulated AC voltage with the same frequency as that of the supply voltage, which has a magnitude proportional to the displacement of the core. By measuring the magnitude of the output AC voltage, the displacement can be measured.

The advantages of differential transducer are the following:

1. High sensitivity and accuracy
2. Output is not effected by temperature variation
3. Effect of variation in supply voltage and frequency is less
4. Resolution is high
5. Due to absence of sliding contact, less force is required for operation
6. Low hysteresis and good repeatability
7. Low power consumption on the order of 1 W

Disadvantages are as follows:

1. Not suitable for very small displacement
2. Highly immune to stray magnetic fields
3. Demodulator is required to get DC output

2.4.3 Capacitive Transducer

The capacitance of a capacitor in many cases can be a factor of measurement of some physical parameters like displacement, pressure, angular position, moisture content, and so on. A capacitive transducer works on the principle of variation of its capacitance by the physical variable. The capacitance C between two parallel plates of a capacitor is given by

$$C = \frac{K\varepsilon_0 A}{d} \tag{2.41}$$

where K = dielectric constant of the medium
A = area of the plates
d = distance between the plates
ε_0 = permittivity = 8.85 pF/m

Capacitance C between the two plates can be varied by varying the distance between the two plates or the area of the medium.

In figure 2.43A, plate B moves toward or away from the fixed plate A, thereby varying the gap between the two plates, whereas in the arrangement shown in figure 2.43B, the gap remains fixed, but the effective area between the two plates changes as plate B moves in an upward or downward direction as shown. In both cases, the capacitance changes proportionately to the motion. Hence, to the object whose displacement is to be measured, plate B can be attached to get the variation of the gap distance. Figure 2.43C shows an arrangement where the capacitance between fixed plate A and movable plate B varies due to the relative angular movement between them.

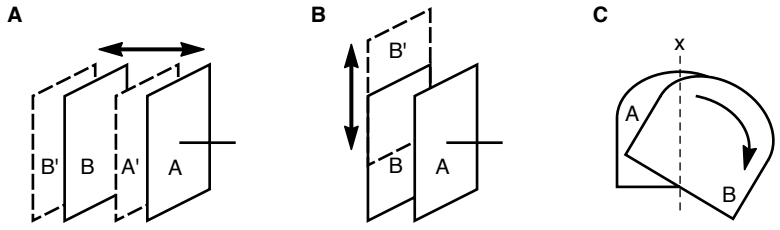

FIGURE 2.43
Capacitive transducer.

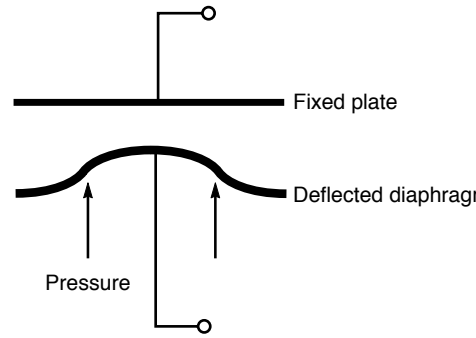

FIGURE 2.44
Capacitive pressure sensor.

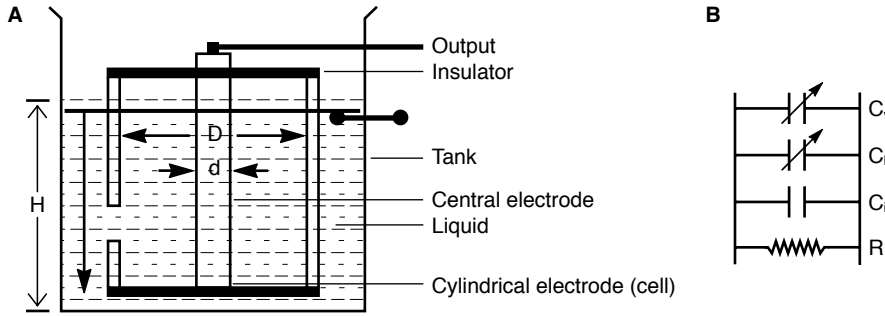

FIGURE 2.45
(A) Capacitive cell for level measurement. (B) Equivalent circuit.

Capacitive transducers can also be used for measurement of pressure using a diaphragm as shown in figure 2.44. A metal diaphragm is allowed to deflect due to application of pressure from one side. Maximum deflection is obtained at a central zone against which a circular fixed electrode is placed. The distance between the two electrodes changes due to the deflection caused by the pressure. The change in capacitance is a measure of the pressure applied.

Another important application of capacitive transducers is as a capacitive humidity sensor. In this type of transducer the gap between the two plates and their cross-sectional area is fixed, but the dielectric constant of the material kept inside the plates varies when it absorbs moisture from the air. The principle behind the function of this transducer is that when water particles are added to a material the dielectric constant of a material changes.

The principle of a cylindrical capacitance is used for measurement of level of liquids in a tank. Figure 2.45A shows the arrangement used for this level detection application.

A cylindrical capacitance cell is placed inside the tank filled with a liquid, the level of which has to be determined. A central electrode and the outer cylindrical cell form the capacitance. The liquid filling the space between the two electrodes serves as the dielectric medium. The capacitance of the cell is given by

$$C_l = \frac{\varepsilon_l h}{2 \ln D / d} \tag{2.42}$$

where ε_l = relative permittivity of the liquid
h = level of the liquid
d and D = radii of the two electrodes as shown in figure 2.45A.

Equation 2.42 shows that capacitance C_l is a linear function of liquid level h. In a practical case, the total capacitance is a parallel combination of capacitance of the liquid (C_l), capacitance of the liquid vapor (C_v), and capacitance of the insulator (C_i). However, C_v and C_i are very small compared to C_l, so these two values can be neglected. In addition to the capacitances, a leakage resistance R of several mega ohms is present between the two electrodes. The equivalent circuit is shown in figure 2.45B. The leakage resistance R can be minimized by using a very high frequency source in the measuring circuit. An AC bridge is generally used for measurement of the level of the liquid. The main drawbacks of this type of transducer are as follows:

1. The capacitance cell does not work if the liquid is conductive, such as citrus juice.
2. An error in capacitance persists due to the fact that the liquid sticks to the electrodes even if it falls down.

Problem 2.7

A capacitive cell is used in a food processing industry to detect the level of squash in a reservoir of height 5 m. The diameter of the central electrode is 1 cm and internal diameter of the cell is 10 cm. The permittivity of squash is 66.8 at a frequency of 200 MHz. Determine the sensitivity of the transducer in capacitance per unit level.

SOLUTION

Given

The diameter of the central electrode = d = 1 cm = 0.01 m
The diameter of the cell = D = 10 cm = 0.1 m
The permittivity of squash = $66.8 \times 8.85 \times 10^{-12}$
The capacitance per unit meter of length (i.e., for h = 1 m) from equation 2.42

$$C = \frac{66.8 \times 8.85 \times 10^{-12} \times 1}{2 \times \ln(0.1 / 0.01)}$$

$$= 128 \times 10^{-12} \text{F}$$

Hence, the sensitivity is 128 pF/m level.

2.5 Digital Transducers

With the advent of microprocessor and microcomputer applications in process instrumentation and control, digital transducers have become more popular than analog transducers. Digital transducers are more compatible with the microprocessor interface than the analog transducers. In a digital transducer, the output is obtained in discrete frequency or in a digitally coded form. The main advantages of digital transducers are as follows:

1. The output can be easily interfaced with a microprocessor or a digital transducer.
2. It becomes easier to display the physical parameter measured by a digital display module.
3. Because the signal obtained in pulse or frequency or digitally coded form does not depend on the amplitude of the signal, there is less noise or distortion during transmission.

Digital transducers have the following different forms:

1. Direct digital encoder
2. Pulse, frequency, or time encoder
3. Analog-to-digital encoder
4. Analog-to-digital conversion

2.5.1 Direct Digital Encoder

A direct digital encoding type is the only real digital transducer that produces a parallel binary coded output without any signal processing or data manipulation operation. Such a type of real digital transducer is rarely developed in practice. A digital shaft encoder is an example of this type of transducer. It basically measures angular position or displacement of a shaft and produces a binary number. This binary number can be comfortably interfaced with a computer without further processing. Figure 2.46A shows this type of transducer.

2.5.2 Frequency, Pulse Encoder

Many transducers produce a train of pulses with a frequency that is directly proportional to the amplitude of the physical parameter. This decoder comprises a transducer producing frequency or pulse signals and a counter to convert the pulse to a parallel digital output. An optical revolution counter,

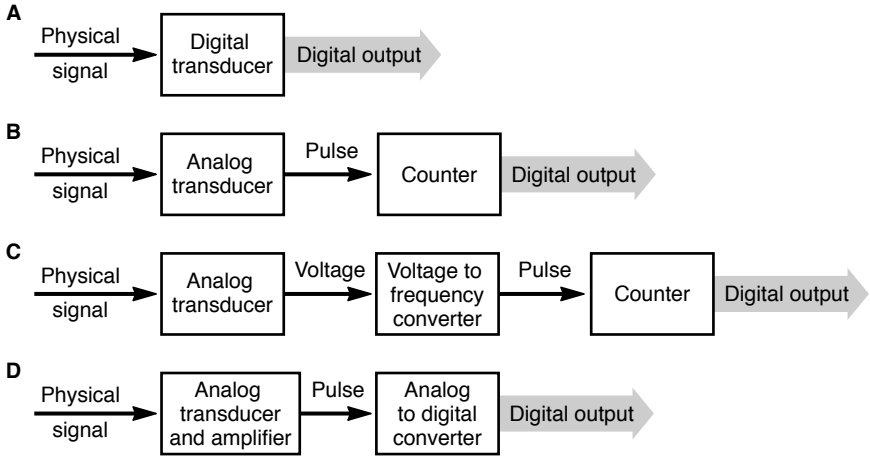

FIGURE 2.46
Block diagrams of digital transducers: (A) Direct digital encoder; (B) Frequency / pulse encoder; (C) Analog-to-digital encoder; (D) Analog-to-digital converter.

a magnetic flow meter, and a radioactive flow meter are examples of this kind of transducer. Because the frequency-dependent signal generated by this transducer cannot be directly fed to a computer, a direct digital signal in parallel binary format is indirectly formed from the pulse signal. This transducer is shown in figure 2.46B.

2.5.3 Analog-to-Digital Encoder

In this type (fig. 2.46C), a digital output is derived in proportion to a physical parameter by connecting an analog transducer, a voltage-to-frequency converter, and a digital counter in tandem. The amplitude-dependent electrical signal obtained from the analog transducer is converted to a frequency-modulated signal (a train of pulses) by the voltage-to-frequency converter. A counter is used to convert the frequency-modulated signal to a parallel binary number.

2.5.4 Analog-to-Digital Converter

In this technique, the output of an analog transducer is converted to a digital code by analog signal processing and analog-to-digital conversion as shown in figure 2.46D. The analog signal processing circuit either amplifies the signal, filters the noise from the signal, or does both. The processed signal of the right amplitude is fed to the analog-to-digital converter to get a digital signal of binary format.

2.5.5 Digital Encoders

The digital encoder is the only digital transducer in the real sense of its structure. The other types of transducers discussed earlier are in some way manipulated digital transducers. A digital encoder directly converts the physical variable to a parallel digital output. The simplest example of a digital encoder is a digital shaft encoder for angular position measurement.

2.5.5.1 Digital Shaft Encoder

A digital shaft encoder (fig. 2.47) is a circular coded disk driven by a rotating shaft. The circular disk is divided into a certain number of sectors (N_s) and each sector is partitioned into a number of tracks (N_t). There is a relation between the number of sectors and tracks, as $N_s = 2^{Nt}$. For generating a 4-bit binary number from the encoder, the number of tracks should be 4, so the total number of sectors is 16. Because the total angular revolution of 360° is divided into 16 sectors, the encoder can encode a minimum of 22.5° angular displacement. Hence, the sensitivity and resolution of measurement can be increased by increasing the number of sectors, which is possible only by increasing the number of tracks. If the number of tracks is doubled (i.e., 8), the resolution becomes 1.4°, which is 16 times higher than using four tracks.

There are three methods of coding the tracks and thereby three encoding or reading methods:

1. Contact encoder
2. Magnetic encoder
3. Optical encoder

2.5.5.1.1 Contact Encoder

In a contact encoder disc, the tracks are inscribed by a conducting and a nonconducting layer. A conducting layer in a track results a binary 1, whereas

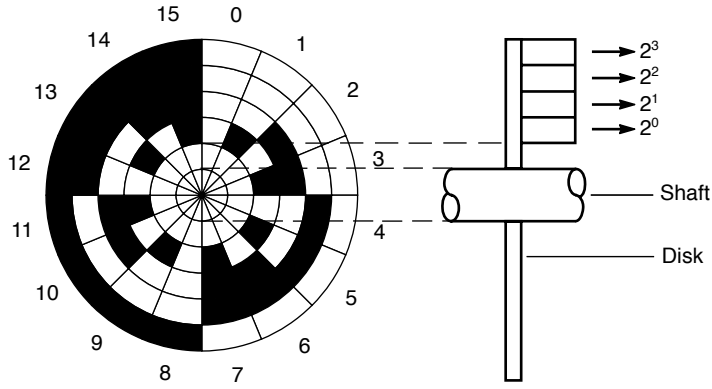

FIGURE 2.47
A digital shaft encoder.

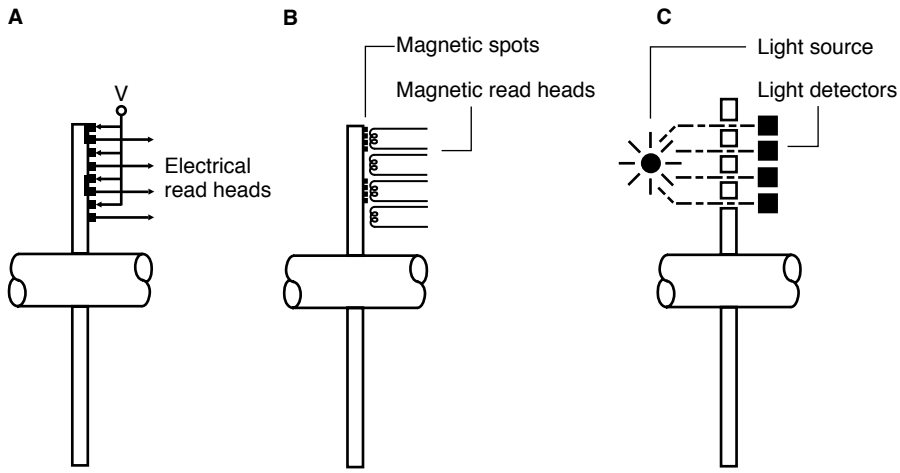

FIGURE 2.48
Digital encoders: (A) Contact encoder; (B) Magnetic encoder; (C) Optical encoder.

a nonconducting layer gives a 0 as the output of the reading head. Brushes are used as the reading heads that collect the electrical voltage or currents. Figure 2.48A shows the arrangement of the contact encoder.

2.5.5.1.2 Magnetic Encoder

In a magnetic encoder the tracks are coated with a magnetic material over which the pattern of digital codes is inscribed. The magnetic spots are either magnetized or nonmagnetized to represent a binary 1 or 0. A tiny pickup coil reads the magnetic spots. Life of the magnetic encoders is longer than that of the contact encoders. A magnetic encoder is shown in figure 2.48B.

2.5.5.1.3 Optical Encoder

An optical encoder (fig. 2.48C) uses a light source in front of an optically coded pattern, through which the light is allowed or restricted to pass through. The pattern is made transparent to code a binary 1 or opaque to code a 0. The light transmitted is picked up by an optical sensor and the electrical signal represents the binary equivalent of the position of the shaft.

2.6 Selection of Transducers

Numerous types of transducers are commercially available for common measurements such as temperature, pressure, flow, displacement, and so on. However, for very rare types of measurements such as compactness of a powdered sample, cracks and voids inside a structure, and others, available

transducers might be limited. For example, one has little choice of electrodes for pH but can choose the appropriate one from a wide variety of transducers for temperature measurement. The selection of the right transducer out of the available types depends on certain factors. The factors on which the selection of a transducer depends are as follows:

- Based on the performance of the transducer:
  1. Accuracy, sensitivity, resolution, linearity, hysteresis, time constant, repeatability, and so on
  2. Type of the output signal needed: analog or digital
  3. Simplicity of the signal processing circuit needed
  4. Mode of indication: local or remote
  5. Type of application: indication, recording, or controlling
  6. Signal-to-noise characteristics of the transducer
  7. Operating range or scale of operation
- Based on handling:
  1. Ruggedness of the transducer required for the application
  2. Ease of operation, like calibration, balancing, zero setting, and so on
  3. Suitability to environmental conditions
  4. Ease of fault detection and maintenance
  5. Safety for the application
  6. Suitability in shape, size, and weight
- Based on cost effectiveness:
  1. Initial cost including procurement and installation
  2. Running cost
  3. Expected working life

The number of transducers for common applications is large, so before selecting a transducer for measurement of a particular variable, these factors should be studied and the merits and demerits should be judiciously analyzed. A good judgment will lead to an optimal selection of the transducer. In selecting a transducer with equal merits for a given application, the simplest one with the fewest moving parts would normally be chosen.

2.7 Actuating and Controlling Devices

The function of an automatic controller is to compare the process output with the ideal or desired value and to generate a control signal that minimizes

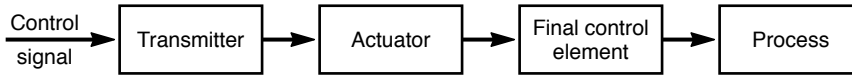

FIGURE 2.49
Block diagram of final control action.

the deviation or error to zero to the smallest possible value with the help of a control action. The process output variable is measured by a transducer or sensor and the measured signal is fed to the controller. The controller consists of an error detector to generate an error signal that is used to vary the input to the plant as per a control law. The controller converts the error signal to a control action (e.g., on–off action, proportional action, derivative action, integral action, etc.). The low-energy control signal is converted to the actual system input like pressure, flow, and so on. This is done by the final control element.

The function of the final control action is to convert the low-energy control signal to an appropriate level to operate the actual process input variables like angular velocity of the drive motor of a food extrusion process, feed rate of fermented tea in a tea dryer, and so on. The signal transmitter is practically a control room device that converts the control signal to an appropriate electrical, mechanical, or pneumatic signal. This conversion depends on the type of actuator used in the next stage to conversion. For example if a solenoid operating at 10 A (full open) is to be actuated to open a valve, the signal conversion to be performed is a voltage-to-current conversion; if a DC motor is to run at 110 V (full speed) to drive a conveyor, the signal conversion would be a power amplification. However, solid state devices like silicon controlled rectifiers (SCRs) and triacs for motor and heater control can be operated with a low energy level signal. The sequence of operation of a final control element is shown in figure 2.49. The actuator is an integral part of a final control action. The actuator finally manipulates the input to the plant and stimulates the final control element. For example, in a conveyor feeder system the conveyor is the final control element and the motor that drives the conveyor is the actuator. Similarly, in a temperature on–off control system, the heater is the final control element and the relay is the actuator. Although the final control element is a part of the plant or process, it is specially designed to fit into the control loop when used for an automatic control system.

2.7.1 Actuators

An actuator is a kind of transducer, in a sense, that converts an electrical control signal to a mechanical form to give a physical effect or action to actuate the final control element. In some cases, an actuator converts a physical signal to give a pneumatic or hydraulic effect, as in pneumatic and hydraulic actuators. Actuators are designed and manufactured with a variety of ratings. Hence, it is important to select the right type of actuator for a

specific application. The following points should be kept in mind to make the actuator selection simpler:

1. Type of power source (electrical, pneumatic, or hydraulic)
2. Reliability required
3. Mechanical power (torque or thrust) required
4. Control functions (on–off, PID, etc.)
5. Cost

The following types of actuators are considered for discussion here:

1. Electrical solenoids
2. Electrical motors
3. Fluid control valves

2.7.1.1 Electrical Solenoids

These work on the simple principle of magnetodynamics. Electrical solenoids consist of a coil and a plunger, where the plunger can be freestanding or spring loaded. The electrical voltage or current signal applied to the coil generates a mechanical motion (usually rectilinear) to make a valve open or close. Solenoids are generally specified by voltage or current ratings and force required to move the plunger. In some applications the duty cycle of the plunger motion (percentage of motion time to total time) is also specified. This rating is important for considering plunger thermal constraints.

2.7.1.2 Electrical Motors

In process industries the control inputs of various categories like conveyor feed rate of raw materials, dosing of ingredients, hot air feeding using blowers, stirring, and mixing are performed by mechanical devices run by electric motors. Sizes and types of such motors depend on the speed and torque required by the process operation. Moreover all motors cannot be controlled with the same precision; therefore the motor employed depends on the control precision.

2.7.1.3 Fluid Control Valves

A schematic cross-sectional view of a control valve is shown in figure 2.50. The fluid control valve accepts a signal from the controller, through the actuator, and adjusts the process fluid to maintain process parameters such as pressure, flow, temperature, level, and composition at a desired level. Control valves are specially designed to meet the needs and characteristics of the process fluid. Control valves are mainly of two types: sliding stem valves with globe or angle configuration and rotary valves with ball and butterfly configuration.

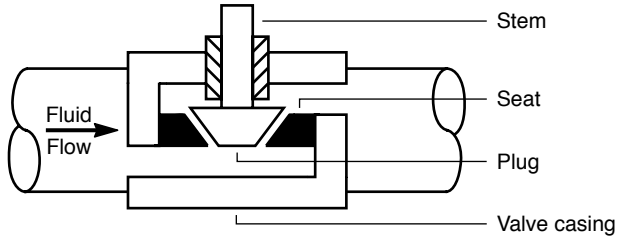

FIGURE 2.50
Cross-section of a control valve.

The basic mechanism of a control valve is the change in fluid aperture to change flow rate.

This is given by the equation

$$Q = Av \tag{2.43}$$

where Q = flow rate of the fluid (m^3/sec)
A = cross-sectional area of the fluid aperture (m^2)
v = velocity of the fluid flow (m/sec)

When the valve opening is varied in a control valve the flow rate is changed due to the restriction imposed by the valve on the pipe. This restriction causes a pressure drop across the valve given by the equation

$$Q = K\sqrt{\Delta P} \tag{2.44}$$

where K = valve constant ($m^3/sec/Pa^{1/2}$)
ΔP = pressure drop across the valve (Pa)

2.7.1.3.1 Sliding Stem Valves

The most common of the control valves are the sliding stem type. Sliding stem valves are designed with different materials, sizes of end connections, and control characteristics. Their guiding designs are cage guided, post guided, and stem guided, and connections are flanged, screwed, or welded ends. Materials used to make these valves include cast iron, carbon steel, stainless steel, and other high-performance materials. Sliding stem valves can be used in rugged field conditions such as under high fluid pressure, vibration, and high temperature variations. Theses valves are manufactured in pipe sizes ranging from 15 to 500 mm.

2.7.1.3.2 Butterfly Valve

The subclasses of butterfly valves are swing-through, lined, and high performance. The swing-through design is the most common and versatile. A

butterfly valve is used for throttling applications requiring shutoff tighter than 1% of full flow. They are manufactured in sizes of 50 mm to 2,500 mm. End connections of butterfly valves are flangeless, lugged, or welded.

Lined or high-performance butterfly valves are used to reduce leakage. In a lined butterfly valve, an elastomer or polytetrafluoroethylene (PTFF) lining gives a contact to the disk, ensuring tight shutoff. High-performance butterfly valves are provided with heavy shafts and disks, full pressure rating bodies, and good quality seals. These valves are manufactured in sizes from 50 mm to –1,800 mm.

2.7.1.3.3 Valve Selection

Although various valve manufacturers claim that their products are suitable for particular applications, selection depends on various factors. The following factors are guidelines for selecting an appropriate valve:

1. Pressure rating and limits
2. Pipe size and flow capacity
3. Flow characteristics and range
4. Temperature limit
5. Shutoff leakage
6. Pressure drop
7. End connection type
8. Material of body
9. Life cycle cost
10. Actuation type

2.7.2 Actuating Motors

Three basic types of motors generally used as actuators—DC motors, control motors, and stepper motors—are discussed in this section.

2.7.2.1 DC Motors

There are many control applications for which DC motors offer many distinct technical and economic advantages due to their versatility in wide ratings. DC motors are more useful where large and precisely controlled torque is required. Speed of DC motors can be exercised with a high degree of precision. Small DC motors can be designed with high-energy permanent magnets, encapsulated epoxy resin windings, and electronic commutation to make it more reliable than AC motors.

The working principle of DC motors is conversion of electrical energy to a rotational mechanical energy with the help of cylindrical armature or rotor between a pair of magnetic poles. The magnetic poles produce the magnetic flux that links with the armature coil for electromechanical energy conversion.

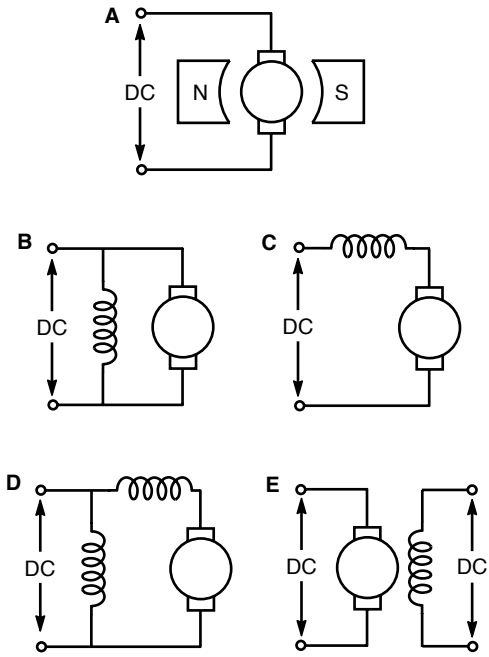

FIGURE 2.51
DC motor configurations. (A) PM; (B) Shunt; (C) Series; (D) Compound; (E) Separately excited.

The armature windings are also accommodated in the slots provided in the armature core. The DC voltage is applied to the rotor through carbon brushes. The magnetic flux is produced in two ways, using permanent magnets and by field coils. In the first type a strong permanent magnet is used to generate the magnetic flux, so the motor is called a permanent magnet DC motor. In the second method, an electromagnet is formed by connecting the field coil in parallel or in series to the armature winding, so the motor is called a shunt field motor or a series field motor, respectively. In DC compound motors both shunt and series field are used. Figure 2.51 shows the various configurations of DC motors.

Different configurations of DC motors with respect to method of excitation give rise to different electromechanical characteristics. A shunt field motor gives a smaller starting torque, whereas a series motor provides a large starting torque. Speed control is more convenient in shunt motors than in series motors. Thus for starting heavy loads and where precise and proportional speed control is not required (e.g., driving of a loaded conveyor at fixed speed), this motor is suitable.

2.7.2.2 Control Motors

Control motors are one of the most important electromechanical control devices. Control motors are used in feedback control loops as positioning systems for precise positioning of an object like a valve, wedge, door, or robot limb. Servomotors and stepper motors are two basic types of control motors.

2.7.2.2.1 DC Servomotors

Although DC servomotors are basically same as DC motors in principle, servomotors are specially designed to work with servomechanism systems. DC servomotors differ from general DC motors as follows:

1. They are designed for low rotor inertia, so the torque-to-inertia ratio is very high.
2. They should have an extremely low time constant.
3. They have a relatively low power rating.

Servomotors are manufactured with medium and high power ratings, which are used in robotics, numerically controlled machines, and so on. In some applications DC servomotors are driven by an electrical controller called a servo-driver. The servo-driver adjusts the speed of the servomotor, such as in motion control drives where pulse width modulation is used for controlling speed. The DC servomotors are operated and controlled in two modes: armature-controlled mode and field-controlled mode.

2.7.2.2.2 Armature-Controlled Mode

The speed or angular displacement of the motor is controlled by varying the armature voltage while the field is separately excited and is held constant. However, in the field-controlled method, the motor is controlled by the separately excited field current and the armature voltage is held constant. Because armature-controlled mode is more popular, only this method is discussed here. Figure 2.52 illustrates an armature-controlled DC servomotor.

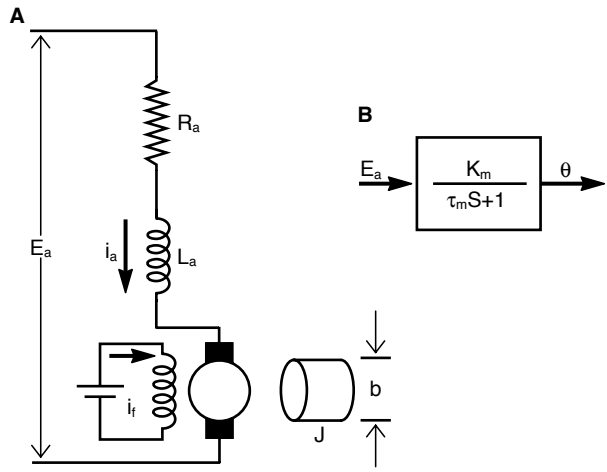

FIGURE 2.52
(A) Circuit diagram of the armature-controlled DC motor. (B) Block diagram of the control system.

The transfer function relating the output angular velocity $\dot{\theta}(s)$ and output control voltage $E_a(s)$ is given by

$$\frac{\dot{\theta}(s)}{E_a(s)} = \frac{K_m}{s(1+s\tau_m)} \tag{2.45}$$

where $K_m = K/(R_a b + KK_b)$ = motor gain constant
$\tau_m = L_a J/(R_a b + KK_b)$ = motor time constant

In this system

R_a = armature resistance (ohm)
L_a = armature inductance (H)
E_a = applied armature voltage (V)
θ = angular displacement of motor shaft (rad)
J = equivalent moment of inertia of the motor (Kg-m^2)
b = equivalent viscous friction coefficient of the motor (N-m/rad/sec)
K = motor torque constant (Kg-m/A)
K_b = back EMF constant (V/rad/sec)

The transfer function indicates that the DC servomotor is a first-order system. The time constant can be made small by using low values of J and R_a. The gain can be increased by using a high torque constant and a smaller back EMF constant, lower values of R_a and b. Typical ratings of commercially available servomotors are as follows:

- Full scale input voltage: 1.5 V to 24 V
- Impedance: 2.8 ohms to 700 ohms
- Time constant: 0.01 sec
- Full scale speed: 1000 RPM to 2000 RPM
- Starting voltage: 4.2 mV to 79 mV
- Load capacity: 1.8 to 12.4 gm-cm at full voltage

2.7.2.2.3 Two-Phase Servomotor

A two-phase servomotor is similar to a two-phase induction motor, with the difference that a servomotor is designed with small diameter-to-length ratio to minimize the moment of inertia. This gives a good accelerating characteristic. Moreover, the power rating of a two-phase servomotor ranges from a fraction of a watt to a few hundred watts. A schematic diagram of a two-phase servomotor is shown in figure 2.53. The fixed phase of the motor is supplied with a constant AC voltage and the control phase is supplied with the control voltage of the same frequency. The frequency of the voltages used is generally 50, 400, or 1,000 Hz. The control voltage (E_c) should be 90° phase

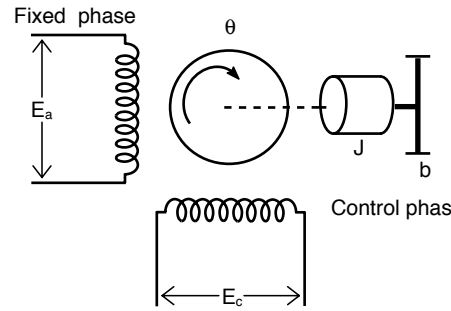

FIGURE 2.53
Schematic diagram of a two-phase servomotor.

shifted in time from the reference voltage to develop torque in the shaft of the rotor. The transfer function of the servomotor is given by

$$\frac{\dot{\theta}(s)}{E_c(s)} = \frac{K_m}{s(1+s\tau_m)} \tag{2.46}$$

where K_m = motor gain constant
τ_m = motor time constant

Parameters such as position, velocity, speed, and acceleration are all motion-related variables and their control is important in transportation of materials by conveyer systems in food industries. In high-speed bottling plants, servomotors can perform orientation of the empty bottles, positioning them on the rails, and feeding them to the fill station. In these motion control applications, servomotors serve as the control components.

2.7.2.3 Stepper Motors

In many robotic and semirobotic industrial automation applications, stepper motors are used due to their special advantages. The main advantage of the stepper motors is that they can be interfaced easily with digital devices. Other advantages include low cost, robustness, simple construction, low maintenance, wide applications, high reliability, and robustness to adverse environmental conditions. Moreover, they provide excellent torque at low speed, which is not obtained in other DC motors. Three main types of stepper motors are permanent magnet type, variable reluctance type, and hybrid type. The hybrid type is the most popular type.

2.7.2.3.1 Permanent Magnet Motors

These stepper motors are used in nonindustrial applications like computer printers, disk drives, and so on. The cost of permanent magnet stepper motors is low but they operate at low speed and low torque. These motors are operated at relatively large step angles for which precise positioning becomes difficult.

2.7.2.3.2 Variable Reluctance Motors

In this type of stepper motor the torque output is small, so it is used for small torque applications like micropositioning tables. Due to their low torque output for a given size, they are not used for industrial applications. Because these motors are not sensitive to current polarity as are permanent magnet stepper motors, they require a different driver circuit compared to other types.

2.7.2.3.3 Hybrid Stepper Motors

A hybrid stepper motor consists of a slotted stator with two or more individual coils. The input digital signals are applied to these stator coils. The rotor does not carry any winding and a magnet is attached to the rotor as shown in figure 2.54. Figure 2.54 shows a four-pole stator and a five-pole rotor structure. The rotor pole pitch is defined as

$$\text{Rotor pole pitch} = 360° / \text{number of rotor poles}$$

The rotor pole pitch of the motor shown is 72°. Each rotor pole is magnetized at one end with N polarity and the poles at the other end are magnetized by S polarity. Moreover, the N-pole set of rotor poles is arranged to be displaced from the S-pole set by half of the pole pitch. When coil *AA'* is assumed to be energized to make pole at *A* an N and pole at *A'* an S, then rotor poles S_1, S_2, and S_5 correspond to N; S_3, and S_4 to S. Similarly N_1, N_2, and N_5 correspond to S; N_3 and N_4 to N.

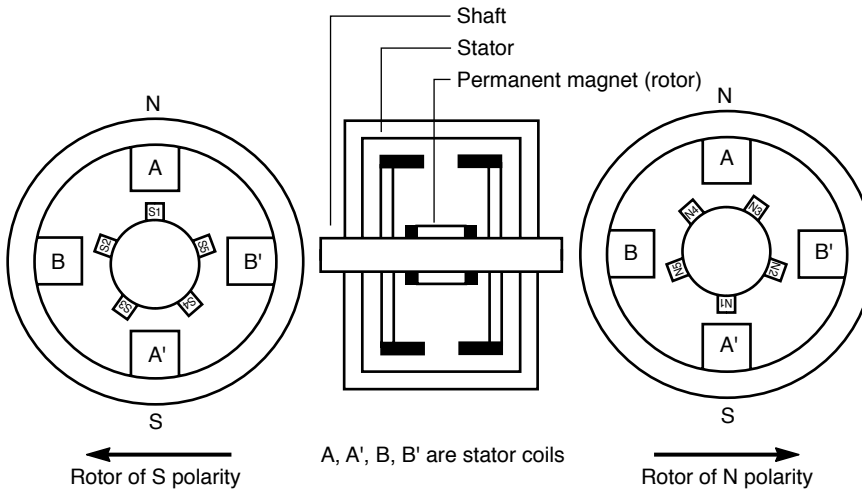

FIGURE 2.54
Cross-sectional view of a hybrid type of stepper motor.

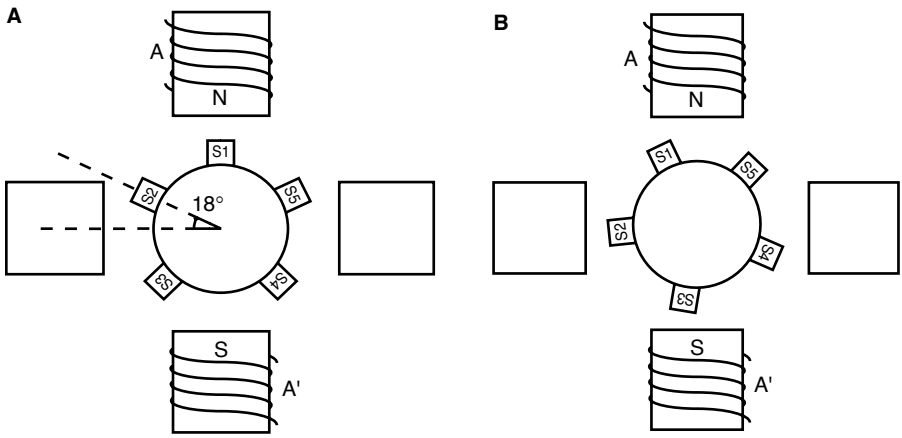

FIGURE 2.55
Rotor positions: (A) initial position; (B) position after one step movement.

2.7.2.3.4 Method of Operation

As shown in figure 2.55, let the starting position be with coil *AA*′ energized to carry a positive DC current so that the upper stator pole becomes N and the lower stator pole becomes S. In this state, coil *BB*′ is assumed to be not energized. The rotor remains in this orientation as long as the stator coil current remains unchanged. In this state S_1 is in alignment with the N poles of the stator. Therefore, the torque produced is zero (as $\sin \theta = 0$ at $\theta = 0°$). The torque developed

between S_5 and N (force of attraction in counterclockwise):

$$\text{Torque} \propto (-\sin 72°)$$

between S_2 and N (force of attraction in clockwise):

$$\text{Torque} \propto (\sin 72°)$$

A similar result is obtained for stator S pole and rotor N poles. The rotor is pulled by equal torques in opposite directions for which the rotor remains in standstill position. On the other hand, torque values between stator S pole and rotor S poles S_3 and S_4 are

between S_4 and S (force of repulsion in clockwise):

$$\text{Torque} \propto (\cos 36°)$$

between S_5 and S (force of repulsion in counterclockwise):

$$\text{Torque} \propto (-\cos 36°)$$

Position 2: Let Coil *AA*′ be de-energized and coil *BB*′ be energized by a positive current. This will cause pole at *B* to be N and pole at *B*′ to be S. The

net rotor displacement for this change in coil excitation is 18°. The orientation of the rotor poles becomes such that it is identical to the starting orientation and so the rotor is again in equilibrium and standstill position. The torque developed when there is a change of stator coil energization from *AA′* to *BB′* is

$$\begin{aligned} T &= T_m\,(\sin(S2 - N) + \sin(S1 - N) - \sin(S3 - N) + \cos(S5 - S) - \cos(S4 - S)) \\ &= T_m\,(\sin 18° + \sin 90° - \sin 54° + \cos 18° - \cos 54°) \\ &= 0.863\ T_m \end{aligned}$$

Because this is a positive torque, the shaft rotates in counterclockwise direction and reaches the equilibrium position.

Position 3: Let us consider that coil *BB′* is de-energized and coil *AA′* is energized by a negative DC current. In a similar way the torque developed can be obtained by

$$\begin{aligned} T &= T_m\,(\sin 18° + \sin 90° - \sin 54° - \cos 54° + \cos 18°) \\ &= 0.00 \end{aligned}$$

Because the torque is zero it brings the rotor to equilibrium position. The complete sequence for operating the stepper motor in counterclockwise direction by steps of 18° is shown in table 2.3. In this example the angle completed in one sequence is 72°, which is known as pole pitch. A two-coil stator with two states needs four switching operations to complete a switching cycle. The angle 18° is known as full step size, which is given by

$$\text{Full step size} = \text{Rotor pole pitch}/N$$

where N is the number of stator poles.

The direction of rotation can be reversed by reversing the switching sequence.

TABLE 2.3

Stator Coil Current Sequence for Full Step Size Rotation

Sequence	Coil AA′	Coil BB′	Cumulative Rotor Displacement
1	ON (+)	OFF	0°
2	OFF	ON (+)	18°
3	ON (–)	OFF	36°
4	OFF	ON (–)	54°
5	ON (+)	OFF	72°

2.7.2.3.5 Half Stepping Operation

The previous analysis was based on the assumption that only one stator coil was energized at a time. This operation is called half stepping. The result will be different if both the stator coils are energized at a certain periods in

TABLE 2.4
Stator Coil Current Sequence for Half Step Size Rotation

Sequence	Coil AA′	Coil BB′	Cumulative Rotor Displacement
1	ON (+)	OFF	9°
2	ON (+)	ON (+)	18°
3	OFF	ON (+)	27°
4	ON (–)	ON (+)	36°
5	ON (–)	OFF	45°
6	ON (–)	ON (–)	54°
7	OFF	ON (–)	63°
8	ON (+)	ON (–)	72°

a cycle. Table 2.4 shows the complete sequence for half stepping operation. Half stepping operation provides more precise control of rotation of the stepper motor. High-resolution stepper motors provide microstepping up to 500 microsteps, giving 100,000 steps per revolution. In a standard 200 steps hybrid motor, the rotor has two sections with 50 teeth on each section.

2.7.2.3.6 Stepper Motor Driver

A digital signal cannot drive the stepper motor directly. Stepper motors are designed with a specified current rating so that the required torque can be developed. Generation of pulses of appropriate current rating is done with the help of a driver circuit. The driver circuit for a four-phase stepper motor is shown in figure 2.56.

2.7.3 Final Control Elements

It has already been mentioned that the final control element is part and parcel of a process plant. A complex process can be composed of many subsystems of control loops where output variables are locally controlled by varying the control inputs. In such cases the individual subsystems also contain a final control element. A control element can be developed in the form of mechanical, electrical, or pneumatic/hydraulic. Some application examples of these types are discussed here and are further discussed in chapter 4.

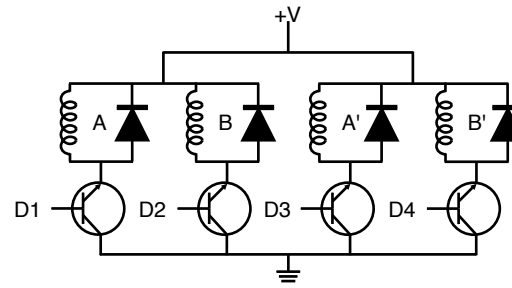

FIGURE 2.56
A basic driver circuit for a four-phase stepper motor.

2.7.3.1 Mechanical Types

When a process needs a mechanical system to be operated by a control element, it becomes a mechanical final control element. Examples from food processing include tea withering fans, dust blowers, grain hopper valves, dozing pumps, and so on.

To understand the function of a mechanical final control element, let us consider a fan reversal control operation in a tea withering system, as shown in figure 2.57. In tea withering, green tea leaves are spread over a wire-netted platform and trough. A fan driven by induction motor pushes air from below the platform to dry the tea leaves. The moisture released from the tea leaves accumulates over the withering troughs, saturating the air with moisture. This disrupts the process of moisture release from the green tea leaves. To avoid this problem, a reversing controller reverses the fan at a regular interval to suck the saturated air surrounding the troughs out and let fresh air move there. If we consider this problem as a closed-loop control system, we can define the moisture releasing operation as the process, air flow rate (both directions) as the input, and moisture content of the air (humidity) as the output. On the other hand, the motor reversing system is the controller, the motor is the actuator, and the withering trough or tunnel is the final control element.

A similar control operation in tea withering is the withering percentage controller (fig. 2.58). Withering percentage is defined as the reduction of moisture level of the green tea leaves as a percentage of the initial moisture content. There is a target set to this value and as soon as this value is achieved the withering fan is stopped. If we consider this as a closed-loop control operation we can define, similar to the fan reversal problem, the parameters, with air flow rate as the input and the withering percentage as the output; and the control components, the fan as the actuator and the withering trough as the final control element. These two control problems are discussed in chapter 4 with more emphasis on control aspects.

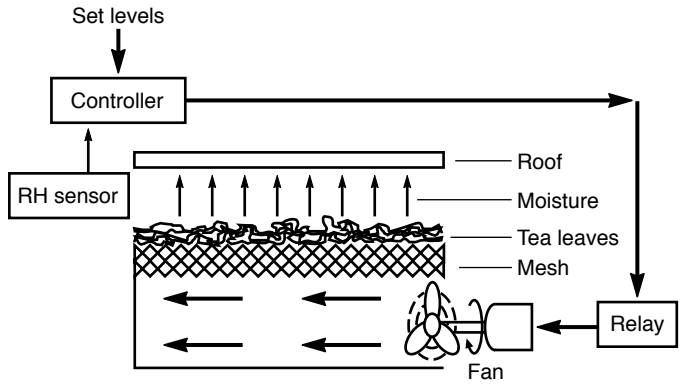

FIGURE 2.57
Schematic diagram of fan direction control in tea withering.

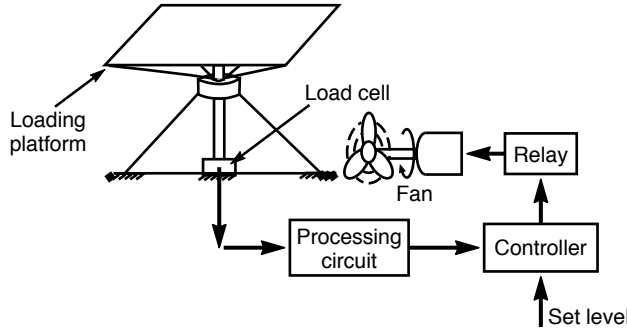

FIGURE 2.58
Schematic diagram of withering percentage control in tea industry.

2.7.3.2 Electrical Types

Electrical heating systems are good examples of electrical final control elements in an industrial environment. In an electrical heater or oven the heat is generated electrically and the supply voltage is responsible for the amount of heat developed. Any temperature variation in the heater or oven can be controlled by manipulating the supply voltage by on–off controller or continuous adjustment by PID controller. In a microwave oven, the heating can be controlled by controlling the output power of the magnetron. In food processing applications, there are many examples in which such electrical heating and control is used. Such examples include microwave tempering of frozen foods, vacuum drying of citrus juice and grains, pasteurization of food, bread baking, and roasting of nuts and coffee beans.

Another important example of electrical control is the motor speed control. Many food process parameters depend on the speed of the drive motor used for various functions such as conveyor feeding, metered feeding by pumps, food mixing and stirring, blowing hot air in dryers, food extrusion, and so on.

2.7.4 Pneumatic Control Devices

Pneumatic devices for sensing and controlling in industrial processes have been successfully used for almost a half-century. With the advent of electrical and electronic components, pneumatic devices were replaced by electrical and analog controllers. In recent times, in most industrial systems, pneumatic controllers have been replaced by electronic analog and digital controllers due to their advantages, such as miniaturization and computerization. In spite of this, pneumatic controllers are still functioning in many industries due to their most significant advantages: safety and reliability. Working principles of a few basic pneumatic devices are discussed here.

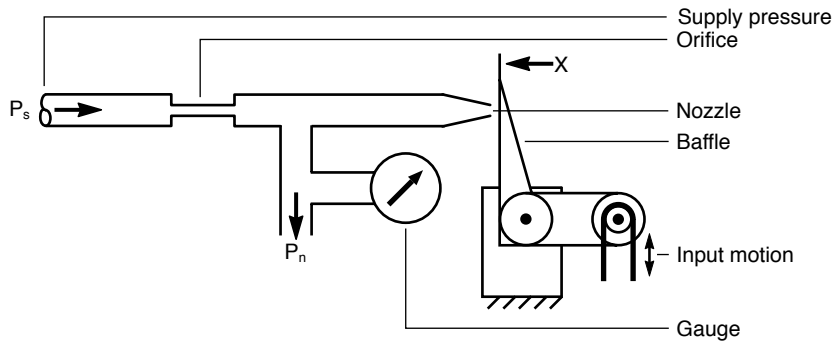

FIGURE 2.59
A baffle-nozzle detector.

2.7.4.1 Baffle-Nozzle Detector

This is a basic type of pneumatic detector that generates a pneumatic signal corresponding to a mechanical motion. Most pneumatic controllers use this detector as a primary sensing element. Figure 2.59 shows a nozzle actuated by a mechanical motion applied through a pivoted baffle. A constant air supply is applied to a fixed orifice that is connected to the nozzle that exhausts directly to atmospheric pressure. In a fixed condition of the baffle, the air from the supply line flows through the orifice and exhausts out from the nozzle through the gap between the nozzle and baffle (x). When the baffle moves closer to the nozzle the pressure in the line between orifice and nozzle pressure P_n rises and again falls when x increases. This back pressure P_n is the transmitted output signal proportional to motion. The highest value of P_n, when x is zero, is determined by air supply pressure P_s. The lower limit is determined by the ratio of resistance to air flow between orifice and nozzle when x is very large. Between these two extremes, various nozzle pressures are established. The linear operating range of 3 to 15 Psi is taken as the standard input and output limits. In most of the pneumatic instruments, supply air of 1.4 kg/cm^2 pressure is used. In the linear range, the ratio of output pressure and input motion is called *nozzle sensitivity* or gain, which is very high in this type of detector because a motion of 0.001 in. in the baffle causes a change in nozzle pressure greater than 8 Psi. The detector shows two other features:

1. It develops only a small reaction force equal to the product of nozzle pressure and nozzle throat area.
2. It uses only a small amount of air.

The force required to move the baffle is directly proportional to the line pressure and the cross-sectional area of the nozzle. For example, when the

nozzle diameter is 1.25 mm, nozzle pressure is P_n; but when nozzle diameter is 0.625 mm the nozzle pressure will be $P_n/4$.

Because the baffle is usually moved by a low-power signal, the force of the output signal is also low. To get a higher output force the nozzle diameter is reduced to the lowest possible value. If the nozzle diameter is reduced, the orifice diameter must also be reduced. For example, when the orifice diameter is 0.625 mm, nozzle diameter is 0.625 mm, and P_s is 1.4 kg/cm^2, then P_n (minimum) will be 0.7 kg/cm^2 with the nozzle wide open. With flapper movement, the maximum variation of pressure can be from 0.7 kg/cm^2 to 1.4 kg/cm^2. On the other hand, with a nozzle diameter of 0.625 mm and orifice diameter of 0.25 mm, P_n (minimum) will be 0.067 kg/cm^2 for an input pressure of 1.4 kg/cm^2. So the variation can be maintained from 0.067 kg/cm^2 to 1.4 kg/cm^2. However, when the orifice and nozzle sizes are reduced, the danger of plugging and subsequent instrument failure increases. Therefore, a limit on nozzle and orifice diameter is estimated as

$$0.5 \text{ mm} < \text{nozzle diameter } (D_n) < 10 \text{ mm}$$
$$\text{and } 0.33\, D_n < \text{orifice diameter } (D_o) < 0.5\, D_n$$

2.7.4.2 Pneumatic Amplifiers

The back pressure developed in a basic baffle-nozzle detector is used to drive some pneumatic control devices. Because the power rating of this signal is not sufficient to drive a control device, the signal strength is increased with the help of amplifiers.

Amplifiers or relays are biased so that no output response occurs until the input pressure has increased to a certain level above its minimum value. Thus the nozzle should operate at the linear operating range. Figure 2.60 shows a schematic diagram of a bleed type pneumatic amplifier. In the pneumatic amplifier the input pressure signal is applied to chamber D, where

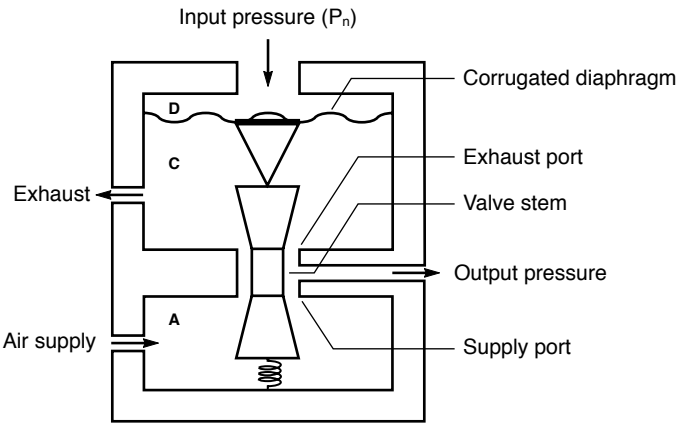

FIGURE 2.60
Bleed type relay pneumatic amplifier.

it exerts a downward force on a corrugated metal diaphragm so that it is flexed downward reducing the exhaust port gap and enlarging the supply port gap. This causes more air to flow from chamber A to output and then to chamber C. The diaphragm is adjusted so that when the supply port is fully closed and the exhaust port is fully opened the input pressure rises to a given value, typically 5 Psi. When no signal is acting or a signal below 5 Psi acts, air supply completely closes the supply port. When the input signal is 1.4 kg/cm^2 the exhaust port is completely closed and the whole air supply moves to output. Therefore, the amplified signal is of the same pressure as that of the control signal, but volume is amplified. This is a forward-acting amplifier because an increase in signal pressure increases the air volume. In a reverse-acting amplifier an increase in signal pressure decreases the air volume. In some designs the output pressure is also increased in addition to the increase in air volume.

2.7.4.2.1 Force Balance Transmitter

To translate a force, a position, or a motion into a corresponding air pressure a force balance transmitter is used. Figure 2.61 shows the schematic diagram of the force balance transmitter. The T beam is free to pivot at P_1. A force F_1 generated by the variable to be measured is applied at one end of the beam. The leg on the T beam carries a flapper in front of which a nozzle is placed. Air supply of 1.4 kg/cm^2 is applied to the nozzle line. An increase in F_1 will create an counterclockwise turning movement on the T beam and so the flapper moves closer to the nozzle. This will increase the back pressure P_n and the output signal is amplified by a pneumatic amplifier. The output pressure is then fed to the feedback bellow. An increase in output pressure will cause the bellow to expand and, thereby pushing one end of the L beam upward

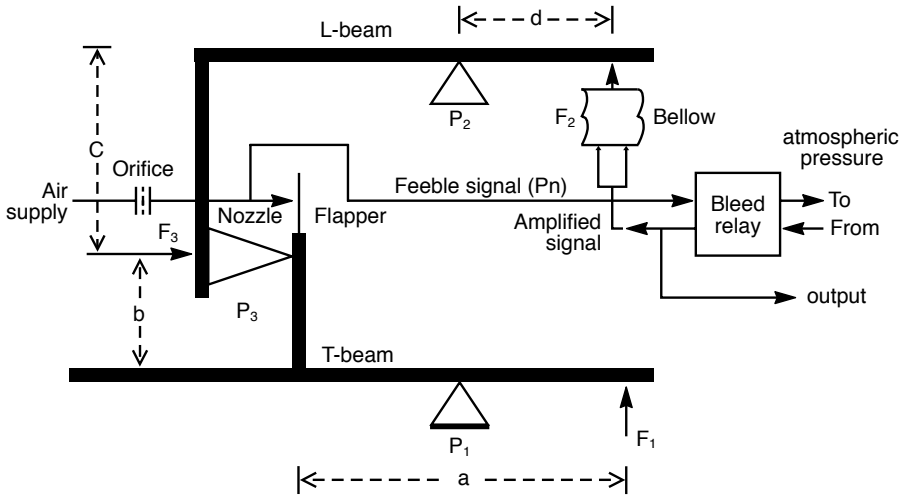

FIGURE 2.61
Force balance transmitter.

with a force F_2. The L beam is connected to the T beam through a movable point P_3 so a force F_3 will act on the T beam at P_3 due to a feedback force F_2.

Considering the moments of F_2 and the reaction force F_3 acting on the L beam at point P_2 and P_3

$$F_3 \times c = F_2 \times d \tag{2.47}$$

and

$$F_3 = \frac{F_2 \times d}{c}$$

Again F_3 causes a clockwise turning movement on the T beam around the pivot P_1 and the balanced condition shall be achieved when this will be equal to the moment created by the force F_1. Therefore the moment equation is

$$F_3 \times b = F_1 \times a \tag{2.48}$$

hence,

$$F_3 = \frac{F_1 \times a}{b}$$

From these two equations, we get

$$\frac{F_2 \times d}{c} = \frac{F_1 \times a}{b}$$

hence,

$$F_2 = F_1 \frac{ac}{bd} \tag{2.49}$$

Again $F_2 = P_0 \cdot A_{eff}$
where P_0 = output pressure
A_{eff} = effective cross-sectional area of the feedback bellow.

the factor $\frac{ac}{bd}$ = constant..

Therefore the output pressure is directly proportional to the force F_1 created by the measurable parameter; that is, a true measure of the input variable. The transmitter is calibrated with the absence of the forces on the beam when the nozzle-flapper gap is maintained to give an output of 0.2 kg/cm^2. This

can be done by adjusting the tension of a spring mounted in the flapper-nozzle assembly. The areas of the diaphragm and bellow and the length of the beams are related to each other in such a manner that the highest force of measurable range will develop an output of 1.0 kg/cm^2. Range of the instrument can be changed by varying the position of the movable pivot P_3.

2.8 Conclusion

Understanding the techniques of measurement and control in food processing mandates knowledge of basic principles of transducers, sensors, and control components. Most of the transducers were developed first to fit them to specific applications; however their working principles propagated rapidly to many other similar applications.

This chapter is intended to provide the reader with sufficient information on principles and easy-to-understand applications of various types of transducers. Actuating and control components were also discussed, but it was not possible to go into depth about control system engineering due to space limitations. With the information provided in this chapter one can hope to understand, design, and apply the concepts of transducers and controllers in food processing.

Further Reading

1. Doeblin, E. O. 1986. *Measurement systems, application and design.* New York: McGraw-Hill.
2. Patranabis, D. 1990. *Industrial instrumentation*. New York: McGraw-Hill.
3. Jones, E. B. 1976. *Instrument technology (Vol. II).* Butterworth & Co..
4. Johnson, C. D. 2000. *Process control instrumentation technology* (6th ed.). Upper Saddle River, NJ: Prentice-Hall International.
5. Toro, D. 1985. *Electric machines and power systems.* New Delhi: Prentice-Hall of India.
6. Anderson, N. A. 1998. *Instrumentation for process measurement and control.* Boca Raton, FL: CRC Press.
7. Barney, G. C. 1988. *Intelligent instrumentation: Microprocessor applications in measurement and control.* New Delhi: Prentice-Hall of India.
8. Liptak, B. G. (ed.). 1995. *Instrument engineers handbook: Process measurement and analysis.* London: Butterworth & Heinemann.
9. Ogata, K. 1982. *Modern control engineering.* New Delhi: Prentice-Hall of India.
10. Kuo, B. C. 1982. *Automatic control systems* (3rd ed.). New Delhi: Prentice-Hall of India.
11. Langton, M. A., and Say, M. G. (eds). 1985. *Electrical engineering reference book* (14th ed.). London: Butterworth & Co.
12. Van Valkenburg, M. E. 1988. *Linear circuits.* New Delhi: Prentice-Hall of India.

3

Measurements in Food Processing

CONTENTS

3.1 Introduction

Most food processing techniques are extensions of traditional kitchen preparation methods that employ scientific techniques, making enough surplus products to be sold outside the household. Current food processing technologies are gradual improvements of old techniques and equipment designs to improve quality and efficiency. As technology advanced, food processing technology also geared up to meet productivity, quality, safety, and economic requirements. To keep pace with quality requirements and government regulations, most food processing industries have a quality control or quality assurance department that monitors raw materials, manufacturing processes, and the finished products. Food quality testing personnel perform many standardized physical and chemical tests on food products, checking physical properties (sizes, weight, density, etc.), chemical properties (pH, vitamin content, fat content, etc.), sensory attributes (appearance, taste, flavor, texture, etc.), and legal requirements or public health considerations (presence of certain microorganisms, insecticides, metal particles, etc.). In objective testing (physical and chemical properties), instrumental methods are preferred, but objective testing of quality attributes like odor, taste, and so on are difficult to carry out by subjective methods. Present-day technology continues to develop and use various modern tools for both monitoring and control of the various food quality parameters. Electronics have long appeared among the tools of measurement and control of food processing, but computer technology became an important part of measurement and control only a few decades ago. The concept of computer-integrated manufacturing (CIM) evolved in the 1970s and has revolutionized this field of engineering. In this chapter, quality factors involved in food processing and their measuring techniques, monitoring systems, and control strategies form the basis of discussion.

3.2 Moisture Content Measurement

3.2.1 Role of Moisture Content in Quality of Food

When food items are processed, water is either mixed in or driven off by the process of drying. Most food items absorb moisture from the air during processing or preservation. Many common foods like potato chips, dry breakfast cereals, crackers, and others absorb water particles when exposed to a relatively humid environment. These foods are generally manufactured at high temperatures and their moisture content is lower. If these foods are exposed to humid conditions, they become moist and their quality deteriorates. When food gets moist, even if the quality is not affected, it might become soggy, rubbery, and unappetizing.

In manufacturing of powered foods like cocoa, milk, gelatins, and dehydrated concentrates, the food items are completely dried to avoid coagulation by tiny particles. If these food items are exposed to moisture, the tiny particles cluster together, causing a problem in free flowing during packaging.

When a food item is processed, the quality of the raw material is also an important factor and it should be monitored as a quality control measure. In general the moisture content of the raw material should not be too high for a good product as well as for economy such as in tomato ketchup, juices, lemons, oranges, mango, squash, jam, jelly, and so on. Table 3.1 shows the moisture content of some dehydrated fruits and table 3.2 shows final product moisture content of some food products. The moisture contents listed are considered the optimal values from a technical, practical, and commercial point of view for delivery to the market or for shipping and safety for the shelf life needed before buying or consumption by customers.

Moreover, the unwanted or free water in food helps the growth of microorganisms, which can cause food poisoning on consumption. Microorganisms like *Entamoeba histolytica* acquired by water particles, resident to the food, causes diarrhea and vomiting. To destroy these microorganisms, heat processing is adopted where the food is subjected to a higher temperature. On the other hand, during the heating process, some wanted water particles are driven off from food, which reduces the quality of the food to some extent.

TABLE 3.1

Ideal Moisture Content of Some Dehydrated Fruits

Fruit	Moisture Content (%)	Moisture Content After Dehydration (%)
Apple	86.5	20
Banana	78.1	15
Lemon	91.2	—
Mango	85.5	15
Pears	83.9	23

TABLE 3.2

Final Product Moisture Content of Some Food Products

Food	Moisture Content (%)
Butter	16
Cocoa bean	4
Coffee bean	12
Made tea	3–4
Fats and oil	0.5–1
Caramels and toffee	6–8

An estimation of the moisture content of the food items during and after processing becomes an essential part of food quality monitoring and control. Estimation of moisture content of the raw materials of the food products is also a routine quality procedure in many industries. Different food products are treated differently for estimation of moisture content. This depends on factors like size, shape, texture, amount of moisture, on-line or off-line requirement, requirement of precision, and so on.

3.2.1.1 Definition of Moisture Content

Moisture content is defined in several ways that are specific to a certain material and application. Moisture content is expressed either on a wet or dry basis. These two definitions of moisture content are

Moisture content (wet basis)

$$M_w = \frac{W_w - W_d}{W_w} \quad (g/g) \tag{3.1}$$

Moisture content (dry basis)

$$M_d = \frac{W_w - W_d}{W_d} \quad (g/g) \tag{3.2}$$

where W_w = weight of wet material (g)
W_d = weight of dry material (g)

Moisture content of unprocessed foods are generally expressed on a wet basis, but many food products after drying have their moisture content expressed on a dry basis only.

One of the most commonly used classical methods of moisture content measurement in food products is the dry and weigh technique. In this technique a representative sample of the food item is dried using a standard drying oven and weighed by a precise weighing balance. The difference in measure of weight gives the moisture contained in the material. In this method there is a standard and predetermined time of drying for a particular

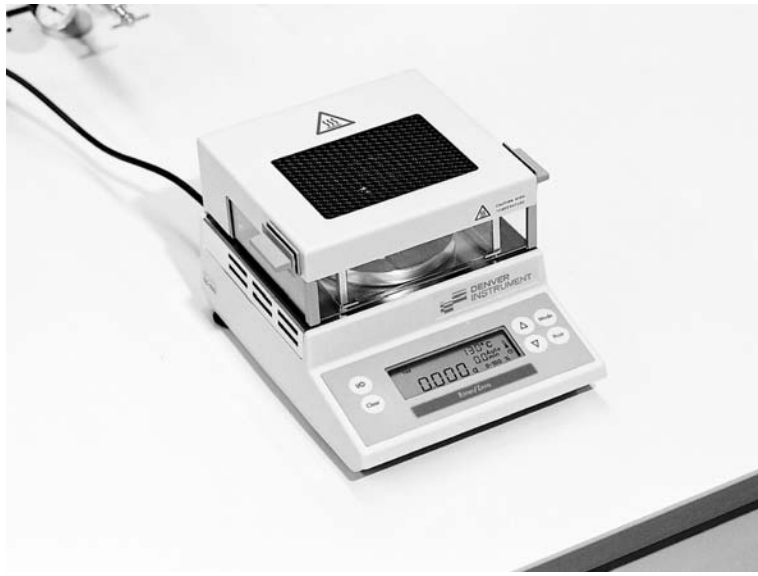

FIGURE 3.1
Infrared moisture meter, model IR-30. (Reprinted with permission from Denver Instruments, USA)

material, during which all moisture particles are driven off. Such a moisture meter (Model IR-30) manufactured by Denver Instruments (USA) is shown in figure 3.1. This instrument utilizes infrared heating and precision weighing for quick and accurate moisture determination. It measures moisture or solids content in a range of samples from powders to liquids.

Radio frequency (RF) impedance measurement and microwave permittivity techniques are most suitable for fruits and grains due to their nondestructive sensing behavior. Many food industries adopt these measuring techniques due to the nondestructive or noncontact procedure and higher accuracy achieved.

3.2.2 Microwave Absorption Method

In microwave absorption techniques, moisture content of fruits and vegetables can be measured in the microwave frequency band of 20.3 GHz to 22.3 GHz. The frequencies 2.45 GHz, 8.9 to 10.68 GHz, and 20.3 to 22.3 GHz are the three regions in which the technique can be utilized. When an electromagnetic wave of these frequencies passes through a material, water molecules greatly moderate the signal of the frequency range 20.3 to 22.3 GHz and water molecules produce molecular resonance. Hence, this frequency is most suitable for moisture content, particularly for free water determination. Figure 3.2 shows the schematic arrangement of the microwave absorption type moisture meter.

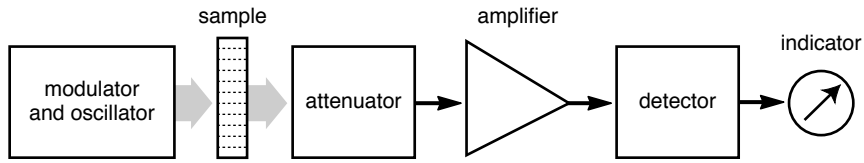

FIGURE 3.2
Block diagram of microwave moisture meter.

In this technique the complex relative permittivity of the material is utilized for measurement of moisture content. The complex relative permittivity of a food material can be represented as

$$\varepsilon = \varepsilon' - j\varepsilon'' \tag{3.3}$$

where the real part ε' is the dielectric constant and the imaginary part ε'' is the dielectric loss factor. This loss factor of a material depends on the moisture present in the material.

3.2.2.1 Loss Factor Measurement

Figure 3.3 shows a loss factor measuring scheme using the microwave technique. The permittivity measurement can be made by measurement on a free-ended semirigid Teflon insulated small coaxial copper conductor as the wave guide of the microwave energy. A wave guide 10 cm long consists of a 7-mm diameter air line that is connected directly to the reflection and transmission set. A 90° bend at 10 cm from the free end of the coaxial copper conductor is provided to facilitate contact with the surface of the sample.

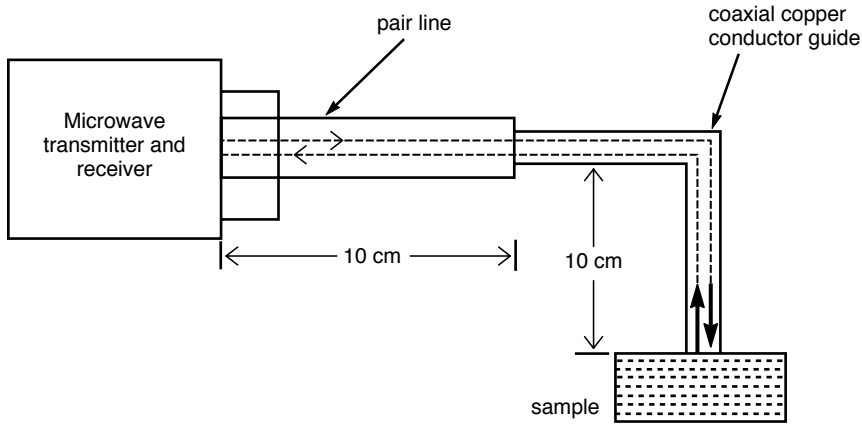

FIGURE 3.3
Setup for loss factor determination of a food sample.

The free end of the cable is cut and polished smoothly to avoid distortion perpendicular to the axis of the line.

The reflection coefficient of the wave guide at the dielectric interface at the tip of the probe is determined by the permittivity of the material in contact with the probe. This technique can be adopted for moisture content determination of fruits and vegetables. The technique provides a nondestructive moisture evaluation of fruits and vegetables that is desired in many food industries.

3.2.3 Radio Frequency (RF) Impedance Technique

The basic principle of the RF impedance technique is that when a radio signal of frequency below 10 MHz is passed through a food item containing water particles, the water molecules absorbs some of the RF energy, causing molecular motion. Figure 3.4 shows a block diagram of the RF absorption technique. This technique is suitable for comparatively dry materials like grains, cereals, corn, and so on. The RF technique of moisture measurement is based on the principle of measurement of the RF impedance of the sample under test. Best results are obtained when the measurement is performed with an individual sample like soybean, pea, gram, or corn. The equivalent circuit and phasor diagram of the measurement is shown in figure 3.5. The impedance model of the sample consists of a capacitance (C) and a parallel equivalent resistance (R). The susceptance of the sample is given by

$$B = \omega C \tag{3.4}$$

when the sample is excited by an alternating voltage of angular frequency ω. The admittance of the sample is

$$Y = G + jB \tag{3.5}$$

where G is the conductance. The phase angle θ and the loss factor angle δ are given by

$$\theta = \tan^{-1}[\omega CR] = \tan^{-1}[B / G] \tag{3.6}$$

and

$$\delta = \tan^{-1}[1 / \omega C R] = G / \omega C = G / B \tag{3.7}$$

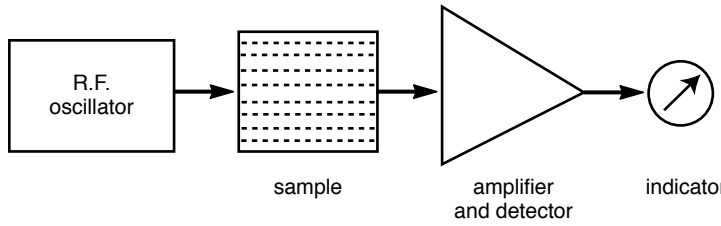

FIGURE 3.4
RF impedance technique.

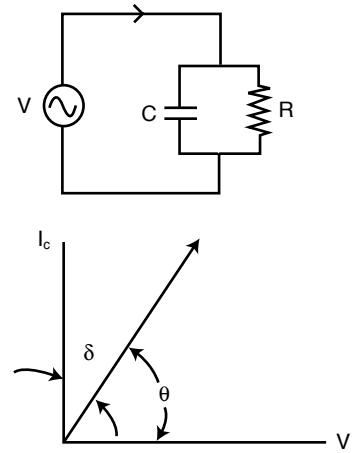

FIGURE 3.5
Equivalent circuit for RF moisture measurement.

The current through the sample has two components, a capacitive and a resistive component. The currents through the capacitor and the resistor are given by

$$I_c = Vj\omega C \tag{3.8}$$

and

$$I_R = V / R \tag{3.9}$$

so the total current through the resistor is

$$\begin{aligned} I &= V / Z \\ &= V(G + j\omega C) \end{aligned} \tag{3.10}$$

where V is the voltage applied and Z is the impedance of the sample.

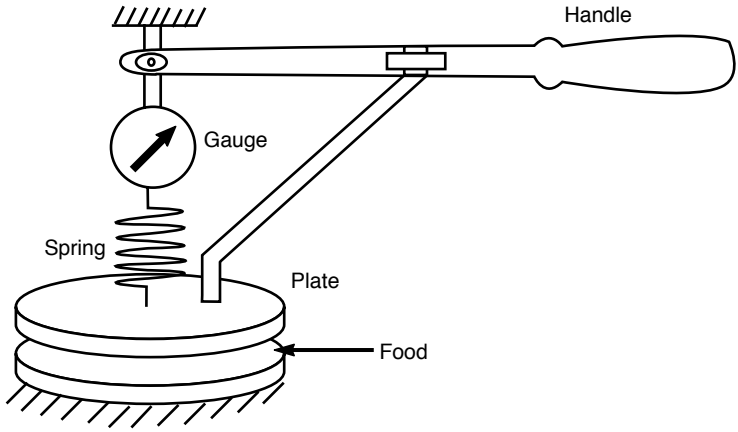

FIGURE 3.6
Fixed pressure application device.

Figure 3.6 shows the electrode setup for the RF impedance technique of moisture content measurement. Two parallel plate brass electrodes are arranged for placing the sample between them. The upper electrode is connected to a spring pressure dial indicator and the lower electrode is fixed to a base. The upper electrode can be moved by a lever connected to the upper side of the dial gauge. The gauge indicates the desired pressure applied to the sample to get proper contact, compactness, and uniformity between measurements.

The capacitance C can be calculated from the following mathematical steps:

$$\omega CR = \tan\theta \tag{3.11}$$

and

$$\begin{aligned} V / I &= R + (1 / j\omega C) \\ &= (1 + j\omega CR) / j\omega C \\ &= (1 + j\tan\theta) / j\omega C \end{aligned}$$

$$\left|\frac{V}{I}\right| = \frac{\sqrt{1+\tan^2\theta}}{\omega C}$$

$$C = \left|\frac{I}{V}\right| \frac{\sqrt{1+\tan^2\theta}}{2\pi f} \tag{3.12}$$

where f is the frequency of the operating voltage.

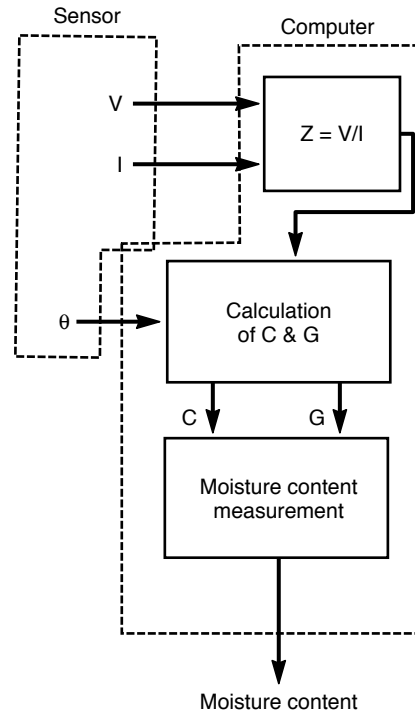

FIGURE 3.7
Schematic diagram of the RF technique.

Voltage and current sensors can produce equivalent DC signals proportional to the AC voltage applied (*V*) and AC current produced (*I*). Figure 3.7 shows the block diagram representation of the technique. The voltage- and current-dependent signals after signal conditioning are interfaced to a computer-based data acquisition system. The phase angle θ is also produced by a phase angle sensor and the signal is interfaced to the computer. The computer is programmed to calculate the value of *C* using equation 3.12. From the capacitance values obtained at different frequencies, the moisture content of the sample can be determined. The RF impedance technique of moisture determination is best suited for low moisture content food products of a dry nature. This technique can provide moisture content readings with errors in the range of 0.6% to 0.7% (moisture content).

3.2.4 DC Resistance Technique

The resistance or conductance of a food item depends, to a large extent, on the amount of moisture present in it. At constant voltage the electrical conductivity increases as the moisture content increases. Total conductivity of the material corresponds to the effective volume and the surface conductivity. Moreover, the specific resistance of a material at constant moisture depends on the following factors:

1. Size and shape of electrodes
2. Distance or gap between electrodes
3. Electric field intensity, temperature, salt pressure, and so on

The electrical resistance of a material with moisture content M_c is given by

$$R = \frac{K}{(M_c)^b} \tag{3.13}$$

where K and b are two constants that depend on the size and shape of electrodes and other structure of the material under test. Although there are various arrangements available in DC conductance techniques, the model-based technique developed by Bhuyan et al. [1] for green tea leaf moisture measurement is discussed here.

In this method pairs of nonopposing penetrable needle electrodes suitable for plant leaves were used. Figure 3.8 shows the basic measuring circuit for leaf moisture dependent resistance. In a basic resistive network, the output voltage V_0 is given by the relation

$$V_0 = \frac{VR_t}{(R_f + R_t)} \tag{3.14}$$

where V is the DC supply voltage, R_t is the leaf resistance, and R_f is a fixed resistance connected to the circuit.

3.2.4.1 Average Moisture Content Model of Plant Leaf

Water particles in a plant leaf reside in structural microcapillaries of the leaf. In most of the plant leaves, the moisture particles do not homogeneously reside over the entire leaf but are distributed in different quantities in different zones. The moisture content is higher near the petiole and midrib than at the apex and edge, respectively. Therefore percentage moisture content measurement in one zone of a plant leaf does not give a true representative value. In a leaf where water particles are distributed nonhomogeneously, moisture content measurement is possible by the dry and weigh method, but this is not an on-line method. To understand an average moisture content measurement principle, the technique based on the model of leaf moisture content developed by Bhuyan et al. [1] is explained next.

The percentage of moisture content (wet basis) of a leaf section as shown in figure 3.9A can be represented by

$$\begin{aligned} M_p &= \left[(W_w - W_d)/W_w\right] \times 100\% \\ &= (W_m/W_w) \times 100\% \end{aligned} \tag{3.15}$$

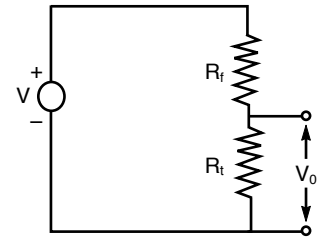

FIGURE 3.8
Equivalent circuit for the leaf moisture measurement.

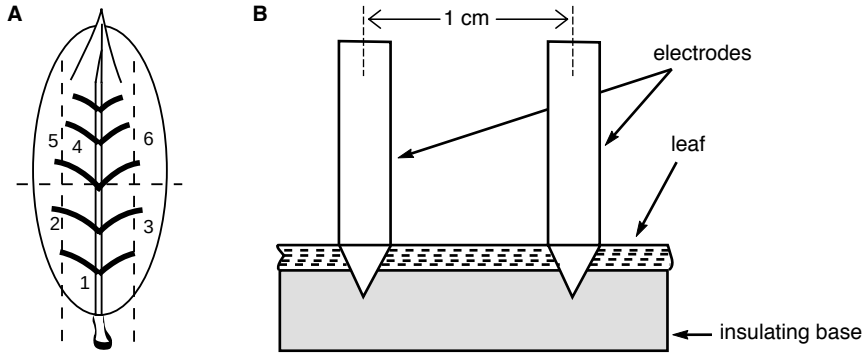

FIGURE 3.9
Model of tea leaf for moisture content measurement: (A) Six moisture zones; (B) electrodes.

where W_w = weight of wet leaf
W_d = weight of dry leaf
W_m = weight of moisture content

The total weight of wet leaf, dry leaf, and moisture of the leaf section can be expressed as a sum of individual zonal weights (for zones 1, 2, …, n)

$$W_w = W_{w1} + W_{w2} + \ldots\ldots + W_{wm} \tag{3.16A}$$

$$W_d = W_{d1} + W_{d2} + \ldots\ldots + W_{dn} \tag{3.16B}$$

$$W_m = W_{m1} + W_{m2} + \ldots\ldots + W_{mm} \tag{3.16C}$$

The moisture content can be expressed using equation 3.15 and equation 3.16C as

$$M_p = \frac{W_{m1}}{W_w} + \frac{W_{m2}}{W_w} \cdots\cdots + \frac{W_{mn}}{W_w} \times 100\% \tag{3.17}$$

The zonal moisture content ratio can be written as

$$M_{ri} = \frac{W_{mi}}{W_w},\ i = \text{zone number} \tag{3.18}$$

From equation 3.18, the average moisture content M_p can be expressed as

$$M_p = \sum g_i M_{ri} \times 100\%, \quad i = 1 \ldots n \tag{3.19}$$

where g_i = zonal weightage factor.
$= W_{wi}/W_w$

Taking P_i as a candidate for measurement of moisture content (M_{pi}) across *i*th sensor electrode pair, the average moisture content can be expressed as

$$M_p = \frac{1}{K} \sum g_i P_i \times 100\% \quad \text{for } i = 1 \text{ to } n \tag{3.20}$$

where $K = P_i/M_{ri}$ = sensor sensitivity.

In this model equation it is assumed that the weightage factor g_i is constant within the boundary of a zone *i*. This factor is different for different plant leaves and for a particular type of leaf the factor is nearly constant. Figure 3.9A shows the tea leaf topology divided into six zones. The relational values of the zonal weightage factors of the leaf can be described as

$$g_1 > (g_2, g_3) > g_4 > (g_5, g_6)$$

The zonal weightage factors g_1, g_2, g_3, g_4, g_5, and g_6 should be estimated for a particular plant leaf and then the sensor outputs P_1, P_2,…P_6 can be used to calculate the average moisture content M_p using equation 3.20. table 3.3 shows the zonal weightage factors for healthy tea leaves. These values were calculated by the dry and weigh method using a KAYBEE™ infrared moisture analyzer.

TABLE 3.3

Mean Values of Zonal Weights and Weightage Factors

Zones	Zonal Weights (mg)	Weightage Factor
1	59	0.23
2	48	0.18
3	47	0.18
4	38	0.15
5	33	0.13
6	32	0.13

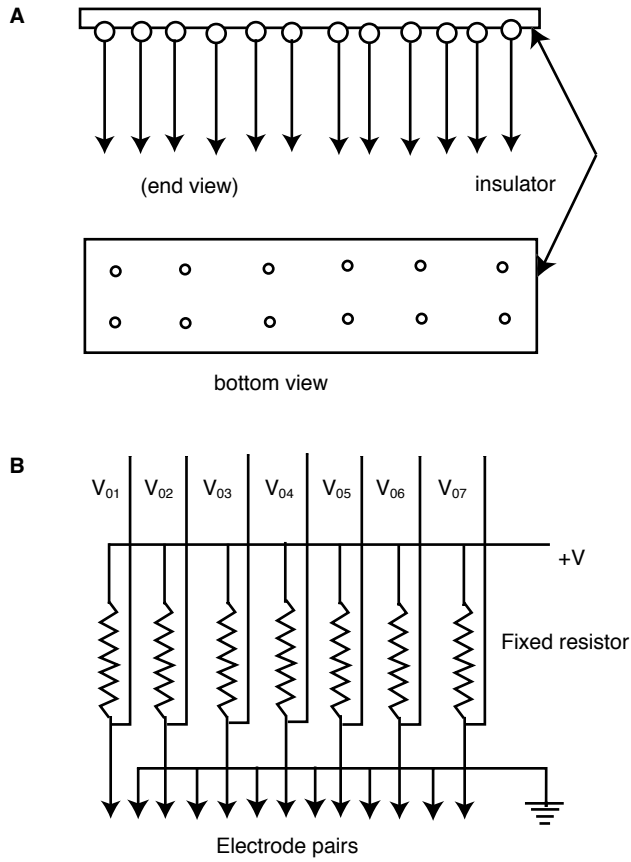

FIGURE 3.10
Electrode system: (A) End and bottom view of the electrode system; (B) six-electrode connection circuit.

3.2.4.2 Measuring Circuit

Equation 3.20 is the basis of measurement of the moisture content of a plant leaf. This equation establishes the condition of the output voltage to vary from +V to 0 when the electrodes are open or short-circuited when the leaf is totally dry (moisture content of 0%) and fully saturated (moisture content of 100%), respectively. A linear variation is established between these two extremes. For average moisture content of the six selected zones of the tea leaf, six electrode pairs are used, as shown in figure 3.10. The seventh electrode pair can be used for calibration of the instrument.

The circuit shown in figure 3.11A is used for generating a calibrated output voltage signal for final display of moisture content. It consists of an averaging, an inverting, and a calibrating amplifier connected in tandem. The averaging circuit gives the average output as per the following equation:

$$V_x = -R_f\left[\frac{V_{01}}{R_1} + \frac{V_{02}}{R_2} \ldots + \frac{V_{06}}{R_6}\right] \tag{3.21}$$

where V_{01}, V_{02}, ……V_{06} are the electrode output voltages and R_f is the feedback resistance of the op-amp amplifier. The estimated weightage factors shown in table 3.3 are simulated by selecting proper values of input resistors so that the following ratios are maintained:

$$g_1 = \frac{R_f}{R_1},\ g_2 = \frac{R_f}{R_2}, \cdots g_6 = \frac{R_f}{R_6}$$

The inverting output obtained from the first summing amplifier is amplified by the second inverting amplifier to get the noninverting output. The third stage is a calibrating amplifier that calibrates the signal linearly from 0 V to 12 V over the variation of moisture content from 0% to 100% in full scale. The characteristic curves for different stages of the measuring circuit are shown in figure 3.11B. The calibrated output V_y is adjusted by the variable

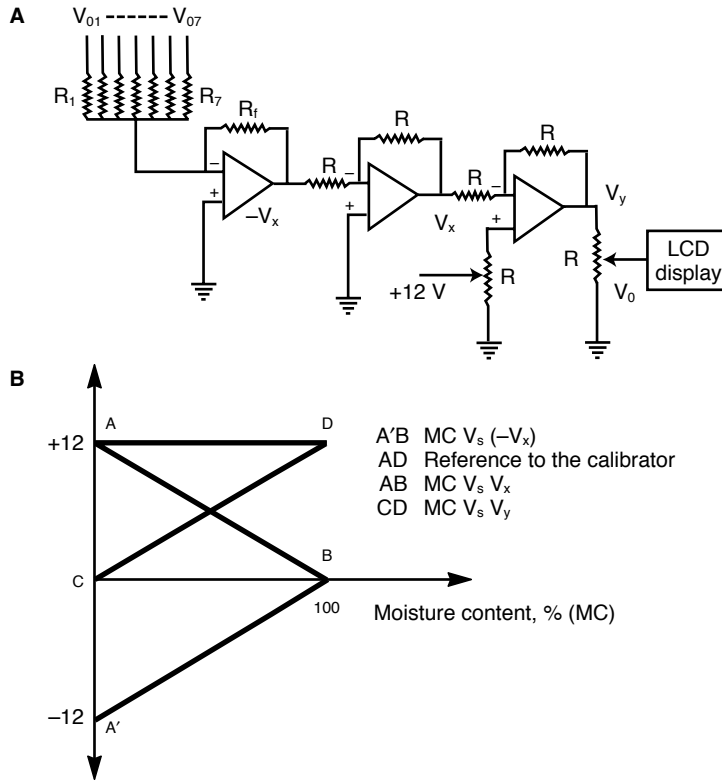

FIGURE 3.11
Amplifier system: (A) Circuit diagram; (B) Characteristics.

output resistor R to the appropriate level for final display of the percentage moisture content in a display module. The reference input to the LCD panel meter is adjusted to display the percentage moisture content in digital form in the range from 0% to 100%.

The instrument was calibrated against known values of moisture content of a tea leaf before using it for measurement. The zero setting calibrating resistance is adjusted to display zero (0%) and maximum (100%) readings, respectively. A moisture content of 0% can be simulated by keeping the electrodes open circuited and adjusting the reference input potentiometer of the calibrating amplifier. Similarly, moisture content of 100% can be simulated by dipping the electrodes in impure water and adjusting the calibrating pot until a display of 100% is achieved. This DC conductance method of moisture content measurement gives a maximum error of ±0.5%.

3.2.5 Infrared Technique

The infrared (IR) technique is used for determination of the constituents of many food items, like oil, sugar, starch, grains, oilseeds, animal feeds, forages, and so on. This technique is based on the principle that water molecules absorb IR radiation selectively. For example, considerable absorption takes place at wavelengths 1.45 μm and 1.94 μm [2], which is generally used for moisture measurement in food materials.

Figure 3.12 shows the schematic diagram of a basic IR moisture meter. The IR source produces wavelengths of the absorption band that are focused and

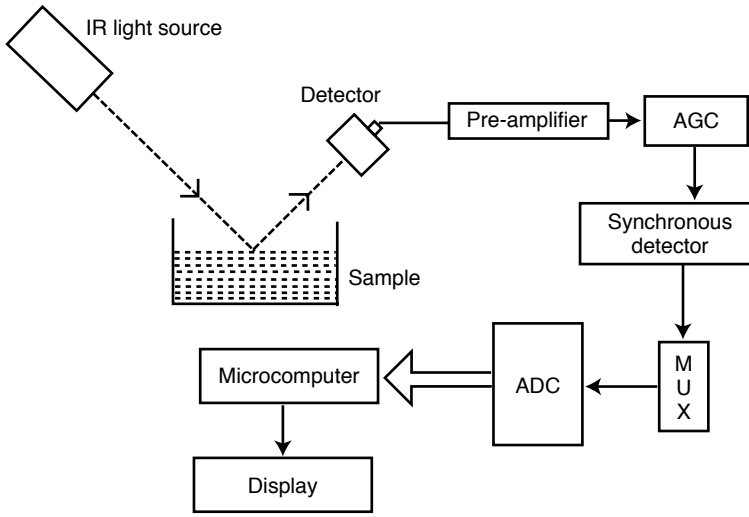

FIGURE 3.12
Schematic diagram of an IR moisture meter.

passed through a filter. The filter isolates two discrete light rays of wavelengths, measuring wavelength and a reference wavelength, which are allowed to fall on the sample. The light reflected back after being absorbed by the water particles is detected by a detector like a lead sulfide detector and converted to a modulated electrical signal. The output signal is amplified by a preamplifier to increase its level and sometimes an automatic gain controller (AGC) is used to feed back the preamplifier. A synchronous detector demodulates the signal to give two DC signals proportional to the reflectance of the sample at the two wavelengths. The ratio between these two signals is a representation of the moisture content of the sample. These two signals are interfaced to a microcomputer after converting them to a digital format. The microcomputer calculates the reflectance ratio and gives a calibrated display of the moisture content. The output signal of the moisture meter has to be calibrated for each material. The actual moisture content of the material should be determined from a set of data for different moisture levels. A quadratic regression equation can be formulated and the regression coefficients can be used for determining the moisture content.

The main advantages of this moisture meter are faster response, on-line use, noncontact and nondestructive, and it is especially suitable for food items. One limitation of this technique is that the instrument gives only representative moisture content because IR does not penetrate very far below the surface of the sample. A commercial IR-based moisture meter (Model-SMART-II) manufactured by Moisture Register Products, a division of AQUA Measure Instruments Co. (California), is shown in figure 3.13.

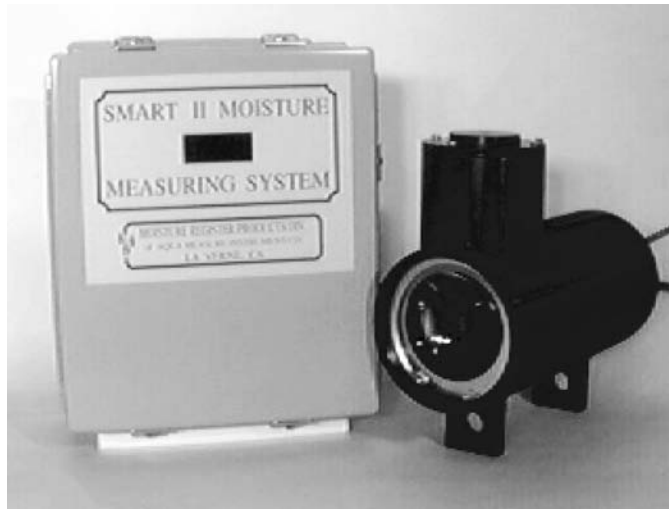

FIGURE 3.13
Online IR moisture meter (Model SMART-II). (*Reprinted with permission from Moisture Register Products, A Division of AQUA Measure Instrument Co., California*)

3.3 Moisture Release During Drying of Food

When a particular food material is dehydrated, cooked, dried, or withered, water particles are released, resulting in some variation in quality of the food. Some foods require slight reduction of moisture, whereas some must be completely dried. The degree of drying might be different for different types of raw materials and food products. In some cases the moisture is released initially or during an intermediate stage, whereas in others the food product is dried at the final stage of processing. In many situations the raw materials require preheating or drying to reduce their moisture content. The amount of water to be reduced depends on the initial moisture content of the raw materials. In such situations it might be necessary to know the moisture content of the raw material, how much moisture is being released, or to what extent the food item has been dried. Controlled release of water particles from a food item is an important criterion in many food processing applications. To achieve the required quality, this factor needs to be measured and monitored. This section describes a technique of measurement of moisture release during withering of tea developed by Bhuyan [3].

3.3.1 Mathematical Representation

The degree of moisture released from a food item can be expressed by a percentage term. Different food processing industries use different terms to represent the same operation. For example, in the tea industry, the initial moisture reduction process of the green tea leaves (the process of withering) is defined by the term *percentage of withering*, which can be expressed by a mathematical expression. If the moisture content of green tea is known, the extent of withering (in percentage) to achieve the final moisture content of the processed food can be calculated as [4, 5]

$$P_w = 96\frac{(100 - M_g)}{(100 - M_w)} \tag{3.22}$$

where P_w = percentage of withering (%)
M_g = moisture content of green leaf in wet basis (%)
M_w = moisture content of withered leaf in wet basis (%)

Equation 3.22 is based on the assumption that about 4% dry substance is lost during withering or drying of most of the food materials. The weight of tea leaf before or after withering is given by

$$W_g = W_{mg} + W_d \tag{3.23}$$

where W_g = weight of green tea leaf
W_{mg} = weight of moisture in green leaf
W_d = weight of dry tea leaf

The instantaneous value of weight of tea leaves during withering is given by

$$W_w(t) = W_{mw}(t) + W_d \tag{3.24}$$

where $W_w(t)$ = instantaneous weight of tea during withering
$W_{mw}(t)$ = instantaneous weight of moisture during withering

The moisture content of tea leaves before and during withering is expressed in wet basis, respectively, as

$$M_g = \frac{W_{mg}}{(W_{mg} + W_d)} \tag{3.25}$$

and

$$M_w(t) = \frac{W_{mw}(t)}{(W_{mw}(t) + W_d)} \tag{3.26}$$

From equation 3.22, equation 3.25, and equation 3.26, the instantaneous value of percentage of withering can be written by the equation

$$P_w(t) = \frac{96\left[1 - (W_{mg} / (W_{mg} + W_d))\right]}{\left[1 - (W_{mw}(t) / (W_{mw}(t) + W_d))\right]}\% \tag{3.27}$$

$$= \frac{96\left[W_d(W_{ms}(t) + W_d)\right]}{W_d(W_{mg} + W_d)}\% \tag{3.28}$$

$$P_w(t) = \frac{96W_w(t)}{W_g} \tag{3.29}$$

Hence, for estimation of withering percentage using equation 3.29, the initial weight of green tea leaves (W_g) and the instantaneous weight of tea during withering ($W_w(t)$) should be measured.

3.3.2 Mechanical Loading Arrangement

For continuous monitoring of withering percentage, the withering trough should be equipped with a representative section of platform placed over

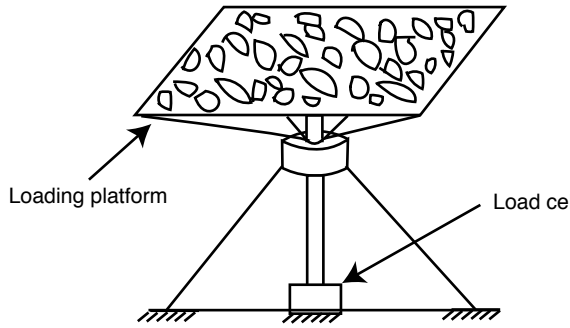

FIGURE 3.14
A loading platform in tea withering trough.

load sensors as shown in figure 3.14. Generally the representative section is positioned at the middle of the withering trough to get a faithful representation of moisture release for the entire trough. To minimize initial cost, the loading system can be constructed with a minimum number of load sensors. Two arrangements are possible: one with four load cells and one with a single load cell (fig. 3.15).

The approximate weight of the tea leaves over the surface area of the representative section should be known to determine the capacity of the load cells. If the total weight of the material is W, the approximate load distribution at each of the load sensors will be W/4 in the arrangement shown in figure 3.15A. Hence, each load cell should have a maximum load-bearing capacity of W/4. The loading platform should be such that it causes a considerable effective transmission of weight of the food material to the load sensors. The arrangement shown in figure 3.15A requires an electronic summing device in the subsequent stages of signal processing.

To reduce this additional cost of four load cells with an electronic summing device, the second arrangement of a single load sensor platform can be used (fig. 3.15B), which does not require a summing device. The load of food materials placed on the representative section is directly sensed by the transmitting rod that is connected to the center of the platform and the load sensor

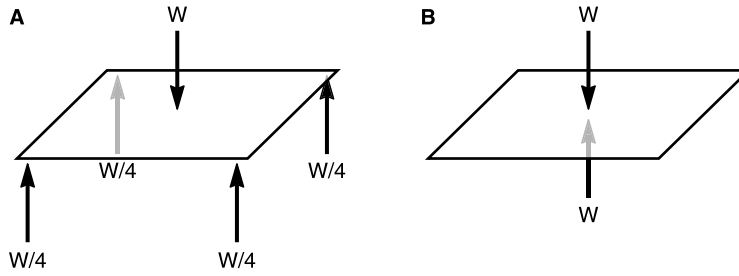

FIGURE 3.15
Loading modes in loading platform: (A) Four load cells; (B) Single load cell.

placed on the floor. This structure ensures that maximum load is transmitted to the load sensor (about 98%).

3.3.3 Measuring Circuit

Load cells are designed either for compressive load, tensile load, or both. In the platform type of loading system, a compressive load cell is required. When a DC voltage of about 5 V is applied to the bridge circuit of a typical load cell, a maximum output voltage of about 50 mV is developed with a sensitivity of 1 mV/V. Hence, for determination of instantaneous load of the representative section, amplification of the signal is necessary because most of the interfacing devices used for displaying and recording operate at voltages in the range from 0 V to 5 V. Figure 3.16 shows an instrumentation amplifier generally used for amplification of signal obtained from a bridge configuration. The major characteristics of the instrumentation amplifier include high common mode rejection ratio (CMRR), high input impedance, low noise, negligible drift, and moderate bandwidth.

Problem 3.1

The amplified output voltage of an instrumentation amplifier (fig. 3.16) is given by

$$E_0 = (e_1 - e_2)\left[\frac{R_4}{R_3}\left(1 + \frac{2R_2}{R_1}\right)\right]$$

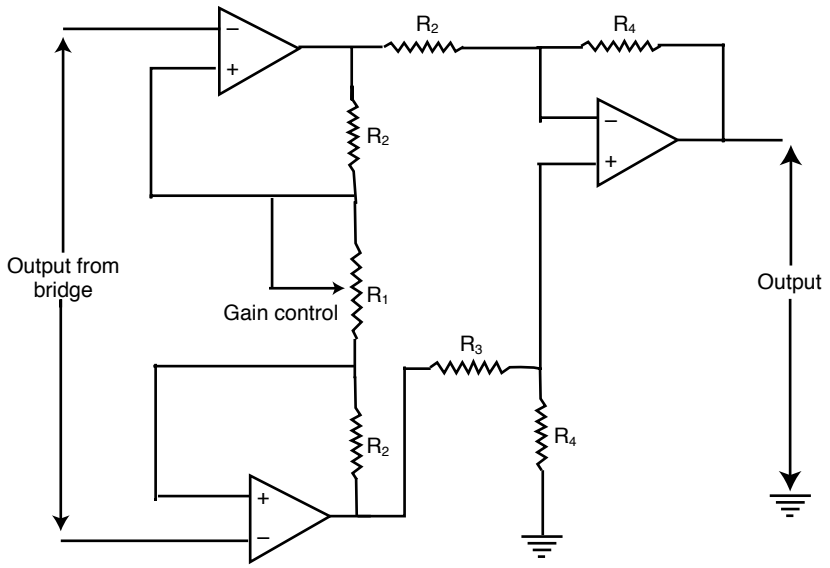

FIGURE 3.16
Circuit diagram of an instrumentation amplifier.

The amplification factor can be obtained by selecting proper values of R_2, R_3, and R_4 and fine adjustment can be done with the variable resistor R_1. For example, let the output voltage of the bridge be 5 mV for a load of 50 kg and the desired amplified output be 5 V. Find proper values of the resistances of the amplifier. What is the sensitivity of the measurement system?

SOLUTION

Given

Output voltage from the bridge = 5 mV
Amplifier output voltage = 5 V

Therefore, the gain of the amplifier is

$$A = 5.0/5\text{mV} = 1{,}000$$

Hence, from the given equation

$$(R_4/R_3)(1 + 2R_2/R_1) = 1{,}000$$

Assuming

$$R_4/R_3 = 100\ \text{k}\Omega/2\ \text{k}\Omega = 50$$

hence,

$$(1 + 2R_2/R_1) = 20 \text{ and}$$
$$2R_2/R_1 = 19$$
$$R_2/R_1 = 9.5$$

If the value of R_2 is chosen as 100 kΩ
then

$$R_1 = 100/9.5 = 10.52\ \text{k}\Omega,$$

so a 15 kΩ potentiometer can be used for R_1.

The sensitivity = output voltage/input weight
= 5 V/50 kg
= 0.1 V/kg

For continuous monitoring of percentage of withering (P_w) a real-time monitoring or data acquisition system is essential. The data manipulation is illustrated by a general block diagram, as shown in figure 3.17.

This topic is discussed in chapter 5 with more details about hardware interfacing components used for implementation of computer-based monitoring and control of the tea withering process.

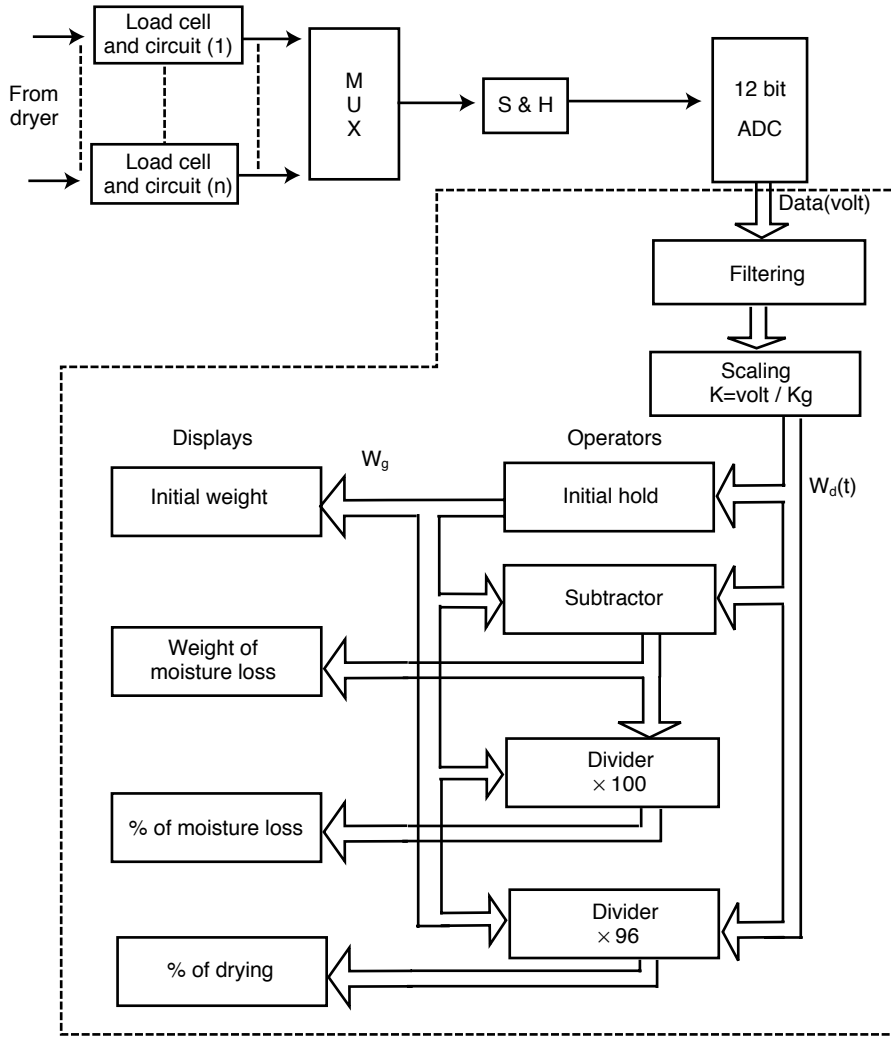

FIGURE 3.17
Block diagram of data manipulation and display operation.

3.4 Humidity in the Food Processing Environment

As mentioned earlier, during processing, manufacturing, and preservation, some food items like potato chips, dry breakfast cereals, and crackers absorb water particles when exposed to relatively humid environments. As a result,

TABLE 3.4

Typical Air Humidity in Food Processing Industries

Food Process	Stage	Humidity (%)
Brewing and distillation	Hops storage	60
	Fermentation	45
	Filter room	45
	Grain storage	40
Baking	Sugar storage	35
	Icing and glazing	35
	Cookie drying	20
	Potato chips	20
Candy	Caramel cooling	40
	Bar cooling	40–50
	Chocolate	13
	Hard candy making	30
	Hard candy packing	30
	Sugar storage	35
Concentrates	Molasses grinding	25
	Honey grinding	25
	Citrus crystal packing	15

the quality deteriorates due to physical, chemical, or biological changes that take place in the food. Physically, food can become soggy, rubbery, and unappetizing. In the case of powdered foods, due to absorption of water, the food becomes coagulated. Packed flour loses weight or dough forms a skin on the surface on releasing moisture under dry air conditions. Similarly granulated sugar cakes when it absorbs moisture under humid conditions. The taste, flavor, and other qualities of some food items deteriorate due to changes in the enzyme formation from excess amounts of water particles absorbed from the air. Apart from physical and chemical deterioration, biological degradation can also take place in the food due to absorption of moisture. Many microorganisms like bacteria and viruses can thrive, making the food hazardous for consumption. Hence, the moisture level of the surrounding air plays a vital role during food processing and preservation. In many food processing and preservation industries, the humidity of the air is regulated to circumvent these problems. Table 3.4 shows different food processing industries with typical humidity values where humidity measurement is essential. In such situations, measurement of humidity is essential so that regulatory actions can be taken. This section describes the different techniques of humidity measurement.

3.4.1 Definition of Humidity

The term *humidity* means a quantitative indication of the amount of water vapor retained by a gas or air. More precisely, however, there are three definitions: absolute humidity, specific humidity, and relative humidity.

Absolute humidity is the ratio of mass of water vapor contained in a gas mixture to the total mass of the gas mixture. *Specific humidity* gives the ratio of mass of water vapor present in a gas mixture to the mass of the dry gas mixture. *Relative humidity* is the ratio of mass of water vapor in a gas mixture to the mass of moisture in a saturated mixture at equal volume, temperature, and pressure. In other words this is the ratio of moisture contained in a gas mixture to the maximum moisture the gas mixture can hold at equal volume, temperature, and pressure.

Two more definitions are also used to define the moisture-carrying property of a gas: dew point and saturation pressure. *Dew point* is the saturation temperature of a gas–water vapor mixture. Dew point is an important parameter to determine the minimum safe temperature of a food product in a cooling machine. *Saturation pressure* is the pressure of a fluid required for condensation to take place at a given temperature. This temperature is called the saturation vapor pressure temperature (SVPT) of the gas.

In most practical applications, humidity measurement aims at measurement of relative humidity, which is expressed as percentage of the ratio mentioned in the definition.

3.4.2 Conventional Types

The most common and conventional humidity meters are the hair hygrometer and wet- and dry-bulb psychrometers.

3.4.2.1 Hair Hygrometer

This traditional method utilizes the change of mechanical and dimensional properties of organic material due to absorption of water particles (fig. 3.18A). In this method a bunch of animal hair is fixed in a frame so that its expansion with an increase in relative humidity actuates an indicating instrument. The amount of moisture the hair can absorb is dependent on the temperature and partial vapor pressure of the atmosphere and thus the expansion of the hair is a function of the relative humidity of the air. In this method the accuracy over a large range is very poor.

3.4.2.2 Wet- and Dry-Bulb Psychrometer

Classically relative humidity is found from the psychrometric chart based on the temperature readings of two mercury thermometers, the dry bulb that reads the air temperature (T_d) and the wet bulb that reads the temperature of adiabatic saturation (T_w). At this wet-bulb temperature the thermodynamic equilibrium is reached between cooling by evaporation and heating by convection. The mercury bulb of the wet thermometer is covered by a cotton wick that gets moistened from a small water pot. For a better response, the wet-bulb thermometer should be subjected to a large draft of air. When the water of the cotton wick of the wet bulb evaporates, it becomes cooled. The amount of evaporation is determined by the amount of water already present

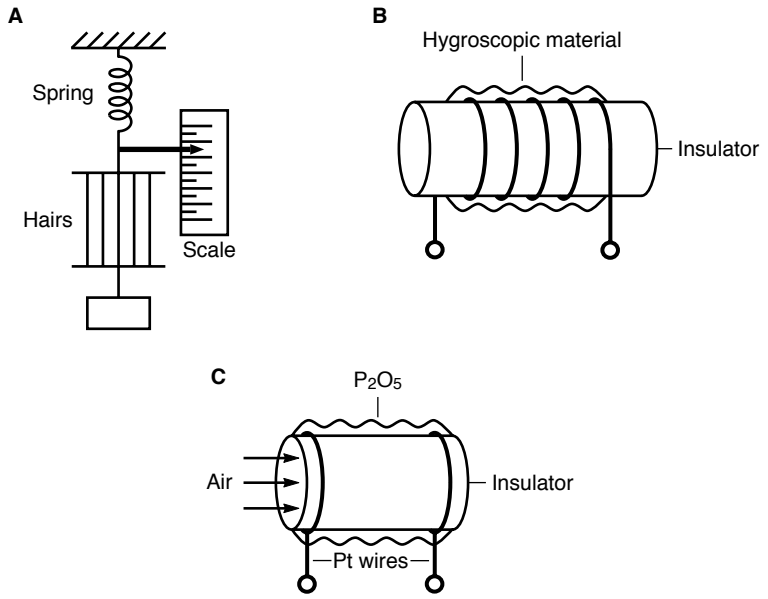

FIGURE 3.18
Humidity sensors: (A) Hair hygrometer; (B) Resistive type; (C) Electrolytic type.

in the surrounding air. In moist air, evaporation will be less, whereas dry air will cause more evaporation. The difference between T_d and T_w is known as depression temperature or hygrometric difference (ΔT). It determines the magnitude of relative humidity for a particular value of T_d and ΔT. The equation relating relative humidity and the two temperature readings can be expressed as

$$RH(\%) = \frac{P_v}{P_{sat}} \times 100\% \tag{3.30}$$

and

$$P_v = P_{sat} - KP_t(T_d - T_w) \tag{3.31}$$

where P_{sat} = saturation partial vapor pressure
P_t = total pressure
K = a constant

The temperatures are expressed in °F.
The constant K is given by

$$K = A\left[1 + B(T_w - 32)\right] \tag{3.32}$$

where A and B are two constants.

Equation 3.30 cannot be used directly for measurement of relative humidity. The psychrometric chart utilizes equations 3.30 through 3.32 to relate T_d and T_w to determine relative humidity. The psychrometric chart gives values of relative humidity corresponding to various sets of dry-bulb temperatures and hygrometric difference temperatures. This hygrometer is a classical device suitable for offline applications.

There are few variations based on this principle by which direct display of the two temperature readings and the corresponding relative humidity is possible, which are discussed in later sections.

This principle of humidity measurement has certain advantages for which these meters are popular. One advantage of this hygrometer is that it covers a wide range of humidity, which is not possible with other hygrometers. Another advantage is that there is no temperature effect on the output because the technique itself is based on temperature measurement.

3.4.2.3 Fluidic Dry- and Wet-Bulb Hygrometer

In one variation of mercury thermometer-type hygrometer, mercury thermometers are replaced by filled liquid thermometers. Filled liquid thermometers are still popular in industries when an electrical signal is not necessary. However, one limitation is that the signals can be transmitted to a remote location to a maximum distance of only about 200 ft. Similar to the mercury thermometers discussed earlier, the dry bulb is kept open in the air, but the wet bulb is wrapped with a knitted or woven cotton wick and placed on the surface of a water vessel. The level of water in the vessel is kept constant with the help of a filling pipe and the excess water is spilled out.

The thermometers transmit fluidic signals through capillary tubes and they drive the stylus of a fluidic recorder. A schematic diagram of this hygrometer is shown in figure 3.19.

This fluidic hygrometer is very simple and also reliable. In situations where automatic control is not adopted and the dry- and wet-bulb temperature readings only are sufficient, this hygrometer stands as the most advantageous.

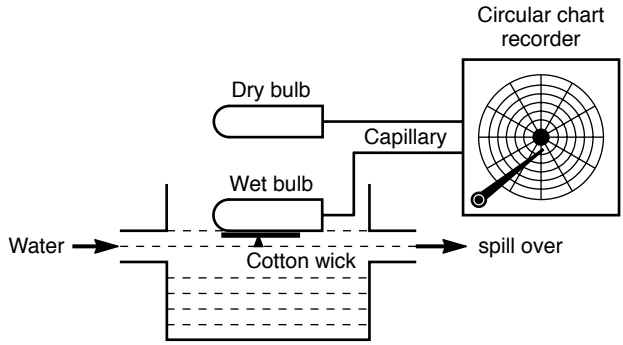

FIGURE 3.19
Fluidic type hygrometer.

3.4.3 Electrical Type of Humidity Meters

Electrical humidity meters are based on sensors that undergo a variation of some electrical parameters such as resistance, conductance, and capacitance. These sensors are discussed next.

3.4.3.1 Resistive Hygrometer

A resistance element type of relative humidity sensor consists of two wires wound over an insulating former and a coating of hygroscopic materials like lithium chloride, phosphoric acid, calcium chloride, zinc chloride, or tin tetrachloride (fig. 3.18B). When the hygroscopic material absorbs moisture from the air, dissociation takes place so the resistance between the two wires changes. The variation of resistance due to humidity is between 10 MΩ and 10 KΩ. The main disadvantage of this sensor is that error due to temperature is high. Moreover, the sensor does not cover the full operating range of relative humidity. Hence, a number of such sensors are necessary to cover the full range. Another disadvantage is that the wires are prone to contamination, so they should be made of noble metals only. An AC circuit performs the measurement to avoid polarization. The accuracy of this transducer is about ±1.5% (relative humidity).

3.4.3.2 Electrolytic Hygrometer

The electrolytic humidity sensor (fig. 3.18C) consists of two platinum wires wound over an insulating tube made of Teflon or Neopherene in duplex helix winding form. The space between the windings is filled up with a hygroscopic compound like phosphorous pentoxide. The test air is then passed through the tube at a rate of about 100 cm^3/min. When the cell is energized by a DC voltage, a current flows through the winding under a constant air flow condition. The system reaches equilibrium when the moisture absorption rate of the hygroscopic material equals the rate of electrolytic decomposition. Therefore the current becomes proportional to the relative humidity of air. The response of this device is slower than other two devices previously mentioned. In addition, a change in temperature tends to change the calibration of the device.

3.4.3.3 Capacitive Hygrometer

In this type of sensor the relative permittivity of a material is allowed to change with the absorption of moisture. Therefore a change in capacitance can be obtained due to a change in relative humidity. These sensors are very precise in design and construction, making them extremely sensitive. The electrodes are made of gold or gold-plated metals, which makes them costlier than other types.

All four types of humidity meters are available in battery-operated, portable forms that are very popular for field measurements.

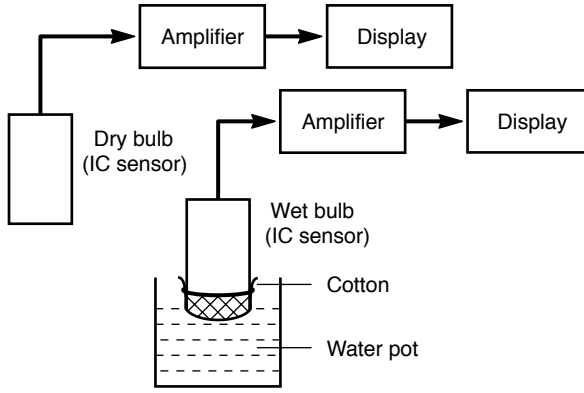

FIGURE 3.20
IC thermal sensor-based hygrometer.

3.4.4 Electronic Wet- and Dry-Bulb Hygrometer

In the electronic version of the wet- and dry-bulb hygrometer, the two thermometers are realized by two IC thermal sensors, either VPTAT or IPTAT. These sensors are available in a three-terminal plastic or metal package capable of working in the temperature range of –50°C to 200°C. The moistened cotton wick is wrapped around the IC that is used as the wet bulb. An electronic circuit is used to amplify the output signal to the desired level for display. Figure 3.20 shows a schematic diagram of this thermal sensor-based device. The amplified signal is displayed in analog meters or digital display modules. The circuit used to amplify the IC sensor signals is shown in figure 3.21A.

In another approach, a copper-Constantan thermocouple is used to implement the wet- and dry-bulb concept [3]. In this method the measuring hot junction is used as the dry bulb and the cold junction is used as the wet bulb (fig. 3.21B). As a result, the thermocouple develops a voltage proportional to the depression temperature. This voltage is amplified by an instrumentation amplifier as shown in figure 3.16. A thermocouple of sensitivity 50 μV/°C will need an amplifier with a gain of about 100 to calibrate the output in the range of 0 V to 5 V corresponding to a temperature range of 0° to 100°C.

3.4.4.1 Microprocessor-Based Wet- and Dry-Bulb Hygrometer

There is no linear equation relating relative humidity with the wet- and dry-bulb temperatures. Some equations are available but they show an error up to ±5%. These equations cannot be used in applications in which accuracy is very important.

In a microprocessor-based device developed by Bhuyan et al. [6], intermediate operating points of the psychrometric chart are stored in an erasable programmable read-only memory (EPROM) chip. The psychrometric chart

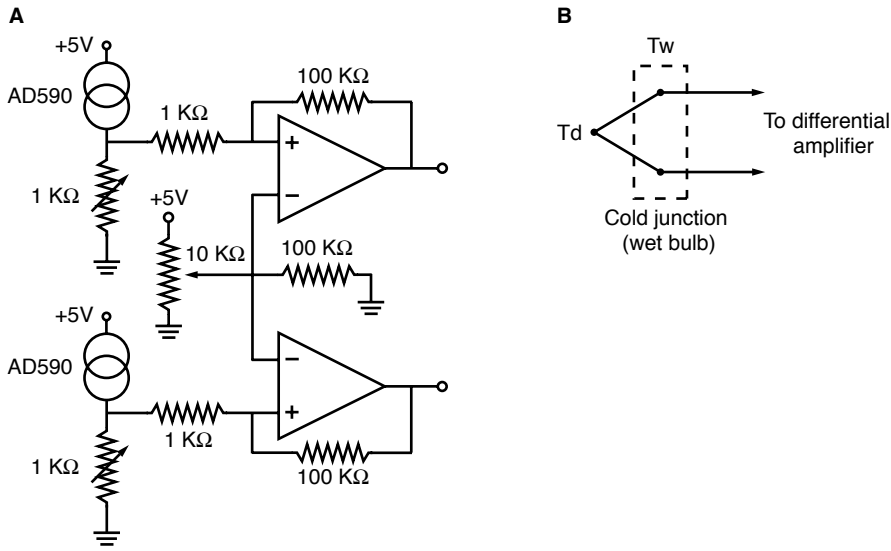

FIGURE 3.21
Generation of hygrometric difference signal: (A) IC thermal sensor amplifier circuit; (B) Thermocouple circuit.

contains a huge amount of data and it is not possible to enter all of the data into the EPROM. The intermediate data stored in the EPROM is used as a lookup table and programmed to interpolate the points, thereby trying to stretch the psychrometric graphs from their actual shape, sacrificing a little accuracy. This technique should be adopted when the operating range is not very wide. Working with a limited operating range will reduce the amount of data, making it possible to enter data of the chart in the actual pattern. Figure 3.22 shows a graphical shape of the psychrometric chart. Values shown within arrows correspond to relative humidity from 75% to 100%. Hence, for applications where relative humidity does not change beyond this

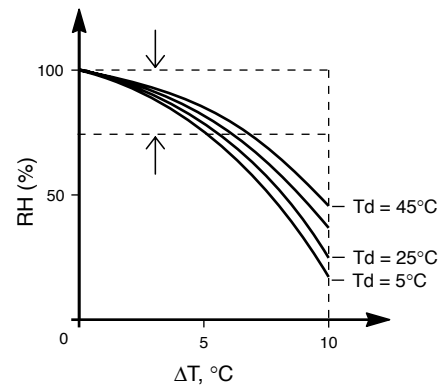

FIGURE 3.22
Variation of relative humidity with depression temperature.

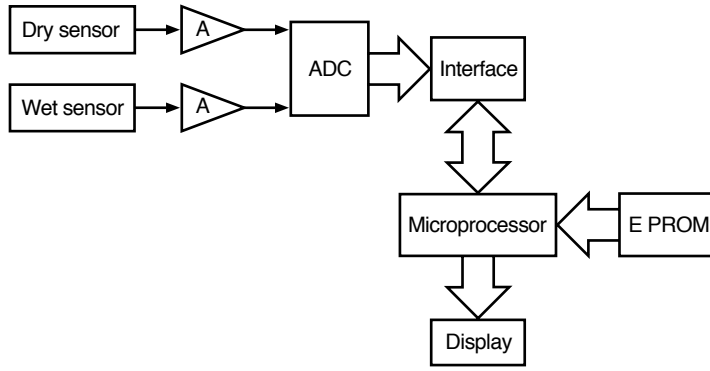

FIGURE 3.23
Block diagram of microprocessor-based hygrometer.

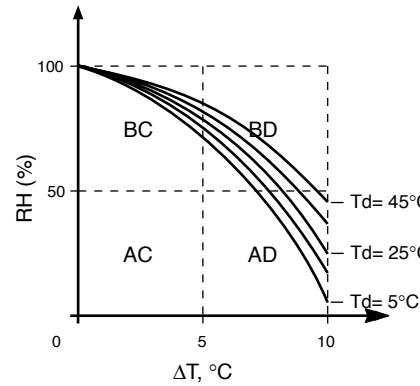

FIGURE 3.24
Four operating zones of the psychrometric chart. (*Redrawn from Proc. Int. Conf. on Industrial Automation and Control, 1995 with permission from IEEE.*)

range, the corresponding data on the chart can be used. This simplifies the technique to a great extent. Figure 3.23 shows the schematic arrangement for the microprocessor application.

3.4.4.2 Hygrometer Based on Linearized Model of Psychrometric Chart

A linearized model of the psychrometric chart was developed by Bhuyan and Bhuyan [7] for implementing the system by a computer. In this technique four piecewise linearized model equations are developed. In the piecewise linearized technique, the data of the chart are divided into four zones that are considered linear within individual boundaries. Figure 3.24 shows the four operating zones AD, AC, BC, and BD in the relative humidity characteristics of the psychrometric chart.

The temperature limits for the zones are as follows:

$$\text{Zone AC:} \qquad 5°\text{C} \le T_d \le 25°\text{C}$$
$$\text{and } 0°\text{C} \le \Delta T \le 5°\text{C}$$

Zone AD: $25°C < T_d \leq 45°C$ and $0°C \leq \Delta T \leq 5°C$

Zone BC: $5°C \leq T_d \leq 25°C$ and $5°C < \Delta T \leq 10°C$

Zone BD: $25°C < T_d \leq 45°C$ and $5°C < \Delta T \leq 10°C$

After linearization the resulting equations for relative humidity (%) for the four operating ranges are

$$RH_{AC} = (0.204\Delta T + 0.072)T_d - 12.76\Delta T + 97.88 \quad (3.33a)$$

$$RH_{AD} = (0.198\Delta T + 0.034)T_d - 12.44\Delta T + 98.67 \quad (3.33b)$$

$$RH_{BC} = (0.251\Delta T + 0.122)T_d - 12.31\Delta T + 94.55 \quad (3.33c)$$

$$RH_{BD} = (0.174\Delta T + 0.111)T_d - 12.28\Delta T + 101.19 \quad (3.33d)$$

Relative humidity can be calculated from any one of the above equations using the dry-bulb temperature (T_d) and the depression or difference temperature ($\Delta T = T_d - T_w$). Calculation of relative humidity using equations 3.33a through 33.3d is performed online with a computer-based data acquisition device. A schematic block diagram of this type of humidity measurement is shown in figure 3.25.

This computer-based wet- and dry-bulb hygrometer has the following advantages:

1. Free from temperature effect
2. Easy to calibrate
3. Covers the entire range (0%–100%)

Calibration in this technique is easy because the relative humidity is calculated from the values of wet- and dry-bulb temperatures. If the temperature readings are properly calibrated the instrument will be automatically calibrated for relative humidity.

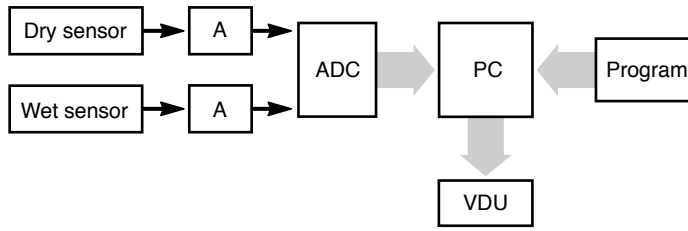

FIGURE 3.25
Block diagram of a computer-based hygrometer.

3.5 Turbidity and Color of Food

Measurements of color and turbidity are important quality control methods in many food processing industries. Table 3.5 shows some natural colors of foods and artificial colors used in foodstuffs. In many food items the chemical and the food values are reflected in their color. Apart from the processed food, the color of the raw materials also plays an important role in quality monitoring in certain food processing industries. Color matching against standard color of brewing conventions is a regular quality check in the alcoholic beverage industry. Similarly, syrup color testing is also conducted in the soft drink industry. Color and turbidity measurement is employed in the sugar industry to monitor the clarity of the juice for further processing. In the tea industry the quality of the tea originates mainly from the process of fermentation. The color of the fermented tea gives an indication of its quality. To improve appearance and to make food attractive, artificial color is added; for example, in margarine, yellow color additive; in sauces and burgers, red color additive, and so on. There are numerous applications of color and turbidity measurement in the food processing industries. This section explains some commonly used techniques.

3.5.1 Turbidity Measurement

Measurement of turbidity has been performed by brewers since the Middle Ages in very crude manners. In those days, a glass of wine was observed by holding up to light; any small reflectance of light from particles present in the liquid was visible. This basic concept of observing the glass of liquid in light is the basis of most present turbidity measurements in the food processing industries.

TABLE 3.5

Natural and Artificial[a] Colors of Some Food Products

Food	Color	Cause
Bread crust	Foxy	Amount of sugar remaining in dough
Cocoa powder	Orange/ginger-dark	Alkalization
Oil	Green/orange	Presence of chlorophyll
Flour	Creaminess	Bleaching
Made tea	Black	Degradation of chlorophyll
Fermented tea	Coppery red	Thearubigin
Colored staff:		
Cocktail cherries	E127erythrosine	
Sauces and burgers	E128 red 2G	
Smoked and cured fish	E154 brown FK	
External coating of confectionaries:		
	E174 Silver	
	E175 Gold	

[a] As per permitted colors in the United States.

Turbidity is defined as an optical property of a transparent or semitransparent material for which light gets scattered and absorbed instead of traveling through the material in a straight line, making the liquid look cloudy or smoky. In other words, turbidity, in most cases, is a measure of relative sample clarity. Color and turbidity are two different properties of a material. Turbidity is due to light scattering, whereas color is developed due to absorption of light. The presence of undissolved particles larger than 0.2μm in a liquid makes it turbid. The undissolved particles scatter a beam of light when passed through the liquid. This causes the attenuation of the intensity of the light beam. The ratio of the intensity of the incident and transmitted light is proportional to the amount of undissolved particles present in the liquid, or the turbidity of the liquid.

3.5.1.1 A Basic Turbidity Meter

The basic components of a turbidity meter are a light source, a photo detector, and a sample container or cell. The light intensity scattered by suspended solid particles due to the Tyndall effect can be related to the turbidity of the sample. The light beam should be of a single wavelength so that the scatter pattern and intensity should always be the same. Any variation in scatter pattern reduces the repeatability of the instrument. Therefore to increase repeatability a monochromatic light is used. Light-emitting diodes (LEDs) or lasers can be used because they produce monochromatic light. If a monochromatic light source is not used, the photo detector should be of a narrow spectral band that responds equally only to that band. A photo detector is placed at an angle of 90° to the transmitted light as shown in figure 3.26. The light intensity detected by the photo detector is calibrated in terms of turbidity of the liquid. As the liquid becomes more turbid the detected light intensity decreases. There are a few variations of this basic type, such as ratio technique, dual beam technique, and ratio four-beam techniques. Essentially these techniques have added advantages; for example, in the ratio technique, the effect of light reduction due to color of the liquid is minimized. In the dual-beam technique, frequent calibration is not required, and the ratio four-beam technique provides superior stability.

3.5.1.2 Standards and Units of Turbidity

A universally accepted standard is used for calibration of all turbidity measuring instruments regardless of type. The most popular unit is the formazin turbidity unit (FTU). Formazin suspension is produced by polymerization of hexamethylenetetramine and hydrazine sulfate solution. In this standard, formazin is used as the standard of calibration material. The U.S. Environmental Protection Agency (EPA) adopts this standard (EPA Standard 180.1), but they define the unit as the nephelometric turbidity unit (NTU). The International Organisation for Standardization (ISO) also adopts this unit as a standard turbidity unit (ISO 7052-1984).

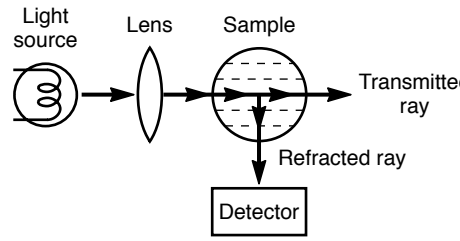

FIGURE 3.26
Schematic diagram of a basic turbidity meter.

The Jackson turbidity unit (JTU) is an optical-based unit, whereas the Keiselgur turbidity unit (KTU) is purely a parts per million (ppm) unit. The turbidity developed when 1 mg of silica is mixed in 1 L of distilled water is called a KTU. This unit is equivalent to the JTU, which equals 6.9 times an FTU unit. Similarly the Mastic turbidity unit (MTU) relates to turbidity resulting when 0.02 ml of mastic solution is added to 50 ml of distilled water. An MTU is equivalent to 0.125 times KTU, 0.0125 times FTU, and 0.125 times JTU.

3.5.1.3 Light Scattering Type Turbidity Meter

The basic setup of a turbidity meter based on the light scattering principle is shown in figure 3.26. One variation of this basic principle is the ratio technique shown in figure 3.27A. It is equipped with two photo cells to detect light scattered in two opposite directions. In some devices a separate control unit is used to enable constant intensity of the light source.

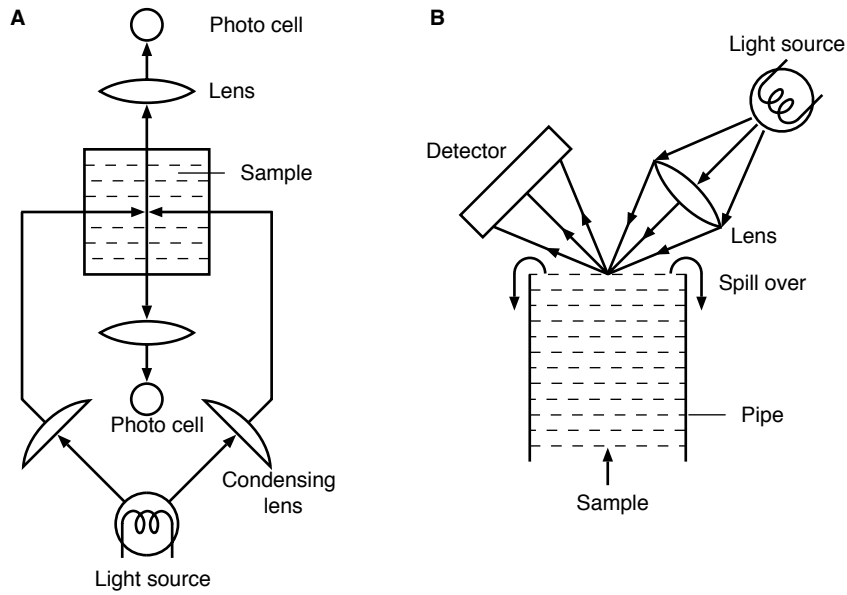

FIGURE 3.27
Basic turbidity meters: (A) Ratio turbidity detector; (B) Back-scattering detector.

The scattering technique is utilized in a different manner in the back-scattering turbidity meter shown in figure 3.27B. In this unit the sample surface is left open to circumvent the problem of window deposit in other meters. The light incident on the sample is scattered from the particles present on the surface and received by a set of photo cells installed at the proper angle and position.

3.5.1.4 Optical Absorption Type Turbidity Meter

Turbidity measurement based on the principle of optical absorption method employs both off-line and on-line techniques. The principle behind this technique is when a visible light ray is allowed to pass through the sample, a certain amount of light energy gets absorbed by the coloring matters and the turbid suspension particles. Dispersion takes place in the incident light ray, causing a spectrum in the range of about 380 nm to 760 nm. The same light ray is also transmitted through a turbid-free reference solution. The frequency of alteration is about 600 cycles per second.

In this technique (fig. 3.28) a visible light is paralleled by using a lens (A) and is passed through a cell of rectangular cross-section containing the sample liquid. The light transmitted through the sample is allowed to fall on a transmission grating kept at normal incidence position with respect to lenses B and C. The dispersion of light takes place in wavelengths between 380 nm and 760 nm and the measurement is performed in this range only. This dispersed spectrum is sensed by an array of photodiodes positioned at correct angles. Each photodiode has a spectral wavelength equal to the total spectral band divided by the number of photodiodes. The photodiodes capture the spectrum and generate electrical signals corresponding to the spectral range from 380 nm to 760 nm at the spectral interval. The electrical signals generated by the photodiodes are multiplexed, amplified, and filtered. The signal is then fed to an analog-to-digital converter and then processed by a computer.

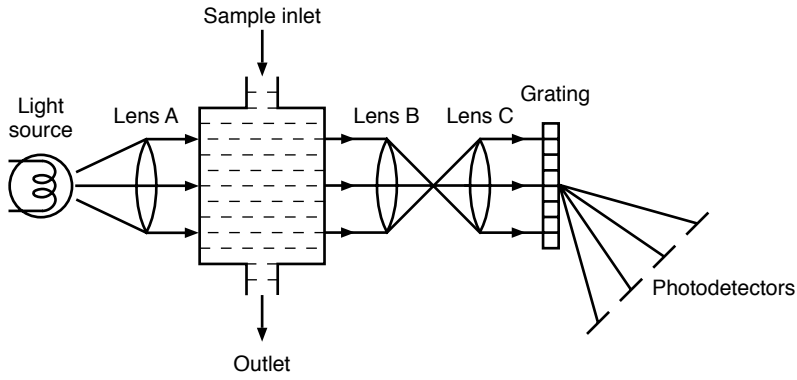

FIGURE 3.28
Setup of an optical turbidity meter.

3.5.1.5 Turbidity Measurement in the Sugar Refining Process

Turbidity measurement is very important in the sugar refining process. The raw sugar juice is acidic and turbid, with a pH value that is maintained at a level of 7.0 by addition of lime, sulfur dioxide, and then by heat treatment. In sugar refining, pH measurement is conducted where lime is added and this factor plays a vital role in determining the color of the refined sugar. The juice is heated after the addition of lime. After this process heavy precipitation is formed containing insoluble lime salts, coagulated albumin, waxes, and gums. These precipitated compounds are clarified in the clarifier. The turbidity of the clarified juice is measured. A sampling line is used to make the juice move from the clarifier continuously to the turbidity meter.

An optical absorption technique was used for relating color and turbidity with the pH value of sugar juice by Govindraj and Sankaranaryanan [8]. In the sugar refining process the color obtained in the refined sugar is amber-brown due to the clarity of the sugar juice. The International Commission for Uniform Methods of Sugar Analysis (ICUMSA) has recommended the optical range of 380 nm to 760 nm in the optical absorption method.

In their investigation the absorption pattern of the sugar juice was observed at 420 nm, 560 nm, and 720 nm. Absorption at these first two wavelengths accounts for color and the last (i.e., 720 nm) accounts for turbidity of the sugar juice. When the turbidity of sugar is minimal, the absorption value at 720 nm is also a minimum. When there is minimum absorption at 720 nm, the absorption value at 420 nm is the effective color value of the juice at 420 nm; the effective color value was also obtained at 560 nm.

In their investigation the pH value of sugar was measured and controlled and the optimum pH corresponding to the best color was detected. The light source used was a halogen lamp and the detector consisted of an array of photodiodes based on an integrated circuit (40-pin DIP Hamamatsu S2312-38Q) with a quartz window. Pure water was used as the reference material.

3.5.2 Food Color Measurement

The color of an object should be determined by studying its spectral characteristics over the entire visible spectrum. When a ray of light interacts with an object, its color is obtained. When a beam of light incidents on an object a part of the light is transmitted, some is reflected back, and some is absorbed by the material. As per this principle, the light that is reflected back is collected and dispersed into its various component wavelengths. The degree of reflectance in these wavelength regions represents the color. Food color measurement concerns only the visible range of the spectrum (i.e., approximately from 400 to 700 μm). Table 3.6 shows the color and visible spectrum wavelength relations and table 3.7 shows some conventioanl color measuring techniques. The fundamental properties of an object responsible for its color are spectral transmittance for transparent materials and spectral reflectance for opaque materials. Because most of the food items can be considered opaque, the reflectance technique is very important.

TABLE 3.6

Color and Wavelength Correspondence

Color	Wavelength (μm)
Violet	400–450
Blue	450–500
Green	500–570
Yellow	570–590
Orange	590–610
Red	610–700

TABLE 3.7

Conventional Color Measuring Techniques for Some Food Items

Food	Color	Measuring Technique (Conventional)
Refined oil	Pale, bright	Color, Colored glass matching
Flour	Creamy, bright	Optical reflectance
Wheat grain	Hard red, soft white, amber	Optical reflectance
Fermented tea	Coppery red	Chemical test, colorimeter
Made tea	Black	Colorimeter
Wine	Black, red, purple, pink, white	Colorimeter

3.5.2.1 Optical Reflectance Method

This method uses a technique of measurement of light reflected from the surface of the sample either in one dimension or in three dimensions. The three stimuli (tristimulus) correspond to amber, green, and blue as per the Commissions International de'Eclairage (CIE) standard. A continuous or on-line color spectrophotometer based on this approach is shown in figure 3.29A. This method uses a sequential comparison and flicker photometer measurement of the sample and a reference. A single filter develops the three stimuli outputs $\overline{X}$, $\overline{Y}$, and $\overline{Z}$. The CIE standard response values of the tristimulus are shown in figure 3.29B.

Another technique using the optical reflectance principle is shown in figure 3.30. It uses the International Commission for Illumination (ICI) recommended viewing and illuminating integrating sphere to illuminate the sample by a light beam sent through paralleling lenses. The color of the sample is measured per unit of percentage reflectance at closer wavelength intervals of the visible spectrum compared to a standard or reference color. The intensity of the light reflected from the sample is collected by the receiving lenses, making the light incident on a plane reflect grating. The spectrum of light is forwarded to a silicon photodiode through a slit. The spectrum resolved by the grating ranges from 400 nm to 700 nm, which is in the visible range. A stepper motor rotates in steps corresponding to the resolved wavelength to control the grating, which is coupled to the stepper motor through a reduction gear. The grating is brought to its normal incidence position with the help of an optical encoder fixed to the sensor and a photo-reflector. The

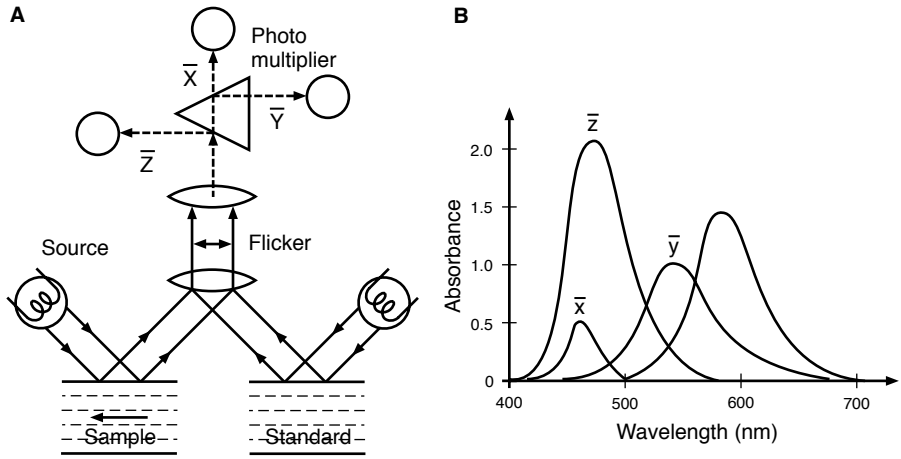

FIGURE 3.29
Fluorescence technique: (A) Schematic diagram of Tristimulus flicker method; (B) Tristimulus CIE color standard. (*Redrawn with permission from* Encyclopedia of Chemical Technology, *Vol. 6, 4e, 849. © John Wiley & Sons, Inc.*)

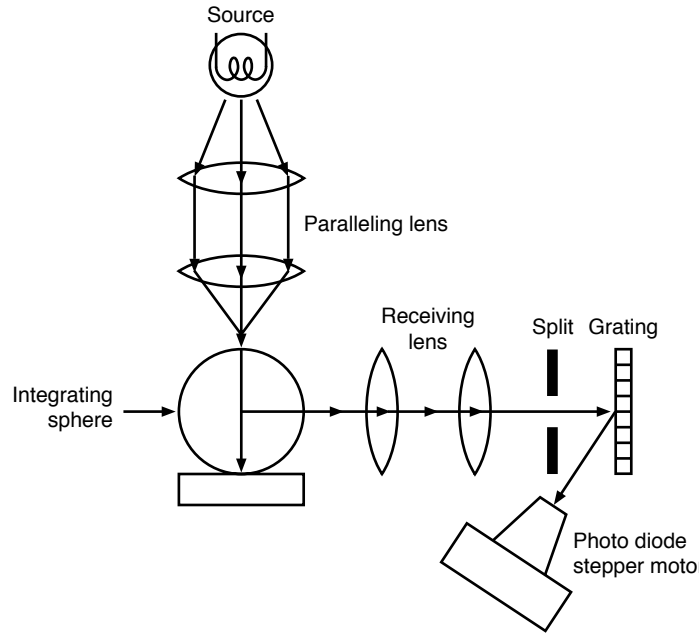

FIGURE 3.30
Schematic diagram of the optical setup of a refractometer.

current produced by the photo detector, proportional to the intensity of light, is first converted into a voltage signal, which is then amplified and fed to a computer.

If the difference of reflectance values for two samples at two equal wavelengths is equal, it can be ascertained that the shades of the two samples are the same but the concentration of color might be different. If the difference of reflectance values is not equal, it can be ascertained that both the color and the concentration are not the same. If the data are exactly the same, then both shade and concentration are the same in the two samples. Appropriate programs can be written to include these conditions in the software. The reflectance values for the sample and the standard color at different wavelengths are determined *a priori* and stored in memory. From these values the parameters are calculated and the variations for the sample and the standard color are compared.

3.5.2.2 Color Reflectance and Digital Color Image Processing in Food Grains

Color is a useful factor in determining quality in grains and an important visual attribute of cereal grains used for grading. Color measure is used to denote class and degree of soundness of grains. For example, wheat is graded on the basis of color as hard red, soft white, or amber durum. Further wheat classification as hard red wheat is made on the basis of hue and concentration. Similarly certain inferior qualities such as stained, pink immature, grass green, or bleached kernels are marks of discoloration of wheat grains.

Reflectance spectrophotometer is one of the methods by which color analysis of grains can be performed. A Spectro-reflectometer is an example of such instruments that measure the reflectance values for grains at different wavelength regions (420 nm–700 nm). These devices measure the spatially averaged color of the entire field. Selective color measurement of specific objects or geometric zones enables better grading and classification of grains. This is possible by integrating the tristimulus value determination with digital image processing capabilities. The schematic setup of this technique is shown in figure 3.31. The color data acquisition system consists of three main components:

1. The sample illumination and viewing device
2. Optical setup and image generation and signal processing
3. Digital image acquisition and processing

The sample illumination is produced by incandescent tungsten filament lamps powered by a highly regulated power supply to minimize the variation of spectra of illumination. The lamps should be hoisted on an annular platform, the height of which can be adjusted from the surface. The platform of the lamps can be centered on the viewing zone of the camera. The sample platform consists of a white, diffusely reflected foamboard for the background against which the samples are compared. Due to this background, necessary contrast is formed to distinguish the grains to be tested and a reference color. The camera is white balanced for this background.

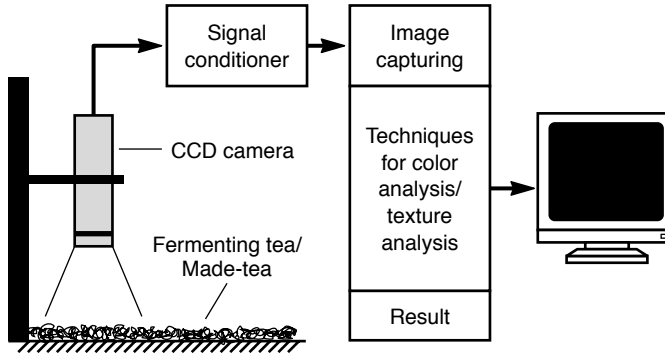

FIGURE 3.31
Measurement setup of the image capturing. (*Reprinted from PhD thesis with permission from S. Borah*)

The color-sensing device is a color television camera or a digital camera with built-in gamma compensation. The camera produces three signals—analog red, green, and blue (RGB)—and National Television System Committee (NTSC)-encoded color signals. The RGB analog signals are then fed to a camera control and signal processing unit. The coded signal from the camera control unit is fed to a color video monitor for viewing of the image to be digitized. The RGB signals are amplified to a level compatible with the inputs to the video digitizer.

The digitizing unit is a frame grabber digitizer. It converts a video frame into a 512×512 digital image with 8-bit resolution per pixel (i.e., 256 gray levels). Sequential images are acquired for digitizing the R, G, and B signals that comprise a single color image. The digitizing unit is controlled by software written in the microcomputer or by using commercial software such as Pixelview™.

System calibration should be done as follows:

1. A small central sample area of interest is digitized in successive R, G, and B images of the reflectance standard and the mean intensity value of this central window is computed. Alternatively the RGB values can be converted to a hue, saturation, and intensity (HSI) model and the hue (H) space can be used for reflectance calculation.
2. Data are collected from images ranging in reflectance from 1% to 100%. A white background is used as reference and data are collected.
3. Reflectance of the images relative to the white background is determined and displayed on the monitor.

The reflectance can be represented as a fractional value relative to the white surface. When the reflectance value increases, the grain pigmentation decreases gradually for a particular color.

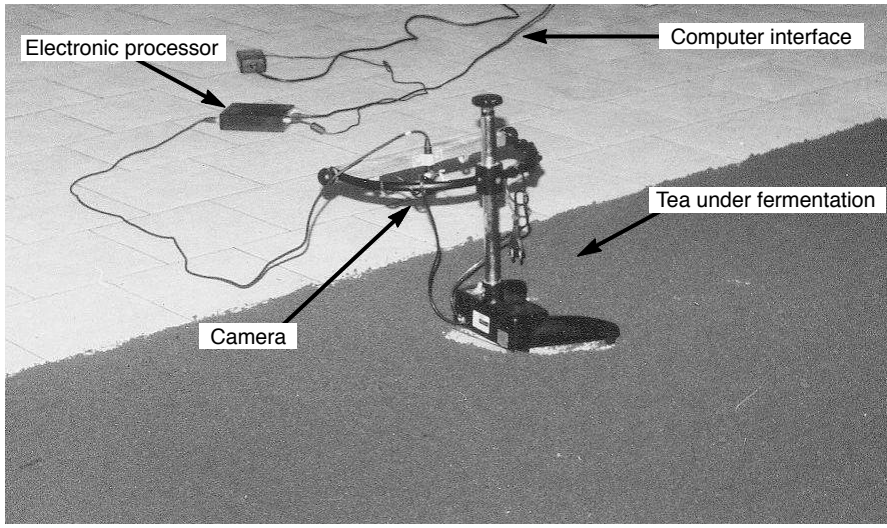

FIGURE 3.32
Photograph during capturing of fermented tea images in a tea factory.

3.5.2.3 Color Matching in Fermented Tea

A digital image processing and machine vision technique for color matching in tea fermentation was developed by Borah and Bhuyan [9, 10]. Figure 3.32 shows a photograph of the experimental setup in a tea factory.

In the black tea manufacturing process, green tea shoots are first withered, and then cut into smaller fragments to speed up enzymatic oxidation of the *catechins*. The cut tea is fermented in a controlled environment to form two groups of color compounds in the tea, theaflavins (TF) and thearubigin (TR). The analysis of the pigmenting compounds formed during fermentation of tea has been suggested by Mahanta [11]. In this method a black tea sample was collected from the dryer mouth and the sample was extracted with 40 ml of aqueous acetone. The filtrate (0.3 ml) containing about 20 mg extract is separated over a Sephadex LH-20 column into six fractions (I–VI) containing TFs and TRs along with chlorophylls and their derivatives. Table 3.8 shows the characteristics of pigment products formed during the fermentation process. The Tocklai Tea Experimental Station under the Tea Research Association, India has developed two methods of color content analysis of tea [12]. The first is based on polyphenol content of tea leaf and the second is based on the measurement of the concentration of TF formed during fermentation.

In a method developed by Borah and Bhuyan [13] color images of fermenting tea are recorded by a digital camera and fed to a signal conditioner, which in turn converts the images to a digital signal. A computer retrieves the images from the digital camera through an image capturing card. The digital camera is mounted over the fermentation table to continuously record

TABLE 3.8

Characteristics of Pigment Products During Fermentation of Tea

Fractions of TF and TR	Color Contribution	Liquor Color
Thearubigin		Reddish brown
I TR-1	8.73	
II TR-2	8.73	
III TR-3	14.3	
Ethyleacetate	28.4	Black
Chlorophylls and their derivatives	30.0	Golden yellow
IV Theaflavins		
V Theflavnimongollate		
VI Theaflavin digallate		

Source: Proc. 30th Tocklai Conference, 1988. Reprinted with permission from Tocklai Tea Experimental Station, Assam, India, Tea Research Association (India).

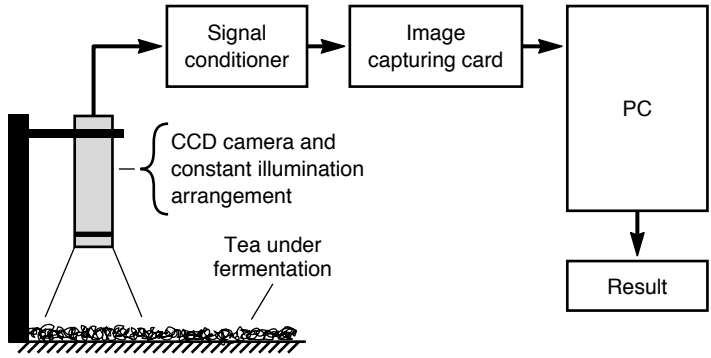

FIGURE 3.33
Schematic of the image capturing setup. (*Reprinted with permission from Int. J. Food Sci. & Tech., Vol. 40(6), Blackwell Publishing Co.*)

the images of fermenting tea. The images used by the signal conditioner are converted into a digital signal in the S-band frequency, which is then fed to the computer. The computer receives the image from the input signal with a Pixelview™ card interfaced to the computer. A schematic diagram of the setup is shown in figure 3.33.

In this technique a histogram comparison algorithm is used in matching color of fermented tea with a standard color image. By definition a color histogram is a vector where each entry stores the number of pixels of a given color of the image in RGB color space. Histogram axes are partitioned uniformly with fixed intervals by a heuristic approach to determine the bin size. The number of bins is kept small for computational efficiency but this reduces recognition accuracy. The histogram bin size fixed in the method was 32. After receiving an image, histograms were developed and plotted for each color space (fig. 3.34) and the corresponding histogram comparison for each color space was performed with the standard image using Euclidean and L1 (Manhattan) norms to quantify a similarity between two colors. Given a pair of

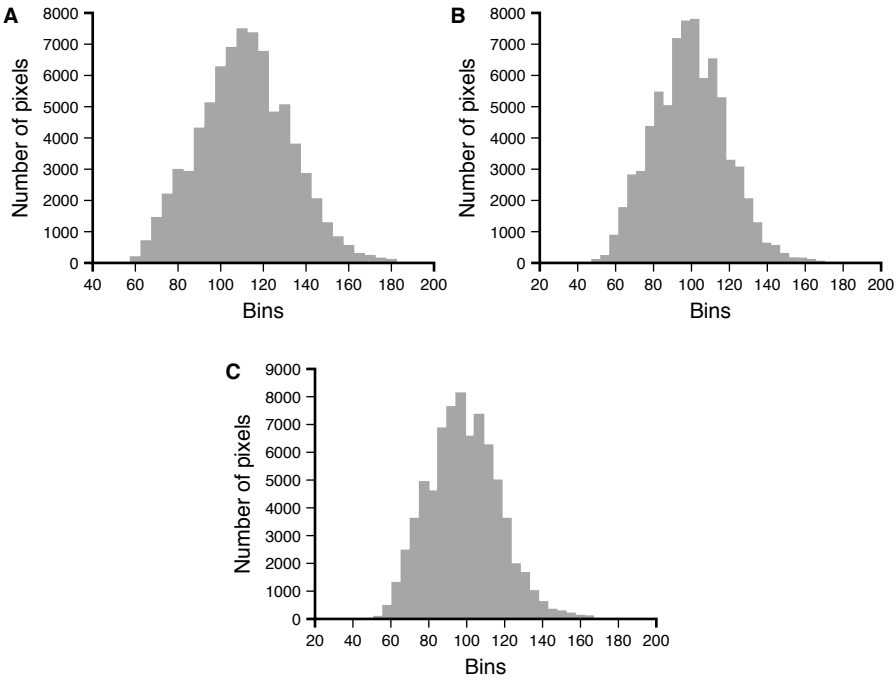

FIGURE 3.34
Color histograms of a fermented tea image: (A) Space R; (B) Space G; (C) Space B. (*Reprinted with permission from Int. J. Food Sci. & Tech., Vol. 40(6), Blackwell Publishing Co.*)

histograms *H(I)* and *H(Q)* of input image *I* and the standard image *Q*, respectively, each containing *n* bins, the defined histograms intersection is as follows

$$S\{H(I),H(Q)\}=\frac{\sum_{j=1}^{n}\min\{h_j(I),h_j(Q)\}}{N_Q\times M_Q} \tag{3.34}$$

where $h_j(I)$ = number of pixels of color j in images I and Q
$N_Q \times M_Q$ = size of the standard image

This measure can be represented by difference form (dissimilarity) as Manhattan norm (L1) as

$$\begin{aligned} D\{H(I),H(Q)\} &= \sum_{j=1}^{N}\left|\frac{h_j(I)}{N_I\times M_I}-\frac{h_j(Q)}{N_Q\times M_Q}\right| \\ &= \frac{1}{N_I\times M_I}\sum_{j=1}^{N}\left|h_j(I)-h_j(Q)\right| \end{aligned} \tag{3.35}$$

where $N_I \times M_I$ = image size

For a given distance T, two histograms are said to be similar if $S \geq T$ or $D \leq T$ and the images are of the same color.

Images of well-fermented (WF) tea (almost deep-coppery red) are stored as a standard image. Tea images were captured sequentially from the start of fermentation to completion to generate a database of images of tea during the fermentation process. This database consists of images under the categories not fermented (NF), underfermented (UF), well fermented (WF), and overfermented (OF). A dissimilarity pixel value (DPV) for all the color spaces—R, G, and B—are determined by comparing each of the sample images with the standard images. The histogram comparison method is adopted for finding the DPV of each image using the standard color images. DPV for all three spaces for the typical fermenting stages are shown in table 3.9. A dissimilarity threshold pixel level was found from a large number of images that was taken as a faithful threshold level for discriminating between

TABLE 3.9

Dissimilarity Measures for R, G, and B Color Spaces

Sample Number	State of Fermentation	DPV for R Color Space	DPV for G Color Space	DPV for B Color Space
1	NF	0.77	0.56	0.61
2	NF	0.39	0.45	0.41
3	NF	0.38	0.70	0.51
4	NF	0.45	0.41	0.62
5	NF	0.67	0.51	0.48
6	NF	0.54	0.56	0.43
7	NF	0.67	0.62	0.73
8	UF	0.36	0.40	0.39
9	UF	0.42	0.30	0.31
10	UF	0.42	0.46	0.37
11	UF	0.37	0.32	0.55
12	UF	0.35	0.43	0.52
13	UF	0.42	0.53	0.41
14	UF	0.35	0.37	0.36
15	UF	0.41	0.36	0.40
16	UF	0.31	0.35	0.41
17	WF	0.57	0.18	0.24
18	WF	0.22	0.10	0.09
19	WF	0.21	0.21	0.23
20	WF	0.13	0.24	0.25
21	WF	0.13	0.18	0.24
22	WF	0.26	0.15	0.20
23	OF	0.60	0.50	0.54
24	OF	0.30	0.48	0.49
25	OF	0.32	0.44	0.34
26	OF	0.28	0.35	0.42
27	OF	0.59	0.56	0.68
28	OF	0.36	0.33	0.51

Source: Int. J. Food Sci. & Tech., Vol. 40(6), 2005. Reprinted with permission from Blackwell Publishing Ltd., Oxford, UK.

the images. DPV calculation for the red (R) color space was done on each test sample and a decision was made as

$$\text{NF for DPV value} \geq \text{Threshold}$$
$$\text{and WF for DPV value} < \text{Threshold}$$

A prominent variation of DPV was observed for the three spaces that revealed a good correlation between sensory panel judgment and the computer-aided approach.

In a variation of this technique they used only the hue (H) space of the HSI model of the images in a similar manner. The HSI color model is better than the RGB model for its illumination intensity invariant property.

This technique shows a potentiality for adopting machine vision techniques to eliminate human error in color matching in the tea industry.

3.6 Food and Process Temperature Measurement

Different types of transducers available for the measurement of process temperature were discussed in chapter 2. However, based on the type of food material, type of control technique, precision requirements, and so on, temperature transducers can take different forms and variations in the food industry. In this section, temperature measurement in food processing situations, with a special emphasis on application conditions, is discussed.

3.6.1 Temperature Measurement in Food Processing

The primary considerations required for food temperature measurement are type of the food item (solid, liquid, viscous, etc.), accuracy needed, dynamic behaviors (stationary or moving), atmospheric conditions, thermal coupling, and so on. The simplest situation of temperature measurement is in a stationary phase of a food (i.e., while storing). For example, in cocoa butter manufacturing, liquid cocoa butter is stored where the temperature should not exceed 45°C. However, dry cocoa beans stored inside jute sacks with an increase in temperature over 20°C can develop mold within a few days. On the other hand, bulk storage of chocolate is generally done at 40°C to 60°C.

Apart from storage heating or drying in stationary mode, treatment of food items with mixing and stirring also requires simple temperature measuring devices. Such a situation might arise in production of milk compounds by mixing condensed milk or reconstituted milk, sugar, and water and heating to 74°C. In the butter manufacturing process, after pasteurization, the cream is crystallized down to 3°C to 5°C in insulated tanks for a period not less than 4 hr. This cream is again heated to a churning temperature of 7°C to 13°C before butter making.

A fundamental difficulty of temperature sensors is thermal coupling. In case of liquid foods like fruit juice, soft drink, and wines, the temperature measurement needs an equilibrium condition between the sensor temperatures. The temperature during heating or drying of moving food products also undergoes rapid variation within a local region, causing unstable sensor output. This necessitates a sufficiently strong thermal coupling and fast response. The thermal difference developed in a temperature sensor can be shown by this equation:

$$\frac{T_1 - T}{T_1 - T_0} = e^{(hA/WC_p)\theta} \tag{3.36}$$

where T = temperature
h = heat transfer coefficient at surface of sensor
A = surface area of sensor
W = weight of sensor
C_p = specific heat of sensor material
θ = time after sensor is in contact with the food

A large surface area (A) to mass ratio enables a shortened response time. Moreover, increasing heat transfer coefficient by forced convection or rapid flow of the liquid will also make the response fast. The following sections address some of these considerations in temperature transducers.

3.6.2 Thermocouples

Although thermocouples were primarily used for high temperature measurement, now they are used for a wide temperature range, from high to low. Most food processing industries use thermocouples because they are supplied with calibration standards. Food industries generally incorporate temperature measurement in the lower range, below 300°C. In most cases storage and heating are to be conducted below 100°C. Materials like lactose, polydextrose, sorbitel, xylitol, and so on melt comparatively at a lower temperature (below 300°C). The following thermocouples are generally used in process measurements:

1. Copper-Constantan
2. Iron-Constantan
3. Chromel-alumel
4. Platinum-platinum/rhodium

However due to lower operating temperatures of measurement in food processing, copper-Constantan is more widely used. The most suitable connecting lead wire for a copper-Constantan thermocouple is copper-Constantan itself. Use of the same material as lead wire reduces the error due to development of spurious thermo EMF.

3.6.2.1 Thermocouple Installations

Thermocouples must be protected from adverse environmental conditions such as corrosion and oxidation using thermal wells. Cast or milled materials such as nichrome, chromel, and iron with thick walls are reactive and give slower responses. From this point of view, ceramic materials such as vycor, sillimanite, and porcelain are more suitable as protecting materials.

To measure temperature of liquids flowing through pipes, thermocouples are employed to ensure true food temperature. A radiation shield is necessary near the hot junction of the thermocouple. To get the maximum heat transfer effect, the thermocouple inserted through the pipe should conduct heat radially and axially at the tip. For this the well should be thin and should protrude slightly beyond the center of the pipe. The well of the pipe at the point of measurement should be properly insulated. If the diameter of the pipe is very small an expander is used or the well is mounted at the bend of the pipe (fig. 3.35 and fig. 3.36).

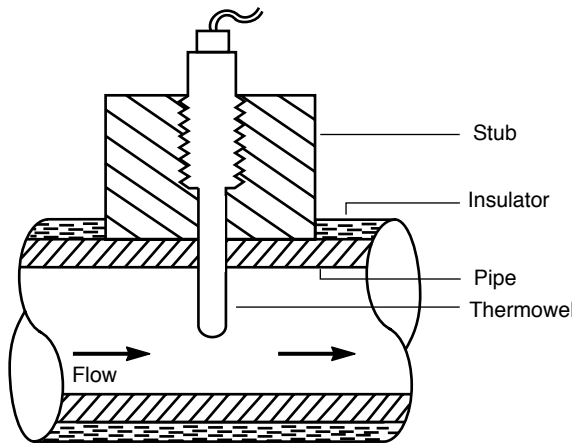

FIGURE 3.35
Thermocouple installation in a pipe.

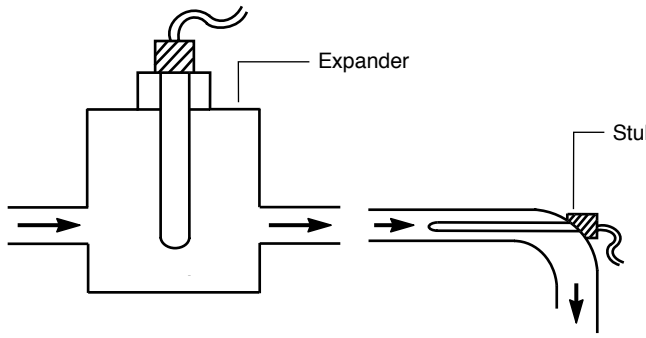

FIGURE 3.36
Thermocouple installation in small pipes.

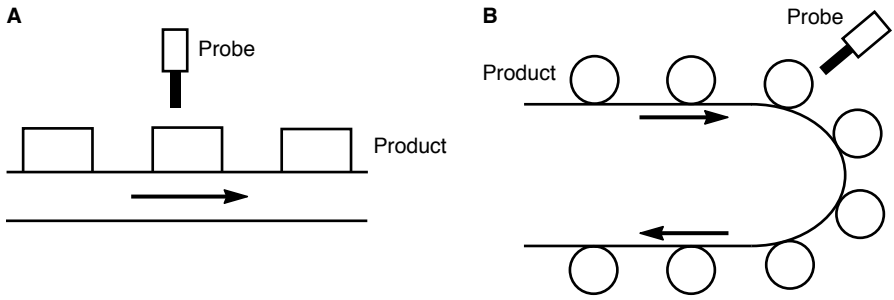

FIGURE 3.37
Temperature measurement under product in moving condition: (a) Packaging and canning; (b) Bottling.

3.6.3 Temperature of Food on a Conveyor

Special arrangements are necessary for sensing temperature measurement of food under moving conditions such as drying and pasteurization, packaging, and bottling. In such situations the sensors are either noncontacting or of traversing brush-skid design (fig. 3.37).

3.6.4 Food Tempering Monitoring

Food tempering is a process where plasticized fat of food is allowed to cool at a controlled temperature until its properties are stabilized. In chocolate manufacturing, chocolate is tempered in a tempering machine. Proper tempering requires measurement of the cooling process, which is generally done in a temper meter. A temper meter basically monitors the relation between temperature and time with the help of a thermocouple and a miniature temperature recorder. It consists of the following elements (fig. 3.38):

1. A vacuum flask
2. Ice powder to cause cooling
3. A sample tube made of good conductive material
4. A probe stud and insulator
5. A thermocouple or thermistor
6. A miniature recorder

The correctness of tempering can be determined by looking at the temperature–time graph plotted by the recorder. When the tempered chocolate (at 30°C) is poured and immersed in the flask, it starts cooling and the thermocouple senses the cooling temperature continuously.

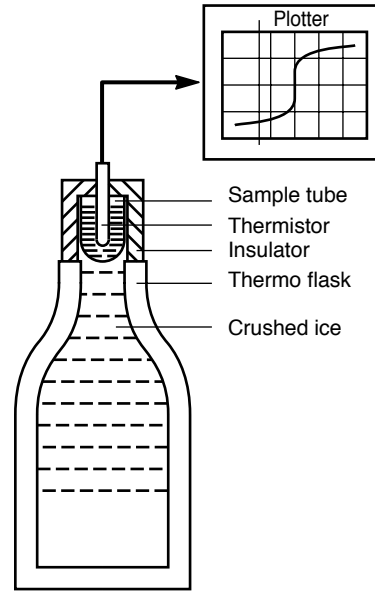

FIGURE 3.38
Apparatus for monitoring cooling curve in food tempering.

3.6.5 Precision Temperature Measurement

For temperature measurement in food processing, accuracy is needed on the order of 0.1°C. A responsible food manufacturer does not disregard a digit after the decimal point. RTDs are among the most widely used precision temperature sensors in the food industry due to their higher accuracy, simplicity, and flexibility of design. Another added advantage is their high resolution on the order of 0.01°C.

RTDs are generally made up of metallic (platinum, copper, or nickel) or nonmetallic (semiconductors) materials, the resistance of which increases as temperature increases. The resistance–temperature coefficient and melting point of platinum are higher compared to nickel and copper, for which it is found to be suitable.

In precision thermometry, platinum is used as a resistive element. A platinum resistance thermometer usually has a resistance between 10 and 35 ohms at 0°C. The element is wound over or etched on in various forms (fig. 3.39). The resistance element of the RTD is connected to the measuring circuit, which is most commonly a Wheatstone bridge circuit. The output voltage produced by the circuit is amplified and recorded or displayed by a suitable meter. Similar to thermocouples, RTD probes are also shielded by a protective sheath or well made of porcelain, brass, or stainless steel. The platinum probe is placed at the end of the well, properly insulated from the body of the well.

A probable application of precise temperature measurement using RTD in food processing is a three-stage chocolate tempering machine. Such machines are used to temper and crystallize cocoa butter to get tempered chocolate. At

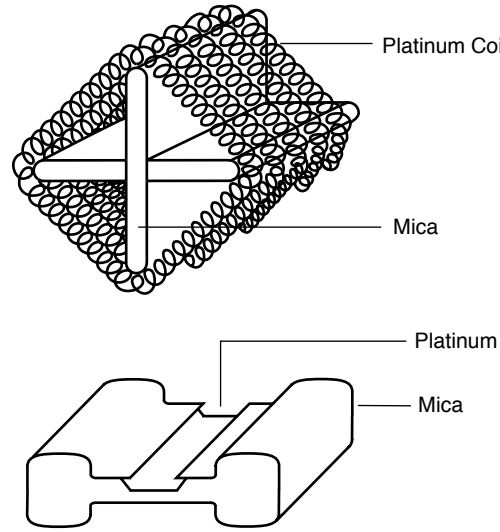

FIGURE 3.39
Platinum resistance thermometers.

every stage of tempering, RTDs can be installed to measure the temperature of both chocolate and coolant fluid. Platinum RTD probes are recommended in tempering machines to achieve accuracy to within a tenth of a degree.

3.7 Food Flow Metering

Flow measurement of liquid food materials is primarily conducted to determine the quantity or proportion of input material introduced into a processing stage. The important aspect of flow metering in the food industry is the quantity control; hence, special attention should be paid to designing a flow meter for a special applications. For example, dealing with products that solidify at high temperature like hydrogenized oil, the flow meter might be fitted with a heater. A wide variety of flow meters are available that work on different physical or electrical principles and have different advantages and disadvantages.

Turbine, variable area gap meters, and vortex shedding meters are widely used flow meters in many industrial applications, but these are not suitable for high-viscosity food fluids. Venturi tubes and ultrasonic sensors are comparatively less obstructive but are practically ineffective for liquids suspended with solid particles.

Pressure difference or the pressure drop principle is used in venture, orifice, and pitot tube flow meters. A positive displacement flow meter uses a rotary piston, oval gear, sliding vane, or reciprocating piston. In all of these techniques, a velocity head is converted to a pressure drop and the flow meter or a part of it has to be inserted into the flow pipe. Due to this obstruction of the

fluid flow, these flow meters are not suitable for food processing applications because they create problems of frequent cleaning and maintenance.

Electromagnetic, ultrasonic, and Coriolis mass flow meters are advantageous for liquids and pasty or viscous food materials.

3.7.1 Magnetic Flow Meters

There are many liquid foods that are suitable for metering by the principle of magnetic flow meter. As per Faraday's law of electromagnetic induction, when a conductor is moved through a magnetic field, an EMF is generated in the conductor that is proportional to the relative velocity between the conductor and the magnetic fluid.

The conductive principle can be applied to food items like fruit juices, yogurt, beer, citrus juice, and so on. Table 3.10 gives the conductance values of some liquid food materials. For liquids with conductivity as low as 0.1 mS/cm, special design considerations have to be made for electromagnetic flow metering. Most of the materials show higher conductivity at higher temperatures, so a liquid with marginal conductivity at a particular temperature can be metered satisfactorily at a higher temperature. Wines generally have smaller conductivity, but flow metering at higher temperature while boiling (i.e., wort) might be possible.

TABLE 3.10

Electrical Conductivity of Some Food Materials

Liquid Food Material	Conductivity (mS/cm)
Molasses (at 50°C)	5,000
Corn syrup	16
Vodka (100 proof)	4
Water (potable)	70

The schematic representation of a magnetic flow meter is shown in figure 3.40. The magnetic field (H) should be perpendicular to the flow direction and voltage induced (E) will be mutually perpendicular to both H and flow velocity (v). The mathematical relation of the induced EMF with other parameters is given by

$$e = BDv \tag{3.37}$$

where B = magnetic field strength (Tesla)
v = flow velocity (m/s)
D = diameter of the flow pipe (m)

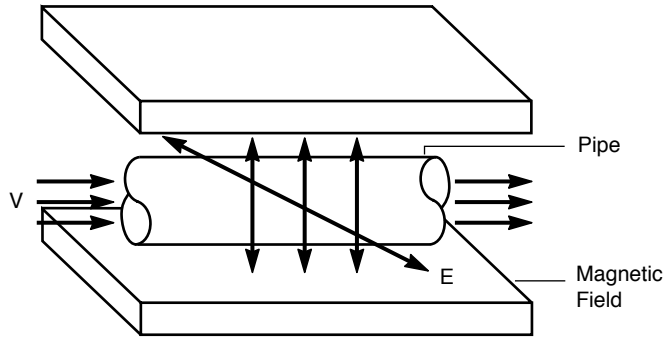

FIGURE 3.40
Schematic diagram of a magnetic flow meter.

The volumetric flow rate Q can be calculated from

$$Q = vA \tag{3.38}$$

where A = cross-sectional area of the pipe

The magnetic coils are energized either by AC or DC voltages. In the case of DC, a pulsed DC excitation can be applied. There are variations of magnetic floweters, including a pitot type. Figure 3.41 shows a pitot type of magnetic flow meter used in irregularly shaped pipes or conduits.

Magnetic flow meters are not affected by viscosity of the material as in the case of molasses or sugar syrup. The capacity of magnetic flow meters ranges from as low as 40 ml/m to 378 kl/m and can be accommodated in pipe sizes ranging from 2.5 mm to 2.4 m in diameter. The power consumption is about 20 W with DC excitation, 30 W for a 50-mm AC unit, and 0.3 kW for a 760-mm AC unit.

3.7.2 Mass Flow Metering

In food processing, in many situations, metered quantity of a food item is fed to the process to get the desired quantity of the product. For example,

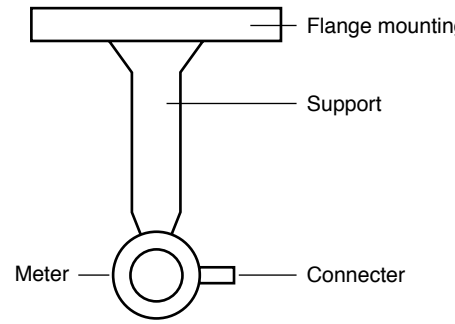

FIGURE 3.41
Schematic diagram of a pitot-type magnetic flow meter.

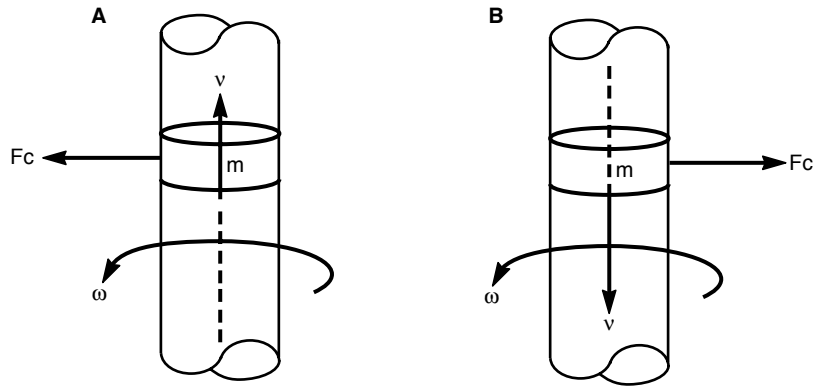

FIGURE 3.42
Fluid element in Coriolis flow meter: (A) Outward motion; (B) Inward motion.

liquid chocolate is a viscous material. When it is applied to a tempering machine in metered quantity, mass flow metering can be selected. Similarly, feeding sugar juice to a yeast fermenter, glucose solution into isomerization, and plant, liquid milk to spray dryer of spray milk production are examples where mass flow metering is essential.

All mass flow meters work on the principle that when a fluid rotates, a force is produced that is proportional to the mass of the fluid. A Coriolis mass flow meter employs a tangential acceleration produced by a fluid flowing through tube that is rotated about a fixed axis perpendicular to the tube axis. Figure 3.42 shows a fluid element of mass m flowing at constant velocity v outward away from the rotational axis of the tube rotating at a constant angular velocity ω. This rotation imparts a Coriolis acceleration given by $a_c = 2v\omega$. A Coriolis force of value $F_c = 2mv\omega$ is exerted on the fluid, which tries to push the fluid element to the left. This force is balanced by the inertial force (F_i) of the fluid pushing the fluid to the left. Due to elasticity of the tube, the inertial force deflects the tube slightly to the right. Similarly, if the fluid mass m moves inward at a constant velocity v in line with the tube axis that rotates at a constant angular velocity of ω, a Coriolis force F_c acts in the opposite direction and it is opposed by the inertial force F_i, causing the tube to deflect slightly to the right. In practice the tube is not rotated but vibrated, and the same effect is observed. A mechanical exciter is placed at the middle of the tube while the ends are fixed. The two halves of the tube act like two different tubes. Two reaction forces due to Coriolis effect are developed with opposing action and create a small displacement in the flow tube. This displacement is proportional to the mass flow rate m given by

$$F_c = 2ml\omega \tag{3.39}$$

and so

$$m = F_c / 2\omega l \tag{3.40}$$

where l is the fluid element length.

Direct measurement of the displacement or force is not possible, but the phase difference between the forces in the two halves can be measured. In practice, the tube is vibrated in sine wave pattern and the motion of the inlet tube lags behind the motion of the outlet tube. This phase difference is detected by placing a detector such as an electromagnetic pickup (measures velocity) or optical pickup (measures displacement). In the case of electromagnetic sensors, a magnet is placed in one of the tubes and a wire is placed on the other, thereby generating an EMF in the coil proportional to the relative positions of the coil and magnet. If the tube is vibrated by a sine wave, both of the detectors produce sinusoidal signals with a phase difference proportional to mass flow rate. When there is no flow, the phase difference is also zero.

An electronic circuit, a microprocessor, or a computer can be used to receive the two signals, determine the phase difference, and calibrate in terms of mass flow rate. In some cases a frequency-dependent signal might also be generated instead of a voltage or current signal. A Coriolis flow meter can be calibrated to measure volumetric flow rate, density, or temperature in addition to mass flow rate. Geometry of a Coriolis flow meter is shown in figure 3.43. Coriolis flow meters are recommended for mass flow measurements of liquids and slurries. The flow meter works well in the flow range up to 11,340 kg/min. The pipe size ranges from 1.5 mm to 150 mm. Although temperature variation might affect the accuracy of this flow meter, viscosity has no effect on its performance.

Mass flow rate of food items like beer, chocolate, fruit juice, honey, ice cream, margarine, milk, molasses, peanut butter, tomato paste, and vegetable oil can be measured by Coriolis flow meter; however, the meters are prone to clogging. The flow meter is not suitable for products in which hardening, freezing, or crystallization is observed because the flow is obstructed. In such cases a single-tube design is preferable to the dual-tube design to make

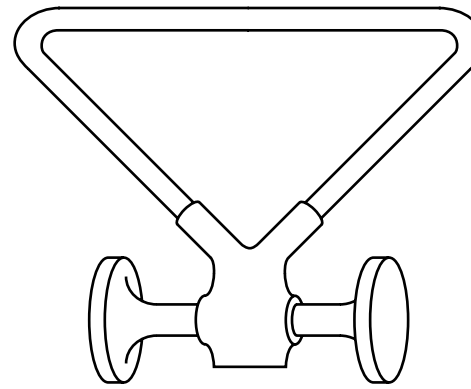

FIGURE 3.43
A Coriolis flow meter geometry.

unplugging easier. Another drawback of the Coriolis flow meter is that it is prone to vibration. This flow meter should not be installed near large pumps, vibrating sorters or sieves, vibrating conveyors, and other such equipment.

3.7.3 Turbine Flow Meter

Turbine flow meters are also in use in some food processing industries, like dairy and beverages, but they have limitations on high viscosity of the food or possible damage due to overspeeding during liquid and gas phases. If these problems can be minimized, turbine flow meters are very accurate and suitable for high-temperature fluids. The output signal of the turbine flow meter is a pulsed waveform and therefore easy to interface with a computer.

3.7.4 Positive Displacement Flow Meter

In the positive displacement flow meter, the fluid is successively divided into segments by directing and discharging it through a chamber of known volume. Oscillating pistons, lobed impellers, sliding vanes, rotating discs, and so on are used to produce the successive revolutions. The liquid should form a seal in the meter; therefore highly viscous liquid foods such as honey are suitable. Because this meter creates narrow tracks to direct and discharge the liquid, the liquid should be free from suspensions or solid particles. Because this flow meter can be operated without a power supply, it is very popular in applications like storage tank loading and process control meters for liquids like edible oil and sugar syrup.

3.7.5 Solid Flow Metering

Flow measurement of liquids and gaseous products is carried out by installing the flow meters in the pipeline or chute through which the product flows. On the other hand, transportation mechanisms like hoppers and feeders are involved in solid flow metering. In most cases of solid flow of food products, flow measurement is performed for metered dosing. The transportation mechanism is automatically controlled to transport or feed a measured quantity of the solid food. For example, in a cocoa butter press, the cocoa kernels are transported from the cocoa kernel container to the hydraulic press through a metered dosing mechanism. In such situations either manual or controlled dosing or an automated set-level dosing method is used. Therefore in designing a solid flow meter, the design aspects of the supply bin and feeder should also be taken into consideration. A good design of the surge hopper is also important to provide an accurate flow metering.

Throttling and metering the flow of solid material to the feeders are performed in various ways. Most of these devices work on the weighing principle, in which they determine the weight of material passing a given point.

3.7.6 Gravimetric Feeder Meters

These meters comprise a weight-rate measuring device with a volumetric control mechanism. The vertical gate gravimetric feeder is not advantageous for throttling flows of large particle size, fibrous materials, and grains of irregular shape. These feeders are generally designed to produce typical material ribbon of widths of 50 mm to 457 mm and to regulate depth of material up to 152 mm on the weight belt. The opening and closing of the gate can be actuated by electromechanical solenoids, pneumatic actuators, or servomotor-controlled actuators.

3.7.6.1 Rotary Vane Feeder

The assembly of a belt type gravimetric meter with a rotary control is shown in figure 3.44. The rotary vane feeder is suitable in a volumetric feed section where the material is aerated and has a low bulk density. Similar to the vertical feeder, a rotary feeder is also not suitable for handling materials that have large particles and in some cases are not desirable for fibrous or stringy materials. The rotor speed determines volumetric capacity. If a very high flow rate is desired the rotor speed must be high; however, in such situations the rotor pockets might not be completely filled with the materials. Under such circumstances, the use of rotary vane feeders is limited to free-flowing materials, such as salt, sugar, and tea grain.

3.7.6.2 Screw Feeder

In a screw feeder, the rotary motion of a screw element controls the delivery of the material. A hopper delivers the material at the start of the screw feeder or at the middle. The hopper is mounted so that the screw feeder is always filled with the material. Screws grooved in one direction deliver material to one end only and screws grooved in the opposite direction from the center

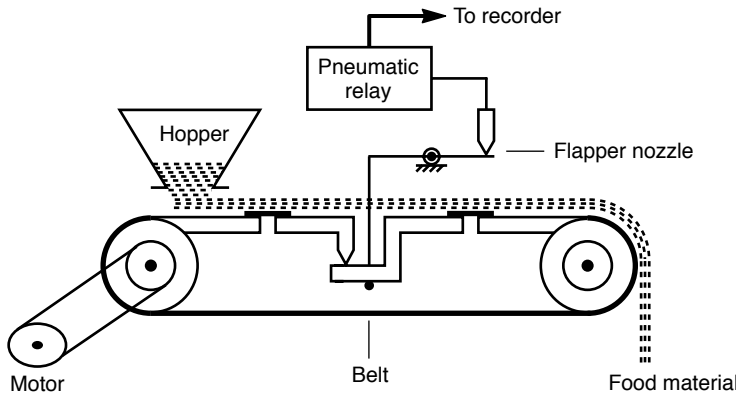

FIGURE 3.44
Schematic diagram of a belt-type gravimetry meter.

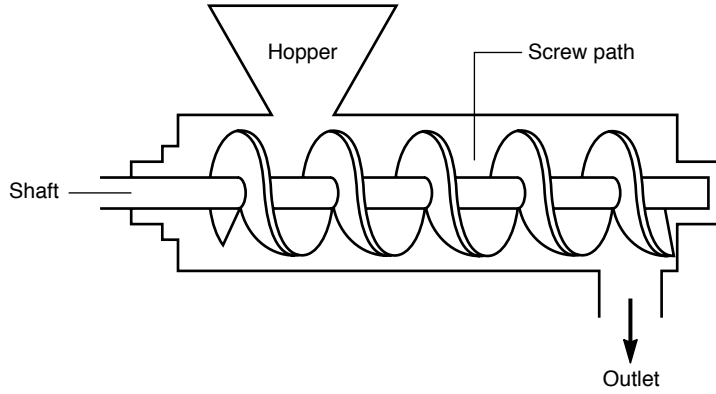

FIGURE 3.45
Sectional view of a screw feeder.

deliver material to both ends. A long screw section prevents flooding of material through the screw feeder. Screw feeders can be custom built to facilitate feeding of fibrous and coarse lumps. Materials prone to clogging can be accommodated using a double-ended screw feeder with lateral oscillatory motion imparting a cleaning action. In such designs the material is fed alternately from both ends and the direction of screw rotation is altered accordingly. Figure 3.45 shows a cross-sectional view of a screw feeder.

3.7.6.3 Belt Feeder

In belt feeder a belt driven by electric motor and revolving around a specific distance is used as the conveyor device. Because the quantity of material is not controlled, the measurement can be performed by metering the belt speed and a weight-sensing transducer installed below the belt. The feeder is added with a volumetric flow regulator that can be a simple gate or a rotary gate, a screw, or other volumetric control devices. Figure 3.46 shows a simple belt feeder added with a flow regulator. The gate is adjusted such

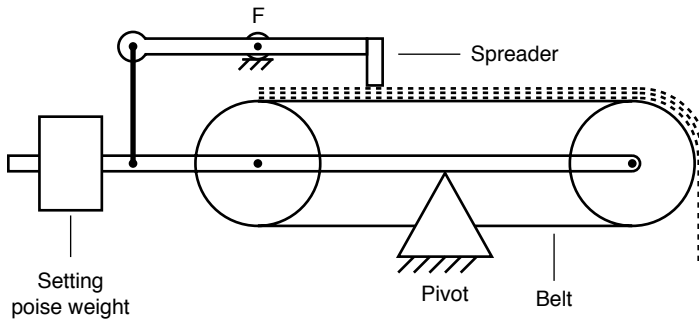

FIGURE 3.46
A belt feeder flow rate sensing and controlling.

that the belt load is balanced by an adjustable poise weight. Although this feeder is very popular in industries, its performance is affected by a number of disadvantages.

3.8 Viscosity of Liquid Foods

3.8.1 Definition and Units

Viscosity is the property of a liquid that describes the amount of resistance offered by the liquid due to shear forces developed within it. Let us consider two parallel layers of a fluid separated by a distance Δy as shown in figure 3.47. The upper layer is subjected to a constant force F and moving in the direction of the force. The upper layer moves at a constant velocity Δu while the lower layer is stationary. It is found that the force F is directly proportional to velocity Δu and surface area A of the layers and inversely proportional to the separation distance Δy. This can be expressed mathematically as

$$F \propto A\frac{\Delta u}{\Delta y} \tag{3.41}$$

or

$$F = -\mu A\frac{\Delta u}{\Delta y} \tag{3.42}$$

The shear stress is given by

$$\sigma = F / A \tag{3.43}$$

where μ is a proportionality constant and is called the coefficient of viscosity or dynamic viscosity. The negative sign indicates that the momentum gradually

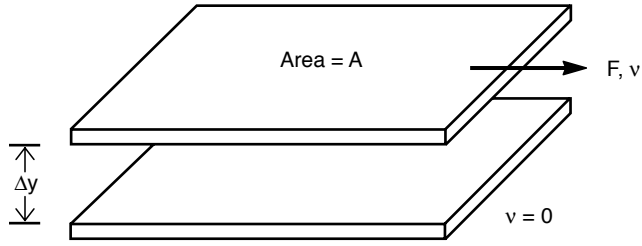

FIGURE 3.47
Fluid layers to illustrate viscosity.

decreases fromtop layer to bottom layer from high- to low-viscosity region. In equation 3.42, if Δy tends to zero the shear stress becomes

$$\sigma = F / A = \mu(-\frac{du}{dy}) = \mu\gamma \tag{3.44}$$

and so

$$F = \mu A \frac{\Delta u}{\Delta y} \tag{3.45}$$

where the term γ is called the rate of shear or shear rate. From equation 3.44

$$\mu = \frac{\sigma}{du / dy} \tag{3.46}$$

The unit of dynamic viscosity in MKS (meter, kilogram, second) system is

$$\frac{N / m^2}{1 / s} = \frac{Pa}{1 / s} = Pa.s$$

The unit of viscosity in a CGS (centimeter, gram, second) system is

$$\frac{dyne / cm^2}{1 / s} = \frac{dyne.s}{cm^2} = poise \qquad [1 \text{ Pa.s} = 10 \text{ poise}]$$

Poise is the practical unit of viscosity and it is often expressed in centipoise (0.01 poise). There is one more way of expressing viscosity, the kinematic viscosity, which is the ratio of viscosity and density of the liquid, expressed as

$$\text{Stokes} = \upsilon = m^2/\text{sec}$$

3.8.2 Newtonian and Non-Newtonian Food Flow

Newton's law of fluid friction gives the relation between shear stress in fluid and the velocity gradient as

$$\sigma = \mu \frac{\Delta u}{\Delta y} = \mu\gamma \tag{3.47}$$

In food industries, food viscosity plays an important role in various situations. For example, during spreading of food, a low viscosity is desirable, whereas for chewing or swallowing, the food should possess a higher viscosity.

Shear thinning behavior is exhibited in some fluid foods where viscosity decreases with increasing shear rate. Fruit purees, chocolates, and meat pastes are examples of such food materials.

Equation 3.44 describes the flow dynamics of a Newtonian fluid. Some food materials like honey, fluid milk, fruit juice, and cold drinks exhibit Newtonian characteristics, whereas molten chocolate is a non-Newtonian fluid. Molten chocolate is a suspension mixture of sugar particles, cocoa, and milk solids. It behaves as a non-Newtonian fluid due to the presence of solid particles. In food industries various fluid food materials, including milk products, glucose syrups, gums, chocolate, praline pastes, caramels, toffee, dough, flour batter, chewing gums, and fats, show non-Newtonian behavior in viscosity. Table 3.11 shows some food items with their viscosity values and table 3.12 gives shear rate for some food items with their importance of processing.

There are basically two types of non-Newtonian liquids: time independent and time dependent. The first type flows immediately when a shear stress is applied. In the second type, there are two classes: shear thinning and shear thickening liquids. In the case of shear thinning liquids, the apparent viscosity decreases as the shear rate is increased; therefore, apparent viscosity is expressed along with the shear rate to define its flow property. Condensed milk, fruit purees, mayonnaise, mustard oil, and vegetable soups are examples of shear thinning liquid foods. When the apparent viscosity increases with shear rate the liquid is called a shear thickening liquid. Examples of

TABLE 3.11

Viscosity Values of Some Food Materials

Food Material	Viscosity (Pa.s)
Coffee cream	0.01
Vegetable oil	0.10
Honey	10.00
Mayonnaise	4.2
Apple sauce	7.32
Banana puree	107.3
Water	0.001

TABLE 3.12

Shear Ratios with Process Importance of Few Food Materials

Food Material	Shear Ratio	Process Operation
Salad dressing	10^{-6}–10^{-4}	Setting of fine suspensions
Vegetable oil	10^{-1}–10^{1}	Gravity draining
Snack food, cereals	10^{0}–10^{2}	Extrusion
Chocolate, sauces	10^{0}–10^{3}	Pipe flow
Most foodstuffs	10^{1}–10^{2}	Chewing and swallowing
Fruit squashes	10^{1}–10^{3}	Mixing and stirring
Margarine, butter	10^{2}–10^{4}	Spreading

shear thickening foods are homogenized peanut butter and a 60% suspension of corn syrup in water.

Time-dependent, non-Newtonian liquids behave as stable fluids only after a finite time of application of a shear stress. Starch paste and fruit juice are examples of time-dependent, non-Newtonian liquid foods. These are also called Bingham liquids. If the response is similar to a shear thinning liquid even after application of yield stress, the liquid is called plastic. Chewing gum is a good example of a plastic food.

Viscosity of food requires measurement and control not only for achieving the required quality of mouthful for bottling and canning, but also to estimate the mechanics of flow, spreading, extrusion, and so on. A pump manufacturer always must know the viscosity and shearing ratio range of the food material before designing a pump for that particular food. Power rating and geometry of mixing and stirring machines depends on the viscosity of the food.

One important factor on which viscosity depends is the temperature. Viscosity decreases rapidly with an increase in temperature. For example, temperature sensitivity of viscosity for water is 3%/°C at room temperature, whereas this temperature sensitivity at 100°C is 1%/°C.

Problem 3.2

Water is mixed with corn syrup and the force needed to mix two layers of the product can be calculated by finding the relative force developed between them. Assume that the layers are 0.15 cm apart. The velocities at which the ingredients are injected into the mixing chamber are 10 cm/sec for water and 8 cm/sec for corn syrup. The temperatures and coefficients of viscosity of water and corn syrup are 15°C and 0.011 poise and 37°C and 280 poise, respectively. Take unit layer areas for both. How can the force on corn syrup be reduced to half? Assume that the temperature–viscosity sensitivity of corn syrup is 5%/°C.

SOLUTION

Given data

Unit area of the layers = A = 1 cm^2
Distance between the layers = y = 0.15 cm
Viscosity of water at 15°C = μ_{25} = 0.011 poise
Viscosity of corn syrup at 37°C = μ_{37} = 280 poise
Velocity of water = 10 cm/sec
Velocity of corn syrup = 8 cm/sec

The relative velocity between water and corn syrup

$$(10 - 8) \text{ cm/sec} = 2 \text{ cm/sec}$$

The force required on the water layer from equation 3.45

$$F_W = (0.011)(1)(2)/0.15$$
$$= 0.146 \text{ dyne}$$

Similarly the force required on the corn syrup layer

$$F_{CS} = (280)(1)(2)/0.15$$
$$= 3733.33 \text{ dyne}$$

The force required to move the corn syrup layer can be reduced by increasing the temperature of corn syrup because viscosity decreases if temperature is increased. If the temperature is reduced, the viscosity of corn syrup can be calculated as follows:

The viscosity of corn syrup at 37°C = 280 poise.

To decrease the viscosity by half (i.e., 140 poise), the reduction percentage is 50%.

The required decrease in temperature

$$= \frac{50[\%]}{5[\%/°C]} = 10°C$$

3.8.3 Laboratory Type Saybolt Viscometer

A Saybolt viscometer is a laboratory type viscometer used to measure kinematic viscosity. The principle of operation of the Saybolt viscometer is based on measurement of the time required to drain a constant quantity of the liquid through a capillary tube. A schematic diagram of the Saybolt viscometer is shown in figure 3.48. In this arrangement a capillary is connected at the bottom

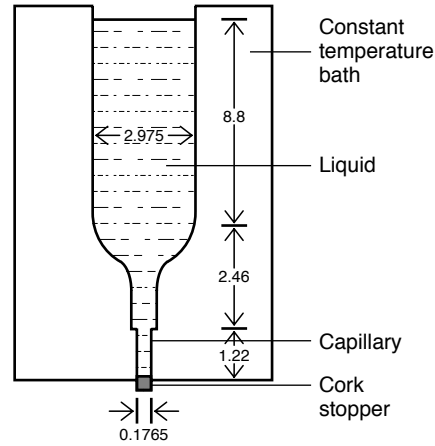

FIGURE 3.48
Schematic diagram of a Saybolt viscometer. (All measurements in cm.)

of a graduated cylinder. The cylinder is placed inside a constant temperature bath. The time (t) required to drain 60 ml of the liquid is used to calculate the viscosity. An empirical equation used for the calculation of viscosity is

$$\upsilon = At - \frac{B}{t} \tag{3.48}$$

where t = time to drain the liquid (in sec or degrees for Engler viscometer)
A and B are two constants

Two variations of the Saybolt viscometer based on the amount of liquid to be drained are: the Redwood viscometer, where the amount of collecting liquid is 50 ml, and the Engler viscometer, where it is 200 ml. The constants A, B and the quantity of collecting liquid for these three viscometers are as follows:

Viscometer	A	B	Q
Saybolt	0.22	180	60 ml
Redwood	0.26	172	50 ml
Engler	1.47	374	200 ml

The unit of kinematic viscosity expressed by these viscometers is m^2/sec. This type of viscometer is also called an efflux cup viscometer.

On-line viscometers commonly used in food industries are capillary tube, rotameter, and rotating cylinder.

3.8.4 Capillary Tube Viscometer

This type of viscometer works on the principle of Hagen Poissulle's laminar flow equation:

$$Q = \frac{\pi R^4 \Delta P}{8\mu L} \tag{3.49}$$

where Q = volumetric flow rate of the liquid through the capillary
L = length of the capillary
R = radius of the capillary tube
μ = dynamic viscosity
ΔP = pressure drop across the capillary

A schematic arrangement of this viscometer is shown in figure 3.49. The liquid is forced to move through the capillary at a constant flow rate by a constant flow pump. A pressure differential transmitter converts the pressure difference between the entry and exit of the capillary to an electrical signal.

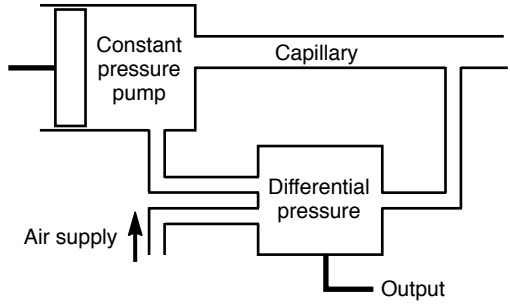

FIGURE 3.49
Schematic diagram of a capillary tube type viscometer.

A commercial model of a capillary flow viscometer is equipped with these other accessories:

- Y strainer: It is externally connected to filter the liquid with an aperture of about 150 microns.
- Filter: It protects the capillary from coke particles smaller than 250 microns.
- Relief valve: It protects the flow system against excessive pressure that might develop due to blockage of capillaries.
- Heat exchanger: It provides constant temperature by an oil bath with deviation less than ±0.005°C.
- Oil bath stirrer: It uses two hollow blades for oil to flow radially.
- Temperature controller: It detects bath temperature by a resistance thermometer and implements a PI controller.
- Heater: It uses an immersion electric heater.
- Temperature set: It is a 10-turn potentiometer resistor.

The measurement range of the viscometer is 0 to 250 poise with an accuracy of ±1%. For implementing the viscometer for on-line application, a sampling system with a bypass line is used to draw a metered quantity of the liquid from the main flow line.

Problem 3.3

A capillary tube viscometer is used to measure the viscosity of vegetable oil at 30°C. The capillary tube measures 2 cm in diameter and 20 cm in length. The differential pressure transmitter transmits a pressure signal of 4.8 Pa at a constant flow rate of 1.55 cm^3/sec. Determine the viscosity of the oil.

SOLUTION
Given data

$$\Delta P = 4.8 \text{ Pa}$$
$$R = 2 \text{ cm} = 0.02 \text{ m}$$
$$L = 20 \text{ cm} = 0.2 \text{ m}$$
$$Q = 1.55 \text{ cm}^3/\text{sec} = 1.55 \times 10^{-6} \text{ m}^3/\text{sec}$$

From equation 3.49

$$\mu = \pi\,(4.8)(0.02)^4/(8)(0.2)(1.55 \times 10^{-6})$$
$$= 0.97 \text{ Pa.s}$$

3.8.5 On-line Variable Area or Rotameter Type Viscometer

A variable area or rotameter type viscometer is shown in figure 3.50. This viscometer works on the principle that under a constant flow rate the position of a viscosity-sensitive float bob in a tapered tube is a function of the liquid viscosity. A constant flow of the liquid is maintained in a bypass line of the flow using a constant flow pump. A flow rate float bob, immune to viscosity, is set to the index mark by adjusting the flow rate. The other bob is viscosity sensitive and its position on the tapered area of the meter indicates the viscosity of the liquid. The core of a double solenoid inductive sensor or a linear variable displacement transducer (LVDT) is attached to the viscosity-sensitive bob so that the inductive sensor can sense its position.

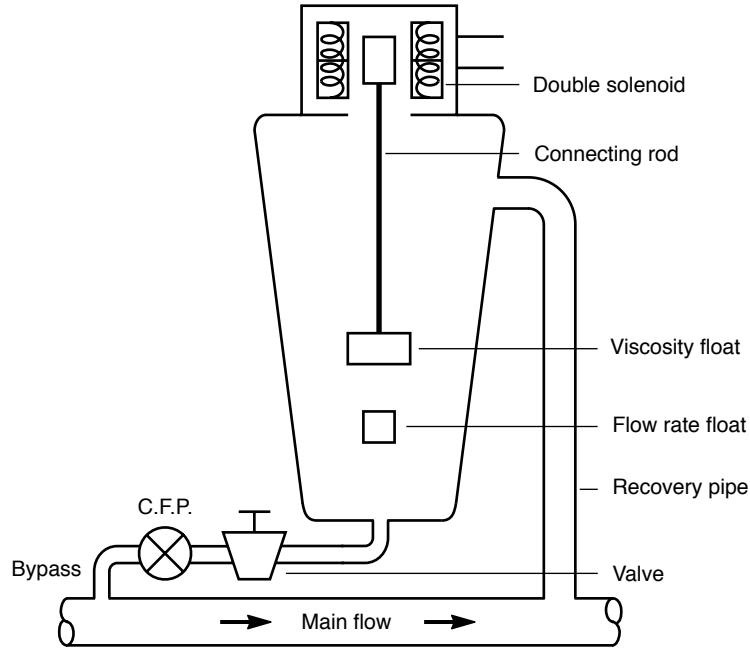

FIGURE 3.50
Schematic diagram of a variable area viscometer.

The force balance conditions of the viscosity-sensitive float bob can be expressed as follows:

Force due to the weight of the bob acting downward is

$$F_w = V_f(\rho_2 - \rho_1)$$

where V_f = velocity of the fluid
ρ_2 = density of the float material
ρ_1 = density of the liquid

If the fluid pressures downward and upward are F_d and F_u, respectively, and the viscosity drag force acting upward is F_v, then under equilibrium condition

$$F_v + F_u = F_w + F_d \tag{3.50}$$

The effect of upward and downward pressures due to flow can be made equal to zero by proper design of the rotameter. Therefore,

$$F_w = F_v$$

$$V_f(\rho_2 - \rho_1) = A\mu \frac{V_f}{d}$$

so the viscosity

$$\mu = \frac{(\rho_2 - \rho_1)d}{A} \tag{3.51}$$

Because the float is free it moves upward in a direction of flow and increases the gap d between the tapered wall and float. The new float position is a measure of the viscosity. The relation between the gap distances d with the linear displacement x is shown in the geometric diagram of figure 3.51. The change in gap distance per unit displacement can be expressed as

$$d = x \tan \frac{\theta}{2} \tag{3.52}$$

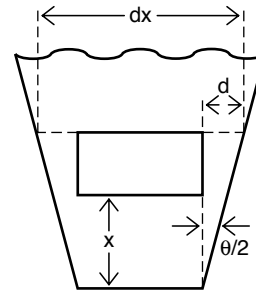

FIGURE 3.51
Geometry of float position, gap distance, and displacement.

Hence the displacement x can be used to calibrate viscosity.

This viscometer is suitable for recording and control applications and can be used in closed or open systems under pressure or vacuum. The measurement range of this viscometer is 0 to 300 centipoise.

In food processing, lower range viscosity of liquids like vegetable oil, coffee cream, fruit juice, and soft drinks can be measured by rotameter type viscometers.

3.8.6 Rotating Cylinder Viscometer

A rotating cylinder viscometer is illustrated in figure 3.52. The inner cylinder is rotated at an angular velocity ω where the outer cylinder is fixed. The gap between the two cylinders is filled with the liquid. The relation between torque T and shear stress σ can be shown by

$$T = 2\pi b^2 L\sigma \tag{3.53}$$

where L is the length of the cylinders and b is the gap between the two cylinders. The shear rate γ for the rotating cylinder as a function of the angular velocity ϖ is given by

$$\gamma = b(-\frac{d\varpi}{db}) \tag{3.54}$$

Using equation 3.45, equation 3.52, equation 3.53, and equation 3.54 we get

$$\frac{T}{2\pi L b^2} = -\mu(b\frac{d\varpi}{db}) \tag{3.55}$$

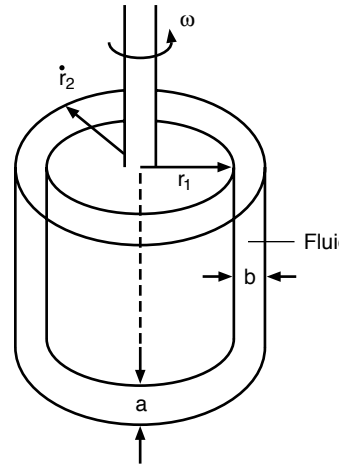

FIGURE 3.52
Rotating cylinder viscometer.

Integrating $d\varpi$ and db terms from the outer layer to the inner layer of the liquid we get

$$\int_0^{\omega_i} d\omega = \frac{T}{2\pi\mu L}\int_{r_2}^{r_1} b^{-3}db \tag{3.56}$$

The outer layer is stationary and the inner layer is moving, and putting these limits in the preceding equation we get

$$\omega_i = \frac{T}{4\pi\mu L}\left(\frac{1}{r_1^2} - \frac{1}{r_2^2}\right) \tag{3.57}$$

then

$$\mu = \frac{T}{8NL\pi^2}\left(\frac{1}{r_1^2} - \frac{1}{r_2^2}\right) \tag{3.58}$$

because $\varpi_i = 2\pi N$.

Using equation 3.58 viscosity of the liquid can be determined by measuring the torque T required to rotate the inner cylinder at an RPM level of N.

The rotating cylinder viscometer can also be implemented by a single inner cylinder on the assumption that the wall of the outer cylinder has no influence on the shear stress on the liquid. This assumption makes r_2 approach infinity and equation 3.58 can be written as

$$\mu = \frac{T}{8NL\pi}\left(\frac{1}{r_1^2}\right) \tag{3.59}$$

Equation 3.59 works well for Newtonian fluids but a careful evaluation is necessary for each liquid.

Problem 3.4

Viscosity of tomato sauce is measured by a rotating cylinder viscometer. The torque and speed of rotation at two different measurements are

N(RPM):	60	120	300
T(N-m):	1.97	2.64	4.09

The inner cylinder has a radius of 2.5 cm and the radius of the outer cylinder is 2.6 cm. The length of the cylinder is 4 cm. Determine the viscosity of the material.

SOLUTION
Given data

$$L = 4 \text{ cm} = 0.04 \text{ m}$$
$$r_1 = 2.5 \text{ cm} = 0.025 \text{ m}$$
$$r_2 = 2.6 \text{ cm} = 0.026 \text{ m}$$

For the first set of measurement data

$$N = 60$$
$$T = 1.97 \text{ N-m}$$

From equation 3.58 the viscosity is

$$\mu = \frac{(1.97)}{(8)(\pi^2)(60)(0.04)}\left[\frac{1}{(0.025)^2} - \frac{1}{(0.026)^2}\right]$$

$$= 1.25 \text{ Pa.s}$$

Similarly for the other two sets of measurement data the viscosity values are calculated as 0.84 Pa.s and 0.52 Pa.s.

Taking the mean of the three viscosity values we get

$$\mu = (1.25 + 0.84 + 0.52)/3$$
$$= 0.87 \text{ Pa.s}$$

A contrave viscometer is the commercial-form design based on the principle of the rotating cylinder viscometer as shown in figure 3.53. In this viscometer the cylindrical measuring bob is rotated at a known velocity by a synchronous motor in the liquid, producing a uniform shear stress. The torque required to maintain the shear stress depends on the viscosity of the liquid. This shear stress is measured by measuring the torque reaction produced on the driving motor balanced by the twisting moment produced in

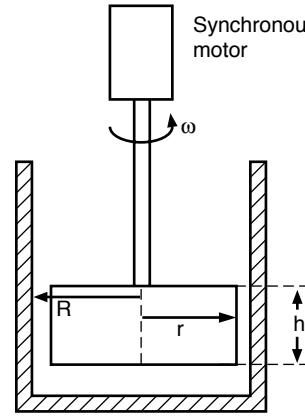

FIGURE 3.53
A contrave viscometer.

a suspension system. The suspended system turns to establish equilibrium and the angle of turn is proportional to shear stress developed on the measuring bob. The torque measuring system is isolated from the process system by a magnetic coupling. By using a linear potentiometer the torque deflection is converted to an electrical signal. In a manual indication system a torque deflection pointer over a calibrated scale is used.

3.9 Brix of Food

Brix is primarily the measure of sugar (sucrose) concentration of a food, but many other quality attributes of food can be ascertained from this parameter. On-line measurement of brix in food processing is important from both the quality and preservation point of view, to prevent the development of bacteria and retain the taste, aroma, and shelf life of packed products like jam, syrup, fruit pulps, juices, and so on. Table 3.13 shows brix degrees of various food products. This parameter is commonly measured by a brix hydrometer calibrated directly to read in percentage w/w of sugar. However, there is a correlation of brix with the refractive index (RI) of sugar-containing liquid foods such as soft drinks or concentrated syrups at 20°C. This measurement is calibrated to the International Sugar Scale that expresses the result in degree brix.

Manufacturing process of chocolate confectionary uses sugar in dry powdered form or in liquid form. Cannery pure sugar, for canning in liquid form, is delivered by tankers and stored in tankers. This sugar is mostly cane or beet sugar dissolved in water to about 65% sugar syrup. The canners generally code and defines fruit juice (10–30), light syrup (15–30), syrup (15–30), heavy syrup (20–40), extra heavy syrup (40–50) and fruit jam (60–68) in terms of degree brix. The best range of syrup strength for dessert meal is 35 to 40 degree brix. Brix of food is related to specific gravity in terms of rheological property. Table 3.14 shows brix and specific gravity relationship of sugar syrups for some specific values.

TABLE 3.13

Brix (%) Values for Some Food Products

Food Product	Brix (%)
Tomato juice	0–25
Light syrup	10–15
Fruit juices	10–30
Syrup	15–30
Heavy syrup	20–40
Exra heavy syrup	40–50
Fruit jams	60–68
Chocolate syrup	12–72
Strawberry jam	36–82

TABLE 3.14

Specific Gravity Corresponding to Brix of Sugar Syrup

Degree Brix (%)	Specific Gravity
10	1.040
15	1.061
20	1.083
25	1.106
30	1.129
35	1.158
40	1.179
45	1.205
50	1.232
55	1.260
60	1.288
65	1.319
70	1.350

Problem 3.5

An on-line brix meter is required to measure degree brix of a sugar syrup and transmit the signal to a controller to control the brix to a value 50° brix. The total weight of sugar used is 500 kg. Find the required volume of the sugar syrup obtained by adding water.

SOLUTION

Weight of sugar = 500 kg
Target brix = 50°
From table 3.15, the specific gravity of sugar syrup at the required brix is 1.232
Hence water to be added = 500/1.232
= 405.84 liters

TABLE 3.15

Refractive Indexes for Some Brix Values of Sucrose Solutions at 20°C

Degree Brix	Refractive Index
4.821	1.34
17.679	1.36
29.376	1.38
40.091	1.40
49.979	1.42
59.170	1.44
67.771	1.46
75.862	1.48
83.500	1.50

Source: TIMA-96, India, 1996. Adapted with permission from R. Sridhar.

3.9.1 Brix Standards

Although degree brix is a standard unit in the sugar industry for indicating the sucrose content, some sugar industries use the Twaddel degree for sugar syrups. The Twaddel degree is defined as

$$°T_w = 200(SG–1.0) \tag{3.60}$$

Here Twaddel divides the specific gravity (SG) range between SG = 1.0 and 2.0 into 200 equal parts each of 0.005 SG values.

The dairy industry uses the Quevene degree for measuring the fat content of milk where each degree corresponds to 0.001 SG (based on water with SG = 1.0) in excess of SG = 1.0, therefore

$$40°Q = 1.04\ SG$$

that is,

$$°Q = (SG–1.0)(1000) \tag{3.61}$$

The brewery industries use Sikes, Richter, or Teller scales on their alcohol meters. This is volumetric percentage of ethyl alcohol in water given as

$$°S, °R, \text{ or } °T = \text{volume } \% \text{ of ethyl alcohol}$$
$$°S, °R, \text{ or } °T \text{ multiplied by } 2 \tag{3.62}$$

$$\text{i.e., Proof} = 2(°S, °R, \text{ or } °T) \tag{3.63}$$

3.9.2 Refractometers

Refractometers are very popular as brix measuring meters that give monitoring in both off-line and on-line environments. Brix has a well-defined correlation with the RI of a liquid. A stick dipped in pure water looks straight, whereas if sugar is added to the water, the stick will appear bent or broken. The reason is that the RI of the sugar syrup is higher than pure water. The RI of air is 1.0003 and for most gases, solids, and liquids it varies between 1 and 2. A basic refractometer measures the RI of a liquid sample, which is given by the following equation:

$$\mu = \frac{v_0}{v_m} \tag{3.64}$$

v_0 = velocity of light in vacuum
v_m = velocity light in the material

Snell's law gives the relation between the angle of incidence and angle of refraction of light. When a ray of light passes through a medium of lower

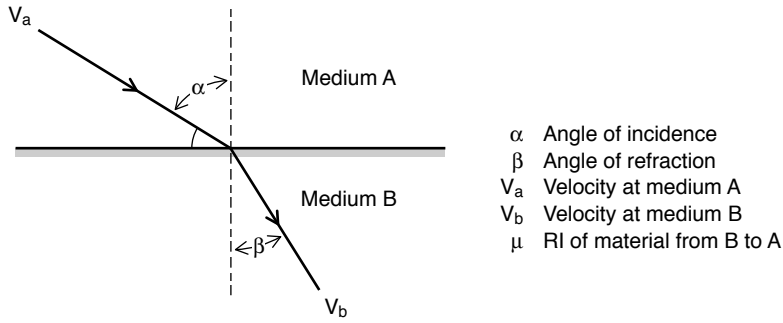

FIGURE 3.54
Illustration of refraction of light.

RI to a medium of higher RI (fig. 3.54), the ratio of the sine of the angle of incidence (α) and the sine of the angle of refraction (β) is defined as the RI of the second medium with respect to the first medium. This can be shown as

$$\mu = \frac{\sin\alpha}{\sin\beta} \tag{3.65}$$

The RI of a material is generally expressed with air as the reference. Therefore, addition of sugar to a liquid changes the RI of the liquid that implies the relation between degree of brix and RI. The RI of sucrose at 20°C related to brix degree is shown in table 3.15 [14]. Because the RI of a solution also changes with temperature, corrective measures or compensation has to be made in brix measurement, of process products, at higher temperatures accordingly.

Refractometers are based on two principles, the refraction angle principle and critical angle change principle, which are discussed next.

3.9.2.1 Refraction Angle Refractometer

The basic concept of this refractometer is measurement of change in refraction angle as a function of RI of the test material. Figure 3.55A shows a schematic diagram of a differential refractometer. It consists of a tungsten filament lamp source, the light from which passes through the combined cell window through a mask. Refraction of light takes place at the window surface. The refracted light is collected by a pair of opposed phototubes ratioed by a beam splitter. The phototube produces the output signal proportional to the refraction through the sample and a reference liquid. The beam splitter is positioned by servo controller so that the light beam falls on the photodetectors equally.

3.9.2.2 Critical Angle Refractometer

A critical angle refractometer is a kind of back-scattering refractometer (fig. 3.55B) where the incident light is reflected back from the surface of a sample

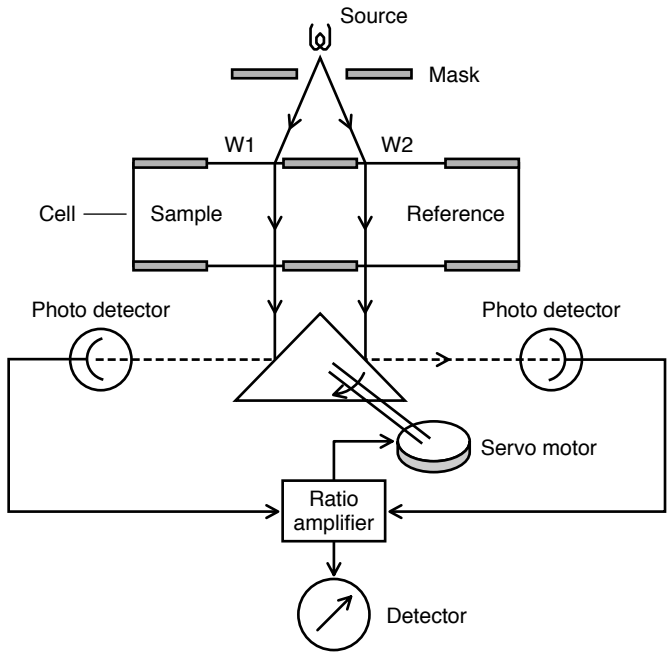

FIGURE 3.55A
Refraction angle refractometer.

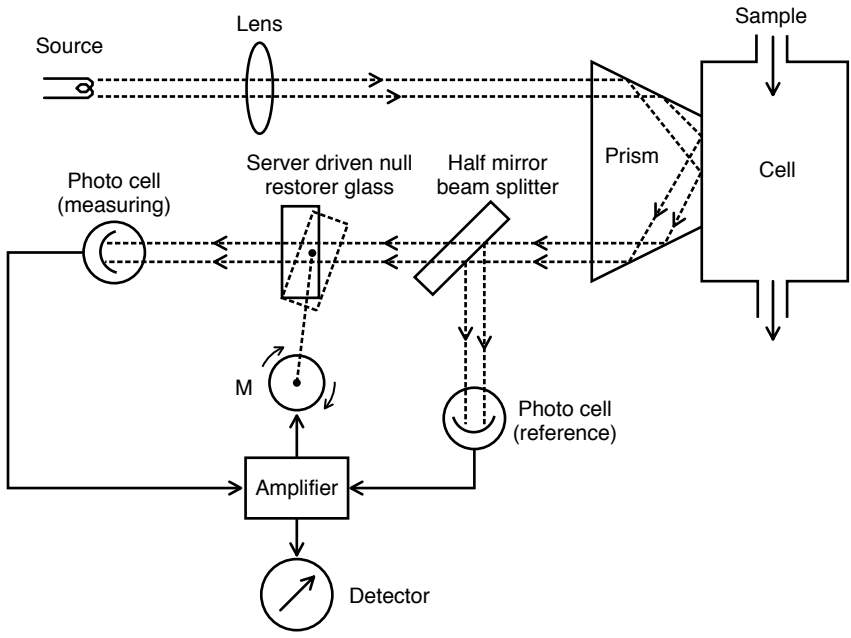

FIGURE 3.55B
Critical angle refractometer.

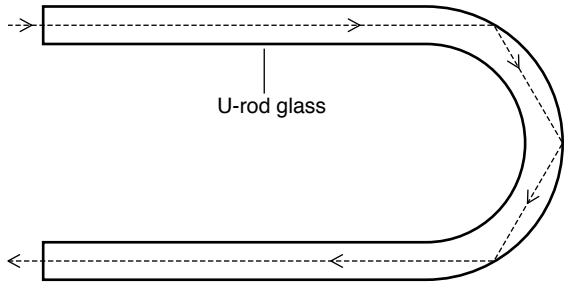

FIGURE 3.56
A U-rod refractometer. (*Redrawn from Proc. TIMA-96, India, with permission from R. Sridhar*)

window. A prism is used to reflect back the light from a source incident at varying incident angles. The reflected light is split using a half-mirror beam splitter. The point of change from refraction is detected by a pair of photocells. An amplifier amplifies the signal proportional to the imbalance and repositions a restorer glass using a servo balance system. A helipot positioned in tandem to the null glass senses the position of the null glass, which is proportional to the critical angle. This refractometer design is utilized in probe type on-line refractometers using fiber optic light transmitters and microprocessor technology.

3.9.2.3 U-Rod Refractometer

Another variation of the critical angle refractometer developed by Sridhar et al. is the U-rod refractometer [14]. The optical geometry of the principle of this refractometer is shown in figure 3.56. A collimated beam of extra bright red light obtained from an LED is allowed to incident through the U-rod and strike the critical surface. The light is reflected back and propagates through the tube by repeated and total internal reflection and escapes at the end of the U-rod. A silicon photodiode is used as a detector to measure the light that escapes at the output end. The LED used was AlGaAs capable of emitting 3,000 mod of red light at 15 mA current. The U-rod size is 10 mm × 10 mm and made of glass with an RI of 1.52. The radius of curvature of the U-rod is 50 mm. A silicon photodiode of active detection area of 10 mm^2 with a peak wavelength detection of 720 nm is used.

The principle behind the measurement is this: A portion of the light gets reflected and absorbed in the medium and the rest gets totally reflected back to the rod depending on the RI and critical angle of the liquid. In this U-rod refractometer, a light–dark boundary (x_c) is related to the RI of the liquid and the radius of curvature (R) as

$$x_c = R(1 - \mu) \tag{3.66}$$

In this experiment, the electrical signal from the silicon photodiode is measured at various sugar solution concentrations of known brix values. Table 3.16 shows some results of this U-rod refractometer with collimated incident lights.

TABLE 3.16

Refractive Indexes and Output Voltages for Few Samples

Sample	Refractive Index	Output Voltage (V)
1	1.3520	0.629
2	1.3665	0.5937
3	1.3835	0.5548
4	1.4040	0.4910
5	1.4245	0.4348
6	1.4440	0.3595

Source: TIMA-96, India, 1996. Adapted with permission from R. Sridhar.

3.10 pH Values of Food

pH is a parameter that determines the quality of a food or any other quality dependent on pH, particularly in packaging, preservation, or canning. Table 3.17 shows pH of some food items and the dependence of pH on quality during processing.

3.10.1 pH Scale

pH is defined as the negative logarithm of the hydrogen ion (i.e., proton) concentration in a solution, which can be expressed as

$$pH = -\log(H^+) \tag{3.67}$$

TABLE 3.17

pH Values of Food Products with Process Factors

Food	pH Range	Process Factor
Cocoa beans	4.75–5.80	Fermentation during chocolate manufacturing
Cocoa powder	5.5	Flavor
Pectin gel	3.0–3.4	Gel formation in jam manufacturing
Beet root	4.0	Canning
Fruit juice	2.5–4.0	Preservation
Vegetables	5.0–6.5	Preservation
Tomato juice	4.5	Heat stability of spoilage organism
Fresh fish	7.05–7.35	Preservation
Stale fish	6.0–6.6	Preservation
Glucose syrup	4.8–5.2	Sugar manufacturing
Jellies	5.0	Preventing hydrolysis of pectin

Taking the antilogarithm of this equation, the hydrogen ion concentration is equal to 10 raised to the power of pH; that is

$$(H^+) = 10^{-pH} \tag{3.68}$$

For a dilute aqueous solution (water), the hydrogen ion concentration is approximately equal to unity and so the pH is 7. A change in pH of one unit represents a change in concentration by a ratio of 10. For example, a solution of pH 8 is 10 times more alkaline than a solution with pH of 7. The practical range of pH is from 1 to 14. An acid solution of unit strength has a pH of 0, whereas a base solution of unit strength has a pH of 14. The relation between hydrogen ion (H^+) and hydroxyl ion (OH^-) concentration with pH value of a solution is illustrated by figure 3.57. The figure indicates that pH measurement can detect 14 decades of hydrogen ion concentration and changes as small as 10^{-14} at pH of 14.

3.10.2 pH Electrodes and Potential

In pH measuring schemes, a pH glass electrode collects hydrogen ions and develops a potential at the glass surface with respect to the solution. The Nernst relationship describes the potential developed due to hydrogen ion concentration as

$$E_g = E_{g0} + \frac{2.303RT}{F} \log_{10}(H^+) \tag{3.69}$$

where E_g = sum of reference potentials and liquid junction potentials that are constants (in mV)
E_{g0} = potential when $H^+ = 1.0$
H^+ = hydrogen ion activity
T = absolute temperature (in °K)
R = 1.986 cal/mol degree
F = Faradays (C/mol)

All aqueous solutions are associated with a water molecule combined with the hydrogen ion. This combination is called hydronium (H_3O^+). When a hydronium ion gets closer to the glass electrode surface the hydrogen ion jumps and becomes associated with hydronium ions in an outer layer of the glass surface.

3.10.2.1 Glass Electrode

The working principle of potential development in a glass electrode (fig. 3.58) is that when two solutions of different hydrogen ion concentrations are separated by a thin glass wall an EMF is developed between the two solutions that

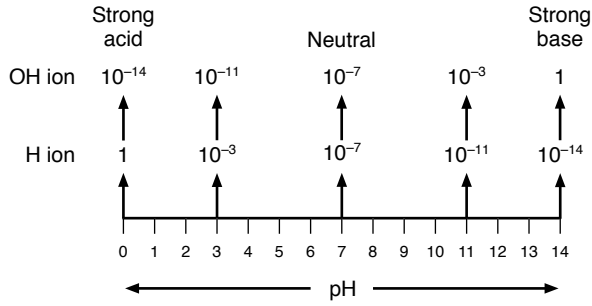

FIGURE 3.57
Illustration of pH scale.

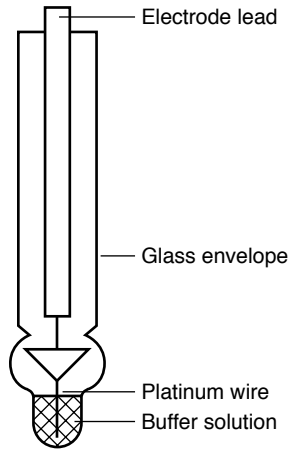

FIGURE 3.58
A pH glass electrode.

is a function of concentration of both. In practice a buffer solution of known concentration is used in a sealed glass electrode surrounded by the measuring solution. Soda lime glass gel (SiO_2, 72.2%; CaO, 6.4%; Na_2O, 21.4% mol) is suitable for development of potential between the separating solutions. This gel is suitable due to its low melting point, reduced hygroscopic, and low electrical resistance. The potential difference between the external glass surface exposed to the measuring solution (E_1) and the internal glass surface at a constant pH of 7.0 (E_2) is given by

$$E_0 = E_2 - E_1 = 0.1984(T + 273.16)(7 - pH) \tag{3.70}$$

This equation accounts for deviation of the constant pH of the internal solution from 7.0 at 25°C due to change in temperature.

3.10.2.2 Calomel Electrode

In this electrode (fig. 3.59) an inner glass tube contains calomel (Hg + HgCl) and is accommodated with a platinum wire. A saturated solution of KCl

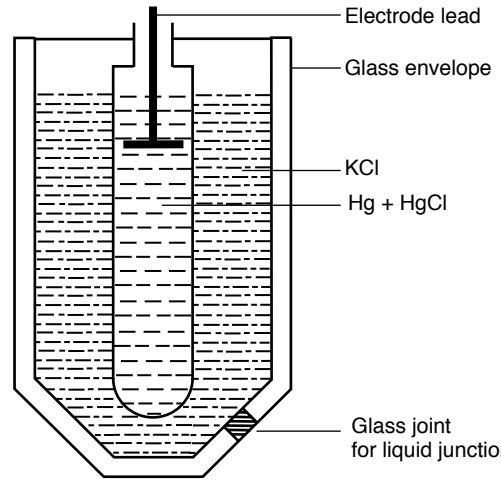

FIGURE 3.59
A Calomel reference electrode.

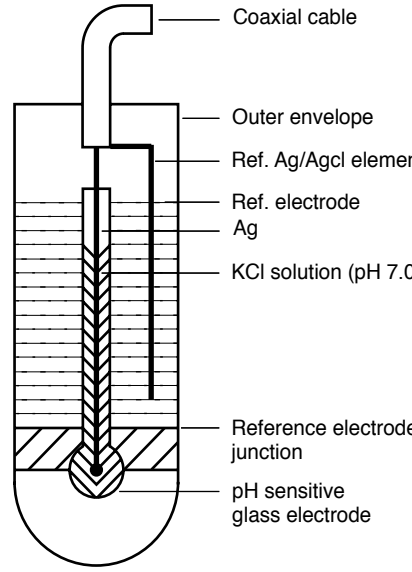

FIGURE 3.60
A combined pH glass electrode.

surrounds this inner glass tube and it remains in contact with the outer measuring solution through a glass joint junction. In some cases a capillary is provided in place of the glass joint junction so that the KCl solution slowly escapes from the electrode into the measuring liquid. The drift due to variation in room temperature is compensated for by a temperature sensor circuit incorporated into the electronic processing circuit.

An industrial pH electrode accommodates both the measuring circuit and reference electrode in a single unit (fig. 3.60). Such electrodes are specially designed to withstand harsh environmental conditions. In practical use, the Nernst equation is taken as

$$E_0' = E_r - 0.1984(T + 273.16)pH \tag{3.71}$$

where E_r is the fixed part of the total potential that depends on the electrode system. The term $0.1984(T + 273.16)$ gives a value of 59.2 mV at 25°C. Although this fixed part of the output voltage also changes with temperature, for practical purposes it can be assumed to be constant.

3.10.3 pH Signal Processing

The measuring circuit for pH signal processing should possess an input impedance fairly larger than the electrode impedance so that the loading effect is minimized. The output impedance of the glass electrode is on the order of 10^9 ohms, so the voltage drop in the electrodes becomes large compared to the EMF developed. Therefore an impedance-matching amplifier is used in the measuring circuit.

Operational amplifiers provide good impedance matching with the high-output impedance glass electrode and high amplification. Standardization is also possible by varying the feedback current of the closed-loop amplifier. For calibration or standardization, the electrode should be cleaned with distilled water between buffer immersions. Calibration with two buffers of 7 pH and 4 pH are generally used. Calibrated buffers can also show deviation in pH due to absorption of CO_2. Electrodes should be stored in the said buffer solutions. Cleaning of the electrodes is very important for storing and reuse after a measurement. Automatic cleaning mechanisms are also available in some pH meters using ultrasonic, brush, water jet, and chemical cleaning devices.

3.10.4 Ion-Sensitive Field Effect Transistor pH Sensors

Glass electrode pH meters are used primarily in laboratories and are difficult to use for on-line applications and in situ measurements. A few glass electrode pH meters have been converted for on-line applications, but problems arise elsewhere, like short circuits in reference electrode to earth, high reference electrode impedance, and so on. With the advent of ion-sensitive membrane sensors (ISMs) and ion-sensitive field effect transistors (ISFETs), on-line detection of pH and other related food quality measures have become possible. Apart from on-line applicability, ISFETs have the following advantages:

1. ISFETs are robust and durable, and cleaning and reusing them is simple.
2. Mass production by IC technology keeps the cost low and size small.
3. ISFETs can be used over an extremely wide temperature range.
4. ISFETs can be made multifunctional by a combination of membranes.
5. On-chip circuit integration is possible in ISFETs.

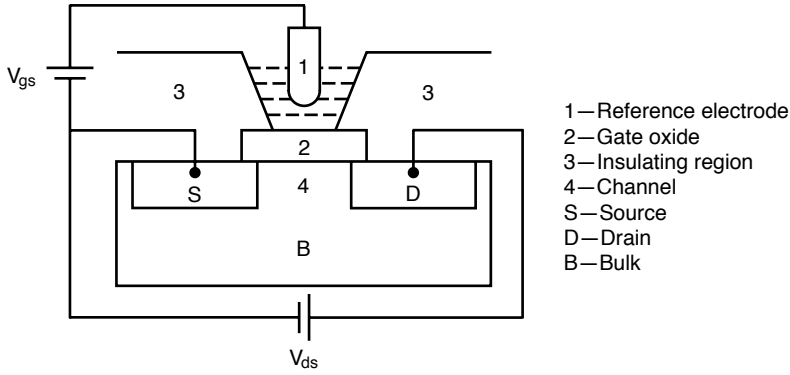

FIGURE 3.61
Schematic diagram of an ISFET sensor.

The structure of an ISFET is shown in figure 3.61. An ISFET is mainly a metal oxide semiconductor field effect transistor (MOSFET), where the metal gate is replaced by a complex structure that is sensitive to hydrogen ions. In place of the metal gate of a MOSFET a reference electrode and a chemically sensitive insulator are placed and the measuring electrolyte is placed in contact between them. The gate voltage is applied to the reference electrode and the electrolyte completes the electric gate-source circuit.

The ISFET sensing is based on a site binding theory [15–17]. According to this theory the insulating surface contains hydroxyl groups that can get positively or negatively charged depending on the concentration of hydrogen ions of the electrolyte. In the case of SiO_2 insulator, the binding sites available are SiOH, SiO^-, and $SIOH^+$ and the ionization reactions are

$$\begin{aligned} &SiOH \leftrightarrow SiO^- + H^+ \\ &SiOH + H^+ \leftrightarrow SiOH_2^+ \end{aligned} \tag{3.72}$$

Thus the surface potential is changed when the surface hydroxyl groups bind with H^+ ions.

The relation between concentration of $[H^+]_b$ of protons in the electrolyte and concentration $[H^+]_s$ of protons in the insulator follows the Boltzmann law:

$$[H^+]_b = [H^+]_s e^{-q\phi/KT} \tag{3.73}$$

where q = Charge (C)
ϕ = potential drop in the electrolyte–insulator interface
K = Boltzmann constant
T = Temperature (absolute)

Writing equation 3.71 in pH terms

$$\varphi = 2.3(KT / q)(pH_s - pH_b) \tag{3.74}$$

where pH_s = pH of electrolyte
pH_b = pH at the surface of the sensor area

Different materials are available as ISFET insulators, but Si_3N_4 has been found to be a very sensitive material [18], with a sensitivity of 56 mV/pH. A drift of 600 μV/h and a temperature dependence of 1.5 mV/°K at constant pH is found on an Si_3N_4 insulator. Figure 3.62 shows such an ISFET package.

Maritonia et al. [19] developed an ISFET pH sensor array in a surface-mounted device package on a printed circuit board (PCB) that is placed in a flow injection microchamber. The sensor chip measures 1.75 cm × 1.85 cm of die housed with an array of 12 ISFETs. Such chips are incorporated with

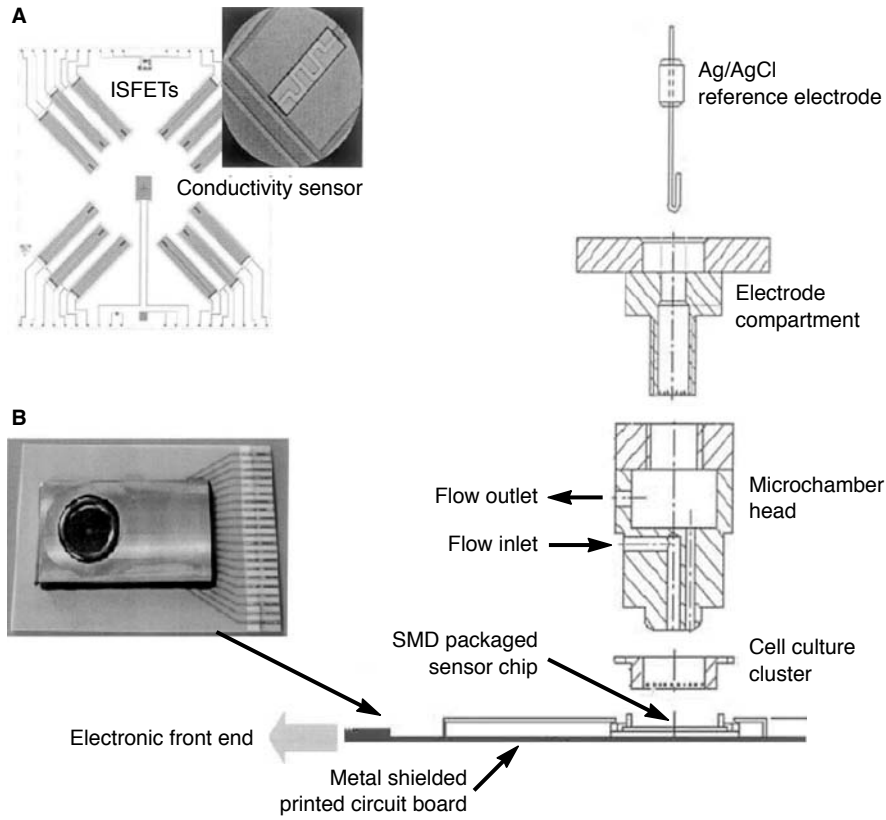

FIGURE 3.62
An ISFET microsystem for pH detection. (A) ISFET array-based sensor chip. The laserscan microscope photograph shows in detail the ISFET sensitive area; (B) The microsystem package photograph and a sketch of the system prototype. (*Reprinted with permission from Biosensors and Bioelectronics, Vol. 18(5–6), Elsevier*)

multifunctional blocks like temperature sensors and conducting sensors. A very large scale integration (VLSI) electronic circuit package can accommodate the sensor chip to be housed to reduce bias current. The sensors are operated at a constant drain source current and high output impedance. The reference currents for the sensor bias is obtained from a stable reference voltage made independent of temperature from a band gap circuit. The circuit can be powered by a 4-V power supply for battery-supplied operation.

A pH-sensitive ISFET has been developed by Artigas et al. [20] for online stabilization of wine by ion exchange resins. They fabricated pH-sensitive Si_3N_4 n-channel MOS (NMOS) gates that were fixed on a PCB and encapsulated with a photopolymer by photolithographic technique. The stabilization of the wine was performed in a cationic exchange resin and samples were alternately collected every 3 min from the inlet and outlet of the resin column using a flow system operated by peristaltic pump. The sample flow rate was maintained at 48 to 50 liters per hour and a filter was used to prevent blocking of the pipes by resin particles. Figure 3.63 illustrates the schematic of the ISFET-based wine stabilization system.

The pH ISFETs were calibrated by two standard solutions: one of aqueous solution and another of ethanol solution. The responses of the ISFETs to the wine solutions and the buffer solutions are shown in figure 3.64. The sensitivity of the ISFETs was 49 mV per decade.

A pH-sensitive sensor with lithium lanthanum titanate materials has been developed by Bohnke et al. [21]. The sensor can also be used for on-line pH control during cleaning of a fermenter that uses hot acidic and alkaline media, control of pH of milk during fermentation, neutralization of acidic foods, and so on. In their method, a polished titanium wire of 1.5 mm diameter was fixed with a silver conducting glue on one face of a pellet of

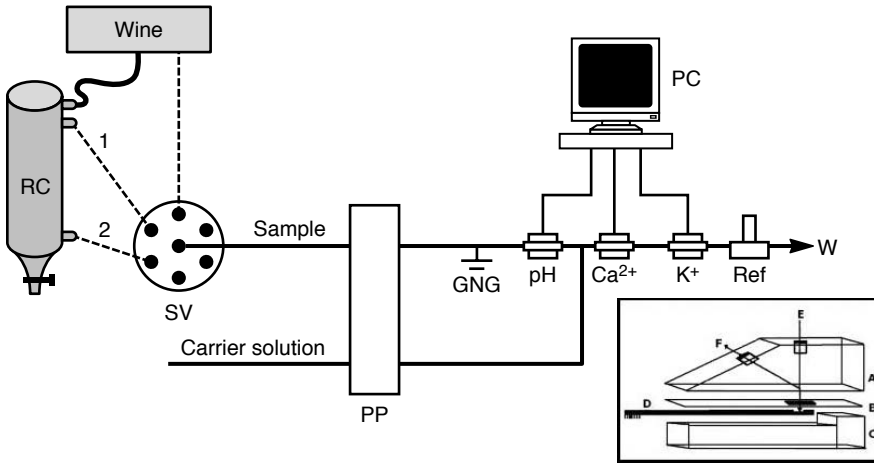

FIGURE 3.63
Schematic of ISFET-based wine stabilization system. (*Reprinted with permission from Sensors and Actuators (B-Chemical), Vol. B 89, Elsevier*)

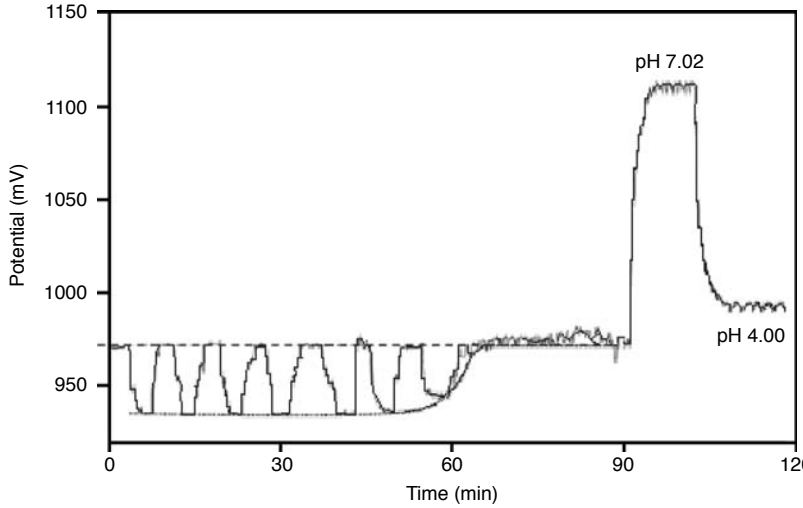

FIGURE 3.64
Responses of ISFET in wine flow system. (*Reprinted with permission from Sensors and Actuators (B-Chemical), Vol. B 89, Elsevier*)

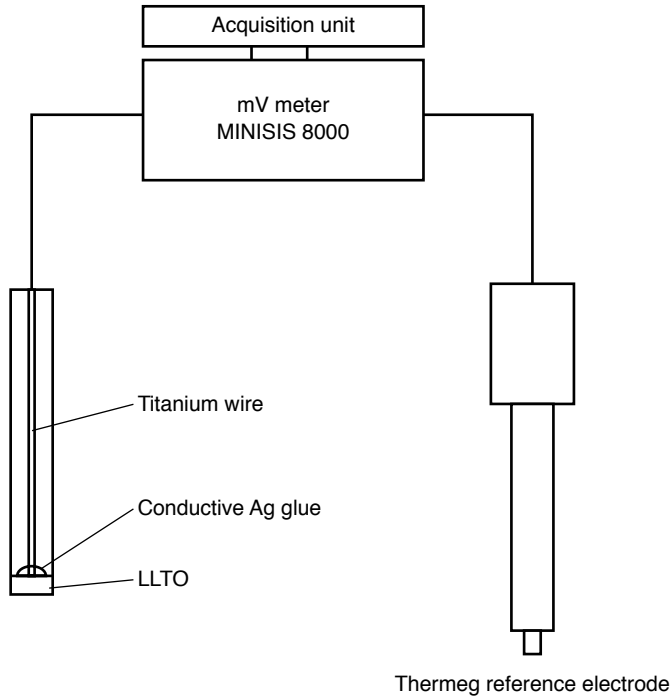

FIGURE 3.65
Measurement setup with the measuring and reference electrode. (*Reprinted with permission from Sensors and Actuators (B- Chemical), Vol. B 89, Elsevier*)

13 mm diameter containing La_2O_3, Li_2CO_3, and TiO_2. The pellet was fixed to the end side of a glass tube using araldite glue. The contact area of the glass with the electrolyte was 0.196 cm^2. A reference glass electrode was connected parallel to the measuring circuit—a millivoltmeter. The temperature of the complete system was controlled from 20°C to 80°C with a temperature bath and the temperature was recorded. The reference glass electrode was used in parallel to the system for different test materials, a Ingold Pro3200™ for orange juice, yogurt, milk, and so on. The setup of the measurement scheme is shown in figure 3.65. The sensitivity of the solid state electrode was found as 16 mV/pH and 36 mV/pH at 25°C and 60°C, respectively. Figure 3.66 shows the response of the sensor in orange juice, milk, yogurt solutions, and two buffer solutions of pH 4 and pH 7. The transition from ample to ample was found to be fast and reproducible.

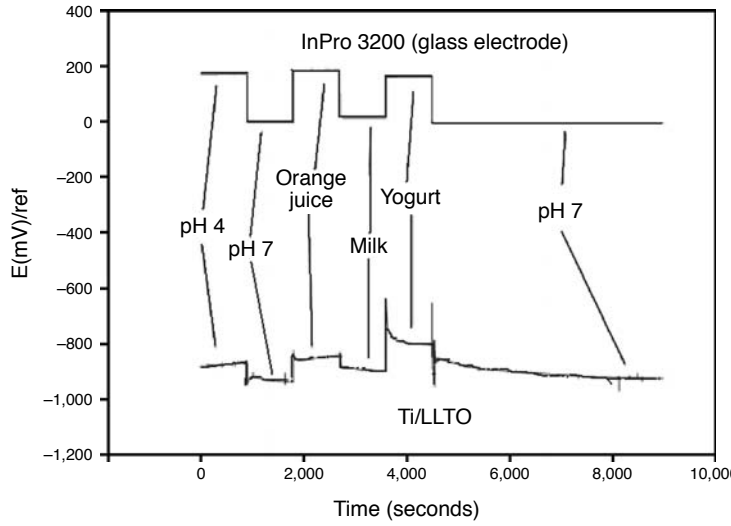

FIGURE 3.66
Response of the Lithium Lanthanum Titanate electrode. (*Reprinted with permission from Sensors and Actuators (B-Chemical), Vol. B 89, Elsevier*)

FIGURE 3.67
An ISFET probe (model-PH-30GS-Epoxy body). (*Reprinted with permission from IQ Scientific Instruments, California, USA*)

Commercial ISFET pH sensors are available in various probe configurations like stainless steel, micro round tip, piercing tip, epoxy body, heavy duty, graphite body, water-resistant rubber armored body, and so on. Figure 3.67 shows a commercial pH ISFET probe (model pH30-GS) manufactured by IQ Scientific Instruments, Inc. (USA).

3.11 Food Enzymes

Because enzyme activities are one of the most important facets of food processing, researchers are currently trying to detect and quantify enzymes using various solid state sensors developed so far. A few of them have been discussed in this section, and many of them are similar to the pH-sensitive ISFET sensors discussed in the last section.

3.11.1 Importance of Food Enzyme Detection

Enzymes are proteins with catalytic and specificity properties important for use in food processing. Enzymes function well within a limited pH and temperature range but their activity varies as pH and temperature vary. Some of the enzymes are naturally present in food materials, whereas others are used to enhance food processing actions or food quality. Table 3.18 gives the properties and uses of some important enzymes found in food materials that will be certainly helpful for sensor researchers in understanding the importance of the enzymes.

3.11.2 Enzyme Sensors

An enzyme sensor is a combination of a bioreceptor and a transducer. The bioreceptor is the primary sensor that responds first to the biological world and converts the biological event to an electrical signal with a secondary device, the transducer. In enzyme sensors the bioreceptor takes the help of an immobilized enzyme as biocatalyst to transform the analyte to a product that can be detected by the transducer. A large number of enzymes are commercially available, but some need to be extracted in specific measurements. Updike and Hicks [22] developed the first enzyme sensor in 1967 by trapping glucose oxidase in a layer of polyacrylamide gel attached to the plastic membrane of an oxygen electrode. Currently, physical entrapment is no longer used due to the short life of enzymatic activities achieved. Therefore, chemical immobilization techniques are more frequently used in enzyme sensors such as cross-linking, immersion method, direct binding method, use of aerosols, use of membranes, electromagnetic multienzymatic techniques, and so on.

TABLE 3.18

Food Enzymes with Their Functions in Food Processing

Enzymes	Food Item	Functions
Pectinases, hemicellulases, cellulases	Apples, pears, berries, and citrus fruits	Added during maceration to enhance extraction of juice and to reduce fermentation time; reduces the viscosity of juices in pectinase treatment
Methoxy-pectin	Jam, jelly, yogurt, and mayonnaise	Gelation formation; film formation
Amylases and cellulases	Immature fruit	Degrade residual starch to impart haze and facilitate maceration and color extraction
β-1, 3/ β-1,6 glucanase	Wine	Clarification and filtration of grapes infected with noble mold; preventing suspension of contaminant microorganisms
Glucanase	Meat	To determine freshness
Immobilized proteases	Wine	Deacidification of wine
Naringinase, limonase	Grapefruit	Hydrolyzing the bitter component without loss of natural yellow color
α- and β-amylase	Wheat	Splitting off maltose from damaged starch, controlling the extract of starch breakdown
Proteases	Biscuit	Breaking down protein, making it more extensible during sheeting and cutting
	Milk	Imparting bitter taste
	Coconut	Breaking down fat, producing rancid flavor
Lipases	Milk	Imparting bitter taste
Gut enzymes	Fish	Autolysis of fish after harvesting
Oxidase	Fish	Degrading
Lecithinases	Pasteurized milk	Imparting sweet curding and bitty cream
Pectinestirases	Pickles	Pasteurization to prevent darkening and softening of vegetables, flavor formation
Hypoxanthine, inosine, inosine-5′-monophosphates	Fish	Freshness
Lactate	Wine	Quality control
Glucose	Wine	Fermentation
Lysine	Wine	Control of proteins
Sucrose	Jam	Syrup formation

3.11.2.1 Principle of Operation

The enzyme sensor is basically composed of three parts: a thin enzymatic layer, the substrate, and the transducer. These layers are shown in figure 3.68. The transducer surface is in contact with an enzymatic layer and the enzymatic layer is immersed in a substrate composed of the solution under test. The substrate has a tendency to migrate toward the enzymatic layer and takes part in reaction with it. Thereby the substrate is transformed into a reaction product. This reaction product migrates toward the sensitive transducer and results in an electrical signal. The cause of the electrical potential is the conversion of the product concentration at the interface. The response time of an enzyme sensor depends on diffusion of the substrate and the thickness of the

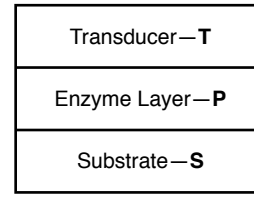

FIGURE 3.68
Schematic of components of an enzyme sensor.

layer. The response time can be reduced by using an extremely permeable membrane and a very thin layer. However the response time of the sensor should be greater or equal to the response of the transducer.

The response of enzyme sensors is mostly asymptotic and it takes a few minutes to be steady depending on the type. Typically the time taken to reach 98% of the final steady value is taken as the time constant. The response with a urease membrane fixed onto a glass diffusion electrode is slower than the response of a membrane fixed to a monovalent cationic electrode [23].

3.11.2.2 Calibration

To calibrate the output voltage to a product concentration first the sensor response is allowed to be stable and then the slope of the linear region is calculated. A urea sensor of such a type gives a calibration factor of approximately 100 mV/10^{-2} M. At low concentrations the response is slow and at higher concentrations the response is fast, giving a nonlinear response. Therefore the nonlinear part of the response is not used for calibration. Figure 3.69 shows such a response of the sensor. An enzyme sensor can also be calibrated in terms of inhibitor substance. When a substrate concentration is fixed, an inhibitor that reduces enzymatic reactions can be detected with varying concentration. Percentage inhibition (%I) is determined, representing the potentials with and without inhibition as

$$I\% = \frac{E_0 - E_I}{E_0} \times 100 \tag{3.75}$$

where E_I and E_0 are the potential differences of the sensor with and without inhibitor for a fixed substrate concentration.

3.11.2.3 Sensor Materials

For determination of various compounds, enzymes are identified either by theoretical modeling or by experimentation methods. For example, two types of alcohols—ethanol and methanol—can be detected by using two enzymes [23]: alcohol dehydrogenases and alcohol oxidases. Alcohol oxidases have regenerating capability in the presence of oxygen, but at low oxygen partial pressure the sensitivity is low at low alcohol concentrations. The other enzymes, alcohol dehydrogenases (ADH), need another coenzyme, nicotinamide adenine

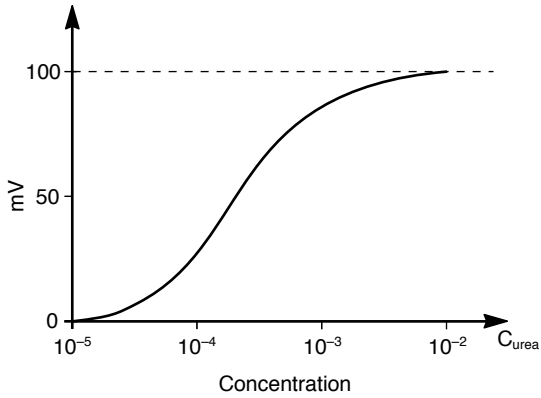

FIGURE 3.69
Calibration curve of a biosensor for urea. (*Redrawn from Fig. 4.8, p. 63, Biosensors, English Edition, 1993, with kind permission from Springer Science and Business Media*)

dinucleotide (NAD), which should be regenerated only by a mediator. A variety of mediators are identified and phenazine metho-sulfate is one of them. The direct electron transfer from the coenzyme to the electrode can be facilitated using organic conducting salts.

In breweries, milk production, and dairy industries, lactate is an important enzyme [23] to be detected. In lactate sensors, enzymes like lactate monooxygenase, lactate dehydrogenase, and lactate oxidase are coupled with amperometric transducers like a pO_2 electrode to detect oxygen concentration. Similarly the amino acid oxidase enzyme can be used to detect amino acids [23]. One electrode suitable for this application is a pO_2 electrode or an H_2O_2 sensitive platinum electrode. When a pO_2 electrode is used, catalase is recommended to be immobilized simultaneously with glucose oxidase so that half of the oxygen can be reused.

3.11.3 Measuring Circuit

The basic requirement of an enzyme sensor is the electrode. It is constructed by coupling an electrochemical sensor, an electrode, and a thin layer of immobilized enzyme [23]. The enzyme produces the electrical signal that is monitored by a potentiometric or amperometric circuit. In a potentiometric circuit the differential voltage between a measuring electrode and a reference electrode is measured and can be calibrated in terms of concentration. An example of a potentiometric electrode is the pH electrode or gas electrode, such as pCO_2 or pNH_3 electrodes. In a glucose electrode, the potentiometric electrode is made by immobilizing glucose oxidase on the sensitive component of the pH electrode. The enzyme catalyzes the oxidation of glucose into glucose acid or glucono lactone as

$$\text{Glucose} + O_2 + H_2O \xrightarrow{\text{glucose oxidase}} \text{gluconic acid} + H_2O_2 \qquad (3.76)$$

The pH electrode detects the gluconic acid and the output voltage is proportional to glucose concentration.

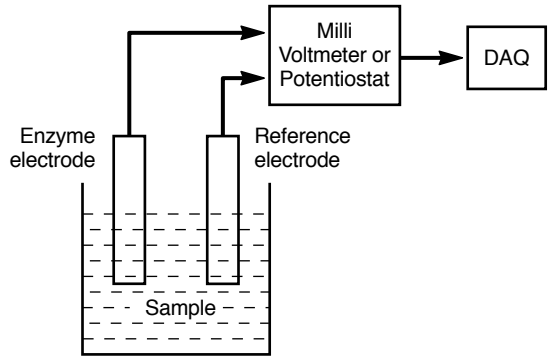

FIGURE 3.70
Use of enzyme sensor in a batch system. (*Redrawn from Fig. 8.2, p. 168, Biosensors, English Edition, 1993, with kind permission from Springer Science and Business Media*)

Enzyme sensor housing can be of two types: measurement conducted directly on the sample medium (batch method; see fig. 3.70) and the sample placed in a measuring cell, ensuring normal temperature and pH conditions [23]. In both of the techniques an enzyme electrode is placed next to a reference electrode such as the standard calomel electrode. In another variation both the electrodes can be combined in a single electrode, as is done in the pH glass electrode.

The differential output is applied to a millivoltmeter in case of the potentiometric measurement or to a potentiostat for amperometric measurements. The output is further connected to a recorder for continuous monitoring. In a more sophisticated situation the output can be connected to a data acquisition system for additional works like data logging, signal processing, and so on.

In the case of an analyte flowing through a pipeline, a flow injection system (fig. 3.71) is more appropriate. A small quantity of the sample volume is

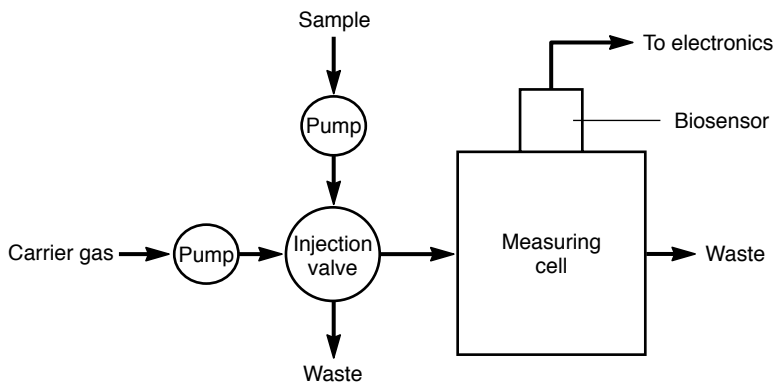

FIGURE 3.71
Use of enzyme sensor by flow injection system. (*Redrawn from Fig. 4.8, p. 63, Biosensors, English Edition, 1993, with kind permission from Springer Science and Business Media*)

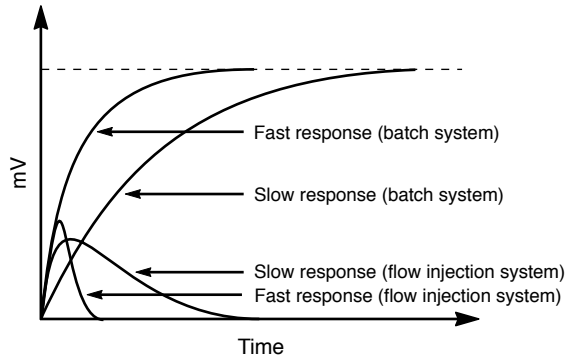

FIGURE 3.72
Typical response of biosensors. (*Redrawn from Fig. 8.3, p. 169, Biosensors, English Edition,1993, with kind permission from Springer Science and Business Media*)

injected into a flow of carrier liquid. An accurately controlled volume of the liquid sample is injected into the carrier line using flow control systems. The carrier or reference liquid and the sample are injected into the sensor through a valve using pumps. The pumps are controlled by a computer to alternately inject the carrier and sample liquid to the cell and the sensor. In a flow injection system the response is slower than the batch system as illustrated in figure 3.72.

3.11.4 Semiconductor Enzyme Sensor

Field effect transistors have been modified recently with the development of enzyme field effect transistors (ENFETs) [23]. They are made by a p-type silicon substrate over which two n-type semiconductor zones are placed as a central channel. These two zones form the source (S) and drain (D) of the transistor. A metallic gate (G) is isolated from the n-type channels by a thin insulating film of SiO_2. To get a MOSFET structure, the substrate and source are grouped (fig. 3.73). When the transistor is not in a saturation state, the drain current is given by the equation

$$I_D = \mu C_{ox} \frac{W}{L}\left[(V_G - V_T)V_D - \frac{1}{2}V_D^2\right] \tag{3.77}$$

where μ = mobility of electrons in the channel
C_{ox} = capacity of the insulating oxide
W/L = width to length ratio of the channel
V_D, V_G = drain-source and gate-source voltages, respectively
V_T = threshold voltage

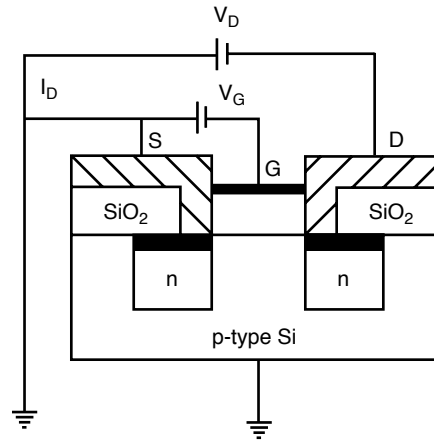

FIGURE 3.73
Schematic of a Metal-Oxide-Semiconductor FET. (*Redrawn from Fig. 4.30, p. 116, Biosensors, English Edition, 1993, with kind permission from Springer Science and Business Media*)

To get a response from this transistor, the metallic gate is separated and the enzyme sensitive to the analyte is used to cover the SiO_2 layer.

A variation of the MOSFET is the ISFET (ion sensitive) where an enzymatic membrane is placed instead of the metallic gate with a reference electrode. A pH-sensitive ISFET can also be used for glucose detection. Glucose oxidase accelerates the transformation of glucose into gluconolactone, which in turn hydrolyzes into gluconic acid that can be detected by the ENFET. Similarly, xanthine oxidase is immobilized on a polyvinylbutyral membrane to get the transformation of hypoxanthine to uric acid, which can be detected by the ISFET. This ISFET can be used for fish freshness detection because hypoxanthine is a fish freshness indicator.

3.11.5 Applications in Food Processing

In view of the information in table 3.18, it seems that enzyme sensors have potential applications in the food industry. The specific applications might be monitoring ingredients, food additives, contaminations, and toxins [23]. For example, a glucose electrode can be used to detect meat contamination by microbes because microbes consume glucose on the meat surface. Similarly fish freshness can be detected by hypoxanthine- or inosine-sensitive sensors. Other examples are detection of lactate in the wine and yogurt industry, amino acids (e.g., lysine) for monitoring proteins, sucrose for syrups and jams, and ethanol for alcohol.

In some cases, enzyme sensors pose a problem of inadequacy of recycling in the fermentation process. The enzymatic reactions produce some waste products and contaminate the fermenter. To avoid this problem a representative portion of the product is tested by the sensors and not recycled. Use of an autoclave also eliminates this problem. Here the sensor is placed in an autoclave and the enzyme is injected separately into the microchamber. When the activity of enzyme is insufficient it is renewed.

3.12 Flavor Measurement

Food items are mostly natural vegetative products that have a certain characteristic flavor. When food items are processed, the flavor pattern might change and new flavor components might be produced. In some cases food flavoring additives are also used to improve its value. In many cases a particular food product is manufactured with different flavors to satisfy different consumers with different tastes. For this, flavor additives, either synthetic or natural, like spices, essences, and oils are used. Flavors and fragrances are the results of substances that stimulate the sense of smell and taste of foods. Besides the four primary taste sensations—sweet, bitter, salty, and sour—flavor characteristics are produced due to our perception of odor.

3.12.1 Sources of Flavor in Food

Most natural flavor compounds are derived from plant substances, either from the aromatic, volatile vegetable oils or from the nonvolatile plant oils known as resins. Some fragrant substances are easily synthesizable like vanillin, the aromatic compound of vanilla. Most of the flavor compounds contain many contributing components, sometimes as many as hundreds. Some of them are organic acids, alcohols, aldehydes, amides, amines, aromatics, hydrocarbons, nitrites, and phenols.

A particular type of food product can have with different flavors due to either raw material of different qualities or different processing methods adopted. Table 3.19 shows various flavor compounds and causes of off-flavors of some food products. Flavors can be technically categorized as follows:

1. Naturally obtained from plants and animal products by physical means only
2. Synthetically produced but known to occur naturally
3. Artificial flavoring compounds produced synthetically only

In most cases the value of the food is determined by its flavor to a great extent. It is customary to say "the smell tells the taste." In most food industries, one of the section of food quality determination is the flavor testing. Hence, estimation or identification of flavor becomes a major function in food industries. Until recently, in most of the food industries this job has been done by organoleptic means: smelling by experienced persons. For example, in the tea industry, tea tasting is a highly specialized profession. However, there are problems associated with human tasters, like individual variability, adaptation (becoming less sensitive if exposed for a long period), fatigue, infections, state of mind, and so on.

TABLE 3.19

Compounds Responsible for Flavor and Flavor Defects of Some Food

Food Item	Process	Compounds	Causes of Flavor Defect
Bread	Yeast fermentation, baking	Organic acids, alcohols, carbonyl compounds	—
Cocoa	Fermentation, drying, bean roasting	—	Mold, excess lactic and acetic acid in bean
Milk	Source and processing	Lactose, minerals	Bacteria, enzyme, feed taints, weed taints
Oil	Refining, deodorization	Fat-soluble flavor compounds	Defective storage
Meat (cured)	Curing	Nitrites	Defective fermentation and storage
Tea	Fermentation	Theaflavin	Defective fermentation drying and storage

Because the odor particles are complex chemical compounds, they are equally sensitive to gas-liquid chromatography and mass spectrometry (GLC-MS). Detection of complex odors by these analytical techniques is expensive, off-line, and time consuming. In many cases odors are not at all possible to detect by GLC-MS techniques. These might be the reasons for the prolonged survival of the old organoleptic methods of odor testing in the food industries. However, E-nose sensor technology has been developed in the last decade that can be used for speedy and sensitive measurement of flavors, which will certainly make quality control in food industries reliable and efficient.

3.12.2 Physiology of Human Olfaction

Odors are sensations caused when volatile organic compounds (VOCs) stimulate our olfactory receptors located in the olfactory epithelium at the roof of the nasal cavity (fig. 3.74). Odor receptors of the human nasal cavity can detect and discriminate up to 10,000 different chemical traces. The olfactory region of each of the two nasal passages in humans is an area of about 2.5 cm^2 holding about 50 million primary sensory receptor cells. The region consists of cilia in the olfactory epithelium projecting down into a layer of mucus about 60 microns thick. The mucus lipids help the transportation of the odorant molecules to the olfactory receptors and produce the signals that our brain receives to interpret the odor. Each olfactory receptor neuron contains 8 to 20 cilia where the molecular reception with the odorant occurs. Information about the stimulus causes a distinctive neuron activity pattern and such patterns allow us to discriminate between vast numbers of different smells.

Odorant particles are volatile tiny molecules of molecular weight of 20 to 300 Daltons. Moreover they are polar and can be detected by humans at concentrations below 1 ppb. The threshold levels of some odorant molecules in water that can be detected by a healthy person are: green leaves, 0.32 ppm;

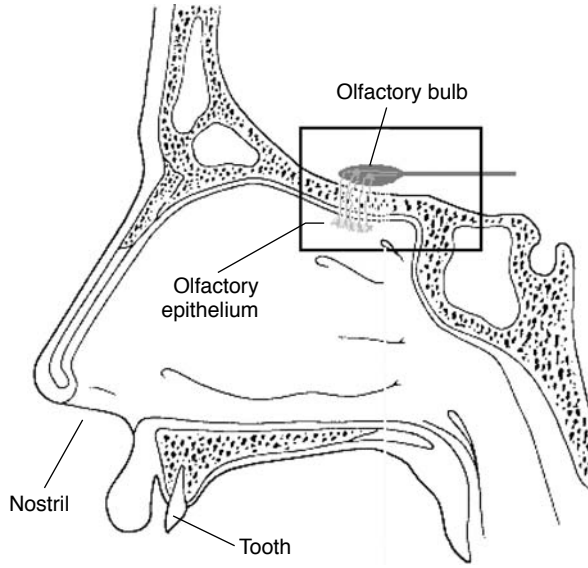

FIGURE 3.74
Human olfactory system.

rose, 0.29 ppm; thyme, 86 ppb; lemon, 10 ppb; off-flavor in white fish, 0.01 ppb; green pepper, 0.001 ppb; and grapefruit, 0.00002 ppb.

The human olfactory system has the limitation of discriminating mixtures of more than three to four components. The current E-nose technology involves a device that mimics the human olfactory system with analogy to an array of olfactory receptors, signal excitation by neurons, and pattern classification in the brain that is discussed next.

3.12.3 Organoleptic Panel

Flavor-related food quality determination requires a reliable organoleptic panel; however human flavor or odor panels show wide variability and nonuniformity. This is due to state of mind, biases, fatigue, and other human factors. Therefore, instead of a single individual, a panel of individuals statistically eliminates the problems to a greater extent. However, a panel cannot circumvent some of the requirements like extreme sensitivity, fastness, short time variability, and so on. In spite of using machine olfaction the training data must be validated by an organoleptic panel only.

In forming a panel of between 5 and 10 people, the panel should pass certain tests: a triangle test, an intensity-rating test, and a multicomponent identification test. In the triangle test, three samples are given to the person at the same time, two of which are identical and third that is of a different intensity or quality. The person has to identify the third one.

In the intensity-rating test, a series of about 20 variations of concentrations of a basic sample is placed in an odorless medium. One sample is removed

and the person is asked to identify its position or order in the series according to its flavor.

In the multicomponent test, there are three mixtures containing two, three, and four components of flavor. The person is asked to identify each of them.

An individual who passes these three tests is considered to have the ability to classify, distinguish, and compare with predetermined standards. An individual can act as a member of an odor panel only after a great amount of experience.

3.12.4 Electronic Nose

The electronic technology of mimicking the human olfactory system by electronic nose is speedy and reliable. It can also make possible continuous real-time monitoring of odor at specific sites and in the field, which was not possible by gas chromatography and mass spectroscopy methods.

3.12.4.1 A Basic Electronic Nose

The electronic nose is made up of three functional components that operate in tandem: an array of gas sensors, a signal processing system, and an intelligent pattern analysis and recognition system. Each sensor in the array has a unique sensitivity profile to the spectrum of odorants and different sensitivity for different odorants. This distinguishability makes the system sensitive to unknown odors.

In a basic electronic nose, the sensor array is housed in an odor-handling and delivery system consisting of a small chamber connected to a tube and a diaphragm pump to pull the sample or a reference gas into the chamber. Figure 3.75 shows a typical headspace sampling setup used with an E-nose. The headspace is the space above the sample inside the container holding

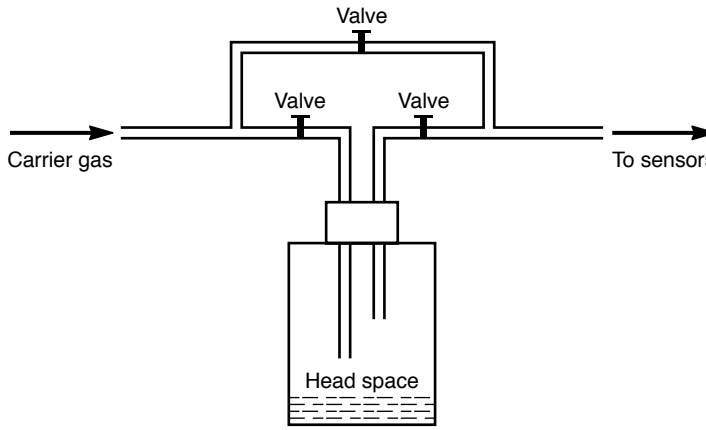

FIGURE 3.75
Setup of a typical headspace sampling system for E-nose.

the sample. A carrier gas such as dry air is supplied so that either the sample vapor carried by carrier gas or the carrier gas alone is supplied to the sensors. Switching the valves with a specific timing program manages this alteration. The sensor behaves steadily to the VOC stimulus after a few seconds, during which the physical variation of the sensor due to the odorant is converted to an electrical signal that is sent to a signal processing circuit.

After getting a response from the sample, a washing gas such as alcohol vapor is passed over the sensor surface for a specific duration to remove the odorant mixture from the surface and the sensor active material. A reference gas is again applied to the sensor array for starting a new measurement. The period during which the sensor is exposed to the odorant is called the *response time* and the period for which the washing and reference gas is applied is called the *recovery time.* In many cases a single gas can facilitate both washing and referencing.

3.12.5 Sensor Types

Table 3.20 lists various sensor types and their measuring principles used in electronic noses. Out of the listed types of sensors, metal oxide semiconductor (MOS), conducting polymers, and bulk acoustic devices are most commonly used.

3.12.5.1 Chemoresistive Sensors

Chemoresistive sensors are of two types: metal oxide and polymer. These sensors are based on change of resistance when exposed to volatile organic

TABLE 3.20

Common E-Nose Sensor Types, Measuring Principle, and Materials

Measuring Principle	Sensor Types	Materials
Chemoresistive	Metal oxide	Tin dioxide, zinc oxide, tungsten trioxide
	Conducting polymer	Polypyrorole, polyaniline, polythiophene, theophene, indoles
	Conducting oligomers	Short chain length conducting polymers
Mass sensitive	Surface and bulk acoustic device	Poly(siloxanes), charged polyelectrolytes, fluoropolymers
Field effect devices	Metal insulator semiconductor or metal oxide semiconductor (MOSFET)	Catalytic metals such as palladium, platinum, iridium, and so on
Fiber optic devices	Polymer bids on fiber optic bundles	Fluorescent, solvochromic dyes to detect solvation of vapors in the polymers

compounds. Of these two types, MOS sensors are more popular in E-nose applications. The typical materials used in MOS sensors are oxides of zinc, tin, titanium, tungsten, and iridium doped with a noble metal catalyst such as platinum or palladium. The doped metal oxide material is then deposited over a glass or plastic substrate between two metal contacts over a resistive heating filament. Two electrodes made of platinum, aluminum, or gold are used to connect the sensor to the output circuit. A heater made of platinum metal trace or wire is used to elevate the temperature of the sensor material from, say 200°C to 400°C. The resistance between the two metal contacts changes in proportion to the concentration of the odorant when the doped oxide material is exposed to the odorant. Different active sensor materials respond differently to an odorant, so for a particular gas, a particular active material is best suited. The sensitivity obtained from these sensors is on the order of 5 ppm to 500 ppm, but a general-purpose sensor array can discriminate a wide variety of odorants.

The most common interfering errors for these sensors are change of conductivity of the sensor material with variation in humidity, susceptibility to poisoning effect of sulfur compounds, and an inherent drift problem over periods of hours to days. Figure 3.76 shows the constructional feature of the sensor.

3.12.5.2 Conducting Polymer Sensors

In this type of sensor the active material is a conducting polymer of the family like polypyrolles, thiophenes, indoles, or furans. The polymer material is electropolymerized between two electrodes with a gap of about 10 μm

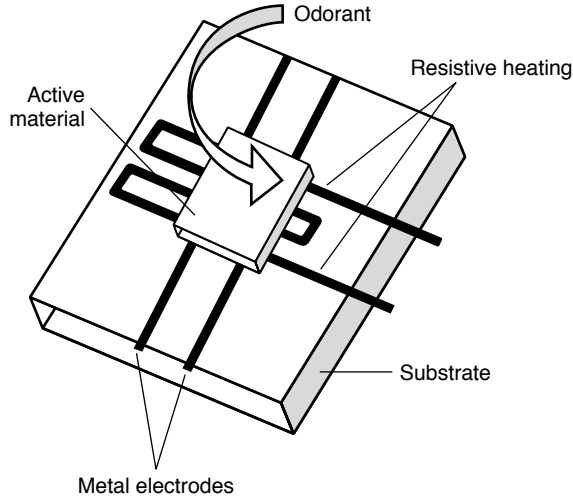

FIGURE 3.76
A chemoresistive sensor.

to 20 μm. When these polymers are exposed to the odorants, the bonding of the molecules changes and affects the transfer of electrons along the polymer chain, causing a change in the conductivity. Conducting polymer sensors can work at ambient temperature and they do not need heaters. The sensitivity obtained from this sensor is 10 ppm to 100 ppm.

The major drawbacks of conducting polymer sensors are that electropolymerization is difficult, time consuming, and prone to be affected by humidity; and some odorants are not retained by the polymer and penetrate through, so it takes more time to recover the odorant particles from the sensor by the refreshing gas.

3.12.5.3 Acoustic Sensors

There are two types of acoustic devices: quartz crystal microbalance (QCM; see fig. 3.77) and surface acoustic wave (SAW) devices (fig. 3.78). These sensors are devised to give a mass changing effect.

The QCM is made up of a resonating disc a few millimeters in diameter and coated with a polymer. Two metal electrodes are connected to each side of the disc. The resonance frequency obtained from the disc is about 10 MHz to 30 MHz when excited with an oscillating signal.

When these sensors are exposed to the odorant, the surface of the sensors absorbs the gas molecules and thereby the mass of the disc increases and reduces the resonance frequency. As an example, say a quartz crystal 166 μm thick cut along a certain axis will have a resonance frequency of 10 MHz. If this sensor gains a mass of 1% from an odorant, a decrease of 1 KHz in resonance frequency results. When the sensor is exposed to a reference gas the resonance frequency comes back to its original value. The selectivity and sensitivity of the QCM sensor depends on the coating of the polymer material. Minimizing the size and mass of the quartz crystal can reduce the response and recovery time of the sensor.

The input–output relationship of these sensors is fairly linear over a wide dynamic range. The effect of temperature can also be made negligible in this type of sensor. The SAW sensor operates at much higher frequency than the QCM sensor, hence the change in resonance frequency is also much higher in this sensor. The resonance frequency of a typical SAW sensor is on the order of several hundred megahertz. Due to higher operating frequency, the

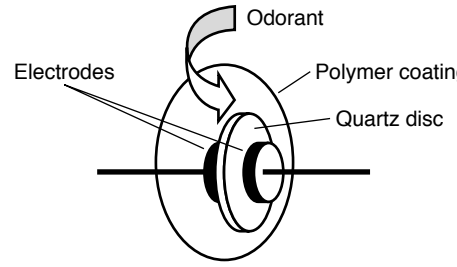

FIGURE 3.77
A quartz crystal microbalance sensor.

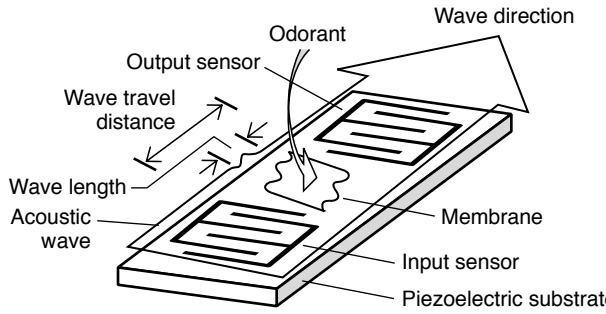

FIGURE 3.78
A surface acoustic wave (SAW) sensor.

signal-to-noise ratio is less in SAW sensors. The only disadvantage with QCM and SAW devices is that they require more complex electronic processing circuits compared to conductivity sensors.

3.12.5.4 MOSFET Sensors

The principle behind the working of an MOS field effect transistor is that when the odorants come in contact with the sensor, a reaction in the metal takes place. The compounds formed due to the reactions can diffuse through the gate of the MOSFET to change the electrical properties. A typical MOSFET structure of the sensor has a p-type substrate and n-doped regions with metal contacts that work as source and drain. The selectivity and sensitivity of the sensor depend on the material and thickness of the metal catalyst operating at different temperatures.

The main advantage of this type of sensor is that they can be manufactured with an IC fabrication process and batch-to-batch variations can be minimized.

3.12.6 The Signal Processing and Pattern Recognition

The four important stages of E-nose signal processing and pattern recognition are as follows:

1. Preprocessing
2. Feature extraction
3. Classification
4. Decision making

Figure 3.79 shows the different stages of the E-nose signal processing operation.

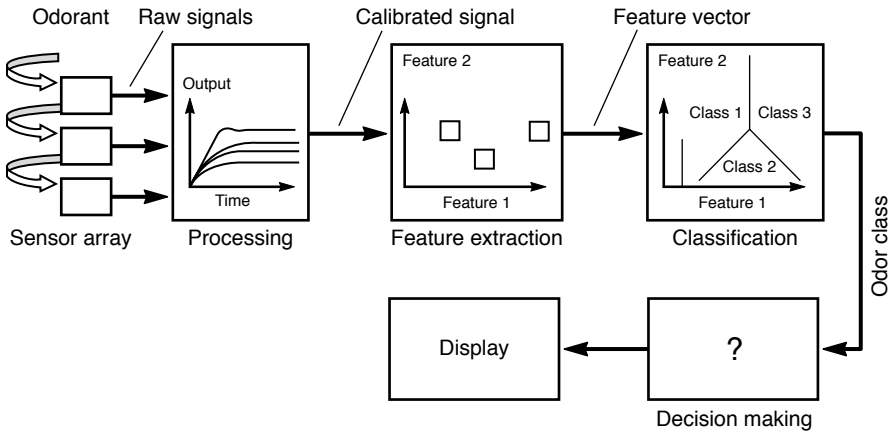

FIGURE 3.79
Block diagram of various stages of E-nose system.

3.12.6.1 Preprocessing

The sensor response in terms of variation of resistance in the case of chemoresistive type and polymer sensors, or variation of mass and resonance frequency in the case of piezoelectric sensors is processed to obtain a variation in voltage or current. In the case of a chemoresistive sensor, a Wheatstone bridge circuit or a current to voltage converter circuit can be used to get a voltage signal, whereas an oscillator circuit or an integrating circuit can be used in QCM and SAW sensors. Sensor drift is one of the factors that has to be compensated for in this stage. The most important function of this stage is the sensor output normalization. Because the sensors in the array will have different sensitivities, the voltage levels of the output signals from the sensors will be different. Hence the signal levels need a standardization or normalization. The voltage signals are then applied to a computer-based data acquisition system and the data are stored in the memory for pattern recognition.

3.12.6.2 Feature Extraction

This process uses mathematical techniques to find relevant but hidden information from the data. The techniques adopted for feature extraction are generally supervised linear transformations such as the classical principal components analysis (PCA).

In PCA, the responses are expressed in terms of a linear combination of orthogonal vectors accounting for a certain amount of variance in the data. Data variance in each principal component is contributed by each eigenvalue with varying importance. This technique removes any redundancy in the response and reduces the dimensionality of the problem. The mathematical and statistical background of PCA is outside the scope of this book.

Nonlinear transforms such as Sammon nonlinear maps and Kohonen self-organizing maps are also used in some feature extraction software.

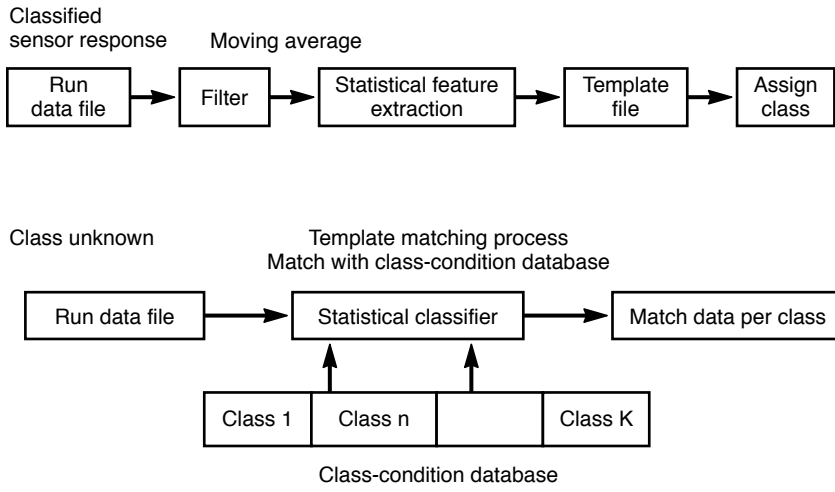

FIGURE 3.80
Block diagram of template learning and matching procedure.

3.12.6.3 Classification

In the classification stage, an estimation of the class for an unknown sample is placed on the class assignment. When the E-nose response data are projected on an appropriate low-dimensional space, the classification stage is used to identify the patterns that are representative of each odor. The classification stage is able to assign to the data a class label to identify the odorant by comparing its patterns with those compiled during training. The different tools used for performing classification work are K-nearest neighbors (KNNs), Bayesian classifiers, and artificial neural networks (ANNs).

The decision-making stage makes modifications if necessary to the classification and even determines that "the unknown sample does not belong to any one of the odorants in the database" or "it belongs" or "it nearly belongs to," and so on. Figure 3.80 shows a functional block diagram of the template learning and matching procedure and figure 3.81 shows the various pattern recognition techniques used for E-nose data processing.

3.12.7 Applications of the Electronic Nose in Food Processing

3.12.7.1 E-Nose Systems Manufactured by Alpha M.O.S. Inc. (France)

In their electronic nose systems, an array of 12 to 32 MOS/CP sensors and pattern recognition software is used. The systems can distinguish between a variety of flavors of beverages like Brazilian and Colombian coffees; two ground coffee varieties (*Coffea arabica* and *Coffea robusta*); freeze-dried and spray-dried commercial instant coffees, and so on. Another electronic nose system has been developed to discriminate among eight different coffee

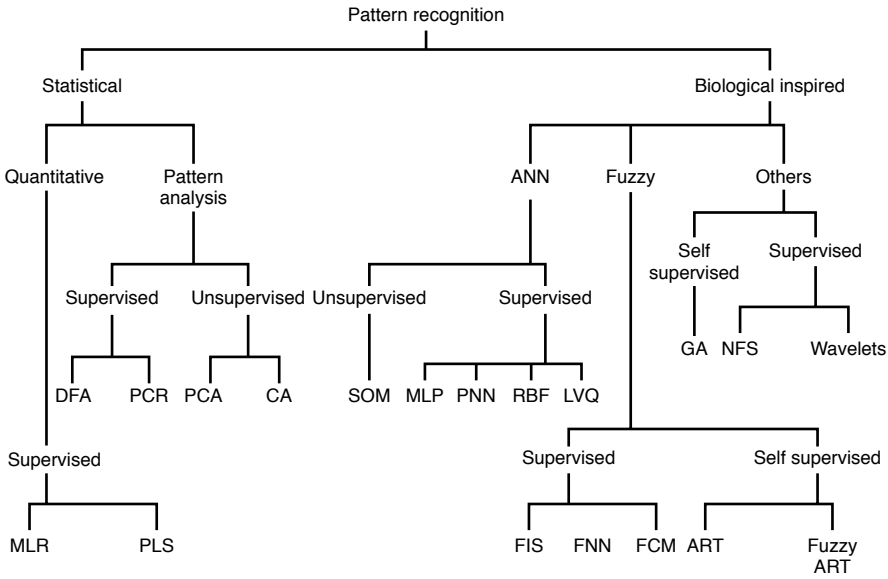

Abbreviations

ANN	Artificial Neural Network	NFS	Neuro Fuzzy System
ART	Adaptive Resonance Theory	PCA	Principal Component Analysis
DFA	Discriminate Function Analysis	PCR	Principal Component Regression
GA	Genetic Algorithm	PLS	Partial Least Square
LDA	Linear Discriminant Analysis	RBF	Radial Basis Function
MLR	Multiple Linear Regression	SOM	Self Organizing Map

FIGURE 3.81
Various pattern recognition schemes.

varieties at five different roasting levels. A photograph of such an E-nose system manufactured by Alpha M.O.S. is shown in figure 3.82.

3.12.7.2 Monitoring of Flavor of Beers

The flavor of beer is composed of hundreds of volatile compounds, but out of them only 122 flavor terms can be separately identifiable. In most beer samples, only 40 or so are detectable and the others, which are considered off–flavor, are less common. Some of the flavor definitions of beer are: alcoholic, estery, diacetyl, hoppy, malty, worthy, spicy, woody, and grainy.

The flavor of beer is traditionally ascertained by conventional methods like human tasters or through analytical tools like gas chromatography. Pearce et al. [24] were able to discriminate between different flavor notes of beer using conducting polymer E-noses.

3.12.7.2.1 The Sensors

The electronic nose used by Pearce for beer flavor detection was made of conducting polymer chemoresistors (fig. 3.83). The sensors were fabricated

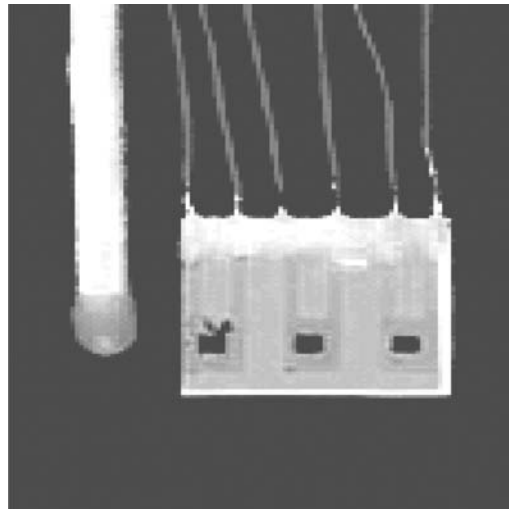

FIGURE 3.82
A conducting polymer E-nose sensor array. (*Analyst, Vol. 118(4); reproduced with permission of The Institute of Physics Publishing*)

FIGURE 3.83
A commercial E-nose system. (*Reprinted with permission from Alpha M.O.S., 31400, Toulouse, France*)

by the method of microtechnology of pure gold on alumina tiles on which an electrode pattern is etched by ultraviolet (UV) lithography and a gap is provided to grow the polymer material.

3.12.7.2.2 Beer Headspace Sampling

The sampling device basically consists of three different units. The chemical unit is made up of a glass vessel (volume = 0.2 m^3) that holds the analyte immersed in a temperature-controlled water bath set at 30°C. At 30°C, the beer sample produces the characteristic odor. The sensor unit is housed with four separate tiles, each carrying three different polymer sensors, for a total of 12 polymer sensors. The devices are wire bonded on one end and soldered onto metal posts. A perplex lid is connected to the post where the sensor head is fastened. The lid is used to close the vessel when the measurement is performed. The mixing unit is formed with a motorized fan connected to the perplex lid. When the device is under operation, the lid closes the vessel and the fan is positioned inside the vessel. A schematic diagram of the beer headspace sampling setup is shown in figure 3.84. The sequence of operation of the measurement is as follows: First, the sample vessel is placed on the water bath and 100 cm^3 of beer sample is placed in the vessel. The vessel is sealed and allowed to remain undisturbed for 20 min so that the liquid and vapor phases come into an equilibrium state. Then, the lid of the vessel is removed and the sensor head is positioned over the sample by lowering it. The circuit is switched on to monitor the change in resistance of the sensors for a period of 10 min.The sensor head is then taken away from the vessel and the sensor head is cleaned with water and dried by clean air for 2 min, which removes any contaminants that might be available. The sensor head is left to recover for 30 min before taking the next measurement.

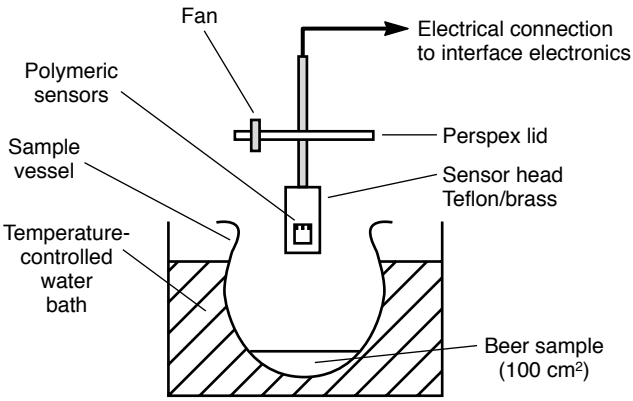

FIGURE 3.84
Beer headspace sampling system. (*Analyst, Vol. 118(4); reproduced with permission of The Institute of Physics Publishing*)

3.12.7.2.3 The Interface System

The variation of resistance corresponding to the beer flavor generated by the polymer chemoresistor sensor array was converted to a 0 V to 5 V analog voltage level for interfacing with the computer through an interfacing card. The circuit for generation of the equivalent analog signal is shown in figure 3.85.

The first stage of the circuit works as a constant current source to the polymer sensor. The sensor is connected across the input port RA and ground. The constant current source is made up of the precision voltage reference diode D2 connected across the output pin and inverting input of the first OPAMP (U2A). The constant voltage offset causes the current through the precision scaling resistors (R3–R10); that is, through the polymer sensor that is only related to the precision resistors selected through the DIP switches (S3). In the second stage, offset voltage nullification is done with the help of the variable resistor (CE2). Scaling of the output voltage is done with the help of a gain adjust resistor (CE1).

Calibration is done by shorting the sensor connection (across RA and ground) and adjusting the null offset potentiometer (CE2) to get zero indication. The standard precision resistors are then selected through the switch S3 so that the output voltage VA reaches the full-scale range of the A/D input device. This gives maximum resolution of the data acquisition system.

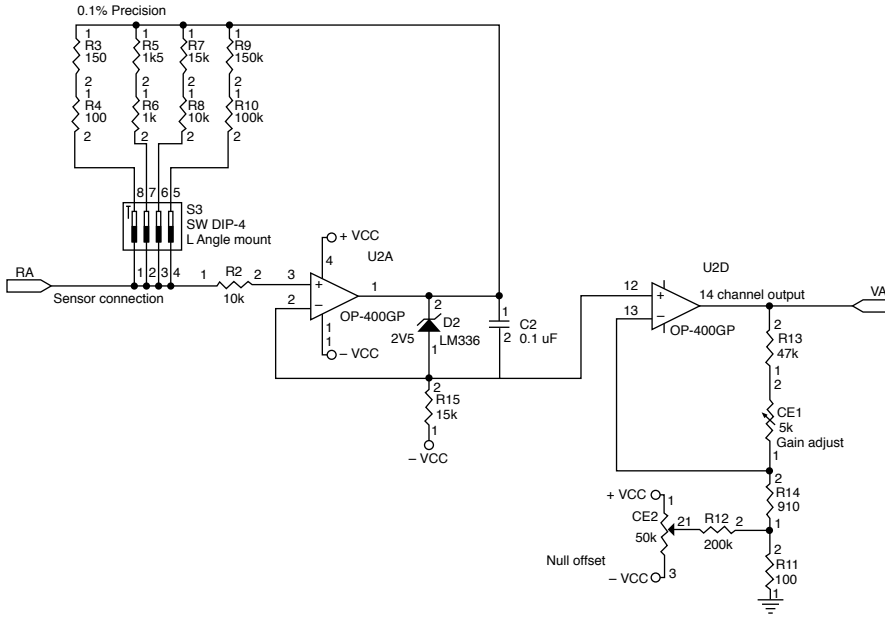

FIGURE 3.85
Measuring circuit for the polymer sensors (*Analyst, Vol. 118(4); reproduced with permission of The Institute of Physics Publishing*)

3.12.7.3 Fruit Ripeness Determination

Llobet et al. [25] developed an E-nose system employing an array of low-cost tin oxide sensors to analyze the rate of ripeness of bananas. The experiment was conducted in a period of 8 to 14 days from the headspace of three sets of bananas during ripening. The multiproduct sensors used in the array were TGS 822 (Figaro, Japan, Inc.), SP-11 (P1) (FIS, Japan), MGS 1100 (Motorola, USA), and AAS14 (Capteur, Ltd. UK). A thin plastic tube was used to collect the banana flavor from a sample vessel and carry it to the sensor head by a diaphragm pump. Data acquisition and storage was done by LabVIEW® software (National Instruments, Inc). A sample measurement took 10 min and recovery to baseline was allowed in 50 min. A long recovery time was allowed to nullify any residual smell.

PCA was used to justify the discriminating power and three supervised classifiers (namely fuzzy ARTMAP, LVQ, and MLP) were used to classify the samples into seven distinct states of ripeness.

In classification of banana ripeness, banana skin color was used as a class reference because skin color is known to correlate well to sugar content. The categories of ripeness of three sets of bananas and their correspondence with skin color are shown in table 3.21.

The response data after normalization were stored for analysis by MLP, LVQ, and fuzzy ARTMAP. Altogether 175 response vectors from the three banana sets were divided into four folds. The results of the classification in terms of number of patterns correctly classified (number of patterns tested) and overall performance is shown in table 3.22.

3.12.7.4 Tea Flavor Detection

More than 500 chemical constituents are found in the organic compounds of tea, both volatile and nonvolatile. The best tea is the most aromatic and full of good flavor. Conventionally, a few chemical tests supplemented by expert human panel decisions ascertain the standard of the tea flavor. These techniques are subjective, influenced by adaptation, and have inherent faults that might even vary with time and the psychology of the panel experts at times.

In the tea industry, from inception of this trade, tea tasters have been using specific terminology; at present there are about 32 classes. Tea industries all over the world presently use these standard terminologies for tea flavor, but there is no mention about quantitative description or score on these flavor terms [26, 27].

It was experimentally established that the application of the E-nose in tea quality and standard flavor determination is highly efficient and accurate. The experiments were conducted on five different overlapping tea samples using four MOS-based E-nose sensors (TGS-2611, TGS-842, TGS-822, and TGS-813-J01) [26–28].

A different experiment was conducted by Kashwan [29] on 10 tea flavors from standard tea terminology and, more important, with nonoverlapping components.

TABLE 3.21

Categories of Banana and Their Relation with Skin Color

Category	Set 1	Set 2	Set 3
A	—	Green-yellow	Green-yellow
B	Yellow, trace of green	Yellow, trace of green	—
C	—	Completely yellow	—
D	Yellow, green tips	Yellow, flecked with brown	Yellow-green tips
E	Yellow, flecked with brown	—	Yellow, flecked with brown
F	—	—	Yellow, flecked with brown
G	—	—	Yellow, blackening

Source: Meas. Sci. & Tech., Vol . 10, 1999. Reprinted with permission from Institute of Physics Publishing, UK.

TABLE 3.22

Results of the State of Banana Ripeness

Method	Fold 1	Fold 2	Fold 3	Fold 4	Overall	Percentage (%)
Fuzzy ARTMAP	38(44)	41(44)	39(44)	40(43)	158(175)	93
LVQ	40(44)	41(44)	39(44)	41(43)	161(175)	92
MLP	36(44)	36(44)	34(44)	40(43)	146(175)	83.4

Source: Meas. Sci. & Tech., Vol. 10, 1999. Adapted with permission from Institute of Physics Publishing, UK.

3.12.7.4.1 Tea Samples

Kashwan [29] collected 10 tea samples with different flavor for the classification. Classification of these 10 flavor terms from standard tea flavor classes is shown here:

Flavor Term	Class
Sweet, minty:	Sweet, aromatic, fragrant
Bakey:	Overfired
Poor:	Poor
Baggy, papery, smoky:	Baggy, papery, smoky
Sour:	Sour
Woody:	Mouthful
Musty:	Fullness

3.12.7.4.2 E-Nose Setup

The experimental setup consists of four MOS-based sensors and a headspace sampling system with flow control devices with a suitable PC control for switching between sample headspace and base room environment. Flow control devices provide constant flow of sample vapor and air to the sensors through connecting pipes. The reference vessel was placed in an open space in a room environment at about 25°C temperature and 65% relative humidity

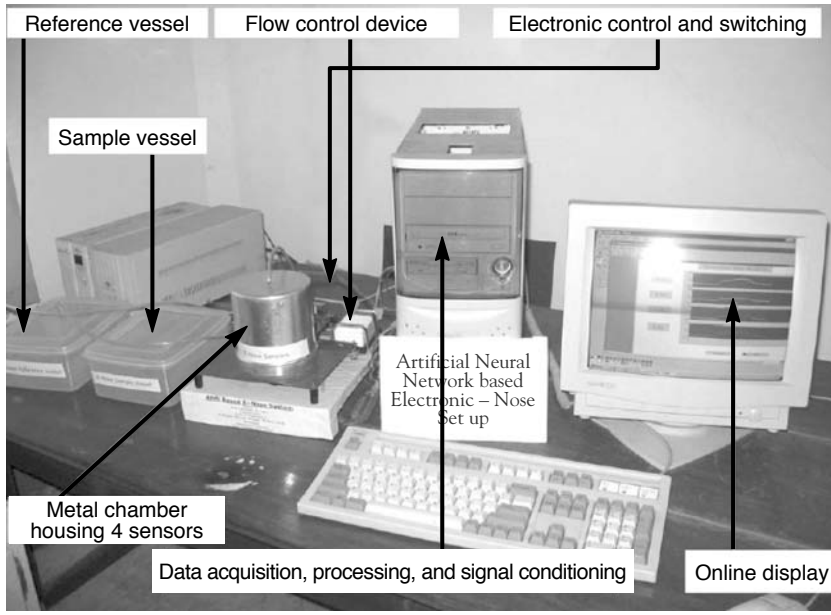

FIGURE 3.86
Photograph of the E-nose setup for tea flavor classification. (*Reprinted with permission from K.R. Kashwan*)

with deviation less than ±2% and the sample vessel inside an oven at constant elevated temperature of 60°C. At elevated temperatures, dry tea was found to emit a higher amount of VOCs. The photograph of the E-nose setup developed for tea flavor classification is shown in figure 3.86.

3.12.7.4.3 Interface Electronics

A computer-controlled relay switching circuit was developed for sampling from the headspace and reference room air. Data acquisition and online logging of the response signals from E-nose sensors was performed by a PCL-708 high-performance data acquisition card from Dynalog (India).

3.12.7.4.4 Data Acquisition

On-line logging and displaying of results were performed by GENIE data acquisition software. They have performed data acquisition for a long duration to generate a database for cluster analysis and ANN classification. The database consisted of 20 data sets for each of the 10 tea flavor samples and each data set consists of 400 data vectors. Room environment was maintained at a temperature of about 25°C and 65% relative humidity with deviation less than ±2%. Each data set was acquired for 200 sec and 300 sec was allowed for refreshing to air. Figure 3.87 shows the display of the sensor responses in a GENIE-based graphic window.

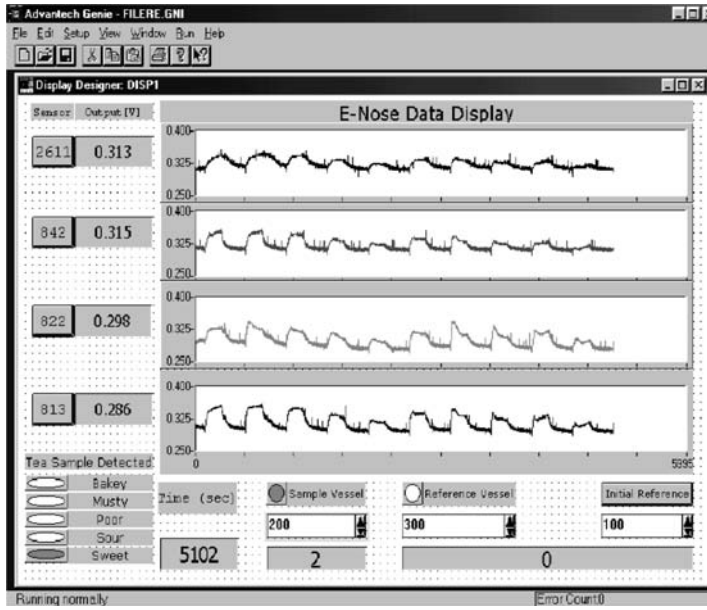

FIGURE 3.87
Display of E-nose responses to tea flavors in GENIE window (*Reprinted from PhD thesis with permission from K. R. Kashwan*)

3.12.7.4.5 ANN Paradigms Used for Data Analysis

The data sets obtained from E-nose responses were analyzed using four ANN classifiers: MLP, LVQ, PNN, and RBF algorithms. Training of the neural networks was performed with first half of the whole data set; the remaining half of the data set was used for testing the neural networks. Table 3.23 lists a summary of results and type of neural networks used for experimental training and testing of tea flavors.

3.12.7.4.6 Principal Component Analysis

The PCA result is shown in figure 3.88 as a graphical cluster classification display and figure 3.89 shows the zoomed display (1,000×) of two clusters. The analysis has established very distinct and separate clusters of 10 non-overlapping standard tea flavors. In the PCA, the first three principal components were analyzed, which resulted in a high classification accuracy of clustering. For example, a "smoky" sample resulted in 99.65% of the variance in the data set (PC #1, PC #2, and PC #3 resulted in 97.58%, 1.23%, and 0.83% of the variance, respectively, whereas PC #4 resulted in only 0.35%). PCA has classified tea flavors correctly at 91.42% (bakey), 94.20% (musty), 99.41% (poor), 98.03% (sour), 99.73% (sweet), 97.33% (woody), 99.65% (smoky), 99.78% (minty), 99.68% (baggy), and 99.06% (papery). Overall, PCA for 10 flavors of tea has accounted for 99.06% of the variance in 10 data sets. The components PC #1, PC #2, and PC #3 accounted for 95.52%, 2.03%, and 1.51%

TABLE 3.23

Architecture of Different Neural Networks and Correct Classification

Neural Networks	Architecture	Classification (%)
MLP	6 hidden neuron, 4 input neurons, 10 output neurons, 0.35 learning rate, with momentum 0.42	87
LVQ	4 input neurons, 10 output neurons, learning rate 0.011, and conscious factor 1	92
PNN	4 input neurons, 10 neurons in output layer, spread constant 0.8	93
RBF	4 input neurons, 10 neurons in output layer, spread constant 0.8	96

Source: *An Artificial Neural Network-Based Electronic-Nose System: Tea and Spice Flavour Discrimination and Drift Parameter Determination,* PhD thesis, Department of Electronics, Tezpur University, India, 2005. Reprinted with permission from K. R. Kashwan.

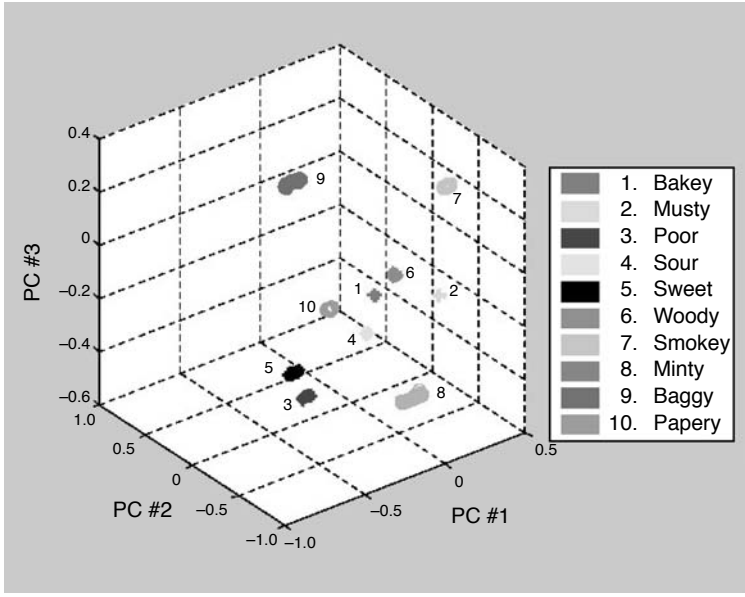

FIGURE 3.88
PCA plot of tea flavorflavor clusters. (*Reprinted from PhD thesis with permission from K. R. Kashwan*)

of variance, respectively, whereas PC #4 accounted for only 0.94%. Figure 3.90 shows a block diagram of the experimental arrangement to verify classification power of the E-nose for tea flavors.

3.12.7.5 Spice Flavor Detection

Spices are popular food additives well known all over the world. Proper ripening of the spices is of utmost importance for obtaining good aroma from them. Agricultural conditions such as type of soil, hybridized seeds,

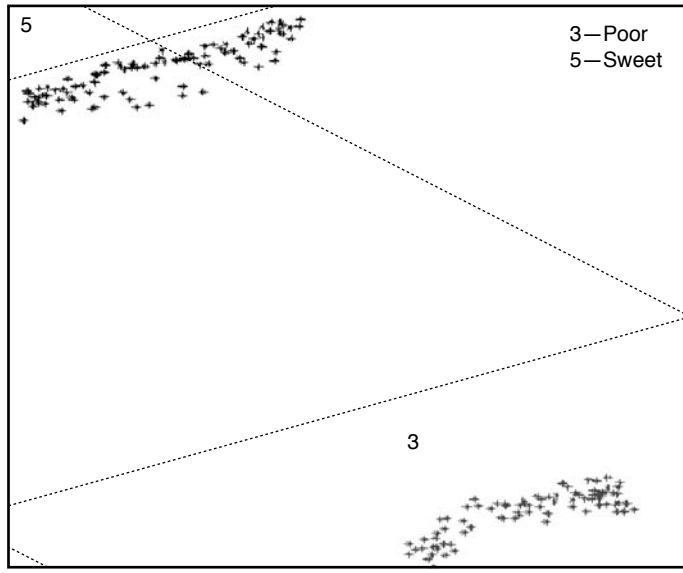

FIGURE 3.89
Zoomed PCA display for two flavorflavor clusters. (*Reprinted from PhD thesis with permission from K. R. Kashwan*)

irrigation, and ecological conditions such as climatic changes and tropical or nontropical weather can have strong correlations with the quality and aroma of the spice. Kashwan [29] used four MOS-based sensors along with an ANN classifier to classify the flavors of five common Indian varieties of spice samples: onion, garlic, turmeric, chili, and ginger. The ANN was trained with a total of 400 sensor response vectors and tested with 200 data. It was found that the classifiers could correctly classify the spice flavors with accuracy of 86%, 93%, 90%, and 95% by MLP, LVQ, PNN, and RBF respectively. The PCA plot for the five spice vectors is shown in figure 3.91.

3.13 Food Texture and Particle Size

Texture plays an important role in many food products to make it more appealing. Analysis of the texture-related qualities of food products is an area for development of new products or improvement of existing ones. The tenderness of peas and poultry, crispness of potato chips, crunchiness of apples, chewiness of chocolate bars, and so on are related to the texture properties of those food items. Although texture features of an object are related to its surface appearance or feel, molecular or crystalline structure of the matter is also greatly related to the surface texture. In nonfood products where surface finishing is an important quality factor (e.g., floor tiles), the

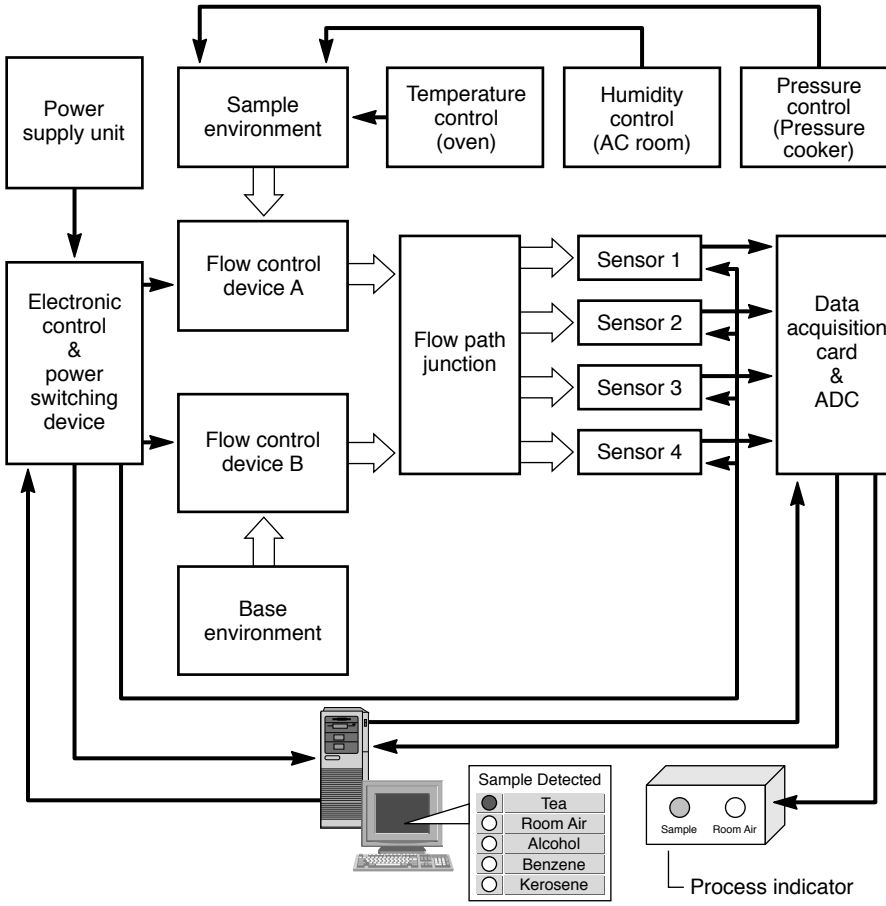

FIGURE 3.90
Block diagram of the tea and spice flavor measurement setup. (*Reprinted from PhD thesis with permission from K. R. Kashwan*)

smoothness or roughness is only related to its surface texture, but with food items there are many factors in the internal structure and constituents for texture. Table 3.24 shows textures of some food items and effects of constituents and treatments on texture formation.

3.13.1 Electromechanical Measuring Techniques

Buyers want a chewing gum to be chewy, crackers and potato chips to be crisp, steak to be compressible and shearable between the teeth, and bread to be soft in their mouth. It is a common practice among buyers to squeeze a bread to test its freshness. It highlights a primary concept of testing the stiffness of some foods, like bread, by measuring the compressibility. When we squeeze bread we apply a force, and the amount being applied indicates

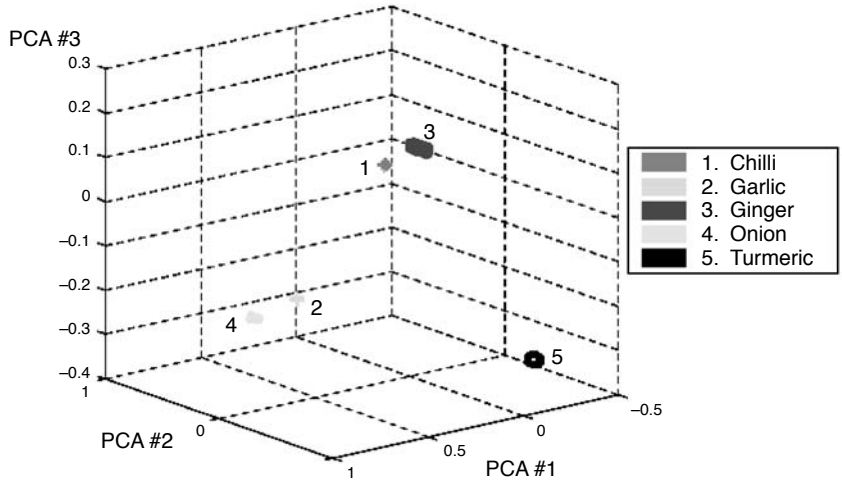

FIGURE 3.91
PCA plot of spice aroma clusters (Reprinted from PhD thesis with permission from K. R. Kashwan)

TABLE 3.24

Texture Factors of Some Food Products

Food	Texture Effecting Factors	Process
Toffee	Dextrose equivalent (DE) value of glucose syrup used	Emulsification
Fish	Freezing below 0°C	Storage
Meat	Toughness of connecting tissues	Tenderizing
Fats	Ratio of solid fat to liquid oil	Tempering
Meat extracts	Isolated proteins	Extrusion
Cheddar	Consolidation and stretching of curd	Cheddaring

the stiffness of the bread. In terms of simple principles of mechanics, this is measurement of resistance or reaction to force applied. When we chew on chewing gum, shear force is applied to slide one layer of the gum past another layer. This shear force is a measure of the chewiness. When we pull apart or tear a muffin by applying outward force, the tensile force applied is a measure of the looseness of the muffin.

Many specialized test instruments are available commercially to measure some attribute of texture with different mechanisms and names. Figure 3.92 shows the mechanical diagram of two types of squeezing testers. These instruments measure the mechanical force applied or a calibrated attribute like a distance moved when the food is tested. For example, a succulometer adopts a force measurement technique where a compressive force is applied to the food to squeeze juice from it. The tenderness of peas can be tested by measuring the compression and shear force applied by a tenderometer. Many such tenderometers are equipped with a recording chart to trace the time–force curve to understand the rheological properties of the food item.

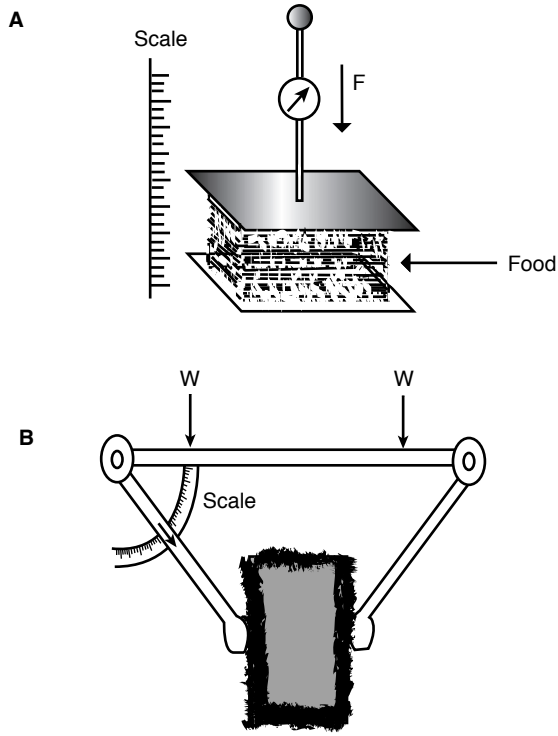

FIGURE 3.92
Food squeezing tester: (A) Single loaded plate; (B) Double loaded beam.

A penetrometer tests the toughness of food by measuring the force required to move a plunger a fixed distance through the food material. In this instrument (fig. 3.93A) a transient force is applied for a short duration that makes a plunger traverse through a food a certain distance to touch a contact. The contact in turn sends a signal (mechanical or electrical) to the pressure gauge to register the force applied. In a variation of this technique (fig. 3.93B), in a Bloom gelometer, lead shots are automatically dropped into a cup attached to the plunger that is positioned above the liquid surface. The plunger moves a fixed distance through the liquid to make contact with a mechanical switch to cut off the flow of lead shot. The weight of lead shots or number of lead shots is a measure of the firmness of the liquid and is defined as degree Bloom.

Mechanical gauges that measure force or pressure have recently been replaced by electrical pressure or force transducers like load cells, and capacitive or resistive diaphragms (discussed in chapter 2) to generate an electrical voltage or current proportional to some texture attribute. Such systems give digital readouts with calibration and recording facilities. In addition to having sensing capability, these devices, as in the case of figure 3.93A and figure 3.93B use mechanical contacts to generate an electrical signal to register the force or load

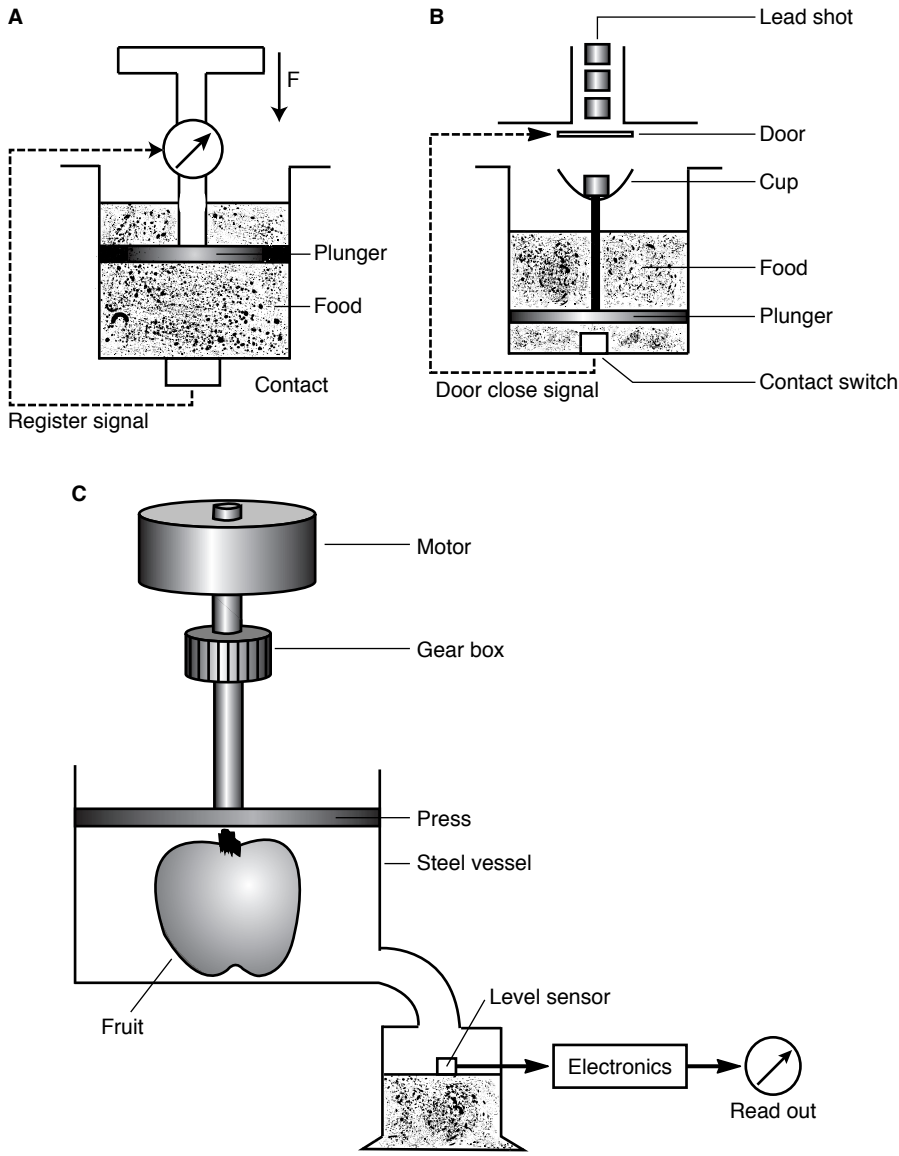

FIGURE 3.93
Schematic diagrams of penetrometers: (A) Force measuring type; (B) Bloom gelometer; (C) Electronic succulometer.

used to penetrate the plunger through the food material. An author's imagination (this might be exaggerated) of an electronic succulumeter is shown in figure 3.93C. A press connected to an electric motor through a gear box applies a constant force to the fruit to squeeze out juice and collect in a beaker. A

miniature level detector generates an electrical signal proportional to the amount of the juice run out and it is calibrated in terms of succulence of the fruit.

3.13.2 Fluorescence Technique for Beef Toughness Detection

The tenderometers discussed earlier in the chapter mostly employ invasive techniques, altering the food sample being tested so the food cannot be reused. Researchers try to predict whether or not the food is tough or tender from a single, rapid, and noninvasive or nondestructive testing.

In the case of beef toughness detection, connective tissue is found to be the prime cause of toughness and fluorescence is a way of detecting it [30]. The reason for using fluorescence is that fibrous materials absorb light energy and re-emit it at a higher wavelength. When a UV (black) light excites fluorescence of the connective tissues, they re-emit the UV light at a longer wavelength (i.e., blue-white). The emitted light can be collected by an optical fiber for measurement, but it is difficult to standardize fluorescence measurements and there could be considerable error due to various florescence properties of the apparatus.

However, Swatland et al. [30] proved that it is possible to obtain similar fluorometry spectra using a fiber-optic probe. This fiber-optic probe method is based on measurement of fluorescence emission spectra of meat through a large stationary window using the shape of the spectrum to measure the biochemical type of collagen in the field. Types I and III collagen have different fluorescence emission spectra. The maximum excitation in most types of collagen in meat is found at 370 nm to 375 nm. An emission spectrum for types I and II collagen is found at 440 nm to 510 nm. A mercury lamp with a 365-nm peak was used to get a prequenching peak (440 nm) due to collagen I and postquenching peak (510 nm) for collagen III. Peak at 440 nm is regarded as the indicator for connective tissue that might cause meat toughness. The postquenching peak at 510 nm is the indicator of low connective tissue in meat.

The Fiber-Optic Probe

It uses the idea of fat-depth probe where a series of measurements are conducted through a small probe window. A single optical fiber probe is penetrated through the muscles through a single window to detect connective tissues. Figure 3.94A shows a block diagram of the setup used for fluorescence of beef. An optical fiber probe (fig. 3.94B) was inserted through the shaft of the probe to form a window behind the cutting head with an optical surface of contact with meat of 1 mm^2. An optical bench was used to link the fiber to the handheld probe. Light from a 100 W short arc mercury lamp was directed through a heat-absorbing filter, a red attenuator filter, and a dichroic mirror. Light at a peak of 365 nm was directed into the proximal end of the optical fiber with a microscope objective. The fluorescence from connective tissue from the end of the optical fiber was measured by a side

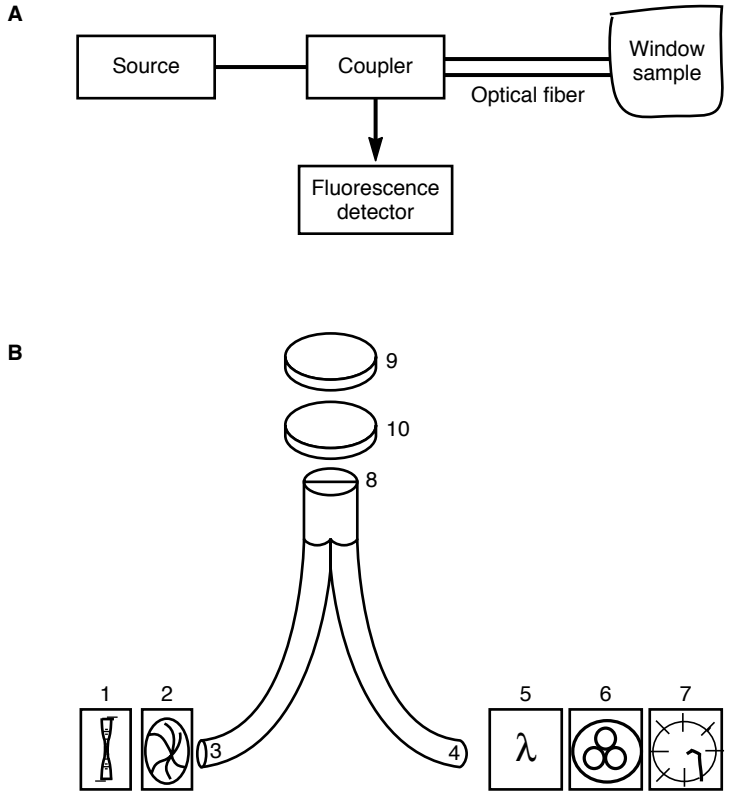

FIGURE 3.94
Fluorescence apparatus: (A) Block diagram of the optical apparatus; (B)Apparatus for measuring back-scattered polarized light. (1) xenon arc; (2) shutter; (3) illuminating branch of light guide; (4) receiving branch of light guide; (5) grating monochromator; (6) stray-light filter; (7) photomultiplier; (8) crossed polarizers on the common trunk of the light guide normally in contact with the samples; (9) pressed plate of barium sulfate powder; and (10) depolarizer, used for standardization shaft had entered the meat. Switches on the MQM probe were used to accept or reject data and to control labeling of the data on disk. A precision potentiometer geared to a plate remaining on the meat surface was used to measure the depth of the optical window in the meat, thus providing depth coordinates (x-axis) for fluorescence signals (y-axis). (*Reprinted from J. Sci. of Food and Agri., Vol. 75, 45–49, with permission from John Wiley and Sons, Inc.*)

window photomultiplier. The dichroic mirror was used to separate out input and output light through the single fiber.

The probe was controlled from a multiprogrammed workstation to control the insertion depth and measurement simultaneously. A precision potentiometer connected to a plate housed on the meat surface was used to measure the depth coordinate of the fluorescence signal. All measurements were performed under computer control using a Hewlett-Packward 360 CMA BASIC workstation operating through an IEEE 488 bus to a Zeiss-MPC controller and an HP Multiprogrammer 6942A.

The relation between fluorescence and connective tissue and error caused by differences in myoglobin content of beef was investigated in this work.

3.13.3 Machine Vision Technique

In image processing, the term *texture* means a structural surface feature of regular or repetitive patterns in certain objects. The repetitive patterns of basic texture elements are called texels. A *texel* is formed by a group of pixels with periodic, quasi-periodic, or random placement. A texture can be coarse, fine, smooth, granulated, rippled, fibrous, and so on. In machine-vision-based food texture measurement techniques, texture features of images are used as the basis of measurement. Image processing techniques adopted in food texture measurement for a few examples are discussed here.

3.13.3.1 Beef Tenderness Detection

Tenderness of certain food items can be predicted by using textural features extracted from gray scale or color images of the food. Such a machine-vision-based technique was developed by Jeyamkondan et al. [31] for predicting cooked beef tenderness. Prior to that, Wulf et al. [32] investigated the correlation between colorimetric readings (L^*, a^*, b^*) and beef tenderness and reported that b^* value showed the highest correlation with shear force (R^2 = 0.4). This concept resulted in the BeefCam™ system to predict beef tenderness developed by Colorado State University and Hunter Associate Laboratory, Inc. However, according to Jeyamkondan et al. [31], there are certain limitations of acceptance of this device due to the system tendency to categorize too many tender caracasses as tough. Later Li et al. [33] developed an image processing technique using textural features from a gray level cooccurrence matrix of pixel values of RGB color space.

Jeyamkondan et al. [31] developed an adaptive thresholding method using the fuzzy c-means (FCM) algorithm to discriminate fat from lean meat. Further they extended the method to predict shear force tenderness using image textural features extracted from CIElab color space. The close-up images of the sample steak, central portion of the ribeye, were captured and used for analysis.

Their computer vision system consisted of a color video camera (A209, MicroImage Video Systems), an image digitizer (FlashPoint 128, Integral Technologies), a 550 MHz PC, and monitor to perform image processing operations. A dedicated lighting chamber was designed for diffuse and uniform distribution of light. The white interior of the arched cover directed base lighting to a 20 cm × 30 cm imaging area. Light was supplied by six 50-W halogen lamps powered by a feedback controller to stabilize illumination level. The camera was mounted above the lighting chamber, viewing the imaging area through an observation port. A removable pan with a matte black surface was used to position the steak in the camera's field of

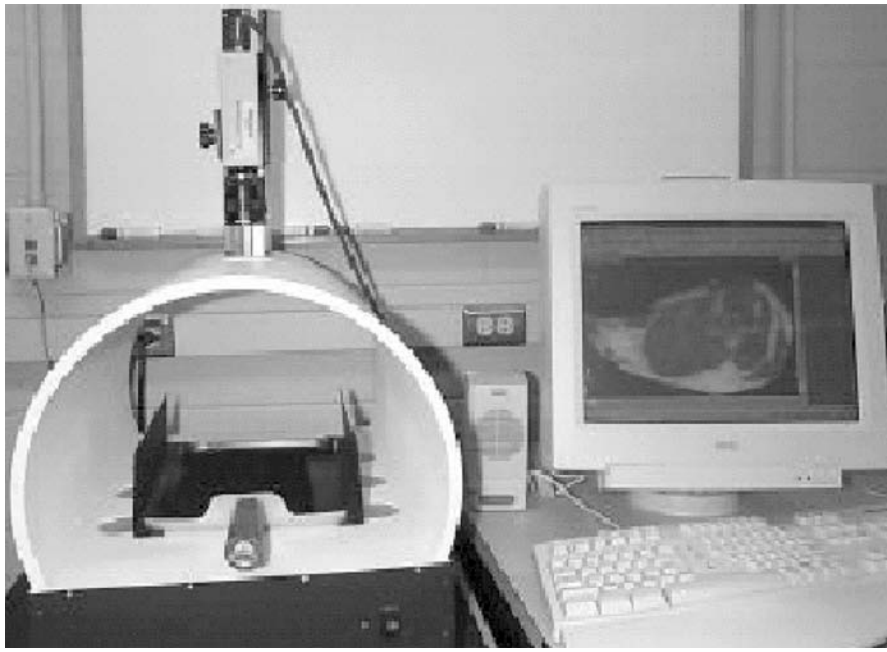

FIGURE 3.95
Photograph of the beef imaging setup. (*Reprinted from ASAE Annual International Meeting Presentation, 2001, Paper No. 01-3063, with permission from American Society of Agriculture and Biological Engineers, 2001*)

view. Camera resolution was 640 pixels × 480 pixels. Output was in RGB format. A calibration grid was employed to quantify pixel size. An 8-mm lens was mounted on the camera to capture a full image of the sample steak. Close-up images of the central portion of the ribeye were obtained with a 50-mm lens. The close-up images obviously provided more textural details. Figure 3.95 shows a photograph of the image-capturing setup. The captured images were preprocessed by segmenting the ribeye from the background, intermuscular fat, and extraneous tissues. Background was removed from the object by an adaptive thresholding method of FCM clustering. Fat and extraneous tissues were also removed by morphological operations.

Color, size, and orientation of the patterns influence the perception of texture. The same texture at two different scales can be perceived as two different textures. Color-textured features were extracted from ribeye segmented from full steak images and from the central region of ribeye.

Spatial gray level cooccurrence matrix (GLCM) analysis was used for extracting 14 textural features from grayscale images. Similarly a gray level difference histogram (GLDH) was also used to calculate seven second-order textural features. The features were used in FCM to discriminate fat from lean meat. The tenderness classification was tested by an Inston Universal Testing machine fitted with a Warner-Bratzler shear head attachment. Percentage

tenderness classified by shear force machine and machine vision technique were compared and a correct classification of tender and tough was found at 92%. This computer vision approach shows the potential for nondestructive and on-line applications in the meat industry.

3.13.3.2 Tea Texture Measurement in Grading

Texture analysis techniques where fractal dimensions have been used to extract texture information have proven to be the simplest method. Borah [10] developed a method for black tea texture measurement based on feature extraction from different subbands of the pyramidal decomposed images. As per this technique the lower subband images of the size 16×16 or 32×32 also contain useful information about the tea grade texture variability. Variance, entropy, and energy features were calculated for all subband images of black tea. This method facilitates categorizing a test image belonging to any one of eight different tea grades of different sizes of granules using k-means and SOM algorithms.

Feature Vectors

The following steps are adopted for feature vector extraction from the gray-scale images of tea:

1. The textured images are decomposed using fast wavelet transform on the subband images with a special set of Daubechie's wavelet for each gray value.
2. Subband images of different levels are stored for feature vector calculation. Mean, variance, entropy, and energy vectors were calculated for all subband images.

Threshold Measurement

The extracted features of all groups were classified using Mahalanabis distance. The Mahalanabis distance was measured in terms of standard distance from mean of samples. The method finds the two most significant images with highest distance that was considered the threshold value. Table 3.25 shows, as an example, all possible combinations of the distances between five test images I_1 through I_5. In the next step the highest distance was picked up as the threshold (Md_{xy}) and the two corresponding images I_x and I_y were considered to be located at the highest distance. When a test image is to be classified under any one of the five groups, the distances are considered the feature vector of the test images.

Tea Grades

Eight varieties of cut-tear-curl (CTC) tea grades were used as the classification groups. Table 3.26 shows these grades of tea with granule sizes and figure 3.96 shows texture images of the tea grades.

TABLE 3.25

Distances Among Five Images

Images	I_1	I_2	I_3	I_4	I_5
I_1		Md_{12}	Md_{13}	Md_{14}	Md_{15}
I_2			Md_{23}	Md_{24}	Md_{25}
I_3				Md_{34}	Md_{35}
I_4					Md_{45}
I_5					

Source: Machine Vision for Tea Quality Monitoring with Special Emphasis on Fermentation and Grading, PhD thesis, Department of Electronics, Tezpur University, India, 2005. Adapted with permission from S. Borah.

TABLE 3.26

Tea Grades with Granule Sizes

Grade Name	Full Name	Granule Size (mm)
BOPL	Broken orange pekoe large	2.0
BOP	Broken orange pekoe	1.7
BOPSM	Broken orange pekoe small	1.3
BP	Broken pekoe	1.0
PF	Pekoe fanning	0.5
PD	Pekoe dust	0.355
Dust	Dust	—
OF	Orange fanning	—

Source: *Machine Vision for Tea Quality Monitoring with Special Emphasis on Fermentation and Grading*, PhD thesis, Department of Electronics, Tezpur University, India, 2005. Reprinted with permission from S. Borah.

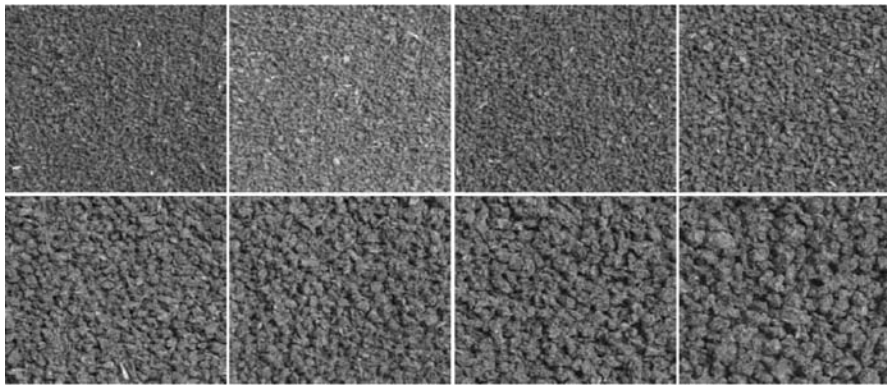

FIGURE 3.96
Texture images of eight tea grades. (*Reprinted from PhD thesis with permission from S. Borah*)

K Means and SOM Clustering

The K-means clustering algorithm adopts a method of estimating the number of heterogeneous clusters present in a given data set by iteratively adding and adjusting cluster center. The algorithm calculates the sum-squared distance of each data point to its cluster center. Eleven images from each of seven different categories (a total of 77 images) were tested. This technique shows how the current manual method of tea grading can be made more efficient by adopting a computer vision technique.

3.13.4 Particle Size Detection

Particle size of powdered foods like cocoa powder is an important factor for producing drinks. In the case of cocoa powder particle size should be very fine (maximum of 75 μm) to avoid sedimentation at the bottom of the drinks. In some other applications like the sugar industry, sugar should be free flowing and should have uniform particle size. The particle size of coarse sugar can be 1.0 mm to 2.5 mm, whereas fine icing sugar should be 0.005 mm to 0.1 mm. Particle size has another important role to play in food grinders, where fineness requirements restrict minimization of probable metal contamination from the grinder discs. The grinder disc pressure can be adjusted and an increase in pressure increases metal contamination in food. Thus particle size detection can optimize the grinder disc pressure and gap to avoid metal contamination.

The conventional method of particle size measurement is dry sieving, best suited for material coarser than 75 μm. The food is shaken through a series of sieve bases that have regularly spaced uniform size openings. The measure of the mass of material retained in the sieve gives the particle size. Particles smaller than 75 μm should be measured using a special type of sieving mechanism.

3.13.4.1 Off-line Methods

Optical microscopy is a standard method of particle size detection for small samples in off-line mode. This technique is also used for calibration of other particle size detectors. The resolution is dependent on the wavelength of light used. The size resolution depends on the electron beam energy and typical resolution values are 0.006 μm to 0.01 μm.

In the optical scattering technique, light rays are allowed to scatter or diffract into various directions and the amount of scattered light is measured. The scattered light from individual particles produces pulses that register counts in counting bins according to size. Resolution of such devices ranges from 1 μm for water-suspended particles.

3.13.4.2 On-line Techniques

On-line particle size measurement can be conducted on flowing or moving food using turbidimetry and the back-scattering principle, but due to variation

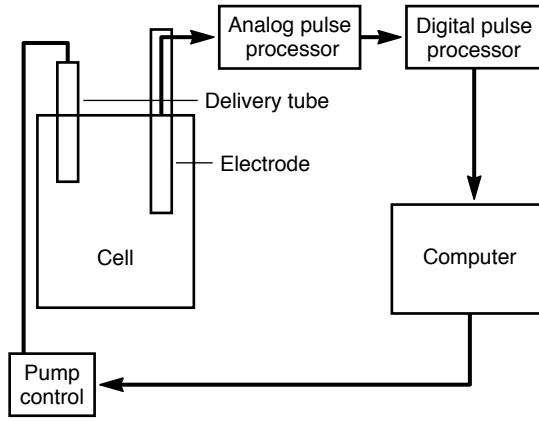

FIGURE 3.97
Block diagram of an online particle size analyzer.

of optical properties for change in composition this method is best suited for monitoring a change rather than absolute value measurement.

An electrical sensor based on the Coulter principle offers resolution around 0.5 μm. In this technique a particle distribution is suspended in an electrolyte and a small orifice immersed between two electrodes draws the particles to pass through it. When a particle traverses the orifice, it displaces its own volume in the electrolyte and causes a momentary change in resistance proportional to the volume of electrolyte displaced. A voltage pulse proportional to the volume of the particle is obtained. The pulse corresponding to a particle is amplified, scaled, and registered into counting bins as per size. The particles drawn through the aperture are precisely controlled to allow the system to count and size particles for an exact reproducible volume. Several thousands of particles per second are counted as per size with great accuracy. The measurement is independent of size, shape, and color of the particles. A fully automated online particle size analyzer (fig. 3.97) for process control can be designed with these accessories: a sampling system to extract a sample from the flow line; a dilution water conditioner and agitator to mix the powder sample with water for circulating through the measuring cell; sampling programmer, timer, and level controller; signal processing electronics with computer-based signal acquisition, logging, and displaying; and a computer-based alarm and process controller to take appropriate measures.

3.14 Food Constituents Analysis

Food is closely related to aesthetic, nutritional value, and safety factors. To maintain these three factors at a standard level food manufacturers need to

analyze constituents of the food they produce. A food process might be completely tuned to a high productivity level, low cost, and high energy savings, but the product might have at low food value, low safety level, and low hygiene level. The tea with the best flavor and best price might carry more insecticide than the permitted level, which is not noticed by the human nose. The food safety regulatory bodies deal with the risks inherent in production, processing, transportation, and preservation of food items. There must be a healthy interface between the technology and law. Food regulatory bodies specify standard chemical and biochemical analyses to be conducted on food. Within the framework of this book it is not possible to provide full guidelines laid by the food-related international or national legislations. In the United Kingdom it is covered by the Food Safety Act (1990), whereas in the United States the Federal Food, Drug, and Cosmetic Act covers similar issues.

Food content measurement and analysis, off-flavor detection, and foreign substance detection are some important issues in food processing. Food content measurement is mostly dealt with in the off-line environment because continuous measurement or analysis is a complex procedure that is difficult to design. Although it is envisioned that in the future food processing will be equipped with fully on-line and automatic analyzing methods, in most of the food industries, routine food sample analysis is done at the laboratory off-line only. This section covers certain off-line or semi-off-line food analysis experiments conducted by researchers. The topics are discussed briefly; however, readers are advised to consult the texts from the references quoted for details.

3.14.1 Carbonates, Bicarbonates, and Organic Matters in Bottled Water

Bottled waters are carbonated beverages developed from the carbonation of mineral waters. Naturally available water is also bottled after adding carbon dioxide, which is called soda water. Some water beverages included added acidified sugar syrup or other sweetener or essence. In some countries, for treatment of malaria, a quinine salt is added to bottled water, known as tonic water. Irrespective of the additional sweetener, essence, or tonic added to bottled water, the carbonates and bicarbonates are important anions found in up to 85% of the inorganic salts.

Mee et al. [34] adopted the autotitralizer technique for rapid determination of CO_3 and HCO_3 in bottled water. Figure 3.98 shows a schematic diagram of such a potentiometric autotitralizer. Such an autotitralizer performs titration in the exact sequence of manual titration by automated opening and closing of valves by an electronic or mechanical (multicam) programmer. The program sequence is as follows: The reagent valve (RV) is opened to fill the burette with reagent from a storage jar to a prefixed mark. At this stage the conducting follower probe is prefixed to maximum height. After this the programmer opens the sample valve (SV) and the flush valve (FV) opens to flush the cell with the sample. After flushing and filling SV and FV, both are closed. The magnetic stirrer is started and the reagent is allowed to mix by

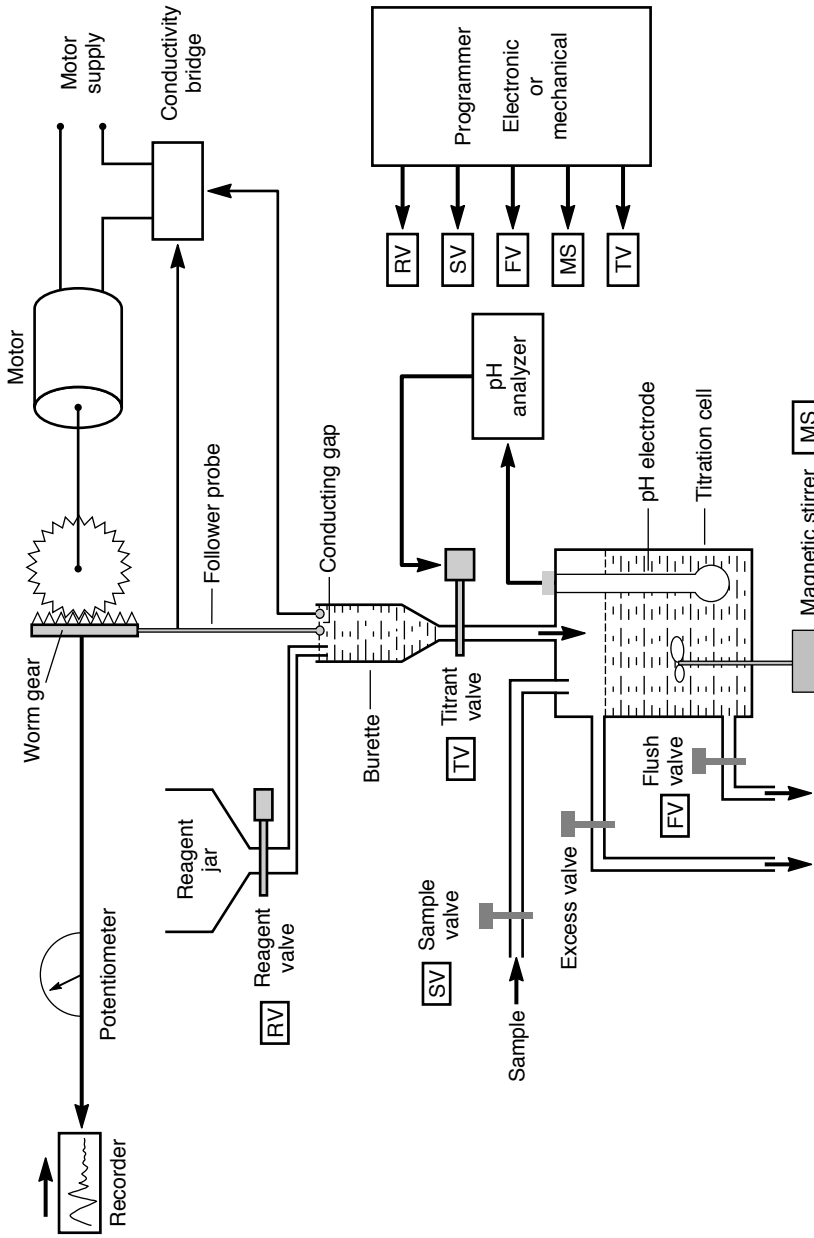

FIGURE 3.98
Flow sheet of an autotitralizer.

opening the titrant valve (TV). As soon as the reagent is added, the pH analyzer is started to measure the pH of the solution of the titration cell. In the burette, the reagent level drops, the conducting gap breaks, and the conducting bridge powers a DC motor to advance the follower probe until the gap is covered. The movement of the follower probe is recovered by a potentiometer attached to the worm gear arrangement. When the end point of the titration is reached, the pH analyzer closes the TV. The potentiometer as well as the recorder record the volume of the reagent and can be calibrated in terms of concentration or ppm.

Mee et al. [34] found that the autotitralizer needs at least 75 ml of the test sample for immersion of the electrode and stirrer, and 100 ml is the recommended volume. The recovery rate of HCO_3 was found to be 98% to 119% by adding from 5 ppm to 100 ppm. Below 10 ppm of CO_3, the standard deviation was 28% and percentage error was 85%. These values for HCO_3 were 10% and 9%, respectively, for less than 5 ppm. The CO_3 ion was not correctly detectable if the pH value of the water sample was neutral or acidic. Therefore, pH values were also continuously monitored using the autotitralizer.

Organic matters in drinking water or beverages change the taste. Mee et al. [35] further analyzed organic maters in bottled water by infrared spectroscopy. They developed a rapid screening test for the detection of organic matters based on $CHCl_3$ extraction by IR spectrometer through 200 to 4,000 cm^{-1} wave number. IR spectra of distilled water samples were taken from $CHCl_3$ extracts of water both at ambient temperature and at an elevated temperature of 110°C (for 1 hr prior to extraction). IR bands were observed at 1,350 cm^{-1} at ambient temperature and two IR bands at 1,600 and 3,680 cm^{-1} were significantly observed at 110°C/1 hr heating due to thermal activation of organics present. They further studied the volatility of organics in water (by PS-SP-080 IR Data System) such as hydrocarbons and chlorinated hydrocarbons, decanol, and benzonitrile.

3.14.2 Volatile Compounds in Tropical Fruits

Tropical fruits are very popular in food processing for their unique flavors and bright colors. Soft drinks and jam and jelly production depend most on tropical fruits: mango, papaya, passionfruit, avocado, and so on. The flavor of these fruits depends on a number of volatile compounds, so the estimation of these compounds is an important tool for food processing. Yamaguchi et al. [36] conducted an investigation on analysis of volatile compounds on those four tropical fruits using GLC and combination of gas chromatography-mass spectroscopy (GS-MS), near magnetic resonance (NMR), IR, and UV spectroscopy.

The peel and seeds were removed from the fruits and edible parts were homogenized with deionized water using a homogenizer. The homogenized fruits were water distilled under reduced pressure in a nitrogen stream at a water bath. The distillate samples were extracted with dichloromethane

using a liquid–liquid continuous extractor. The extract was dried and the solvent was removed under vacuo. A Hewlett-Packard Model 5710-A GC with a flame ionization detector was used for volatile profile analysis. Fused silica capillary columns were developed and used in the GC.

Another GC, Hitachi Model M-80 combination MS-GC (HP-5710A) was used with the same GC column and oven temperatures. The following are the results obtained from the GC-MS analysis:

Mango: 21 constituents; highest constituent, monoterpenes with 42.32% of total GC area.

Papaya: 20 components; highest, butyric acid with 37.34% of the total GC area.

Passionfruit: 21 constituents; highest constituent, n-hexyl n-butyrate with 14.34% of total GC area.

Avocado: 52 constituents; highest constituent, trans-2-hexanol with 58.95% of total GC area.

3.14.3 Moisture, Protein, Fat, and Ash Content of Milk Powder

A near infrared reflectance spectroscopy (NIRS) analyzer has been established by Ereifej et al. [37] as an efficient technique for detecting moisture, protein, fat, and ash content in dried milk powder. NIRS was initially used for moisture analysis in food products, but researchers later extended its use to protein and oil content. Several manufacturers have developed sophisticated instruments based on NIRS techniques for compositional analysis of grain and oilseeds. NIRS has also been successfully used for monitoring sugar and carbon dioxide in carbonated beverages by Frant et al. [38]. In their study, Ereifej et al. [37] used a Neotec NIRS model GOA-41 to detect moisture, protein, fat, ash, and lactose content in four different milk samples: milk powder prepared by spray drying mixtures of skim and whole milk, milk powder prepared by mixing predried skim and whole milk, commercial samples, and commercial cheese powders.

The instrument used spectra in the 1800 nm to 2320 nm region for the analysis with four selected wavelengths. These wavelengths were used to calibrate the readings with known composition. The results were justified by conventional oven, dry ashing, and the Microkjeldahl method for moisture, ash, and nitrogen content determination. Fat content results were correlated with the Mojorrier procedure.

3.14.4 Components in Alcoholic Beverages

The finished products of alcoholic beverages range from pure aqueous alcohol to complex mixtures such as vermouths. Most of the volatiles of interest obtained in alcoholic beverages are present at a level of less than 50g/l. Liddle

et al. [39] adopted a very simple and fast analysis technique with a simple sample preparation method. They used a capillary GC using glass or fused silica columns. This facilitates faster analysis, allowing simple sample preparations. They were able to detect contaminants such as residual monomer, plasticizer, and antioxidants contributing to off-flavors. Total number of volatile compounds detected was about 21. Similarly, about 14 compounds were detected in dry white wine. The diminishing of many volatile compounds was noticed in 8-year-old rum, where only six components were found.

Apostolos et al. [40] detected mineral constituents such as aluminum, calcium, magnesium, and vanadium in Greek wines. For analysis of trace elements of wines, flameless atomic absorption (FLAA) and neutron activation analysis (NAA) were found to be the most sensitive and accurate methods.

3.14.4.1 Minerals in Wines

Analysis of the minerals in wine, particularly aluminum, calcium, magnesium, and vanadium, is very important for quality control and handling wines. Aluminum in wine is found in concentrations of 0.5 to 10 mg/l due to possible contamination from storage in aluminum containers. Aluminum is undesirable in wine because it makes the wine cloudy. Calcium and magnesium present in wine combines with tartarates and precipitates as calcium and magnesium tartarates, even months after bottling. Calcium and magnesium contents in wine can be due to soil conditions of grapes, treatment with fining agents, storage in concrete tanks, use of ion-exchange resins, and so on. Vanadium content in wine gives an off-flavor either by poisoning the yeast or by changing the morphology or physiology of the yeast.

A coaxial germanium-lithium drifted Ge(Li) detector (ORTEC Model WIN 15 Series) can be used for this analysis. In this detector the output signals are fed to a preamplifier (ORTEC Model 119) and a spectroscopy amplifier (ORTEC Model 571). The pulse height of the spectrum detected by the Ge(Li) detector is analyzed by a pulse height analyzer. The radiation detector is considered an ideal method for simultaneous determination of a large number of trace elements due to its sensitivity, rapidity, precision, and accuracy. The precision of measurements reported are 0.72 mg/l for Al, 26 mg/l for Ca, 64 mg/l for Mg, and 1.0 mg/l for vanadium.

3.14.5 Quality Parameters in Cereals and Cereal Products

Protein quantity and quality are of basic interest to cereal and food technologists in assessment of the overall quality and the most important correlation to the final product. Starch is another constituent responsible for CO_2 production during the baking process. Additions in flours (e.g., dry gluten, oxidizing agents, malt flour, enzymes, organic acids, emulsifier, etc.) are also important detectable matters. Pattakou et al. [41] assessed wheat flour to detect its water absorption capacity by Farinograph and mechanical properties of dough by

Extensograph. The Extensograph properties of dough indicate suitability for making bread and puff pastry goods. In addition, Extensograph properties indicate the action of oxidative agents and ingredients and percentage of gluten to be added to improve rheological behaviors to wheat flour.

They also conducted Amylograph tests on wheat flour, and b-amylase activity, gassing power, and falling number tests to assess starch behavior; and Fermentograph tests on wheat flour to assess CO_2 production during yeast formation.

3.14.6 Meat Content

Protein and moisture content in pure meat is almost constant, but the nitrogen content is different in different meat. As specified by the Society for Analytical Chemistry, the Royal Society of Chemistry, the highest nitrogen content (percentage nitrogen on fat-free basis) is 3.9 in chicken breast and the lowest is 3.0 in tongue of animals in the United Kingdom. In other countries, composition of meat products is represented by nitrogen or protein content of water/protein (e.g., in muscle meat 77% water/23% protein = 3.35), indicating the fat-free meat content.

In Germany, the Feder number, the ratio of water to organic nonfat content, is used. This ratio is

$$\text{Feder number} = \text{water}\%/(\,100 - (\text{fat}\% + \text{water}\% + \text{ash}\%\,)) \quad (3.78)$$

In France the moisture of the defatted meat is used as the meat content indicator. In the United States, the term *protein on fat free* is used:

$$\text{PR}_\text{f} = (100 \times \text{protein}\%)/(100 - \text{fat}\,\%) \quad (3.79)$$

Rapid analytical methods have been developed for determination of meat content components, such as fat, protein, nitrogen, and water. The methods are utilized in the following commercial analyzers:

1. The Infralyzer and the Foss SuperScan analyzer™ are convenient as far as their operational techniques are concerned. In both the analyzers, infrared light rays are passed through the sample and the energy absorbed by the sample is measured. The system is comprised of an IR source, electronic balance for accurate sample weight placement, a reactor for sample preparation, and a detecting unit for fat, protein, carbohydrate, and water. The system is controlled by a desktop computer.
2. The AnylRay™ machine works on X-ray diffraction technique and detects the fat content of meat. The sample requirement is comparatively high (1–15 kg), but the sample can be reused.

3. The CEM Meat Analyser™ dries the sample in a microwave dryer and treats it in an automatic fat extraction unit with an automatic solvent extraction and recovery system. The analyzer can give results in under 10 min.
4. The Dickei-John ground meat tester is an electrical device with which an EMF in a piece of meat is developed by electromagnetic induction principle. The EMF is calibrated in terms of lean meat content to give an instant readout.

3.14.7 Bacteria and Foreign Body Detection

3.14.7.1 Bacteria Detection

Microbiological infection and food poisoning is a matter of concern for food manufacturers and food testers. Poisoning by foodborne bacteria is mostly associated with large-scale food service operators rather than food manufacturers; however, food packaging sectors should take every possible measure to prevent bacterial infection. The most common foodborne bacterias are *Listeria monocytogens, Salmonella, Campylobacter, Clostridium botulinum, Aeromoas hydrophila,* and *Bacillus subtilis*. Bacteria growth in food is encouraged by moisture and osmotic pressure in food.

The conventional method of bacteria assessment is the plate-count method, which is very slow and can take several days. Therefore food manufacturers use rapid methods like the Lumac method based on bioluminescence. A widely used method was developed by Bactomatic, in which a sample is mixed with a medium and placed in an impedance-sensing cell under controlled temperature conditions. The impedance detection time (IDT) to reach a number of organisms with a specified concentration is used to quantify the quality of many foods.

Rapid detection of pathogenic bacteria has been successfully tested by Tsen et al. [42] using a DNA hybridization technique. They used the probe for detection of *Salmonella* spp in soy flour, macaroni, meat, and fish. The detection takes 70 hr and counts as low as 1.6 per gram are possible.

3.14.7.2 Foreign Body Detection

Foreign bodies in food primarily include metal particles. In an on-line method the technique is similar to that of a general metal detector, but with a small aperture. The food is carried over a nonmetallic conveyor and allowed to pass through a small aperture around which three coils at a symmetrical electrical axis are placed. A central coil is excited by a high-frequency voltage inducing identical voltages in the other two coils connected in phase opposition. A voltage is induced due to imbalance in the coil induction when a metal particle passes through the aperture. The equal induced voltages are cancelled out when there is no metal particle.

Another method of metal detection is the X-ray inspection in gross items in bulk materials. In materials in sheet form, optical detection methods offer good resolution at high speed. In an optical inspection system, images or scan data are acquired by video camera or a photodiode array. The output from the array in successive scans can be analyzed on-line to detect the presence of any foreign body.

3.14.7.3 Removal of Stalks from Tea

Due to improper withering, cutting, or drying, colored stalks are sometimes developed in CTC tea. Stalk particles are amber to brown in color, whereas clean tea granules are black. The presence of stalk is detected by an array of photocells that receive filtered light reflected back from a single layer of tea. The filter selects the band of light nearest to the stalk color when the corresponding photocell sees a stalk color to develop an electrical voltage. The voltage in turn activates a small air jet to blow off the selected stalk instantly. An electromagnetic high-frequency vibrating conveyor is used to spread the tea with stalk across the width of the machine. The vibrator spreads the tea into a single layer, minimizing ejection of black tea particles. The filters are cleaned periodically by compressed air. A commercial and automated tea stalk sorter machine manufactured by Senvec, Inc. (Japan) is shown in figure 3.99.

FIGURE 3.99
Photograph of a tea color stalk sorter (Model-BTR-C Series). (*Reprinted with permission from Hattori Seisakusho Ltd., Japan*)

3.15 Conclusion

There is a large gap between the food industries and food scientists. In spite of tremendous developments in the fields of electronics, instrumentation, and computer technology, the food industries have been facing many difficulties in measurement of food-related parameters. One reason for this gap is the development toward generalized applications of electronic sensors, leaving food-specific sensors far behind. For example, the new sensors like ISFET, ENFET, and E-nose sensors can detect food pH, enzymes, and flavors, but these new sensors must be adapted properly to make them effective for food-related applications. Similarly. image processing has shown powerful feature extraction and classification capabilities, but food-related issues are very limited.

This chapter provides sufficient information on the available methods in food-related measurement techniques with respect to various process parameters. Some examples of applications are provided to guide one to implement these techniques in one's own applications. For a particular measurement, there is no common or single transducer for each type of food material. Therefore, in every section of this chapter, in discussing a particular measurement technique, the relevance of the technique for a particular food material has been explained. This should help the reader in identifying an appropriate technique for a specific application.

References

1. Bhuyan, M., Gogoi, S., and Choudhury, A. 1996. A novel technique of moisture measurement in green tea leaves. *Proc. of Int. Conf. Trends in Industrial Measurements and Automation*, 78–84.
2. Subramanyam, K., Venkataraman, V., and Sankaranarayanan, P. E. 1994. Online moisture analyzer for tea industry. *J. Instr. Soc. of India* 24(3&4):124–130.
3. Bhuyan, M. 1997. An integrated PC-based tea process monitoring and control system. PhD Thesis, Department of Electronics, Gauhati University, India.
4. TRA. 1991. Calculation of percentage of wither and corresponding moisture content of green and withered leaf. *Res. Bulletin*, Sr. No 184. Jorhat, India: Tocklai Tea Experimental Station.
5. TRA. Moisture 1962. content of green leaf and its relation to yield of made tea. *Res. Bulletin*, Sr. No 18. Jorhat, India: Tocklai Tea Experimental Station.
6. Bhuyan, M., Dutta, V., Sharma, P. K., and Choudhury, A. 1996. A microprocessor based relative humidity measuring technique using piece-wise linearised model of psychrometric chart. *Proc of Int. Conf. Trends in Industrial Measurements and Automation*, 78–84.
7. Bhuyan, M., and Bhuyan, R. 1995. An on-line method for monitoring of relative humidity using thermal sensors. *Proc. of IEEE Int. Conf. on Industrial Automation and Control*, 7–11.

8. Govindraj, R., and Sankaranaryanan, P. E. 1996. Estimation of color and turbidity and pH values of sugar juice during sugar refining process. *Proc. of Int. Conf. Trends in Industrial Measurements and Automation*, 94–98.
9. Borah, S., and Bhuyan, M. 2002. Non destructive testing of tea fermentation using image processing. *Int. Conf. of Non Destructive Testing*, Southport, UK.
10. Borah, S. 2005. Machine vision for tea quality monitoring with special emphasis on fermentation and grading. PhD Thesis, Department of Electronics, Tezpur University, India.
11. Mahanta, P. K. 1988. Biochemical basis of color and flavor of black tea. *Proc. of 30th Tocklai Conf.*, 124–134.
12. TRA. 1988. Polyphenol content and theaflavin concentration analysis. *Res. Bulletin*. Jorhat, India: Tocklai Tea Experimental Station.
13. Borah, S., and Bhuyan, M. 2005. A computer based system for matching of color during the monitoring of tea fermentation. *Int. J. Food Sci. Tech.* 40:675–682.
14. Sridhar, R., Anil, P. K., Sankaranarayyan, P. E., and Rakowski, R. 1986. New refractometer for on-line brix measurement in the food processing industry. *Proc. TIMA-96*, 85–90.
15. Yates, D. E., Levine, S., and Healy, T. W. 1974. Site binding model of electrical double layer at the xide/water interface. *J. Chem Soc. Faradays Trans.* 70:1807–1819.
16. Fung, C. D., Cheung, P. W., and Ko, W. H. 1986. A generalized theory of an electrolyte-insulator semiconductor field effect transistor. *IEEE ED* 33(1):8–18.
17. Ogrodzki, J., and Opalski, L. 2000. Modeling of semiconductor pH sensor for CAD. *Proc. 7th Int. Conf. on Mixed Design of IC and Systems, MIXDES 2000,* 259–264.
18. Leandro, L., Lorenzelli, L., Margesin, B., Martinoia, S., Tedesco, M. T., and Valle, M. 2003. Bio-electrochemical signal monitoring of in-vitro cultured cells by means of an automated microsystems based on solid state sensor array. *Biosens. Bioelectr.* 18(5–6):621–626.
19. Martinoia, S., Rosso, N., Grattarola, G., Lorenzelli, L., Margesin, B., and Zen, M. 2001. Development of ISFET array-based microsystem. *Biosens. Bioelectr.* 16:1043–1050.
20. Artigas J., Jimenez, C., Dominguez, C., Minguez, S., Gonzalo, A., and Alonso, J. 2003. Development of a multi-parametric analyzer based on ISFET sensors applied to process control in the wine industry. *Sensors and Actuators* B89:199–204.
21. Bohnke, C., Duroy, H., and Fourquet, J. K. 2003. pH sensors with lithium lanthanum titanate sensitive materials: Application in food industries. *Sensors and Actuators* B89:240–247.
22. Updike, S. J., and Hicks, G. P. 1967. The enzyme electrode. *Nature* 214:986–988.
23. Canh, T. M. 1993. *Biosensors* (English ed.). New York: Springer Science.
24. Pearce, T. C., Gardner, G. W., and Friel, S. 1993. Electronic nose for monitoring of the flavors of beer. *Analyst* 118:371–377.
25. Llobet, L., Hines, E. L., Gardner, J. W., and Franco, S. 1999. Non-destructive banana ripeness determination using a neural network based electronic nose. *Meas. Sci. Tech* 10:538–548.
26. Dutta, R., Hines, E. L., Gardner, J. W., Kashwan, K. R., and Bhuyan, M. 2003. Tea quality prediction using a tin oxide based electronic nose. *Sensors and Actuators* 94:228–237.
27. Dutta, R., Kashwan, K. R., Bhuyan, M., Hines, E. L., and Gardner, J. W. 2003. Electronic nose based tea quality standardization. *Neural Networks* 16:847–853.

28. Dutta, R., Hines, E. L., Gardner, J. W., Kashwan, K. R., and Bhuyan, M. 2003. Determination of tea quality by using a neural network based electronic nose. *Proc. International Joint Conference on Neural Network* 1:404–409.
29. Kashwan, K. R. 2005. An artificial neural network based electronic-nose system: Tea and spice flavor discrimination and drift parameter determination. PhD Thesis, Department of Electronics, Tezpur University, India.
30. Swatland, H. J. 1997. Relationship between the back-scatter of polarised light and the optical detection of connective tissue fluorescence in beef. *J. Sci. Food and Ag*. 75:45–49.
31. Jeyamkondan, S., Kanzler, G. A., and Lakshmikanth, A. 2001. *Predicting beef tenderness with computer vision* (Paper No.01-3603). ASABE Annual Meeting Presentation. St. Joseph, MI: American Society for Agricultural and Biological Engineers (ASABE).
32. Wulf, D. M., O'Connor, S. F., Tatum, J. D., and Smith, G. C. 1997. Using objective measures of muscle color to predict beef longissimus tenderness. *J. Anim. Sci.* 75:684–692.
33. Li, J., Tan, J., Martz, F. A., and Heymann, H. 1999. Image textural features as indicators of beef tenderness. *Meat Sci.* 53:17–22.
34. Mee, J. M., Jahangir, M., Faruq, I. M., and Al-Salem, S. 1983. Analysis of carbonates in bottled waters by autotitraliser. In *Instrumental analysis of foods: Recent progress*, ed. Charalambous, G. and Inglett, G. (Vol. 2), 21–32. London: Academic Press.
35. Mee, J. M., Khan, P., and Ahmed, S. 1983. Application of direct mass spectroscopy for rapid analysis of organics in water beverages. In *Instrumental analysis of foods: Recent progress*, ed. Charalambous, G. and Inglett, G. (Vol. 2), 33–40. London: Academic Press.
36. Yamaguchi, K., Nishimura, O., Toda, H., and Mihara, S. 1983. Chemical studies on tfopical Fruits. In *Instrumental analysis of foods: Recent progress*, ed. Charalambous, G. and Inglett, G. (Vol. 2), 93–117. London: Academic Press.
37. Ereifej, K. I., and Markakis, P. 1983. Analysis of dried milk and cheese powders by near infrared reflectance spectroscopy. In *Instrumental analysis of foods:Recent progress*, ed. Charalambous, G. and Inglett, G. (Vol. 2), 237–242. London: Academic Press.
38. Frant, M. S., and Labutti, G. 1980. Process infrared measurements. *Anal. Chem*. 52:1331A–1344A.
39. Liddle, P., and Bossard, A. 1983. Glass capillary GC in wine and spirit industry. In *Instrumental analysis of foods: Recent progress*, ed. Charalambous, G. and Inglett, G. (Vol. 2), 307–321. London: Academic Press.
40. Apostolos, P. G., Vassilaki-Grimani, M., and Kanias, G. D. 1983. Instrumental neutron activation analysis of aluminum, calcium, magnesium and vanadium in Greek wines. In *Instrumental analysis of foods: Recent progress*, eds. Charalambous, G. and Inglett, G. (Vol. 2), 323–334. London: Academic Press.
41. Vassiliki Pattakau, V., and Voudouris, E. 1983. Analytical instrumentation and assessment of quality parameters in cereals and their products. In *Instrumental analysis of foods: Recent progress*, eds. Charalambous, G. and Inglett, G. (Vol. 2), 479–492. London: Academic Press.
42. Tsen, H., Wang, S., and Green, S. S. 1991. Salmonella detection in meat and fish by membrane hybridization with chromogenic/phosphatase/biotin DNA probe. *J. Food Sci.* 56:1519–1523.

4

Controllers and Indicators

CONTENTS

4.1 Introduction

Due to the advent of modern electronic techniques and automatic control devices supported by instrumentation, power electronics, and digital systems, the control of machines in industries has been revolutionized. Even today, however, many food processing industries are run by either outdated mechanical means or manual methods. As a result maximum quality, productivity, and efficiency are not ensured. Therefore, there are obvious reasons for incorporating scientific and electronic control devices in food industries. For example, most of the tea factories in India use single-phase or three-phase induction motors ranging from 0.5 hp to 25 hp, totaling around 50 to 60 in a tea factory of normal size for 10 to 12 different process operations. However, these machines are still manually operated today. For a production of 5×10^5 kg/year of processed tea, the average power consumption of a tea factory is about 600 MWh and the total energy requirement of the entire tea sector in India is about 7×10^5MWh [1]. This implies that there is ample opportunity to save a substantial amount of electrical energy in the tea industry alone. Automatic control for food processing not only contributes toward saving energy, but substantially improves quality and efficiency as well.

The usage of controllers in food processing is improving with greater application of engineering capabilities. Applications of computer control,

instrumentation, neural networks, and artificial intelligence techniques are gaining importance in the food processing industries. A responsible food manufacturer is very much concerned about manufacturing a product to a certain standard and selling the food for profit. Control of food quality begins with the raw materials and it continues through various manufacturing processes to storage and packaging. Good Manufacturing Practice (GMP) aims at well-designed manufacturing operations, quality control systems, and quality assurance systems. It is the duty of food manufacturers to adopt process instrumentation and process control devices to achieve reliable and effective control at a reasonable cost.

During my research in development of computer control techniques for the tea industry, it became apparent that there are many innovations yet to be made to make tea processing automotive. Even today, in most tea factories, the quality of the tea during various processes is assessed by smelling, touching, and visual inspection, and machines are controlled by manual operators. There are many similar examples in other food processing industries in which control strategies are known and well defined, but design and development of control techniques has yet to be done.

Examples of industrial controllers and annunciation applications in food processing include temperature and moisture content control in dryers and ovens, flow control in rotary dryers in the sugar industry, withering control in the tea industry, cooling surface area control in chocolate tempering, automated sorting and bottling, and atmospheric control in food storage. This chapter describes a series of examples of food processing systems highlighting the process parameters, control actions adopted or recommended by food scientists, and timers and annunciators associated with the control strategies. The chapter also presents a general overview of classical and modern control schemes used for food processing control.

4.2 Temperature Control in Food Dehydration and Drying

The principle purpose of food dehydration and drying is removal of water before preservation; however, food can be dehydrated to decrease its weight. In such applications, the size and shape of the food is retained, only the weight is reduced. The shipping cost based on weight is reduced, but when shipping cost is based on volume, not on weight, dehydration might not be useful. Another aim of dehydration is production of instant food items. In such production, the cooking and other processing is conducted before the food is dried. Before consumption, the consumer has to make only a simple preparation effort (e.g., mixing with hot water, adding spices or sauces, etc.).

Although sun drying is still popular for many agricultural products, due to its inherent disadvantages, sun drying is not considered an efficient method for many reasons: it is slow and not suitable for many high-value

products, the space required for drying is greater, moisture content below 15% is not achievable, and the food being exposed is subject to contamination and losses due to various reasons.

The term *food dehydration* technically refers to drying artificially under controlled conditions. Although many other food processes like cooking, frying, and broiling involve removal of water from the food, these processes are not considered dehydration. Strictly speaking food dehydration means removal of water without any change in the food; that is, the food should be able to be reconstituted with its original taste, flavor, and other properties by the addition of water or other liquid. Therefore drying with maximum product stability and low moisture level is difficult to achieve. A precise and accurate control of the drying phenomenon is necessary to achieve these criteria.

4.2.1 Control Parameters for Heat and Mass Transfer in Drying

In any type of food drying process, dehydration involves heat transfer from the drying air of the surrounding medium to the food and release of moisture from the food to the air. These two stages of heat and mass transfer should be easily facilitated without any obstruction to achieve fast and efficient drying. Factors affecting the drying process include surface area of the food being exposed, temperature difference between the heating medium and the food item, velocity of the heating air, humidity of the air collecting the moisture from the food, and atmospheric pressure of the heating air.

To speed up heat and mass transfer during drying, the food is generally spread widely to an optimal thickness. However, there must be a compromise between spread thickness and the size of the conveyor floor, volume of the dryer, and the feed rate of the food. The drying air drives off moisture from the food and the hotter the air, the more moisture it can drive off, making the drying process faster. Therefore, a higher temperature difference between the heating medium and the food speeds up drying. Air in motion can sweep up more moisture than stationary air. Therefore a high draft of air, if the medium is air, will facilitate a high uptake of moisture from the food.

The capacity of the air surrounding the food to hold moisture depends on its humidity. Less humid air permits release of more moisture, facilitating faster drying. This is the reason why an air hygrometric difference (difference between dry-bulb and wet-bulb thermometer) not less than 3°C is necessary during tea withering. Again, on a very rainy day with a relative humidity (RH) at more than 90% and temperature at 20°C, hot air is used to achieve a proper withering.

Another important factor determining the minimum moisture content level to which a food can be dried is the equilibrium RH of the food item. At this equilibrium RH, the food neither loses nor gains moisture. Below this level, food can be further dried; above this level it cannot be dried because it absorbs moisture from the surrounding air. However, this humidity level

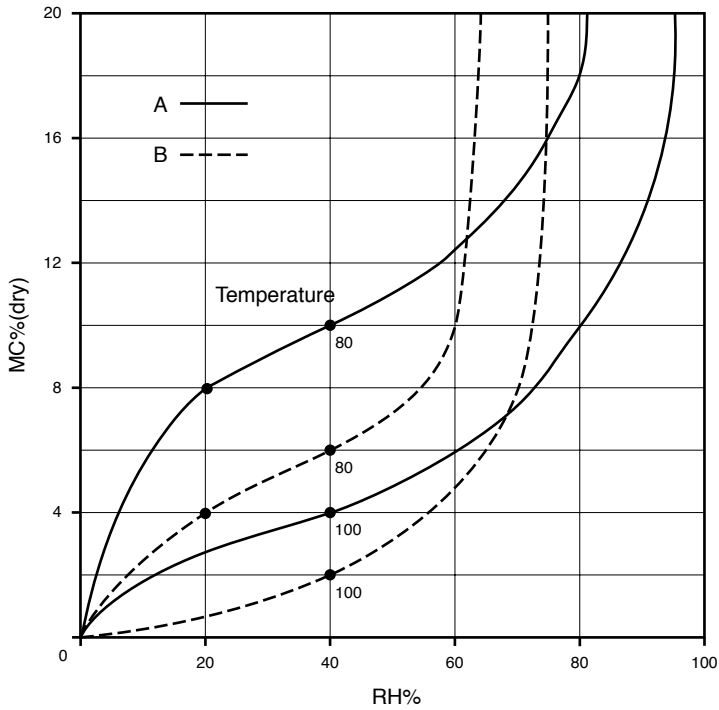

FIGURE 4.1
Example of water sorption isotherm of two food items, A and B.

is different at different temperatures. Graphs of moisture level with RH at different temperatures are called water sorption isotherms of the food. Figure 4.1 shows an example of the water sorption isotherm of two food products, A and B. It is clear from the graph that, say at 100°C and 40% humidity, product B can be dried down to 2%, whereas product A can be dried only to 4%. At 80°C product B can be dried to 6% and product A only to 10%. Again, if it is sufficient to dry product A at 80°C down to 8%, and product B down to 4%, then the RH of the air should be 20%. It is not difficult to experimentally determine the water sorption isotherm of a food product. This can be done by drying the food at different temperatures and RH levels and determining the moisture content by drying and weighing or any other method. Such plots are very important in designing the control strategy for a drying system.

Drying food at higher temperature and for a longer duration could damage the constituents of the food. The drying rate can be made faster at lower temperature by exposing the food at a lower atmospheric pressure. Drying food in a vacuum chamber releases moisture at a faster rate at lower temperature than drying at normal atmospheric pressure. Moisture in food is generally distributed from its surface to its core. Surface moisture, when drying, is released faster, and it takes longer to draw off the inner-level moisture.

TABLE 4.1

Salient Features of Common Food Dryers

Type	Feed Form	Handling Style	Main Features	Heating Method	Temperature	Other Variables
Drum or roller	Liquid, pastes, purees, mashes	Material moves, equipment moves	Heated drum or roller moving in opposite directions	Steam	100°C–150°C	Speed of drums, gap between drums
Spray dryer	Liquid, paste, purees	Liquid sprayed in droplets	Spray dryer, towers	Furnace, electrical	200°C	Air velocity
Vacuum shelf	Liquid, thin solid	Material static, equipment static	Condenser to collect released water	Hot air, steam, electrical	30°C–40°C	Vacuum pressure
Vacuum belt	Liquid, thin solid	Material moves, equipment moves	—	Steam	—	Vacuum pressure
Tunnel dryer	Solid pieces	Material moves, equipment moves	Hot air direction	Furnace	90°C–110°C	Velocity of air, speed of truck
Trough dryer	Solid pieces	Material static, equipment static	Hot air blown by fan	Furnace	90°C–110°C	Velocity, humidity, and temperature of air; spread thickness of food
Belt trough	Solid pieces	Material moves, equipment moves	Hot air blown by fan	Furnace	90°C–110°C	Velocity, humidity and temperature of air; spread thickness of food
Fluidized bed dryer	Particulates, granules	Material moves, equipment static	Hot air blown suspends particles in gentle boiling	Furnace	100°C–120°C	Temperature and velocity of hot air, feed rate

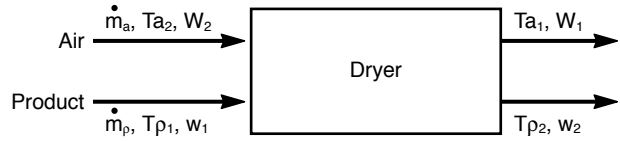

FIGURE 4.2
Representation of heat and mass transfer in a dryer.

4.2.2 Feedback and Feedforward Control in Dryers

In this section we discuss control strategies necessary to control the drying action in dryers.

Table 4.1 outlines classifications and features of some common types of dryers. The table reveals that controlling parameters of the drying process can be different in different types of dryers. For example, in a drum or roller dryer, the drying depends not only on the temperature of the steam, but also on the gap between the rollers and their speed; whereas in tunnel, trough, or belt trough dryers the controlling parameters are the speed of the belt, the velocity and temperature of the drying air, and the RH of the surrounding air. In view of different feed forms, handling styles, and other parameters responsible for drying, the control problems of dryers can be broadly divided into two categories as discussed in the next sections.

4.2.2.1 Mass and Energy Balance in Dryers

Figure 4.2 shows a block diagram of a drying system with mass and energy balance variables. For energy balance, the dryer must fulfill the following condition:

heat in = heat absorbed by the product

This can be expressed by the energy balance equation

$$M_a H_{a2} + M_P H_{P1} = M_a H_{a1} + M_P H_{P2} \tag{4.1}$$

where M_a = air flow rate (kg dry air/hr)
M_p = product flow rate (kg dry solid product/hr)
H_a = heat content of air (kJ/ kg of dry air)
H_p = heat content of product (kJ/kg of dry solid product)

The heat content of air is given by

$$H_a = C_s(T_a - T_0) + WH_L \tag{4.2}$$

where C_s = humid heat (kJ/dry air) = 1.005 + 1.88W
T_a = air temperature (°C)

T_0 = reference temperature (°C)
W = absolute humidity (kg water/kg dry air)
H_L = latent heat of vaporization of water (kJ/kg water)

The heat content of product is given by

$$H_P = wC_{Pw}C_{PP}(T_P - T_0) \tag{4.3}$$

where w = moisture content of product (kg water/ kg of dry solid product)
C_{Pw} = specific heat of water (kJ/kg.K)
C_{PP} = specific heat of product (kJ/kg.K)
T_P = product temperature (°C)
T_0 = reference temperature (°C)

The overall moisture balance equation of the dryer is given by

$$M_aW_2 + M_Pw_1 = M_aW_1 + M_Pw_2 \tag{4.4}$$

Combining equations 4.1 through 4.4 we get the following expression for air flow

$$M_a = \frac{M_p\left[C_{pp}(T_{p1} - T_{p2}) + C_{pw}(w_1T_{p1} - w_2T_{p2})\right]}{C_{s1}T_{a2} - C_{s2}T_{a1} + H_L(W_2 - W_1)} \tag{4.5}$$

where $C_{s1} = 1.005 + 1.88W_1$
and $C_{s2} = 1.005 + 1.88W_2$

Problem 4.1

A conveyor belt dryer is used to dry fermented tea from 60% moisture content (wet basis) at 25°C to 5% (wet basis). Dry hot air from the furnace enters the dryer at 110°C and 1% (wet basis) RH. The drying air leaves the dryer at 30°C and 70% RH. The temperature of tea throughout drying process is 25°C. Compute the drying air requirement per kg of solid tea.

SOLUTION:
The given data:

Initial fermented tea moisture content = $w_1 = 0.6/0.4 = 1.5$ kg water/kg solid tea

Final fermented tea moisture content = $w_2 = 0.05/0.95 = 0.052$ kg water/ kg solid tea

Initial air temperature = 110°C and 1% RH
Exhaust air temperature = 30°C and 70% RH

Using equation 4.4

$$\frac{M_a}{M_p}W_2 + w_1 = \frac{M_a}{M_p}W_1 + w_2$$

a) Using Microsoft Excel software for psychometric calculation from KW Engineering, 360 17th Street, Suite 100, Oakland, CA 94612 (see Appendix F):

W_1 = 0.0186 kg water/kg dry air (at 30°C and 70% RH)
W_2 = 0.009 kg water/kg dry air (at 110°C and 1% RH)
Using the preceding equation

$$\frac{M_a}{M_p}(0.009) + 1.5 = \frac{M_a}{M_p}(0.0186) + 0.052$$

$$\frac{M_a}{M_p}(0.0096) = 1.448$$

$$\frac{M_a}{M_p} = 150.83 \text{ kg dry air/kg solid tea}$$

The drying air requirement is 150.83 kg dry air/kg solid tea.

4.2.3 A Single-Input, Single-Output (SISO) Dryer Model

This is the simplest type of structure for a dryer when the control input is the heating air temperature (manipulated variable) and the controlled output is the moisture content of the food product. Because the moisture content of the product depends on a few other parameters, such as velocity and humidity of the drying air, pressure and humidity of the surrounding air, and the residence time, these parameters are kept constant or manually controlled to a desired or predetermined value. Because residence time of the food determines the bulk of heat transferred, which is responsible for overdrying and underdrying, this parameter can be considered as fixed for a batch type of drying process. The air flow rate is kept at a constant level to compromise between dryer capacity and energy consumption. With these conditions in mind, a SISO dryer control scheme is shown in figure 4.3.

In such a control system the only manipulated variable is the drying air temperature. A resistance temperature detector (RTD) or thermocouple temperature sensor probe properly sheathed and sufficiently long to reach the hot air passage through the dryer wall can be installed to measure the average

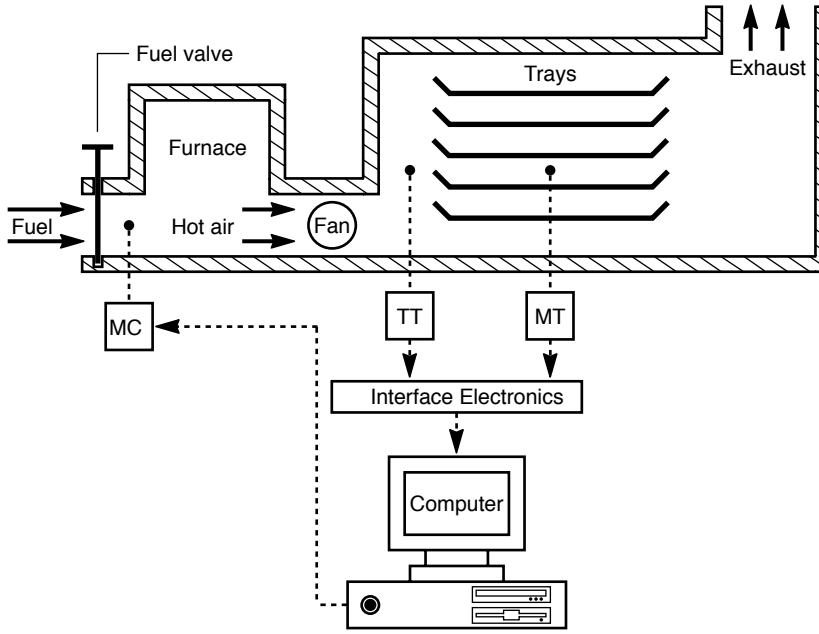

FIGURE 4.3
A dryer control system in SISO model.

temperature of drying air. A 4–20 mA temperature-to-current converter is the most common module to condition the sensor output voltage. For measuring the moisture content of the food placed on trays, online moisture sensors like an infrared moisture sensor can be installed. Such on-line sensors convert the voltage signals to a 4–20 mA current signal. Another possible moisture sensor in this application is a radio frequency (RF) absorption type.

The most common disturbances to the system include nonuniform moisture level and nonuniform drying characteristics of the product. These noises cause fluctuations in the output. Another noise source to the system might arise from fluctuations of flow rate of drying air due to various design parameters of the dryer in spite of constant speed of the drive motor.

4.2.4 A Multiple-Input, Multiple-Output (MIMO) Dryer Model

In some dryers more than one practical input controls the drying process; for example, in a belt conveyor dryer, drying depends on the speed of the conveyor in addition to the temperature of the drying air. The input variables that affect the final moisture content of the food in a dryer are as follows:

1. The drying air temperature and humidity
2. The drying air flow rate
3. The residence time (i.e., speed of the conveyor)

Although the output or controlled variable in most of the drying applications is considered to be moisture content, in some applications some special quality parameters like color, flavor, texture, tenderness, and others might also be considered output variables. However, in view of the complex biochemical phenomena taking place in a food product, apart from release of moisture during drying, it is difficult to model a correlation between input variables and such output variables of special interest. In many food-drying situations, such cross-correlations are not yet theoretically established, so dryers are controlled manually or from experience considering such additional output variables. This situation leads to the concept of a MIMO control strategy in a drying process.

Let us consider the tea dryer to understand a MIMO controller. The fermented tea is dried to reduce the moisture content from 65% to 70% to 2% to 5% during a residence time of 20 to 30 min. Two types of dryers are very common in the tea industry: a conventional conveyor belt dryer and a fluidized bed dryer. In a conveyor belt dryer operating at atmospheric pressure, the fermented tea is carried by a perforated steel belt. There are three to four parallel and vertical arrays of conveyors moving at different speeds. The dried tea drops from the end of one belt to the next belt and traverses to the finishing end. The hot air from the furnace is blown over the belts and the heat is evenly distributed. The tea is spread uniformly with the help of spreaders. The first conveyor moves at a slower speed so that the fresh tea has a higher residence time to release more moisture initially. The speed of the subsequent conveyor belts is higher to allow the tea to pass quickly so that the remaining small amount of moisture gets released.

Overdrying and underdrying are two serious problems in tea drying. This occurs if the fermented tea is not fed at a proper rate or the temperature of the drying air is not maintained at a proper level. In many tea factories the feeding mechanism is manual, which results overdrying or underdrying. Aside from the flavor components, tea color can be considered an output parameter because improper drying causes tea color to deviate from the targeted black color. Therefore tea color can be attributed to a kind of quality parameter during drying. Keeping this view in mind, we are now in a position to make a structure of a MIMO model of the tea dryer as shown in figure 4.4A. The output variables of the dryer are the moisture content and color of the processed black tea. In the SISO model of figure 4.3, the sensors suitable for moisture content and temperature measurement were already mentioned. In a MIMO structure the additional output variable—the color of the tea—can either be detected by optical methods or machine vision techniques as discussed in chapter 3. The detected signals are interfaced to a computer to determine the manipulated input variables by a control law program.

In a MIMO model, when each input has effect on only one kind of output it is called a noninteractive model, and it is easier to keep each output value at its desired level when there are no disturbances. Dryer models are mostly interactive, a MIMO model of which is shown in figure 4.4B.

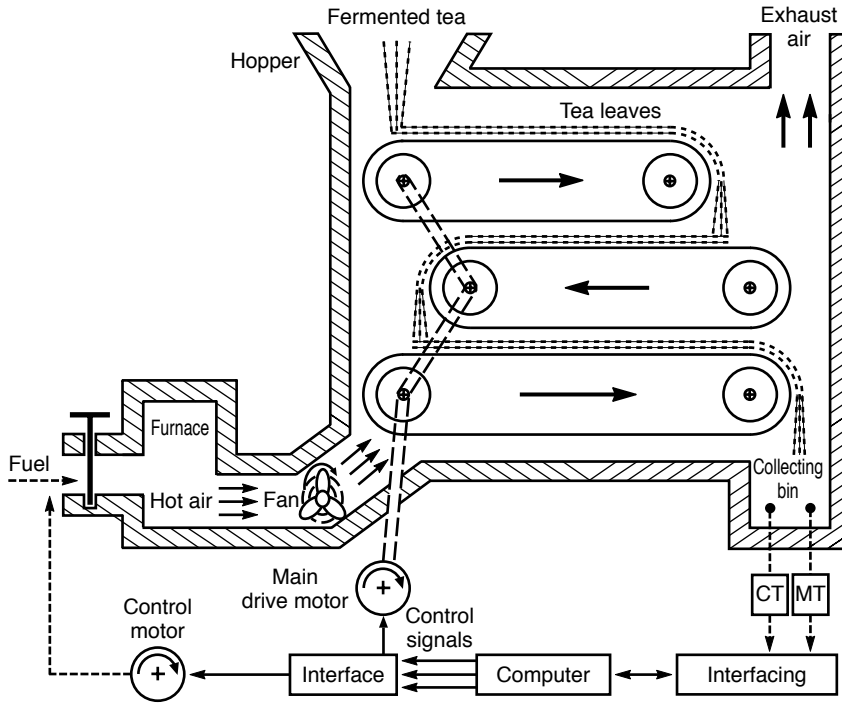

FIGURE 4.4A
A tea dryer control system in MIMO model.

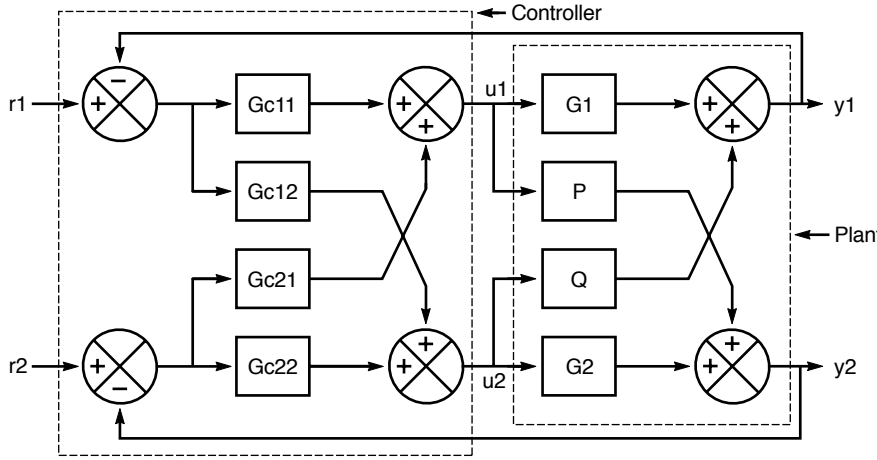

r1—reference temperature input; u1—actual temperature input
r2—reference conveyor speed input; u2—actual conveyor speed input
y1—moisture content of black tea; y2—color of black tea
Gc11, Gc12, Gc21, Gc22—controller interactive transfer functions

FIGURE 4.4B
Interactive MIMO model of a tea dryer control system.

In the interactive model of a dryer, a fan blower blows the hot air to the conveyor bed at a constant flow rate. Therefore the dryer outputs can be controlled by the remaining manipulated input variables (i.e., the temperature of the drying air and the residence time). The residence time depends on the speed of the conveyors, so the practical input to control the residence time is speed of the drive motor that drives three conveyors by a gear arrangement. The control signals obtained from the controller are used to vary the input variables to the final control elements accordingly. The controller output signals are first conditioned to make them compatible with the control devices. For example, the valve that controls the fuel to the furnace is operated by a solenoid; a strong DC current should be applied. On the other hand, the supply to the drive motor used for controlling the conveyor speed depends on the type of the motor (i.e., a DC motor or an AC induction motor). Various types of final control elements were already discussed in chapter 2.

4.2.5 Feedforward Control in the Food Dryer

The dryer controller will not take corrective measures until an error is developed. Most of the thermal systems have a large time lag, so it takes some time before any corrective measures take place. Because the error is developed after a time gap and after this corrective measure begins, there could be considerable damage to the quality of the product. In such cases feedforward control becomes more effective. In feedforward control, corrective action works immediately and simultaneously with the occurrence of any disturbance. The disturbance to the dryer is mainly due to inaccurate feed rate of the material. If there is any deviation of feed rate from the designed value, the feedforward control action corrects it by adjusting the heat input to the furnace.

To realize a feedforward dryer controller, both the signals—the output and the disturbance—are fed to the controller. The speed of the conveyor can be measured by a DC tachometer. This provides the controller a combined feedforward and feedback control. A feedforawrd control can minimize the transient error, but it has some limitations; for example, it cannot cancel stochastic disturbances alone. Figure 4.5 shows a block diagram of the feedforward–feedback controller. The dryer transfer function $G(s)$ and the disturbance transfer function $G_n(s)$ in figure 4.5 should be known to design the controller. The controller transfer function $G_c(s)$ and the feedforward transfer function $G_1(s)$ are the design objectives. The disturbance input signal is $N(s)$ and $R(s)$ is the set point or reference input to the controller. The output $C(s)$ is given by

$$C(s) = G_c(s)G(s)E(s) + G_n(s)N(s)$$

where the error is

$$E(s) = R(s) - C(s) + G_1(s)N(s)$$

so we get

$$C(s) = G_c(s)G(s)[R(s) - C(s)] + [G_c(s)G(s)G_1(s) + G_n(s)]N(s)$$

The effects of $N(s)$ can be eliminated by choosing $G_c(s)$ so that

$$G_c(s)G(s)G_1(s) + G_n(s) = 0$$

This gives the feedforward transfer function as

$$G_1(s) = -\frac{G_n(s)}{G_c(s)G(s)} \tag{4.6}$$

By proper design of the controller transfer function $G_c(s)$, the feedforward transfer function $G_1(s)$ can be determined from equation 4.6.

Figure 4.6 shows the feedforward control scheme of a conveyor belt tea dryer. In the feedforward control of the dryer, the air flow rate can be calculated from equation 4.5, which is used as set value of drying air flow rate. As per equation 4.5, the input and output variables that need to be measured are as follows:

- Temperatures of tea at inlet and outlet: T_{p1} and T_{p2}
- Moisture content of tea at inlet and outlet: w_1 and w_2
- Humidity of drying air at inlet and exhaust: W_1 and W_2
- Temperature of drying air at inlet and exhaust: T_{a1} and T_{a2}
- Feed rate of tea: M_p

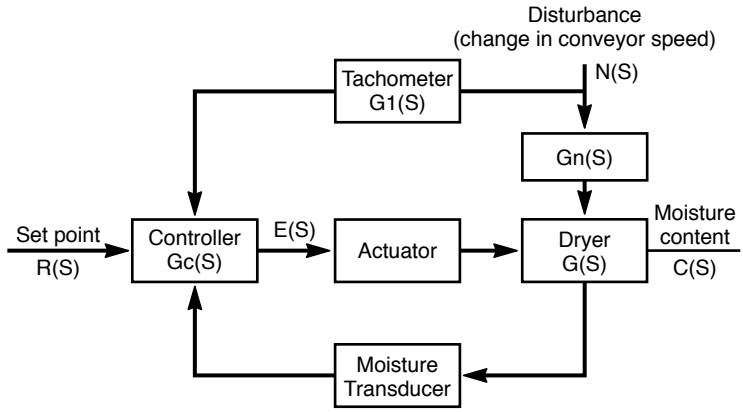

FIGURE 4.5
Block diagram of feedforward control of tea dryer.

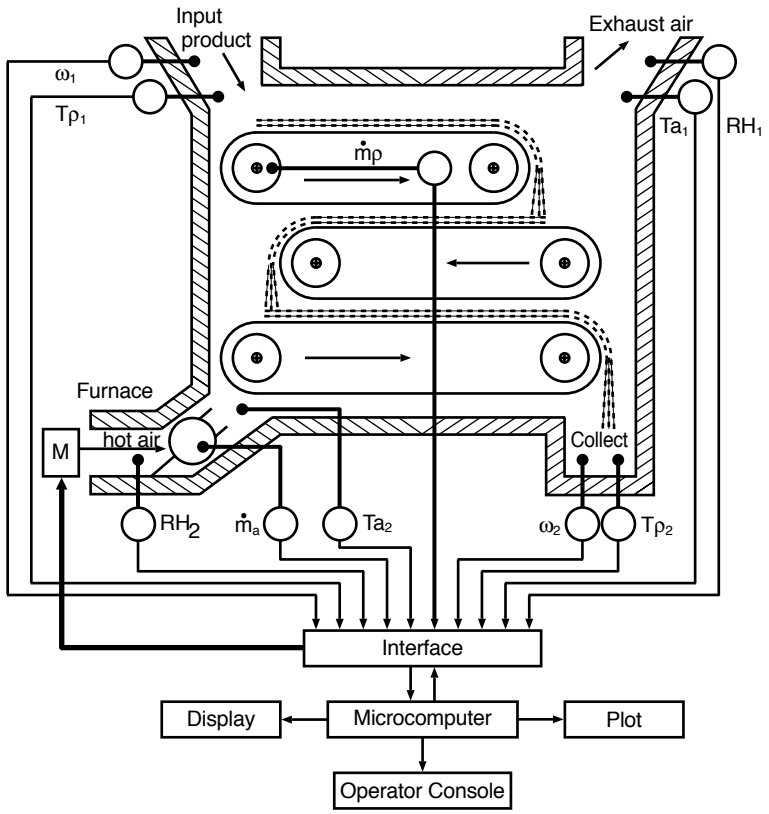

FIGURE 4.6
A schematic diagram of a feed-forward dryer control system.

The temperature signals can be measured by sheathed thermocouples suitable for the operating temperature range of the dryer (ambient to 150°C). A thermocouple will give a fairly linear response in this range of temperature. The most suitable moisture content sensor that can be used for measurement of tea moisture is an infrared sensor that can be used online and in a noninvasive manner. Among various online humidity measuring techniques, the suitable method in this application will be an electronic dry- and wet-bulb psychrometer. The feed rate of tea in the conveyor can be detected by a tachometer connected to the drive motor directly or through a gear arrangement.

4.2.5.1 The Control Functions

For calculation of the manipulated variable M_a using equation 4.5, the following steps are involved:

A device calculates $(T_{p1} - T_{p2})$ and then multiplies with C_{pp} to get $C_{pp}(T_{p1} - T_{p2})$.

The signals T_{p1} and T_{p2} are scaled properly to get (w_1T_{p1}) and (w_2T_{p2}) and a summing device adds them with the second term as negative input. The summed output is scaled by C_{pw} giving

$$C_{pw}(w_1T_{p1} - w_2T_{p2})$$

C_{s1} and C_{s2} values are calculated from the factor (1.005 + 1.88W). This can be implemented by two scaled summers with a bias of 1.005. These values are used to calculate

$$(C_{s1}T_{a2} - C_{s2}T_{a1})$$

Finally, the manipulated variable M_a is calculated by two summers: one multiplier and one divider. These operations can be done either by an electronic controller or a computer. Various types of electronic controllers are available that are discussed briefly next.

4.3 Electronic Controllers

Implementation of a specific controller can be achieved in various ways depending on the complexity, reliability, and cost factors. Mechanical or pneumatic controllers are still in use in many applications despite their disadvantages. Electronic and computer control techniques are becoming more popular. Electronic analog controllers are widely used for the following reasons:

1. Electrical signals are easy to transmit over a long distance.
2. Digital computers are compatible with electrical signals only.
3. Electrical and electronic devices are almost maintenance free and free from leakage, wear and tear, and so on.
4. Intelligent and adaptive controllers can be designed with electrical systems.
5. Electrical systems are less expensive, require less space, and are easy to install and operate.

Operational amplifiers are versatile in designing electronic controllers due to their various analog computational facilities like summation, subtraction, multiplication, integration, differentiation, squaring, relational operations, and so on.

A common operation in a controller is error detection. A differential amplifier can be used in inverting mode with the signal voltage applied to the inverting terminal and the set-point voltage to the noninverting terminal (fig. 4.7A). The feedback resistor value can be adjusted to get an amplification

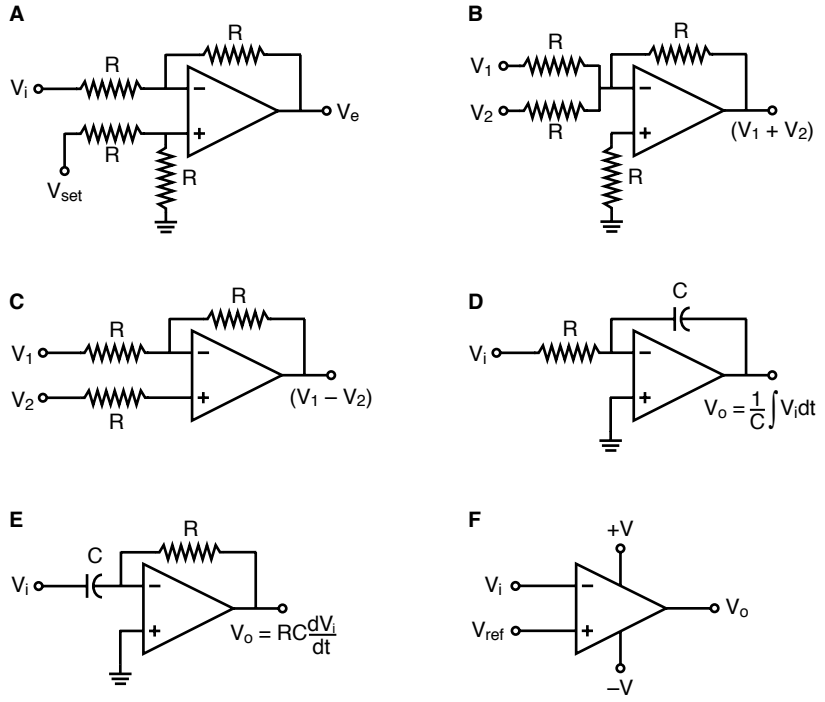

FIGURE 4.7
Operational amplifier circuits for controller design. (A) Error detection; (B) Summer; (C) Substractor; (D) Integrator; (E) Differentiator; (F) Comparator

factor based on the sensitivity of the transducer, but if the transducer output has already been amplified by the transmitter, further amplification might not be required.

Analog controllers need to compute the control signal by using a control law. The complexity of the control law determines the complexity of the circuit. For example, a proportional controller amplifies the error signal by a proportional gain whereas a PID controller must cascade with the proportional amplifier, an integrator, and a differentiator with proper gain constants. Analog computations like summation, subtraction, integration, and differentiation can be performed by operational amplifiers of various types. The basic forms of the circuits are shown in figure 4.7B–E.

Performing control operations often requires generating a signal based on a relation between an input signal and a reference signal. The relational signals are an equality signal, a greater than signal, and a less than signal.

Such signals are used to trigger a control component like a relay, motor, or solenoid. For relational operation an op-amp comparator circuit is used where the inputs are applied to the two input terminals and the op-amp is operated in open-loop mode (fig. 4.7F). The output changes from $-V_{cc}$ to $+V_{cc}$ when the signal applied to the noninverting terminal becomes equal and

greater than the signal applied to the inverting terminal. Thus depending on relational signal needed (i.e., greater than or less than), the input signal and the reference signal should be properly connected. A signal based on only the relational operator "equal" can be generated by applying the outputs obtained from "greater than" and "less than" relational circuits to a digital logic circuit.

4.3.1 On–Off Controller

A two-position or on–off controller generates a control signal based on a relational condition of the input signal with a reference signal (i.e., greater than or less than). Due to oscillations of the output of the process for continuous on–off action generated by the single reference on–off controller, an on–off controller with a differential gap is more suitable. In this type, two set point or reference levels are imposed on the controller: an upper reference level and a lower reference level. An operational amplifier circuit implementing this operation is shown in figure 4.8. The upper comparator generates a signal transition from low to high (e.g., from 0 V–5 V) when V_{in} crosses the level of lower set point V_L and the lower does the reverse; that is, the output traverses from high to low (e.g., 5 V–0 V) when the input crosses the upper set-point level $V_{H.}$ A logical operation of the outputs from the two comparators gives the on–off controller output with a differential gap. The controller can be made to act in reverse by reversing the comparators.

4.3.1.1 Bimetallic Thermal On–Off Controller

Another convenient form of on–off controller used in thermal devices is the bimetallic strip controller. The temperature sensors discussed in chapters 2 and 3 fall under electrical types that generate an electrical signal proportional to temperature. In many applications in which a physical contact or deformation signal proportional to temperature is essential, bimetallic strip sensors are useful. Liquid expansion type temperature sensors also work by a similar principle of thermal expansion, but bimetallic sensors are more popular due to their inherent advantages. The most important advantage is that due to its conductivity to electricity the strip can be used as a thermal switch.

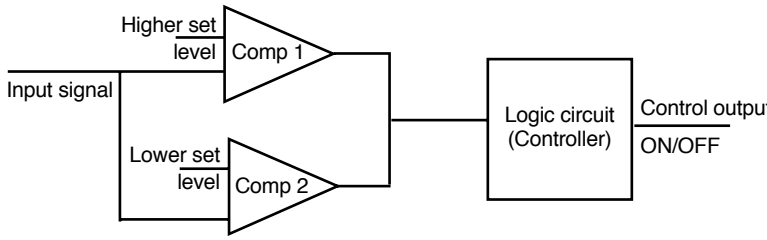

FIGURE 4.8
Block diagram of an on–off controller.

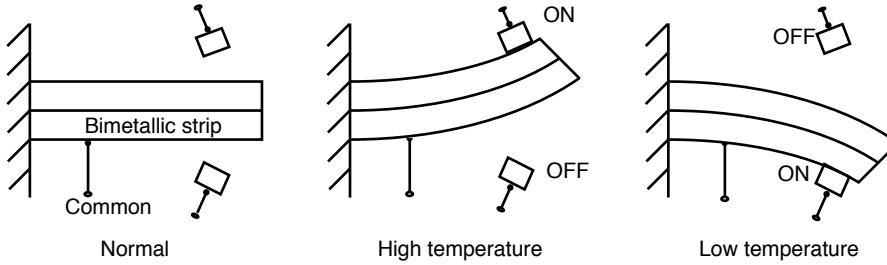

FIGURE 4.9
Schematic diagram of a bimetallic strip on–off switch.

The sensor serves two purposes at the same time: a temperature sensor and also an electrical switch. Although this sensor performs temperature sensing with lower accuracy, higher hysteresis, and slow response, the sensor is used in numerous applications of on–off temperature controls.

When two metal strips made of two materials and with two different thermal expansion coefficients are bonded together, it forms a bimetallic thermal strip sensor. As shown in figure 4.9, when one end of the strip is fixed and the other end is free and the strip is heated, it bends downward if the thermal expansion coefficient of the lower strip is smaller than that of the upper strip. The strip thickness and the deflection are exaggerated in the figure; in practice the deflection is very small.

Many household and industrial thermal systems like ovens, air conditioners, refrigerators, and so on employ a bimetallic strip switch to implement an on–off controller. From figure 4.9 it is understood that when the bimetal strip bends downward it closes an electrical switch. The switch remains in this closed position until the bimetal strip is cooled and returns to its original set-point level position. Hence a temperature signal is sensed and made to actuate a control component like a solenoid valve, control motor, and so on. The switch can be used to actuate two different devices above and below the set-point level.

4.3.2 Controller Modes

The basic concept of conventional and linear controllers was discussed in chapter 1. In this section their mathematical representation and implementation by analog circuits are presented.

4.3.2.1 Proportional Controller

The theory behind a proportional control action was discussed in chapter 1. The response equation of the controller is given by

$$P = K_p e + p_0 \tag{4.7}$$

where P = proportional control output (0%–100%)
K_p = proportional gain
e = error as a percentage of range of variables
e_0 = control output with no error

To implement equation 4.7 the op-amp circuit involved is a summing amplifier with a gain to each part selected by resistors, as shown in figure 4.10. Therefore an equivalent voltage equation of the circuit in the line of equation 4.7 can be written as

$$V = AV_e + V_0 \tag{4.8}$$

where V = controller output voltage
A = amplifier gain to input error = R_2/R_1

The correspondence between the output range, input range, and the proportional band of the controller should be determined prior. For example, for varying a servo-controlled valve operating in the range of 0 V–5 V (fully closed to fully open), a swing to 75% refers to (0.75)(5.0) = 3.75 V. Similarly, for a dryer, the moisture content of the product is measured and controlled in the range of 3% to 6%, which is converted by a moisture sensor to a voltage of 1 V to 4 V. The span or range of the signal is (4 – 1) = 3 V. Thus the physical variable versus electrical voltage correspondence is

$$= \frac{3\,Volt}{(6-3)\%}$$

$$= 1\,Volt\ /\ moisture\%.$$

On the other hand, proportional gain K_p determines the relation between the error and the controller output. Let us assume that K_p = 5% per 1% error with the voltage ranges mentioned earlier. As per the value of K_p, the controller adjustment should be 5% for a 1% change in the error. This means for a change of (0.01)(3.0) = 30 mV in input voltage the controller output should

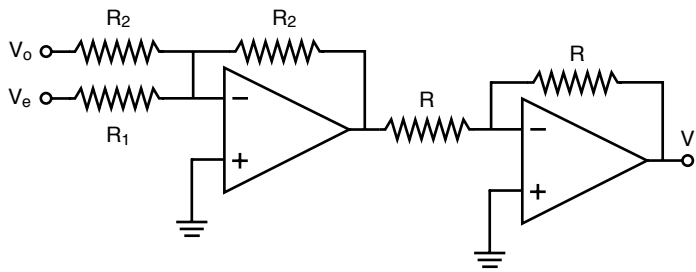

FIGURE 4.10
Proportional controller circuit.

be changed by (0.05)(5.0) = 250 mV. Therefore the gain of the amplifier (A) should be equal to (250/30) = 8.33. This can be obtained by tuning the ratio of the feedback resistor and the input resistor of the op-amp amplifier circuit to 8.33.

4.3.2.2 Integral Controller

The output equation of an integral controller is given by

$$p(t) = K_I \int_0^t e_p(t)dt + p_I(0) \tag{4.9}$$

where $p(t)$ = controller output , % of full scale
K_I = integral gain (s^{-1})
$e_p(t)$ = error in percentage from full scale value
$p_I(0)$ = controller output at t = 0

When realizing equation 4.9 in an op-amp circuit (fig. 4.11), the corresponding voltage equation is given by

$$V_0 = A \int_0^t V_e\,dt + V_0(0) \tag{4.10}$$

where V_0 = output voltage
A = integral gain = $1/RC$
V_e = error voltage
$V_0(0)$ = initial output voltage

The rate of the integral controller is determined by the integration time constant. If the integral gain K_I is too large, the output increases very fast, producing oscillations before settling. The gain implies that a 1% change in the error causes an output that changes K_I% per second. Let the controller

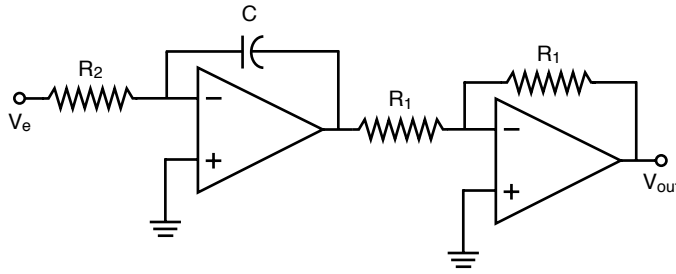

FIGURE 4.11
Integral controller circuit.

use an output range of 10 V and input range of 5 V with a controller gain $K_I = 3.6\%/(\%/\text{min})$. Converting the time unit of K_I from minutes to seconds

$$[3.6\%/(\%/\text{min})][1/60] = 0.06\ \%/(\%/\text{sec})$$

An error of 1% for 1 sec is given by

$$(0.01)(5\ \text{V})(1\ \text{sec}) = 0.05\ \text{V/sec}$$

$K_I\%$ of the output is

$$(0.0006)(10\ \text{V}) = 0.006\ \text{V}$$

Therefore the integral gain for the circuit as amplifier gain should be

$$A = (0.006)/(0.05) = 0.12/\text{sec}$$

The values of R and C can be selected as

$$\text{Let}\ \ R = 100\ \text{K}\Omega\ ,\ \text{since}\ A = 1/RC,\ \text{hence}\ C = 83.33\mu\text{F}$$

4.3.2.3 Derivative Controller

The output equation of a derivative controller is given by

$$p(t) = K_D \frac{de}{dt} \tag{4.11}$$

where p = controller output in percent of full output
K_D = derivative time constant (sec)
e = error in percent of full scale

An op-amp derivative controller circuit is shown in figure 4.12. The preceding theoretical equation can be written in a practical op-amp circuit equation as

$$V_0 = -RC \frac{dV_e}{dt} \tag{4.12}$$

where V_0 = controller output voltage, V
RC = time constant of the circuit, sec
V_e = error voltage, V

To understand the derivative control action, let us consider a case where a derivative control action with $K_D = 0.05\%/(\%/\text{min})$ is used to control the

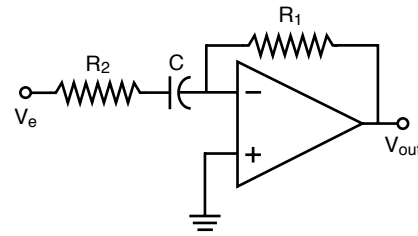

FIGURE 4.12
Derivative controller circuit.

viscosity of chocolate by controlling the flow of lecithin (derived from oilseed) for a maximum period of 2.0 sec. The viscometer output range is 0.4 V to 2.0 V and the controller output range is 0 V to 5.0 V. The derivative gain expressed in units of seconds is

$$[0.05\ \%/(\ \%/\text{min})](60) = 3.0\ \%/(\ \%/\text{sec})$$

This means that a 1% change in viscosity should change controller output by 3.0% per sec. The 1% of the input is

$$0.01(2.0 - 0.4) = 0.016\ \text{V/sec}$$

and therefore 3.0% of the output means

$$0.03(5) = 0.15\ \text{V}$$

The derivative time constant is

$$RC = 0.15/0.016 = 9.37\ \text{sec in the op-amp circuit.}$$

Taking the value of C = 20 μF, the value of

$$R = 468.5\ \text{K}\Omega$$

It was mentioned in chapter 1 that each control mode has its advantages and disadvantages and using a single control mode is not recommended. The best way is to combine the control modes like proportional plus integral (PI), proportional plus derivative (PD), or proportional plus derivative plus integral (PID) mode. These combined control modes can be implemented by cascading the op-amp circuits in tandem.

4.3.3 Fan Direction Control in Food Withering

It has already been mentioned that food dehydration is a controlled process for removing moisture from food. Although the principal aim of food dehydration is to reduce weight or volume for preservation and transportation,

there can be other specific reasons in some foods. For example, in tea processing, withering is a process of dehydration in which the freshly picked tea leaves are withered in withering troughs by blowing air for about 10 to 12 hr. The principal aim of withering is to expedite the chemical changes taking place in the leaf cells, which is called chemical wither. If the tea leaves are not withered, it takes 15 to 20 hr to complete chemical withering. Moreover, tea processed from long chemical wither is less valuable than tea obtained from controlled chemical withering for 10 to 12 hr.

The withering time varies depending on the relative humidity of the surrounding air, temperature, and flow velocity of the withering air. The moisture released from the tea accumulates over the trough during withering and gradually the air becomes more saturated with moisture. Over the course of time, say 2 to 3 hr, less moisture can be released from the tea and the process slows. Therefore the saturated air is required to be sucked out so that fresh air can replace it. To do so, normally the withering fan direction is reversed several times during withering [2]. This process is shown in figure 4.13. Traditionally fan direction reversal is performed manually at assumed regular intervals. In this manual method, three-phase supply to the induction motor is connected to the starter through a phase change switch. The direction of the motor is reversed when any two phases of the supply are interchanged. With the help of a phase changeover switch, the connection of one of the three phases is kept fixed as the other two phases are interchanged. The manual method of fan speed reversal is not recommended because if withering is continued beyond the time of air saturation, rate of release of moisture becomes slow. To avoid loss of time, energy, and quality, fan direction control operation should be done at the correct time for a correct duration. To circumvent this problem an automated withering fan speed reversal technique for the tea industry was developed by Bhuyan [1].

The device works on the principle of a simple closed-loop control system in on–off controller mode. The RH of the air above the withering trough is the key factor for the control device. An electrical transducer continuously measures this RH and the signal is used for generating a command signal using a comparator. The comparator compares the RH signal with two setpoint levels, one high and the other low. When the RH signal is above the

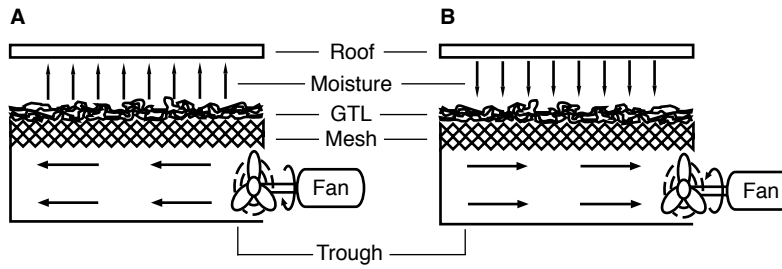

FIGURE 4.13
Schematic diagram of air flow in tea withering: (A) air blowing; (B) air sucking.

high level, the comparator sends a signal, REVERSE, to a logic control circuit. However, before reversing, the braking of the motor has to be performed for at least 20 sec and then the motor has to be stopped. If the RH value is less than the low level, the motor has to be run in forward direction, sending a signal, FORWARD, to the logic control circuit. Therefore the following logic was used to develop the command signal:

1. When RH > high, Command = REVERSE
2. When RH < low, Command = FORWARD

Here REVERSE and FORWARD states can be any conventional digital logic levels, which are most commonly 0 V and 5 V for transistor–transistor logic (TTL) technology. This command signal is used to generate the final logic state signals for the power control circuits. The power control circuit consists of controlled switches (commonly relays) triggered by the logic state signals to reverse the connection of any two phases of the power supply to the motor. The connection of the induction motor to the three-phase supply through the controlled switch array is shown in figure 4.14.

Switches SW1 and SW2 are complementary for a particular direction of the motor, so that when SW1 is closed, SW2 should be open and vice versa. SW3 must be closed for running the motor in both directions. Table 4.2 is a

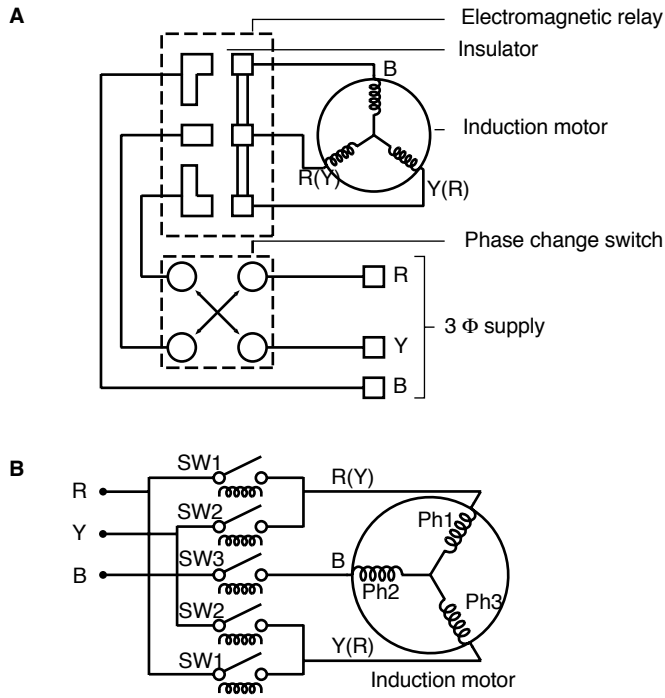

FIGURE 4.14
Switch array for motor reversing: (A) conventional device; (B) relay circuit.

TABLE 4.2

State Table for Switches and Phases

	Switches			Supply Phases		
Direction	**SW1**	**SW2**	**SW3**	**Ph_1**	**Ph_2**	**Ph_3**
Forward	1	0	1	R	B	Y
Stop	0	0	0	0	0	0
Reverse	0	1	0	Y	B	R

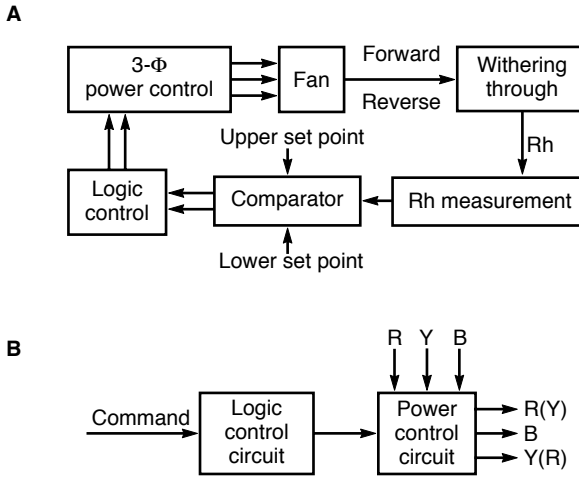

FIGURE 4.15
Withering fan reversal controller: (A) block diagram representation; (B) basic control block; (C) logic control circuit.

state table of the switches and phases. Hence, properly closing and opening the switches supplies the motor with supply phases either in the sequence RBY or RYB for forward and reverse directions, respectively. This phase reversal is mediated by a power control circuit. A block diagram of the controller is shown in figure 4.15A.

4.3.3.1 The Relay Circuit

The function of the relay circuit is to interchange the supply of any two of the three phases and keeping the third phase fixed. The circuit consists of five electromechanical relays. The logic table for the relay coil signals (S_1–S_3), relay states (RL_1–RL_5), and directions are shown in table 4.3.

4.3.3.2 Logic Control Circuit

The requirement of the logic control circuit is that when the command signal from the comparator undergoes a transition from low to high or from high to low, the logic circuit generates signals for triggering the right set of relays.

TABLE 4.3

State Table for the Relay Circuit

Relay Coil Signals			Relays					Supply Phases		
S_1	S_2	S_3	RL_1	RL_2	RL_3	RL_4	RL_5	Ph_1	Ph_2	Ph_3
0	0	0	0	0	0	0	0	0	0	0
1	1	0	1	0	1	1	0	R	Y	B
0	0	0	0	0	0	0	0	0	0	0
0	1	1	0	1	1	0	1	Y	B	R

The circuit that performs this function is shown in figure 4.17. The circuit consists of two parts, a delay circuit and a gate control circuit.

The delay circuit is clocked by a timer. The switching transistors generate high spikes that are applied to the trigger terminal of the timer. When the command signal changes state from 0 V to 5 V, transistor T_1 gives a positive spike to the input trigger and the timer produces a delay of 20 sec. This delay is set by the time constant of an RC circuit externally connected to the timer. Similarly, when the command signal changes from 5 V to 0 V, transistor T_2 generates the spike, producing a delay of 20 sec.

When the command signal changes value from 0 V to 5 V, the output of the timer remains low for 20 sec, resulting in the relay trigger signal being low for 20 sec, after which the motor is stopped. After 20 sec the output of the timer becomes high. Because the command is already high, the trigger signals RL_1 and RL_2 are high but RL_3 is low. On the other transition of the command signal, RL_2 and RL_3 become high but RL_1 remains low (table 4.3).

4.3.3.3 The Comparator Circuit

The comparator circuit is designed to generate the command signal corresponding to the value of the RH values. The command signal is generated with the following logic in mind:

1. When the RH exceeds the upper set level (SPH), the command signal changes from 0 V to 5 V.
2. When the RH decreases below the lower set level (SPL) the command signal changes from 5 V to 0 V.

The timing diagram of the logic states with RH values is shown in figure 4.16. Two comparators generate outputs C_1 and C_2 based on the level of RH with respect to the set levels. The comparator outputs are applied to an RS flip-flop to trigger it as per the state table. The operation of the RS flip-flop as command signal generator is shown in table 4.4.

It is evident that a positive transition of C_1 triggers the command signal generator for positive transition and negative transition of C_2 triggers for negative transition of the command signal. The flip-flop is set when RH exceeds SPH because at this transition the comparator output becomes high. It resets when RH decreases below SPL.

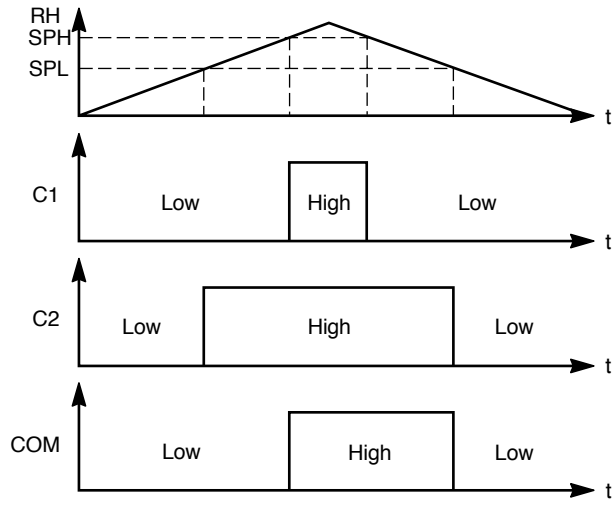

FIGURE 4.16
Timing diagram of comparator outputs.

TABLE 4.4

State Table of the Command Signal Generator

	Comparator Outputs		Command Signal
Relative Humidity Ranges	C_1	C_2	C
RH > SPH	1	1	↑
SPH > RH > SPL	0	1	1
RH < SPL	0	0	↓

In most of the tea industry, the RH is specified by the depression temperature (refer to chapter 3) considering that the dry-bulb temperature does not vary much. In summer (in India), at an ambient temperature of 32°C, a depression temperature of 2°C is equivalent to RH of 88%; similarly a depression temperature of 5°C is equivalent to 70%. Hence, for the higher and lower limits of RH of 88% and 70%, respectively, depression temperatures of 2°C and 5°C respectively can be used. Similarly, in winter with an ambient temperature of 25°C, RH of 88% and 70% is equivalent to depression temperatures of 1.7°C and 4°C, respectively. Depression temperature can be used in this application to simplify the RH measuring circuit. The differential output from the dry-bulb and wet-bulb IC thermometer, instead of a RH signal, has been used to trigger the comparators. Hence, when there is no significant variation in dry-bulb temperature the depression temperature is suitable for simplicity. A circuit diagram of the controller is shown in figure 4.17.

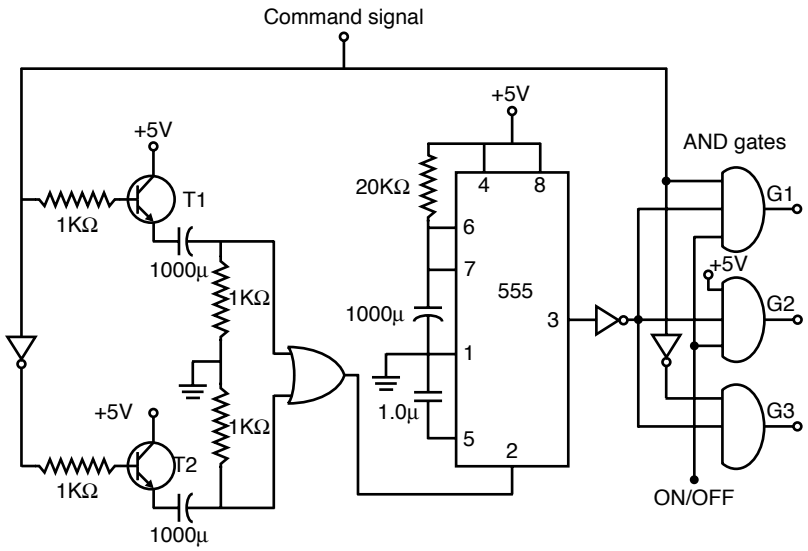

FIGURE 4.17
Withering fan reversal controller circuit.

4.3.4 Cooling Surface Area Control in Chocolate Tempering

In chocolate manufacturing, tempering of chocolate is an important issue. Although chocolate tempering is theoretically very simple, it requires a great deal of experience, skill, and technique so that the chocolate is suitable for the molding plant or enrober. Chocolate tempering requires sufficient cooling to form crystals; hence, temperature control during tempering is very essential. Various chocolate tempering machines are available with electronic controllers. For example, the MSV Turbo model incorporates a new automatic capacity control system. This control adjusts the cooling surface area based on deviation of flow rate and temperature of chocolate. This ensures a uniform degree of temper throughout the process. Additionally, the machine provides a continuous cooling curve sampling unit. The machine is automated by a programmable logic controller (PLC) with automatic startup.

4.4 Flow Ratio Control in Food Pickling Process

In preservation of foods, acetic acid is the main acid constituent found in vinegars. The commercial name of this preservative is glacial with 99% to 100% acid. Acetic acid is used in pickle and sauce manufacturing alone or with vinegar. Lactic acid is also an important edible acid used in brining

preservation of vegetables. The process of adding vinegar or acetic acid to a permitted ratio with water in a tank is called pickling. Controlling a proper ratio of fruit, pectin, acid, and sugar is also an important task in jam and jelly making. In such situations a fixed ratio between the flow rates of the two (or three) liquids is to be controlled. During food pickling, acid to water ratio, acid to pectin ratio, or water to brine ratio has to be controlled at a prespecified value. A strict adherence to the accurate proportion minimizes the use of preservatives.

4.4.1 Ratio Controller

A schematic diagram of the flow ratio control in a pickling tank is shown in figure 4.18. For example, in this application the flow of acid is to be controlled at a preset ratio to flow of water. The flow of water is measured by a flow transmitter and is applied to a ratio relay multiplier, which multiplies the flow of water by a preset factor. The output of the ratio relay is applied to the flow controller along with the acid flow signal in a ratio. The voltage signal and ratio factor of the control action can be expressed by the equations

$$V_{ro} = KQ_w \tag{4.13}$$

and

$$R = \frac{Q_a}{Q_w} \tag{4.14}$$

where V_{ro} = voltage signal from ratio relay
K = preset factor of ratio relay
R = ratio factor
Q_a = flow of acid (to be controlled)
Q_w = flow of water

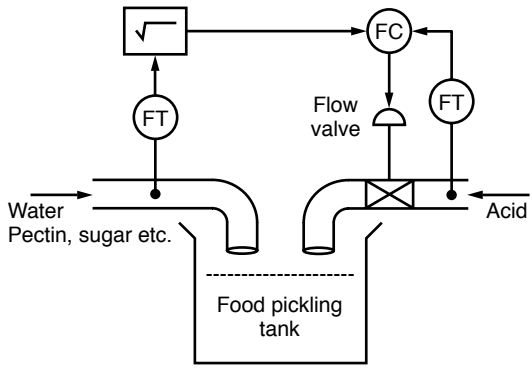

FIGURE 4.18
Schematic diagram of a pickling ratio controller.

To maintain the ratio, the flow of water is calculated at a set point by a preset factor. When the flow of water deviates from a set-point level, it fouls with the ratio relay deviating its output also as per equation 4.13. In turn this deviated output signal calculates the controller output according to equation 4.14. Therefore the flow rate of acid is automatically compensated or adjusted to the predetermined ratio. To understand the operation we can assume some numerical values. Let the maximum flow rate of water be 100 liters per minute (lpm) and that of acid be 50 lpm. The ratio relay is adjusted to a ratio of 1:1, which means that a measured signal of 1 lpm flow of water makes the controller allow an 0.5 lpm flow of acid; that is, if 60 lpm of water flows then 30 lpm of acid will also be allowed to flow. Again if the ratio factor changes to 1:2, then for 60 lpm of water flow, 120 lpm of acid will flow. Now, if the maximum flow rate of acid decreases to 25 lpm (the ratio factor already set to 1:1) then a new ratio factor of 1:2 will be established in the controller that changes the flow rate of acid from 25 lpm to 12.5 lpm. Hence, the ratio factor is established based on the range of the flow transmitters and the multiplying factor set into the ratio relay. Generally a flow range is chosen so that the ratio factor is set at the middle.

The flow meters recommended for this application are differential pressure transmitter type, turbine flow meter, or magnetic flow meters. Magnetic flow meters will be more suitable for the acid line than the water line. In the case of a differential pressure transmitter using an orifice type restriction, the output signal will be proportional to the square root of the flow rather than giving a linear relationship. If the ratio relay factor is to be set to 0.5:1 to 5:1, then in case of orifice flow metering, the actual flow ratios will be

$$[(0.5/1)^{1/2}] \text{ to } [(5/1)^{1/2}] = [0.70{:}1] \text{ to } [2.23{:}1]$$

Use of two output modes of flow meters (i.e., square root and linearly proportional) is not recommended unless one is converted to the other mode. Controlling the ratio between more than two flow signals will require a more complicated ratio control system.

4.4.2 Control Valves

A food process control operation involves, in most cases, control of manipulated variables like flow of raw materials and intermediate products from one point to another. In many applications the flow control requires control of variables like density, viscosity, and composition. The control signals generated, based on some quality parameters of the product, are applied to the control valve to regulate the manipulated inputs. A control valve regulates materials to a process by opening or closing a variable orifice in a pipeline. The word *material* in food processing denotes either gases or liquids, but in most cases the material handled is in liquid, pasty, or semisolid phase.

Flow rate in food processing is generally expressed in volume per unit of time and mass flow rate is very seldom used. Mass flow rate is related

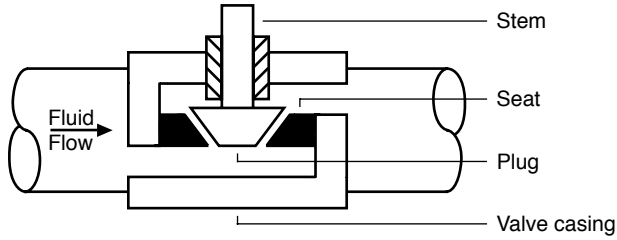

FIGURE 4.19
Cross-sectional view of a control valve.

primarily to the density of the food material. The volume flow rate of a material through a pipe is expressed as

$$Q = Av \tag{4.15}$$

where Q = Flow rate (m^3/sec)
A = Area of pipe (m^2)
v = Flow velocity (m/sec)

Obviously equation 4.15 indicates that the flow rate can be varied by varying the cross-sectional area of the flow line. If we can provide a system by which the cross-sectional area can be varied using a variable-sized restriction, as shown in figure 4.19, the flow rate can be controlled. Figure 4.19 shows that when the stem and plug moves up and down, the area of the restriction increases and decreases, respectively. Bournoulli's theorem establishes the pressure drop developed in the valve opening by the equation

$$Q = K\sqrt{\Delta p} \tag{4.16}$$

where K = proportionality constant ($m^3/sec/Pa^{1/2}$)
$\Delta p = p_2 - p_1$ = pressure drop (Pa)

The proportionality constant is determined mainly by the size and geometry of the valve opening; however, the flowing material also influences this constant to some extent.

4.4.2.1 Types of Control Valves

The performance of a valve is normally specified by many factors and features but the primary factor of the classification of valves is the relation between valve stem position (stroke) and the flow rate. Valves are classified into three different types based on this relation between the stem position (as percentage of full stroke) and flow rate (as percentage of full range). The following are three different types of control valves:

1. Quick opening: In this type of valve a small opening results in maximum possible flow rate. As soon as the valve stem is moved by a small amount, say 30%, the flow rate jumps to 90% in this type of valve.
2. Linear valve: This type of valve presents a linear variation of flow rate with stem travel.
3. Equal percentage: In many situations it is required that at a given percentage change in stem travel the flow rate also should change by the same percentage. Here the flow rate does not become zero at maximum stem travel to close the valve and this can be specified as Q_{min}. When the valve is fully open it gives the maximum flow rate (Q_{max}). The range can be defined as

$$R = \frac{Q_{max}}{Q_{min}} \tag{4.17}$$

The characteristic of this valve is exponential and the flow rate can be expressed as

$$Q = Q_{min} R^{S/S_{max}} \tag{4.18}$$

where S = the stem travel

For example, in an equal percentage valve, maximum flow rate is 100 cm^3/sec and minimum is 2 cm^3/sec. The full stem travel of the valve is 3 cm. The range is

$$R = (100 cm^3/sec)/(2\ cm^3/sec) = 50$$

The flow rate at any valve travel, say at 2 cm, can be determined as

$$Q = Q_{min}\ R^{S/Smax} = (2\ cm^3/sec)(50)^{2cm/3cm} = 27.14\ cm^3/sec$$

Figure 4.20 shows an electronically controlled valve manufactured by Omega Engineering, Inc. (USA).

4.4.2.2 Valve Sizing

The performance of a control valve depends on its design to the required specifications. An oversized valve will fail to block the fluid even at the higher side of the closing due to less effective resistance. Thus, it becomes difficult to control the fluid. Moreover, it is not economical to use an oversized valve for the same flow of liquid. Again, if the valve is undersized it will not pass the necessary flow and a problem of plugging occurs. From a

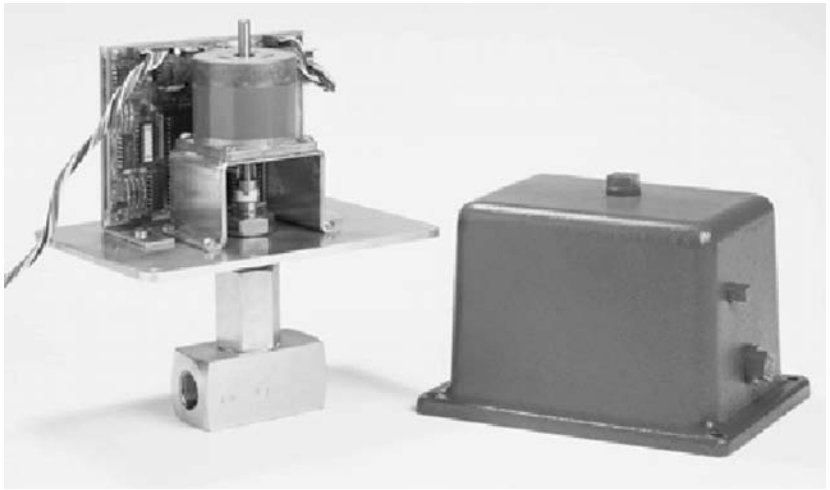

FIGURE 4.20
Photograph of an electronically controlled valve (Model PV14). © Omega Engineering, Inc, All rights reserved. (Reproduced with the permission of Omega Engineering, Inc., Stamford, CT 06907; www.omega.com).

design point of view, the liquid volumetric flow rate can be defined by an equation as

$$Q = C_v \sqrt{\frac{\Delta p}{S_G}} \tag{4.19}$$

where C_v = Valve flow coefficient
Δp = Pressure across the valve
S_G = Specific gravity of the liquid

Values of C_v for different sizes of valves are shown in table 4.5.

TABLE 4.5
Valve Flow Coefficients

Valve Sizes (in.)	C_v
0.25	0.3
0.50	3
1.00	14
1.50	35
2.00	55
3.00	108
4.00	174
6.00	400
8.00	725

4.5 Atmosphere Control in Food Preservation

Food preservation is mainly aimed at controlling growth of microorganisms like bacteria, yeasts, and molds. In addition to use of preservatives, an acceptable atmospheric condition also contributes a lot to food preservation. For example, fruits and vegetables can be preserved well if their respiration rate is reduced by reducing the oxygen content of the storage atmosphere and increasing the carbon dioxide content. However the required levels of oxygen and carbon dioxide content can vary for different fruits and vegetables. Oxygen content not only reduces respiration, but it also limits oxidation spoilage in oxidation-sensitive products like coffee, nuts, and others. Carbon dioxide levels can be increased by adding the gas in liquid or gas form, but reduction requires scrubbing the air. Scrubbing can be done by passing the air through bags of solid calcium hydroxide or through a spray of caustic soda. Ripening of fruits like bananas or tomatoes can be controlled by reducing ethylene levels in the storage atmosphere.

Moisture in the storage environment inhibits growth of microorganisms in food.Therefore humidity of the air plays an important role in food storage preservation. Equilibrium RH of a substance indicates how hygroscopic the substance is. The equilibrium RH of a substance is the humidity value of the air at which the substance neither absorbs nor releases moisture.

Temperature of the surrounding air also matters for food spoilage. At lower temperatures the biochemical degradation of food is low. However, this is not true for all types of food. There are numerous examples of how food storage at low temperature spoils foods; for example, low temperatures in meat freezing damages the muscle cells, and tissue cell breakdown takes place in apples. Therefore temperature measurement and control is an important strategy in food preservation.

4.5.1 Control Scheme

Control of atmospheric storage air parameters as mentioned earlier should be performed, keeping economic considerations in mind. From a control point of view, the atmospheric storage control problem is well defined and distinct and can be addressed by a noninteractive MIMO structure as shown in figure 4.21. Here the control scheme consist of four individual control loops that are noninteractive.

Measurement and control of temperature and humidity have already been discussed. Two new parameters, oxygen and carbon dioxide, are included in this application. On-line detection of oxygen can be performed by high zirconium oxide (voltage or current mode) fuel cells. These detectors do not require a sampling system and the probes can be inserted directly into the process. Probes are available in lengths from 1.5 ft to 12 ft and should be inserted into the process at the most representative region. Measurement ranges of these

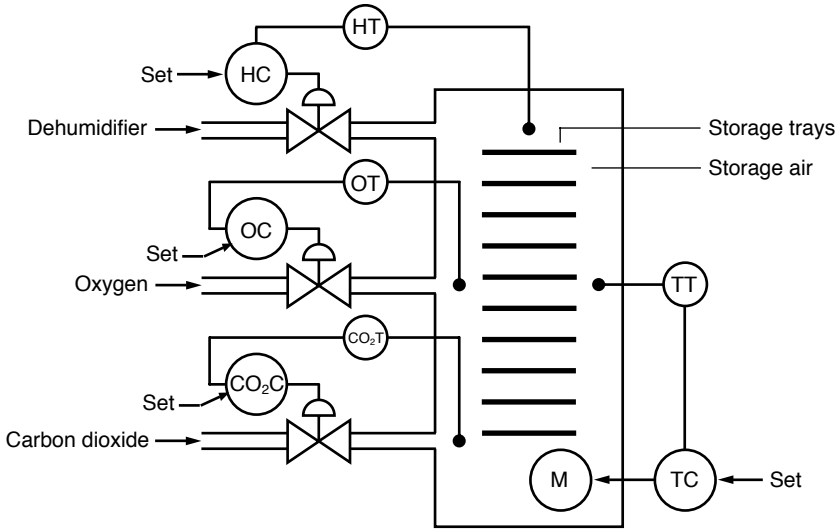

FIGURE 4.21
Schematic diagram of a storage atmosphere control system.

detectors are 0% to 100%. Another suitable and more sensitive oxygen detector for this application is the galvanic detector, but this type of detector requires temperature and gas flow rate compensation. Carbon dioxide gas detection can be performed using nondispersive infrared analyzers or mid-IR filter analyzers, which are available in cell or probe structure. MOS-based gas sensors are also available in a variety of forms and ratings. These sensors are mostly general gas sensors in terms of selectivity and sensitivity and so calibration for a particular gas has to be performed by trial.

The controllers to drive the actuators and control valves shown in figure 4.21 can be implemented by electronic controllers, but microprocessor- or microcomputer-based controllers can also be used. Simple proportional controllers suffice for the control problem because the signals are mostly the slow-varying type without many jumps.

4.6 Timers and Indicators in Food Processing

Earlier it was mentioned that a food processing industry can adopt either a continuous or batch processing system. Most chemical- and petroleum-based industries adopted batch processing earlier but gradually realized that a continuous process is more efficient and cost effective. Most food processing industries prefer batch processing to continuous processing due to the many inherent biochemical factors of food. In batch processing, a particular intermediate

product is transferred to another stage with a time lag. The time lag might be intentional to allow development of a particular taste or flavor. In some cases the time lag is due to shortage of sufficient machines to process the food.

For example, in a food processing industry an intermediate product A is developed at a rate of 1,000 kg/day for a time period of 2 hr in the morning. Product A should be transferred to stage B for the next processing phase between 7:00 and 9:00 a.m., and it takes 15 min to transfer the product from stage A to stage B. There are four machines to operate stage B and each machine takes 30 min to process 125 kg of the product. To schedule this operation a timing sequence must be maintained in the following manner:

Machine Number	Time of Operation (a.m.)
1	7:00–7:30
2	7:15–7:45
3	7:30–8:00
4	7:45–8:15
1	7:45–8:15
2	8:00–8:30
3	8:15–8:45
4	8:30–9:00

If the total processing in stage B requires 60 min, this timing sequence should be arranged in two batch sequences to facilitate easy transfer in the machine room as shown here:

First Sequence		Second Sequence	
Machine Number	Time of Operation (a.m.)	Machine Number	Time of Operation (a.m.)
1	7:00–7:30	3	7:40–8:10
2	7:15–7:45	4	7:55–8:25
1	7:45–8:15	3	8:25–8:55
2	8:00–8:30	4	8:40–9:10

In such operations, factory managers generally use a programmed time scheduling book, however such books are fiction compared to reality! The main disadvantage of this manual timing control is that it is very difficult to track the sequence due to human error. With several machines, operators cannot decide immediately which machine is being charged, discharged, or recharged within the allotted period of time. On the other hand, deviation from the programmed operation leads to loss of time, money, and quality. The only solution is to use an electronic programmed time sequence indicator to provide a visual indicator or alarm on each machine to indicate the charging and discharging time of the machines.

4.6.1 Rolling Program in Tea Manufacturing

The electronic programmable timer developed by Bhuyan [1] for the rolling process in the tea industry is discussed in this section. The percentage of

total tea leaf handled daily out of the total annual crop varies from factory to factory within a range from 0.35% to 1.25%. Factories are equipped with machinery according to their handling capacity. For a 5×10^5 kg annual production with a provision for intake of 0.85% of the annual crop in 10 hr/day will be able to handle 18,800 kg of fresh leaf [3]. The rolling machinery requirement can be determined based on the capacity of the rolling sequence or program used. The aim of such a rolling program is to produce as much fermented leaf per hour as will keep the dryers full.

The total amount of handled fresh leaf of 18,800 kg/day with a moisture content of 66% will wither down to 12,200 kg of leaf with 65% wither. To handle the amount of withered leaf in the rolling section daily, the per-hour handling capacity becomes 1,220 kg. This throughput can be obtained by proper programming of the rolling sequence, which depends on the number of rollers, desired number of rolls, and the period of rolling. For a two-roll system with 30 min rolling time the rolling program will be different for 6 46-in. rollers (6×46 in.) and 14 36-in. rollers (14×36 in.). The rolling programs [3] are as shown here:

Program I

3 × 46-in. rollers		**3 × 46-in. rollers**	
A B C		**D E F**	
First Roll		**Second Roll**	
Roller	**Time (a.m.)**	**Roller**	**Time (a.m.)**
A	7:00–7:30	D	7:40–8:10
B	7:15–7:45	E	7:55–8:25
C	7:30–8:00	F	8:10–8:40
A	7:45–8:15	D	8:25–8:55
B	8:00–8:30	E	8:40–9:10

Program II

7 × 36-in. rollers		**7 × 36-in. rollers**	
A B C D E F G		**H I J K L M N**	
First Roll		**Second Roll**	
Roller	**Time (a.m.)**	**Roller**	**Time (a.m.)**
A	7:00–7:30	H	7:40–8:10
B	7:06–7:36	I	7:46–8:16
C	7:12–7:42	J	7:52–8:22
D	7:18–7:48	K	7:58–8:28
E	7:24–7:54	L	8:04–8:34
F	7:30–8:00	M	8:10–8:40
G	7:36–8:06	N	8:16–8:46
A	7:42–8:12	H	8:22–8:52
B	7:48–8:18	I	8:28–8:58
C	7:54–8:24	J	8:34–9:04
D	8:00–8:30	K	8:40–9:10

For simplicity, the corresponding timing diagram for the roller charging and discharging for Program I is shown in figure 4.22. Generally a 46-in. roller has a capacity of rolling 260 kg to 325 kg of withered leaf and the capacity for a

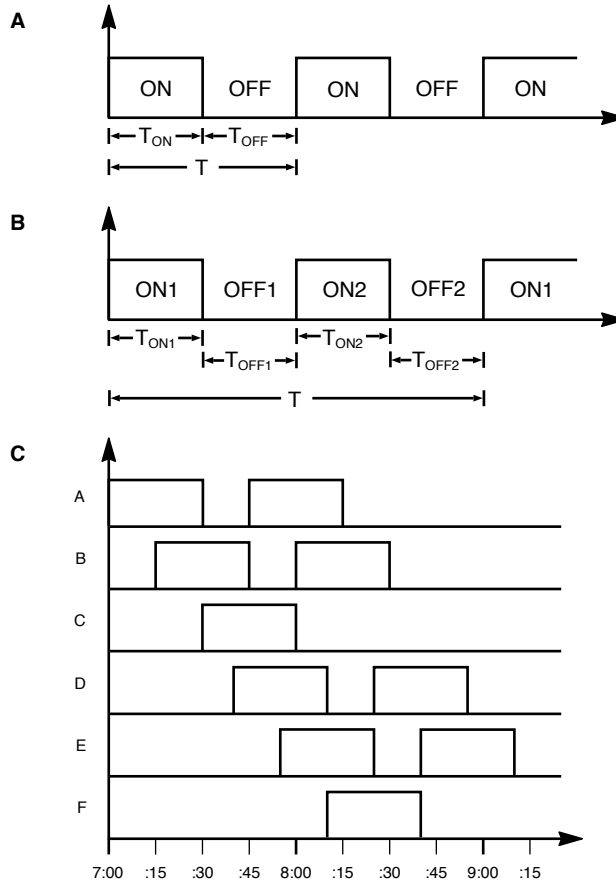

FIGURE 4.22
Timing diagrams for rollers: (A) basic timing; (B) double mode timing; (C) timing for Program I.

36-in. roller is 120 kg to 145 kg. With these capacities, if the rollers are charged as per Programs I and II, the throughput of rolled leaf per hour with 6 46-in. rollers will be between 1,120 kg and 1,300 kg and throughput for 12 36-in. rollers will be between 1,040 kg and 1,160 kg. Including 1.5 hr for shifting, the entire rolling operation will be completed within 11 to 12.5 hr with 6 46-in. rollers and within 12 to 13 hr with 12 36-in. rollers [3].

4.6.1.1 Roller Timing Sequence

Figure 4.22A shows a basic on–off timing, and figure 4.22B shows a dual on–off timing sequence. As seen from the timing diagram of figure 4.22C, each of the rollers A to F is charged and discharged for a specific period of ON time and OFF time, respectively. These ON and OFF time sequences are not the same for all the rollers. For example, roller A starts charging from 7:00 a.m. with the following ON and OFF times as per Program I:

The ON and OFF times for roller A are:

ON1 = 7:00–7:30 (a.m.) = 30 min
OFF1 = 7:30–7:45 (a.m.) = 15 min
ON2 = 7:45–8:15 (a.m.) = 30 min
OFF2 = 8:15–9:10 (a.m.) = 55 min

The ON and OFF times for roller B are:

OFF1 = 7:00–7:15 (a.m.) = 15 min
ON1 = 7:15–7:45 (a.m.) = 30 min
OFF2 = 7:45–8:00 (a.m.) = 15 min
ON2 = 8:00–8:30 (a.m.) = 30 min

Hence, the rollers are required to be charged and discharged with two ON times and two OFF times. This timing sequence can be generated by a programmable timer circuit, as discussed in the next section.

4.6.1.2 Programmable Timer Circuit

A basic timer circuit is capable of producing ON and OFF pulses cycling at a specific frequency and ON/OFF time duration (duty cycle) as shown in figure 4.22B. The programmable timer circuit (fig. 4.23) consists of two major parts: Circuit 1 (CK1) generates the required time delays for the ON/OFF pulses, and circuit 2 (CK2) is used to select different modes of duration. The circuit is made up of the following major components:

1. A timer
2. Decade counters
3. 4 to 16 decoder

The IC timer works as the main clock generator with a minimum of 1-min clock pulses. The CKT1 selects ON/OFF modes sequentially by changing the outputs A, B, C, and D. The correspondence of the modes with outputs is as follows:

When A = 0, mode 1 = ON1
B = 0, mode 2 = OFF1
C = 0, mode 3 = ON2
D = 0, mode 4 = OFF2
E = 0, mode 1 = reset and restart

Reset is initiated by applying the inverted output of E to pin 2 and 3 of the decade counter of CK1. When a particular mode is in action, depending on any one of the values of A through D, the duration of the mode is set by the action of the 4 to 16 decoder of CK1; selector switchesthrough S_1(P, Q)

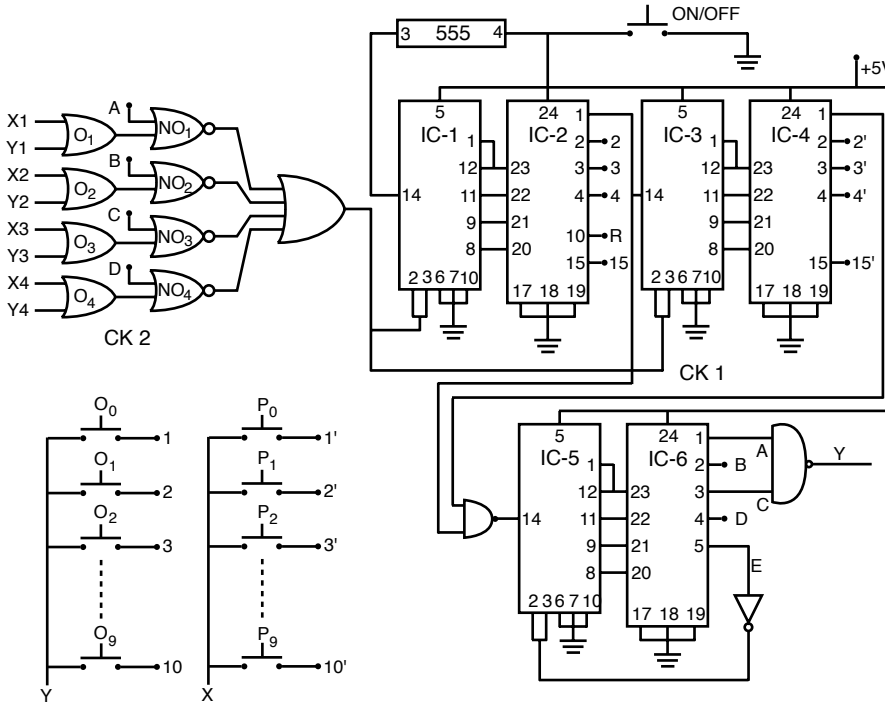

FIGURE 4.23
Circuit diagram of a programmable timer.

to $S_4(P, Q)$; and the OR-NOR-OR gate combination. The time duration of any mode can be adjusted from one basic pulse duration to 99 times that basic pulse duration. For example, when a basic pulse duration is 1 min, the time duration can be set from 1 (1×1) min to 99 (1×99) min.

In each mode there are two sets of switches P and Q. The outputs of IC4 are 10 times the duration of outputs of IC2. For mode 1, let the required mode duration be 25 min. To set this duration, switch P_1 of P and Q_4 of Q are closed; that is, P_1 gates output 2' to X and Q_4 gates output 5 to Y from IC4 and IC2, respectively. Therefore, the total duration selected is

$$P_1 = 2 \times 10 = 20 \text{ min}$$
$$Q_4 = 5 \times 1 = 5 \text{ min}$$
$$\text{Total time} = 25 \text{ min}$$

When output 2' of IC4 and output 5 of IC2 are both low, then the output of OR gate O_1 will be low, causing the output of the NOR gate N_1 to become high because at the same time A is also low at mode 1'. The COM signal becomes high, resetting IC1 and IC3. This makes both outputs 1 and 1' low, which are applied to the clock input of IC5 after OR operation. When IC5 undergoes low to high clock transition, it starts counting to the next state;

TABLE 4.6
Truth Table for IC6 and Final Output

	Outputs of IC6					
Clock	**A**	**B**	**C**	**D**	**Y**	**Mode**
1	0	1	1	1	1	ON1
2	1	0	1	1	0	OFF1
3	1	1	0	1	1	ON2
4	1	1	1	0	0	OFF2

that is, B becomes low, making mode 2 active. The duration of mode 2 can be set by switch S_2 like mode 1. After completing mode 2, the counter advances to mode 3 and then mode 4 sequentially, the time durations of which are set by mode duration selector switches S_3 and S_4. All the mode duration selector switches are separate and each switch comprises two lines of switches P and Q. When the maximum time duration of all the modes lies within a range of 10 times the basic clock pulse duration, the P line switches are not required and the X inputs to the OR gates O_1 through O_4 were connected to high. For example, if the clock pulse duration is 1 min and the maximum duration of the modes is 5 min, by closing switches Q_0 through Q_4, all the durations—1 min, 2 min, 3 min, 4 min, and 5 min—can be programmed without using switch line P. This reduces the numbers of switches to be used.

The output signal for indicating the state of the timer in the four different positions (i.e., ON1, OFF1, ON2, and OFF2) is obtained by NAND operation of the outputs A and C of IC6. The truth table of the IC output and final output is shown in table 4.6. The output Y can be used for indication of the four different ON/OFF times. A relay can be driven through a transistor-switching circuit for indication with the help of colored lamps.

The circuit just described refers to a single roller timing sequence. For N numbers of rollers, N numbers of timer circuits should be used. The pulse generator can be common, triggering all the timer circuits simultaneously. A schematic diagram of the sequential timer for N numbers of rollers is shown in figure 4.24. Outputs Y and R are applied to the switching circuit from which the RED and AMBER lights are turned on. The RED lights are used to indicate the state of the rollers and AMBER lights can be used to check the function of the pulse generator. The programming of the timer as per Program I is shown in table 4.7.

4.6.2 Temperature Indicator for Tea Dryer

Tea drying is carried out on the fermented tea leaf (FTL) in drying machines. In traditional dryers, FTL is transported onto perforated moving trays and hot air is blown through it. Fluidized bed dryers are also very popular compared to traditional dryers due to more homogenous and uniform mass and heat

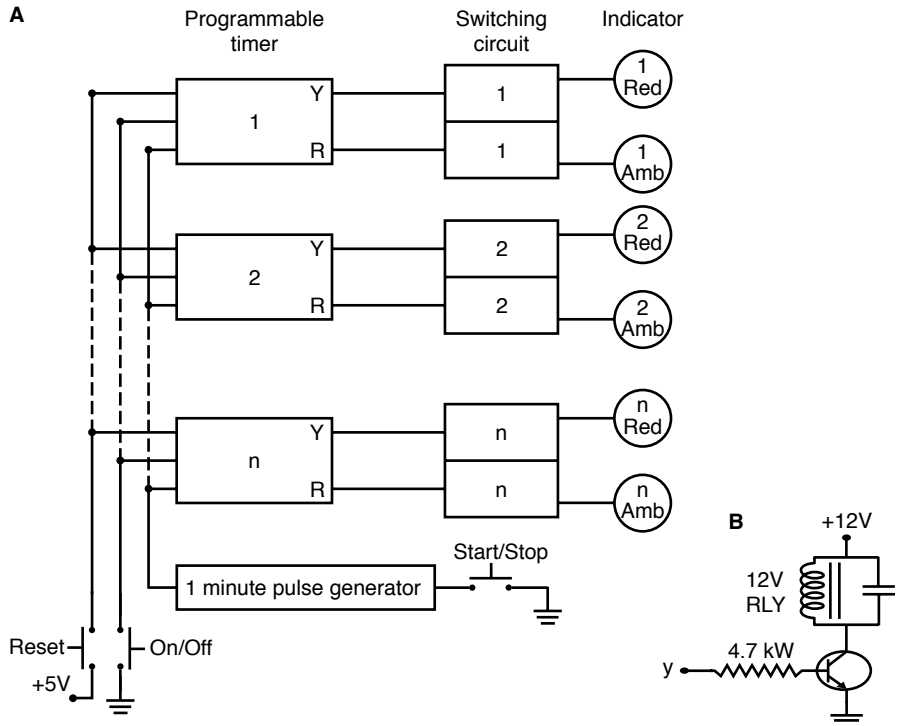

FIGURE 4.24
(A) Schematic diagram of sequential timer/indicator. (B) The relay control circuit.

TABLE 4.7

Timer Sequences

	Duration of Rollers (min)					
Mode	**A**	**B**	**C**	**D**	**E**	**F**
ON1	30	0	0	0	0	0
OFF1	15	15	30	40	55	70
ON2	30	30	30	30	30	30
OFF2	15	15	15	15	15	15

transfer. The quality of the final processed tea during drying depends on the following parameters:

1. Inlet and outlet temperature of the drying air
2. Run-through time or feed rate of the FTL
3. Volume of air

Conventionally, the inlet temperature is kept constant by regulating the temperature and velocity of the drying air obtained from the furnace. On the other hand, even if the inlet temperature is maintained at a constant level,

TABLE 4.8

Logic States for the Three Level Indicators

Ranges of Exhaust Temperature	Drying Status	Feeding Status	Indication		
			Red	Blue	Green
$T_h < T_0 < T_i$	Over	Under	Off	Off	On
$T_l < T_0 < T_h$	Normal	Normal	Off	On	Off
$T_a < T_0 < T_l$	Under	Over	On	Off	Off

Note: T_h = high set-level temperature; T_0 = exhaust temperature; T_i = dryer inlet temperature; T_a = ambient temperature; T_l = low set-level temperature.

the exhaust temperature cannot be maintained if the feed rate is not constant. This is because at a specific inlet temperature the total heat content of a fixed volume of air is also fixed. Therefore the feed rate of FTL should be maintained at a desired value to maintain good quality of the processed tea.

In the dryer the temperature of the exhaust air is a faithful representation of the feed rate of FTL. Therefore its measurement and monitoring becomes essential. The outlet temperature goes down with the feed rate of FTL, hence, FTL temperature increases and the tea is burnt, whereas at a higher feed rate FTL is underexposed to heat, which results underdried tea. If this phenomenon is not remedied for a long time, the whole lot of tea in the dryer gets spoiled. Pressure spring thermometers are normally used to measure the drying air temperatures, but these units fail to give any intelligent information about overdrying or underdrying of tea. To monitor drying conditions of tea, many researchers have suggested continuous measurement of dryer inlet and outlet temperature [4–6].

A three-level dryer temperature indicator system has been developed by Bhuyan [1] to quickly respond to overdrying and underdrying of tea. The device is based on measurement of dryer exhaust temperature and development of a logical decision. The logic table of the three-level indicator system is shown in table 4.8.

A block diagram of the indicator system is shown in figure 4.25. An IC thermal sensor is used to measure the dryer exhaust temperature and an

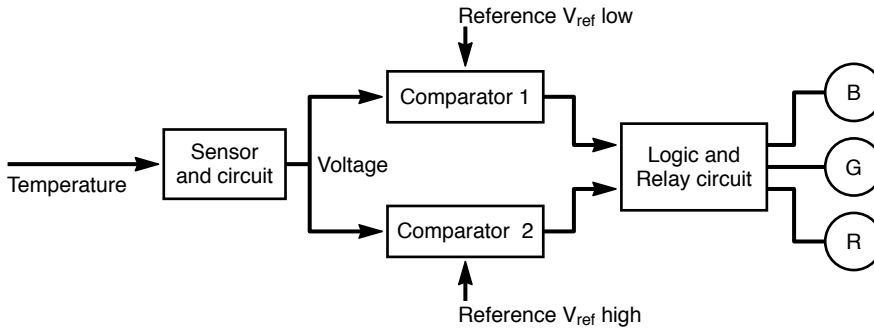

FIGURE 4.25
Block diagram of the three-level temperature indicator.

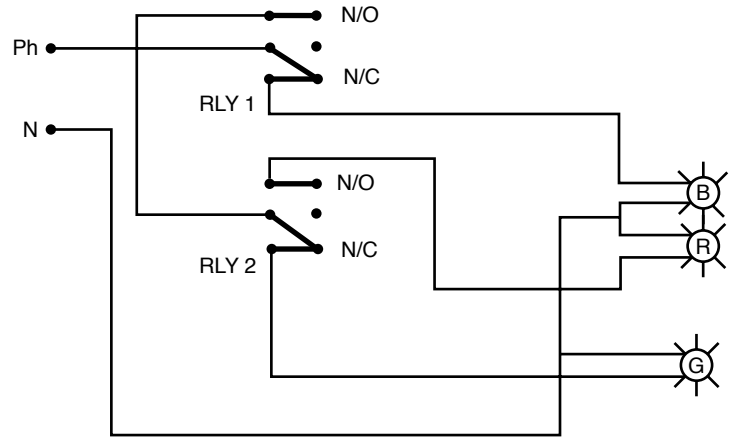

FIGURE 4.26
Relay connection diagram for indicators.

amplifier is used to amplify the signal. The amplified signal is applied simultaneously to two op-amp comparators that compare the signal with the low-level and high-level temperature set points. The comparator individually compares the temperature-dependent voltage signal and produces two signals, V_{c1} and V_{c2}. These outputs are applied to a logic and then to a relay triggering circuit as shown in figure 4.26. By properly selecting the reference inputs to the comparators using selector switches, different levels of high and low temperature can be set for varying conditions of the initial moisture content of the FTL. This fulfills different climatic conditions during drying.

4.7 Food Sorting and Grading Control

4.7.1 Objective of Sorting

Maintaining quality of products manufactured in a food processing industry is a continuous process of assessment in the various processing stages. Sorting and grading is one such stage where cleaning, inspection, or measurement of certain quality parameters is performed. The main objectives of sorting and grading are contaminant detection; elimination of undesired substances; assessment of dimensions, shape, and density; chemical composition determination; detection of dry soluble matters, detection of off-color and off-flavor product; detection of pesticide residue; and so on. The sorting operation is performed on both the raw materials and the final product. For example, in the wheat milling process, the wheat grain is put through a sorting process to remove impurities larger or smaller than the grains, similar to other cereals such as barley and oats. Other substances such as light grains, seeds, stones, and so on, are also removed during the sorting process.

In coffee manufacturing, uniform green coffee bean sizes are preferred before roasting and grinding. Defective beans are also sorted out and removed before processing. Defects such as broken eggs in food processing are called *wholeness,* or the degree of whole and broken pieces. Appearance of food also determines good or bad quality, like defects in moldy bread. Fruits and vegetables can be sorted before processing based on shape, size, and ripeness. Tea is graded as per grain size (as discussed in chapter 3) before packaging. If the lowest grade, "dust." is mixed with the higher grades, "BOPL" or "BOP," it does not command a good price.

Food color also can indicate quality or defects in food. Fruit color can indicate both ripeness and spoilage. Deep or dark color of fried foods indicates overfrying. Shapes can also become an important quality attribute, like the degree of curvature of pickles. Some machines are designed to dispose of the odd-shaped pieces automatically.

4.7.2 Various Sorting Techniques

Conventional sorting and grading based on sizes and shapes is done using mechanized openings called sieves or screens. The food items are allowed to pass through sieves of various sizes to sort out the food as per different grades. Examples of sieving operations include removing other cereals from wheat, sorting and grading of tea by grain sizes, and separating defective beans in coffee manufacturing.

During tea manufacturing, tea ball sizes ranging from 0.5 cm to 1.0 cm formed with rolled or cut tea are removed using a special kind of machine called a ball-breaking machine. Here the rolled tea mixed with balls is allowed to fall inside a rotating cylinder. Due to centrifugal force, the balls find a different outlet and get separated from the smaller grains. All such sorting machines are mechanically vibrated or rotated at a certain frequency using electrical motors with cam arrangements. The sorting machines are designed based on the mass of the food items, providing a relative motion on the platform to an outlet.

Many other sorting machines have been developed based on air-lifting mechanisms, where the lighter objects such as rice husks, get separated from the heavier grains due to velocity of aspirating air. Wheat flour of especially high quality can be manufactured based on particle size and protein content by the air classification method. Here sieving cannot be used because particles below 80μ cannot be separated. In this technique the centrifugal force is balanced by air drag produced on individual particles. Manipulating the air volume can control the particle classification size. Adaptive controllers have also been developed to change the velocity of the air based on variations in mass of the grains.

Sorting based on color attributes of the defective items has become popular recently. Traditionally color sorting is done manually in many food processing industries, but manual methods are monotonous and prone to human

error. In coffee manufacturing, a single black-colored coffee bean can spoil a whole lot of coffee. Therefore black coffee beans are sorted out by optical sorting machines. A similar colored stalk separating technique for tea was discussed in chapter 3.

Separating unripe fruits from ripe fruits can also be done using color sorting and automated techniques of door closing and opening in a conveyor system. Belt sorter conveyors are typically 48 in. wide, traveling at a speed of 600 ft/min, and carrying a total of about 40,000 pounds of the product per hour. Cameras with lights are installed over the conveyor and images of the products are continuously monitored. When a defective item appears in front of the camera, a computer detects the defect by image processing techniques. The computer also determines the x-y coordinates of the location of the item on the conveyor and then sends a signal to one or more fast-acting air jets installed over the conveyor to eject the defective item to a reject conveyor. The time taken from detection to ejection can be only few microseconds. Most of the devices use a single SISO model in on–off control mode. The color or optical signal triggers a threshold circuit to generate the control signal to perform some action to reject the defective item.

Similar sorting and grading devices based on many other quality attributes are in the process of development.

4.7.3 Automated Packaging and Bottling

Packaging of food is aimed at protecting the food from physical, chemical, and microbiological spoilage. There are many types of food packaging methods, but cans and bottles are the most popular for liquid foods. Bottling techniques are different for different materials; for example, soft drink bottling needs only a simple method, whereas fruit juice bottling involves hot filling, bottle pasteurization, or aseptic filling. Bottling includes three main stages: bottle washing, scanning, and filling. Automated bottle-washing machines that maintain correct detergent strength and temperature are available. Scanning detects the presence of any foreign object, any residual liquid, or cracks in a refilled bottle. Manual scanning requires a very high concentration level and good eyesight. Many automatic scanners have been developed, in which a light beam is illuminated through the bottle. Any defect interrupts the light beam, which can be detected. Automated bottle scanners can supplement human scanners, but total replacement is not recommended.

Filling of bottles with beverages is performed by different techniques such as vacuum filler, piston filler, cup-type filler, time-cycle filler, and so on, but vacuum filling is the most popular method. Speed of filling is a matter of concern to achieve production targets. High-speed bottling can be achieved by automated bottling techniques, where sensors and pneumatic actuators play an important role. Pneumatic operations include orientation of the empty bottles, positioning them on the rail, and sending them to the filling

station. Sensors detect the presence of and defects in the bottle. A computer controls the sequence of operations.

4.8 Discrete Controllers

Industrial food processing machineries are run mostly by motors, heaters, coolers, blowers, extruders, stirrers and other equipment that needs electrical power. For example, when a tea withering system is started, the withering fan motors of several withering troughs start simultaneously. The controller continuously determines the withering percentage of tea; when the target value in a particular trough is reached, the motor automatically stops. The stopping operation for a high-current AC machine can be handled by a control relay with a contact rating of high current. A control relay (fig. 4.27A) is an important component of discrete controllers. A control relay is basically an electromagnet that, when energized by a control signal of relatively low power, develops a magnetic force to make a physical contact between two terminals. The relay contact includes three terminals: a common (C) terminal, a normally open (NO) terminal, and a normally closed (NC) terminal. By altering the connection from NO to NC terminal and vice versa, the polarity of the controller action can be reversed. For example, if a control signal needs to start a machine, the connection should be made to terminal C and NO; however, if the control signal needs to stop the machine, the connections should be made to the C and NC terminals. The symbols used for designating a control relay in an electrical diagram are shown in figure 4.27B.

When an industrial control requires operation of several machines in a sequence with definite time intervals, the array of such control relays is used in appropriate places and a sequential control signal triggers the relays to turn the machines on or off. Such control operations are called relay controls. In discrete state control, all inputs and outputs have only two states—true

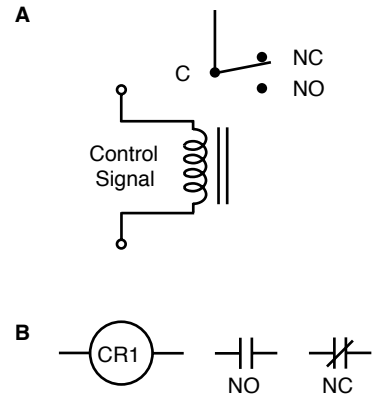

FIGURE 4.27
Control relay: (A) relay contacts; (B) symbols.

or false—such as temperature high or low, heater on or off, withering achieved or not, or fan forward or reversed.

4.8.1 Ladder Diagram

A relay control operation for driving certain machines sequentially in an industry based on certain input parameters can be expressed by a ladder diagram. The ladder diagram follows some symbolic representations of the control elements. In this diagram, all the circuit hardware is connected in parallel across the power supply line. Each branch of the ladder involves a single input or combinations of inputs and a single command output. The inputs and outputs are of the true–false nature.

A ladder diagram can be developed from the description of the control problem. If the control problem is very simple it can be directly transformed to the ladder diagram, whereas a complex operation needs several attempts to complete the ladder diagram. The ladder diagram of the following example shows the development procedure.

In figure 4.28 a relay is used to activate the green light on a machine when the normally open (NO) switch SW1 is not depressed and the relay is not latched. The relay is latched to activate the red light when the switch SW1 is depressed. Hence, the relay is latched, and to unlatch the relay the normally closed (NC) switch SW2 is depressed, which opens the circuit and the releases the relay. The ladder diagram for this problem is shown in figure 4.29. The diagram has three parallel branches. In the first branch the control relay CR1 latch is shown. In the next two branches the two lights—green and red—are connected to the main branch through the control relay contacts. The green and red lights are connected to the power supply through the NC and NO contacts of the relay, respectively.

The ladder diagram also shows how physical connections should be made for the hardware components. This type of relay-based controllers is popular due to their simple and straightforward logic. In many industries, relay controllers are not replaced by computer control techniques. The programming of the relay controller is done by hard-wired connections of the components to the AC power line. Once the components are connected, as per

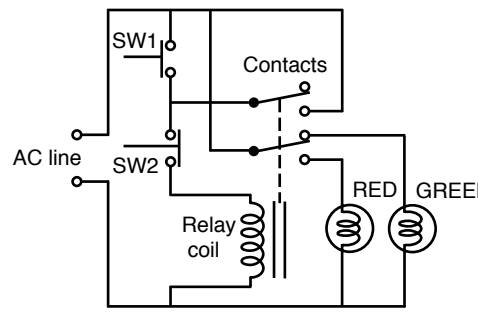

FIGURE 4.28
Connection diagram of a relay used in an indicator latch control.

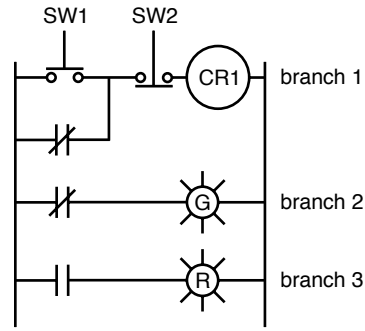

FIGURE 4.29
Ladder diagram of the indicator control.

the ladder diagram, each component will follow the logic, making the system a relay sequencer.

4.8.2 Programmable Logic Controllers

Another alternative and modern technique of discrete control is the programmable logic controller (PLC). The relay control is fully hardware based and the only peripheral to the system is the machines, but in the case of PLCs, many other electronic devices such as comparators, integrators, summers, delays, and so on can be added. Because a PLC uses memory and a processor, many of the relaying actions can be implemented in software.

A PLC can be represented by the diagram shown in figure 4.30, where the processor accepts the input signals and performs logic calculations based on the inputs, and then generates an output command signal.

4.8.2.1 Input and Output Modules

The input signals represent all discrete states of physical operations like switch position, motor condition, and so on. These inputs are received by an input module that converts the signals to an acceptable level for the computer. For example, a power line switch will send a 230 V AC when it is closed and 0 V when it is open. These power line voltage levels are converted

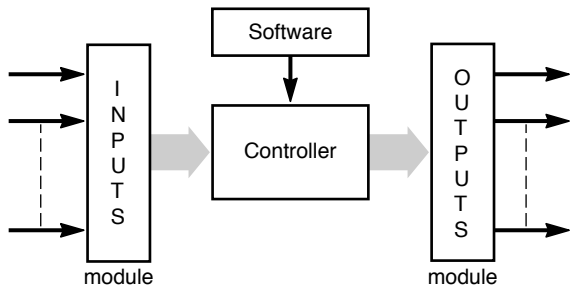

FIGURE 4.30
A basic PLC structure.

to TTL or CMOS levels of digital states, say +5 V and 0 V, respectively. An input module can accommodate a certain number of channels.

The output modules receive digital signals from the processor to drive control devices like motors, solenoids, and so on. Intermediate devices such as relays, silicon controlled rectifiers (SCRs), and triacs are used to operate the control components. Some of the output modules provide sequential signals like pulses to drive stepper motors. PLCs mostly discard the electromagnetic relays, as in the case of relay controllers, and replace them with solid state relays and software operations.

4.8.2.2 Programming

For programming a sequential control action based on some logical conditions of the inputs, the processor must detect the input and output signals. This detection is possible by addressing the locations or channels as in the case of addressing the locations of peripherals like printers and plotters in computers. Each input and output channel is specified by an address in hexadecimal format as shown here:

Input channels (8 numbers): 00 to 07
Output channels (8 numbers): 08 to 0F
Internal relays (8 numbers): 10 to 17
Timers (8 numbers): 18 to 1F

Apart from addressing physical devices, the programming needs to address software-based devices for relay, delay, counters, and so on. A timer is activated based on some condition of a device and when the condition is fulfilled the appropriate device is activated after the time indicated by the timer. Similarly, counters count some events and after the specified number of events is reached the controller makes some contacts.

Modern PLCs not only handle discrete controls, but can implement many other continuous control actions like proportional, derivative, and integral controls as well. Intelligent controllers like fuzzy controllers have also been made possible in PLCs.

4.9 Adaptive and Intelligent Controllers

Adaptive controllers are control systems that can automatically adjust or adapt to variations in the process or environment by adjusting the controller settings. The variations can take place in the process variables or in the process parameters. Based on the adaptation strategy, adaptive controllers can be classified into two major types: self-tuning controllers (STCs) and

model reference adaptive controllers (MRACs). The salient features of the adaptive controllers, for which they are so popular, are the following:

1. They can accommodate uncertainty in constant or slow-moving parameter changes in the process.
2. They require very little *a priori* knowledge about the plant parameters.

In designing an adaptive controller, the major task involves development of a control law with adjustable controller parameters and design of an adaptation law for adjusting the controller parameters. After designing the controller, the convergence of the error (the difference between the ideal controller parameters and the adjusted controller parameters) must be analyzed to avoid delay and oscillations. However, the convergence problem can be avoided to a great extent with *a priori* knowledge about the plant parameter variations [7].

4.9.1 Self-Tuning Controllers

STCs are based on the continuous identification of the closed-loop model of the plant. Figure 4.31 shows the structure of an STC. The main control loop consists of the plant and the controller and the outer loop performs the self-tuning of the controller parameters. A parameter estimator takes the process inputs and outputs to estimate the process parameters on-line. Any variation in the process parameter is fed to a block that determines the controller parameters based on the variations. These controller parameters are used to adjust the main controller parameters. A recursive identification method is used to estimate the plant parameters. The identification algorithm should not take much time so that the adjustment can be made immediately before the next variation of plant parameters takes place. Various parameter estimations techniques include least square, stochastic approximation, maximum likelihood, instrumental variables, extended Kalman filtering, and so

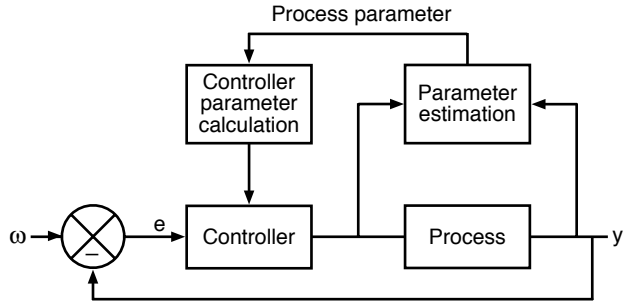

FIGURE 4.31
Structure of a self-tuning adaptive controller.

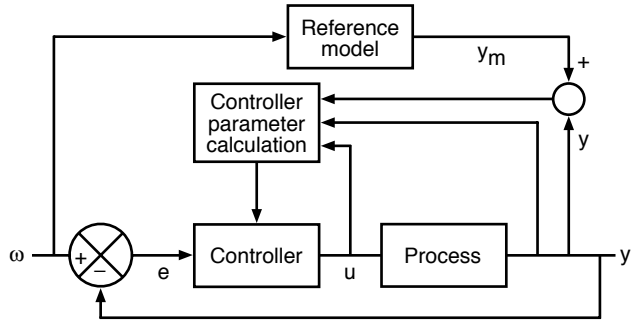

FIGURE 4.32
Structure of an MRAC.

on. The estimation algorithms for these techniques are available elsewhere and readers are advised to consult other references for details.

4.9.2 Model Reference Adaptive Controllers

Figure 4.32 shows a basic structure of an MRAC. Based on the ideal conditions a model of the process is used to generate the ideal or model outputs (Y_m). An error detector generates the error as the difference between Y_m and the actual plant outputs Y. A calculation unit takes the error, the inputs, and the outputs to calculate the controller parameters, which are then used to adjust the controller parameters. The detailed techniques of MRACs can be obtained in works by Landau [8, 9] and Parks [10].

4.9.2.1 Some Design Criteria of Adaptive Controllers

STCs can be designed based on the following criteria:

- Process model
- Process identification model
- Knowledge about the process
- Control design criteria
- Control algorithm

The techniques for the design criteria of these models are available in Isermann [11, 12], Wittenmark [13], and Goodwin et al. [14]. The different control algorithms of adaptive controllers are minimum variance controller [15], pole placement controller [16], linear quadratic Gaussian controller [17], and generalized predictive controller [18, 19].

Table 4.9 and table 4.10 describe the salient features of some practically implemented and commercial adaptive controllers for food processing, respectively.

TABLE 4.9
Salient Features of Some Practical Adaptive Controllers

Function	Type	Model	Controlled Variable	Disturbance Parameters	Convergence
Cross-flow grain dryer	STC	Pole placement	Exhaust air temperature	Grain moisture content	Fast
Air conditioning	STC	Supervisory	Temperature	Air flow rate, heat transfer	Fast
Food extruder	STC	GPC/SISO	Product pressure	Moisture content (square wave)	After learning

TABLE 4.10
Salient Features of Some Commercial Adaptive Controllers

Manufacturer	Model Name	Type	Controlled Variable	Target or Tested Industry
ASEA, Stockholm, Sweden	Novatune	MVC	—	Various
Predicted Control, Norwich, UK	Connoisseur	MPC	Temperature, product flow rate	Dairy, coffee, sugar
Universal Dynamics Tech, Canada	Brain Wave	MRAC	—	Brewery
CyboSoft, Ranch, Cordova, CA	CyboTune	Model free	—	Waste water in food processing

4.9.3 Intelligent Controllers

Intelligent control methods are becoming popular in the control world, which supports the traditional controls to a great extent. Intelligent controllers can endow a control system with flexibility and tunability that conventional methods could never exhibit.

Intelligent controllers are designed for processes with complex dynamics to meet some of the following requirements:

1. Heuristic approaches to tune the controller parameters
2. Knowledge about the process from the past
3. Fault detection techniques

A properly designed intelligent controller can reduce the monotonous and traditional behaviors of a controller. Intelligent controllers can substantially reduce development time and cost. Further, intelligent controllers use far less computational time compared to traditional controllers due to the heuristic approaches used. The most popular intelligent control approaches are fuzzy logic and neural networks. Neither of them can replace the traditional controllers, but they can provide support as an additional tool for the traditional systems. Because fuzzy controllers are more applicable in a control system, this type of controller is discussed here.

4.9.3.1 Fuzzy Logic Controller

Fuzzy control has many advantages compared to linear PID control for the following reasons:

1. It can circumvent the problems of nonlinear control.
2. Because it uses a rule-based approach, it is more familiar to the operators.
3. The controller can be made more user friendly by using a graphical user interface (GUI).
4. Because the control approach is designed for nonlinear systems, it works better in a linear environment.

Fuzzy sets, a basic component of fuzzy control, were first introduced by Zadeh [20] and then were developed in various applications including control problems. Fuzzy logic is said to be a better approach in food processing control because most of the biological products do not follow a strict pattern or rule that can be defined by heuristic or rule based on experience only [21].

4.9.3.1.1 Fuzzy Logic Principles

Most food quality attributes are very difficult to quantify and are generally termed very good, somewhat good, poor, and so on. These are the terms used by sensory panels in food quality testing (tasting). Each of these terms covers a range of measurements. Let us take as an example the grading of tea based on the flavor of a cup of tea. If the flavor profile is measured by points on a scale of 1 to 10, most tea testers grade tea as follows:

- Below 4: The tea flavor is poor.
- From 4 to 6: It is somewhat good.
- Above 6: It is very good.

This classification in fuzy logic is shown in figure 4.33, which shows that unlike classical logic, the uncertainty region of "somewhat good" is eliminated by using a triangular function instead of using a sharp rectangular

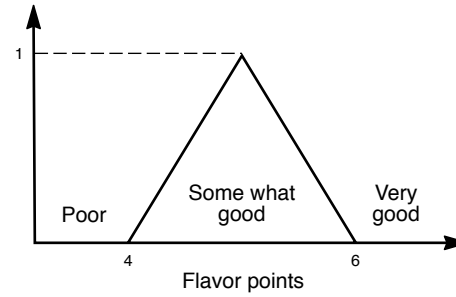

FIGURE 4.33
Fuzzy logic classification of tea flavor.

function. In fuzzy logic a degree of membership varying from 0 to 1 is used to define the classes, whereas in classical logic the function takes values 0 and 1 only. In fuzzy logic flavor points 4 and 6 mean somewhat good with degree 0, whereas point 5 means somewhat good with a degree of 1. Such definitions of uncertainty regions are not possible in classical logic. Fuzzy logic uses logical connectives such as

$$\text{IF (condition) THEN (conclusion).} \tag{4.20}$$

The classification of tea flavor (x) as per the this condition can be described as:

IF $x < 4$ OR $x > 6$ THEN "the tea is of somewhat good color" is false (= 0)
IF $x \geq 4$ OR $x \leq 6$ THEN "the tea is of somewhat good color" is true (= 1)

Very often the logical connectives AND and OR are used in the condition part of the rule. The AND (conjunction) connective takes a minimum degree of truth as in:

IF x_1 is true with a degree of d_1 AND x_2 is true with a degree of d_2,
THEN x_1 and x_2 are true with a degree $\min(d_1, d_2)$.

The OR (disjunction) connective takes a maximum degree of truth.
These concepts of fuzzy logic are used in fuzzy controllers by addition of a conclusion part. For example, in a tea fermentation process the humidity of the fermenting room is to be adjusted by water sprinkler based on the color of the tea. We can write a rule so that if the color is not good, the humidity should be adjusted.

Condition: The color of tea is not very good.
Decision: Adjust the humidity slightly.

The characteristic of humidity adjustment and color point is shown in figure 4.34.

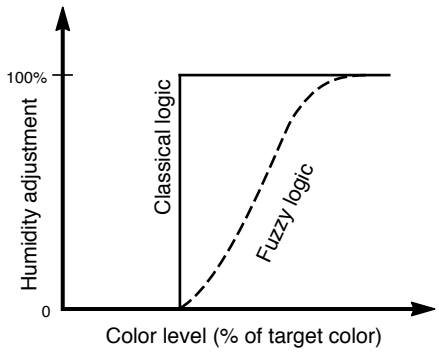

FIGURE 4.34
Fuzzy logic control in tea fermentation.

Fuzzy control uses a fuzzy set for each element of the condition with noncrisp boundaries, whereas classical logic uses a crisp boundary. A fuzzy set A is defined by its membership function as $\mu_{A:[0,1]}$. Fuzzy sets with union and intersection are given as

$$\begin{aligned} x \text{ is moist AND hot} &\Leftrightarrow x \in A_{moist} \cap B_{hot} \Leftrightarrow \mu_{A_{moist} \cap B_{hot}} \\ x \text{ is moist OR hot} &\Leftrightarrow x \in A_{moist} \cup B_{hot} \Leftrightarrow \mu_{A_{moist} \cup B_{hot}} \end{aligned} \tag{4.21}$$

4.9.3.1.2 Fuzzy Logic Control

Considering a process with control input u, error $e(w - y)$ where w is the set point and y is the process output, a fuzzy control law can be written as

$$\begin{aligned} &IF\ e(k)\ is\ A_i^o\ AND \ldots AND\ e(k-n)\ is\ A_i^n\ AND \\ &u(k-1)\ is\ B_i^l\ AND \ldots AND\ u(k-n)\ is\ B_i^n \\ &\qquad THEN\ u(k)\ is\ B_i^o \quad l \le i \le N \end{aligned} \tag{4.22}$$

where N is a number of rules and A_i and B_i are fuzzy predicate symbols.

Let a fuzzy logic controller try to make a variation in the control input (Δu) based on the error (e) and change in error (Δe). The pattern of error and variation in error has many influences on the control action. The pattern of the error and variation in error can be of the following types:

$$e(k) = w - y(k)\text{: negative, zero, positive}$$
$$\Delta e(k) = e(k) - e(k-1)\text{: decreasing, constant, increasing}$$

defining three membership functions for these patterns as

$$\begin{aligned} e &: \mu_{negative}(e), \mu_{zero}(e), \mu_{positive}(e) \\ \Delta e &: \mu_{decrease}(\Delta e), \mu_{const}(\Delta e), \mu_{increase}(\Delta e) \end{aligned} \tag{4.23}$$

Let the control variable take three values—low, medium, and high based on three conditions of error—then the control laws can be written as

IF e is negative AND Δe is increasing THEN set Δu to high.
IF e is negative AND Δe is constant THEN set Δu to medium.
IF e is negative AND Δe is decreasing THEN set Δu to low. (4.24)

There will be a total of nine combinations for the rules similar to these, but all of them might not be useful and in practical cases only a few of them will be operative. Similarly an OR connective can also be used in the rule or a combination of both can be used, such as

IF e is negative AND Δe is increasing THEN set Δu to high, OR

IF e is negative AND Δe is constant THEN set Δu to medium. (4.25)

A fuzzy controller consists of three basic components: a fuzzifier, a fuzzy inference, and a defuzzifier (fig. 4.35). The fuzzifier transforms the crisp variables received from the process to noncrisp fuzzy variables. Fuzzy variables are linguistic variables like good, very hot, slightly hot, and so on. The fuzzifier takes values of a membership function for the transformation. Some of the typical membership functions are triangular, trapezoidal, Gaussian, and bell-shaped. The membership function determines the degree of the crisp variables.

The inference step applies the fuzzy rules on the fuzzy variables similar to equation 4.24 and equation 4.25. For the final output inference, either max-min, max-prod, or add-prod methods are used. For the connective OR, maximum function is used, and for AND minimum function is used.

After applying the rule by the inference, the control output (u) must be applied to the process in its engineering form. This transformation of the fuzzy output variable to crisp variable is done by a defuzzifier. The most common defuzzification method is the center of gravity method given by

$$u = \frac{\int_{-\infty}^{\infty} \mu(x)x.dx}{\int_{-\infty}^{\infty} \mu(x).dx} \tag{4.26}$$

where terms μ and x in equation 4.26 are defined earlier.

Equation 4.26 calculates the ratio between the moment and area of the fuzzy sets.

A nonlinear PID controller has been developed by Årzén et al. [22]. The controller is designed and tuned for processes in which an explicit model or model-based fuzzy control is available. Perro et al. [23] developed fuzzy control in the biscuit baking process where the air temperature in each zone and air flow rate were controlled.

4.10 Conclusion

To make a food processing system efficient, use of automatic controllers is obviously helpful. Objectives of process automation are numerous. However, the manual or traditional controllers in the most sensitive stages

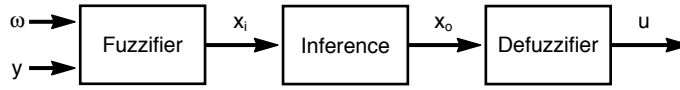

FIGURE 4.35
Block diagram of a fuzzy logic controller.

involving safety and hygiene of food cannot be completely replaced by machine controllers. For example, a tea taster can fine-tune his or her parameters by using a computer based E-Nose system, but it might not be possible to depend entirely on the machine.

The control problems of most food processing methods are complex and a structured approach is required to solve the problems with the help of known or tested methods with the simplest possible framework. There are many situations in which problems are identical, only a slight modification or variation of a tested method can be used to solve them.

In this chapter, various control system parameters, control system models, components, and control laws were discussed. Examples were cited from different food processing situations and more specifically from tea withering and drying controls. Indicators, timers and annunciators are operator-friendly devices. Example applications of timers and indicators were also discussed in this chapter. The knowledge on controllers and indicators gathered from this chapter will carry forward into the understanding of computer-based process measurement and control discussed in the next chapter.

References

1. Bhuyan, M. 1997. An integrated PC based tea process monitoring and control system, PhD Thesis, Department of Electronics, Gauhati University, India.
2. TRA. Withering. *Res. Bulletin*, Sr. No. 185. Jorhat, India: Tocklai Tea Research Station.
3. TRA. 1993. Factory requirement for 500,000 kg annual production. *Bulletin,* Sr. No. 83. Jorhat, India: Tocklai Tea Research Station.
4. Zahed, A. H., Zue, J., and Grace, J. R. 1995. Modeling and simulation of batch and continuous fluidized bed driers. *Drying Technology* 139(1&2):1–28.
5. Chang, D. I., and Chung, D. S. 1978. *Simulation of natural air drying of rough rice.* Manhattan: Food and Feed Grain Institute, Kansas State University.
6. Borbora, B. C. 1992. Techno-economic development of tea industry and role of electronic process controlled instruments. *Seminar on Application of Electronics in Tea Industry.* Jorhat, India: TRA.
7. Bhuyan, M., and Kandali, A. B. 1991. A model reference adaptive control system with *a priori* knowledge about the plant parameter variations. *IEEE Conf. TENCON-91*, Asia Pacific Region, India.
8. Landau, I. D. 1974. A survey of model reference adaptive techniques: Theory and applications. *Automatica* 10:353–379.
9. Landau, I. D. 1979. *Adaptive control: The model reference approach.* New York: Marcel Dekker.

10. Parks, P. C. Stability and convergence of adaptive controllers: Continuous systems. In *Self-tuning and adaptive control: Theory and applications*, eds. C. J. Harris and S. A. Billings. London: Peregrinus.
11. Isermann, R. 1982. Parameter adaptive control algorithms: A tutorial. *Automatica,* 18:513–528.
12. Isermann, R. 1989. *Digital control systems: Vol. 2. Stochastic control, multivariable control, adaptive control, applications.* New York: Springer Verlag.
13. Wittenmark, B. 1988. Implementation and application of adaptive control. In *Proc. IFAC*: *Adaptive control of chemical processes,* ed. M. Kummel, 9–14. Copenhagen, Denmark: IFAC.
14. Goodwin, G. C., and Sin, K. S. 1984. *Adaptive filtering: Prediction and control.* Englewood Cliffs, NJ: Prentice-Hall.
15. Clarke, D. W., and Hasting-James, R. 1971. Design of digital controller for randomly distributed systems. *Proc. IEEE* 118:1503–1508.
16. Clarke, D. W., and Gawthrop, P. J. 1979. Self tuning control. *Proc. IEEE* 122:929–934.
17. Clarke, D. W., Kanjilak, P. P., and Mohtadi, C. 1985. A generalized LQG approach to self tuning control: Part II. Implementation and simulations. *Int. J. of Control* 41:1525–1544.
18. Clarke, D. W., Mohtadi, C., and Tuffs, P. S. 1987. Generalized predictive control: Part I. The basic algorithm. *Automatica* 23:137–148.
19. Clarke, D. W., Mohtadi, C., and Tuffs, P. S. 1987. Generalized predictive control: Part II. Extensions and interpretations. *Automatica* 23:137–148.
20. Zadeh, L. 1965. Fuzzy sets. *Inf. Control* 8:338–353.
21. Davidson, V. J., Brown, R. B., and Landman, J. J. 1999. Fuzzy control system for peanut roasting. *J. Food Eng*. 41:141–146.
22. Årzén, K., Jahanson, M., and Babuska, R. 1999. Fuzzy control versus conventional control. In *Fuzzy algorithms for control*, ed. H. B. Verbruggen, H. J. Zimmerman, and R. Babuska. Boston:Kluwer Academic.
23. Perrot, N., Agioux, L., and Ioannou, I. 2000. Feedback quality control in the baking industry using fuzzy sets. *J. Food Proc. Eng*. 23:249–280.

Further Reading

1. Seborg, D. E., Edgar, T. F., and Mellichamp, D. A. 1989. *Process dynamics and control.* New York: John Wiley.
2. Nybrant, T. 1986. *Modelling and control of grain dryers* (UPTEC 8625 R). Uppsala, Sweden: Institute of Technology, Uppsala University.
3. Isermann, R., and Lachmann, K. H. 1985. Parameter adaptive control with configuration aids and supervision functions. *Automatica* 21:625–638.
4. Chang, Z., and Tan, J. 1992. *Adaptive control of food processes with time delay* (Paper No. 92-6544). St. Joseph, MI: American Society of Agricultural Engineers.
5. ÅstrÖm, K. L., and Wittenmark, B. 1990. *Computer controlled systems: Theory and design.* Englewood Cliffs, NJ: Prentice-Hall.
6. Ungar, L. H., Hartman, E. J., Keeler, J. D., and Martin, G. D. 1996. Process modeling and control using neural networks. *AIChE Proc.* 312(92):57–67.
7. Årzén, K., and ÅstrÖm, K. J. 1996. Expert control and fuzzy control. *AIChE Proc.* 312(92):47–56.

5

Computer-Based Monitoring and Control

CONTENTS

5.1 Introduction

There has been tremendous advancement in science and technology with the advent of modern digital computers that can process a large amount of information with fantastic speed, precision, and accuracy. A digital computer has the capability of performing on the order of a man's life calculations. The applications of computers are various and vast. To use a computer for a specific application it is necessary for the user to decide if it is cost effective.

Effective strategy-based computer integrated manufacturing (CIM) solutions are a competitive advantage in today's marketplace. Although the cost of CIM technology has declined steadily, small manufacturing units are reluctant to adopt CIM for automation. At present, a strategy-based approach to CIM is directed toward managing processes and measures to improve quality, reduce cycle time, eliminate waste, and increase productivity. Many powerful CIM tools are available that offer an integrated set of solutions for bridging the gap among manufacturing, engineering, and management. Worldwide manufacturing is reaching such a stage where a better effort for process automation is a necessity for survival and not just better profitability. In particular, automation promises to become a universal remedy for many manufacturing organizations. New emerging CIM technologies are useful for industries of various sizes. With the help of client–server technology, personal computers can be used as engineering stations sharing data over the networks.

A PC-based monitoring and control system can go a long way toward making food processing and manufacturing more scientific and cost effective. The basic requirements that must be satisfied for implementation of PC-based monitoring and control are as follows:

1. Willingness of top officials to adopt automation
2. Involvement of all employees
3. Good infrastructure and the ability to invest resources in training
4. Positive attitude toward quality initiative
5. Effective communications among different functions of the company
6. Detailed knowledge of the production process and its limitations
7. Efforts and involvement toward continuous improvements

5.2 Importance of Monitoring and Control with Computers

A PC can be used extensively for performing complicated analyses and making them simpler. Real-time microcomputers have the capability of performing data acquisition, recording, analysis, and presentation simultaneously.

An ideal on-line computer employing real-time techniques can perform complex analysis with its special hardware features. It can collect data at very fast sampling rates, up to several thousands of readings per second. A real-time monitoring and control system can determine whether some prespecified criteria for a process are being met and if not, possibly take action to fulfill the criteria.

A complete manufacturing plant that involves interrelated or independent operations should preferably be controlled by a single operator, but due to limitations on human operations, an on-line computer is often necessary. Operator control becomes impossible in the case of enormously fast process changes, and in these cases an on-line computer better handles control and data logging. The advantages of a PC for automation can be summarized as follows:

1. A single operator or a few operators can keep watch of the parameters. Therefore, the system can be centralized and simplified to a great extent.
2. The information is displayed instantaneously in a condensed, understandable, and logical manner. Because the information relayed to the operator is not complex, it becomes easy to quickly understand any abnormal condition in the factory.
3. The information can be stored for future reference.
4. Use of PCs makes monitoring and control faster and more accurate.
5. Data analysis and performance calculations become easy.

In a PC-based control system, the process variables can continuously be monitored and output can be sent to the electromechanical actuators, which in turn control the process variables.

5.3 Hardware Features of a Data Acquisition and Control Computer

A PC structure for the purpose of data acquisition and control consists mainly of the following components (fig. 5.1):

1. Central processing unit (CPU)
2. Input devices
3. Output devices
4. Storage devices

A CPU is the primary module. It stores information and program instructions, performs computations, and outputs decisions. It contains the arithmetic

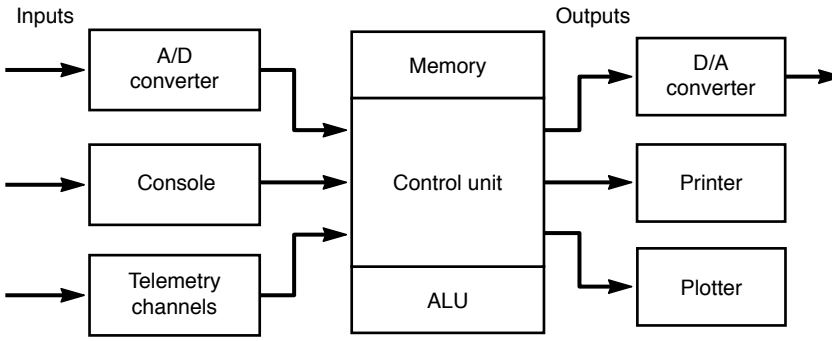

FIGURE 5.1
Block diagram of a digital microcomputer with input and output units.

and logical unit (ALU) to perform arithmetic and logical operations. The CPU reads instructions from the memory and performs the instructions. It also communicates with the input/output device to send and accept data. It is the central player in communicating with various devices, such as memory, input, and output devices. The ALU performs operations such as additions, subtractions, and logical operations such as AND, OR, EXOR, and so on. The register unit of the CPU consists of various registers that are used primarily to store data during the execution of the program. The control unit provides the requisite timing and control signals to all the operations in the microcomputer. It controls data transfer between the CPU and peripherals.

The input devices are the different sensors connected to the CPU through analog-to-digital converters (ADC) for accepting signals from the outside world. Other input devices include devices such as the keyboard, mouse, switches, ADC, and so on.

Output devices such as printers, plotters, magnetic tapes, LEDs, alarms, cathode ray oscilloscope (CRO), and digital-to-analog converters (DACs) transfer data from the CPU to the outside world. In the case of an online control computer, the major focus is on output devices such as telemetry channels, control components, alarms, indicators, timers, and so on.

Storage of data and instructions is accomplished using memory. It stores instructions, data, and results for use whenever necessary. When results are not directly transferred to output, these are stored in the memory. Semiconductor memory is relatively faster, but for large quantities of data storage, floppy disks, compact discs, and magnetic tape disks are more commonly used.

5.4 Remote Data acquisition with PCs

A major part of industrial process data acquisition activities has to deal with the real world of analog and digital signals available from sensors and

transducers. By far, the majority of sensors for these and many other process parameters happen to be analog by nature. They produce a varying voltage, current, or resistance in response to varying stimuli. Another important characteristic is that the electrical signal generated is small in magnitude and can get easily mixed with noise. The processing equipment to accept such low-level signals and represent them in the proper engineering unit requires signal conversion. The output must be indicated near the sensor or in an operator's room for remote operation. Hence, the analog signals are transmitted to such different places. Most likely, each place will receive different readings from the same sensor because of the different distances involved and the resulting signal attenuation or compensation differences along the path. The solution to this problem of carrying such a low-level signal to different locations can vary. A simple suggestion is to amplify the signal with high gain or to convert the voltage signal before transmitting to a form such as current or pulses. Transmitting the signal in the current mode is more efficient from a noise reduction point of view, but these schemes cost more than simple voltage mode transmission. Commonly used standards of current-driven instrumentation are 0–20mA or 4–20mA DC loop. A 4–20mA standard provides an additional facility to sense signals below 4mA in a fault condition, like a break in continuity in the loop.

One common problem of voltage and current telemetry schemes is that each sensor has to be individually wired to the monitoring system. Further, the signal needs to be specially twisted and shielded, which is expensive. If there are more channels, consider that the cabling cost is directly proportional to the number of channels.

Measures for safe operation of the modules in the plant environment include isolation among sensors, computer, and the module power supply. The common feature of the module can be grouped into two distinct categories, functional and electrical.

In the functional category, all the modules from sensor to computer and computer to actuator interface should be intelligent, switchless, jumperless, and preset or potless with autocalibration. All the modules should speak and understand the same languages. This format should be truly universal.

A simple example of a command of a typical analog input module might be this:

```
Port % = & H300
 CH % = INP (PORT %)
```

In this example, the command requests the latest data from the input device having an address 300 (Hex). Such an easy-to-understand program shows how to communicate with a typical input module.

In the electrical category, data acquisition with switch-selectable 16 single-ended or 8 differential analog input channel configurations with a maximum sampling rate of 100 KHz or more, are typical for general applications. In an industry-standard 12-bit successive approximation ADC is used to convert

analog inputs. Two modes of analog input range control are possible: local mode and remote mode. The local mode is switch selectable, whereas remote mode is programmable through software control. Each channel has its own range and the range setting can be stored in onboard RAM.

5.4.1 Analog Signal Interfacing Card

A high-performance, high-speed, multifunctional data acquisition card with programmable gain can be used for the data acquisition and control operations. The high-end specifications of such an interfacing card with complete software support make it ideal for a wide range of applications in an industrial environment. The key features of such cards are as follows:

1. Switch-selectable 16 single-ended or 8 differential analog inputs.
2. A 12-bit successive approximation A/D conversion with 100 KHz or above sampling rate.
3. Analog input ranges:
   a. Bipolar: ± 0.5 V to ± 10 V
   b. Unipolar: 0.2 V to 10 V
4. Software A/D triggering.
5. A/D converted data transfer by direct memory access (DMA) transfer.
6. 8254 programmable counter.
7. Digital output channels (TTL compatible)
   0 V to 5 V
8. Analog output: 0 V to 10 V (DC)

5.4.2 Connector Arrangements

Such cards are equipped with 20-pin insulation displacement (mass termination) connectors. These terminals can be connected to the same type of flat cables connected to 37-pin D-type connectors.

Correct signal connection is one of the most important steps to ensure data are sent or received correctly. A good signal connection can avoid a lot of unnecessary and costly damages to the valuable PC and hardware devices. The cards accept either single-ended (unipolar) or double-ended (bipolar) signals. The single-ended configuration has only one signal wire for each channel, where the voltage to be measured is the voltage of the wire referred to as the common ground and is also called a floating source. A standard wiring diagram of a single-ended or unipolar signal connection is shown in figure 5.2A. On the other hand, the differential configuration has individual pair of signal wires for each channel and these channels respond only to the voltage difference between the high and low inputs. If the signal source has

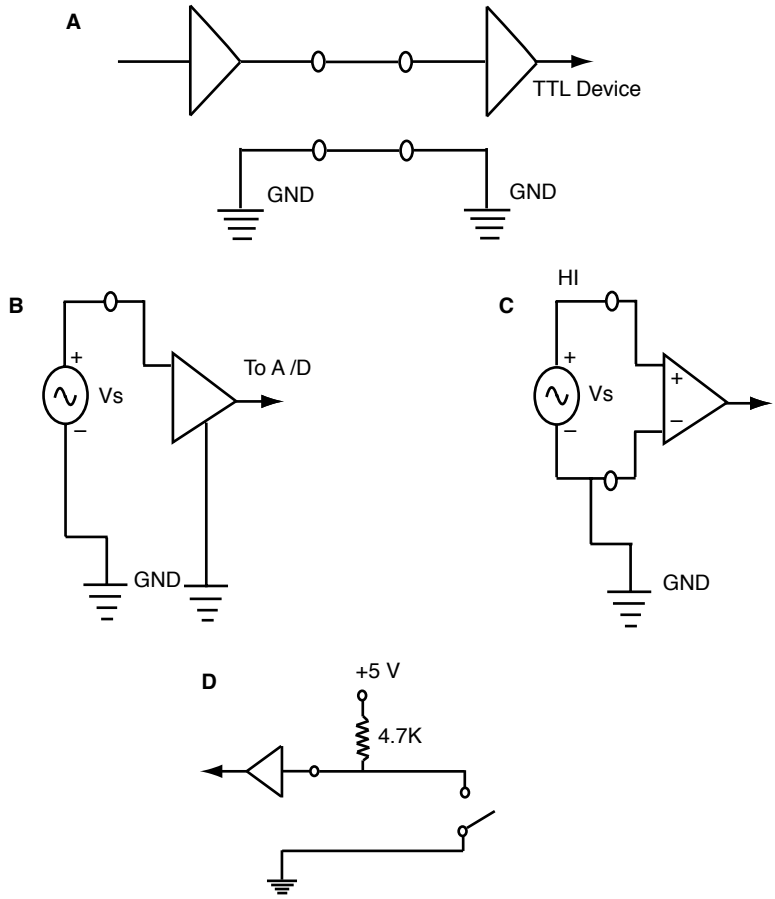

FIGURE 5.2
Signal connector arrangements for a data acquisition.

no ground, it is called a *floating source.* A connection must exist between low input and ground to define common input voltage for the floating signal source. To measure a floating source, the input channel should be connected as shown in figure 5.2B. If the signal source has one side connection to the local ground, the card ground will not show exactly the same voltage, as they are connected to the ground return of the equipment and the main wiring. The difference between the ground voltages forms a common mode voltage. To avoid the ground loop noise the signal ground should be connected to the low input. The low input should not be connected to the card ground. For digital output the 16-channel digital outputs transmit digital signals from the card to the outside connection, which is shown in figure 5.2C. To receive the open/short signal from a relay, a pull-up resistor must be added to ensure the high level when it is open. Figure 5.2D illustrates the relay connections to the coils.

5.5 Signal Interfacing

The term *interfacing* in computer-based data acquisition means a combination of hardware and software modules used to flexibly connect signals between a process and a computer. On the process side, various sensors, transducers, limit switches, and so on generate analog or digital signals that are sent to the computer for on-line acquisition and monitoring. Similarly the computer also generates the control signals that are used to actuate various control components in the process. Figure 5.3 shows a typical process–computer interface. The components used in the interface system are discussed next.

5.5.1 Input Signal Processing

The transducers, sensors, and actuators used in a computer-based data acquisition system were discussed in chapter 2. Signals generated by transducers and sensors can be classified into two basic types based on the level of the signal. As shown in figure 5.3, the low-level analog signals that are less than 1 V are generated by transducers like thermocouples (50 mV at 100–500 μA), strain gauges (10 mV at 50 μA), and so on. High-level signals above 1 V are obtained from resistance thermometers (1 V at 5 mA), digital limit switches

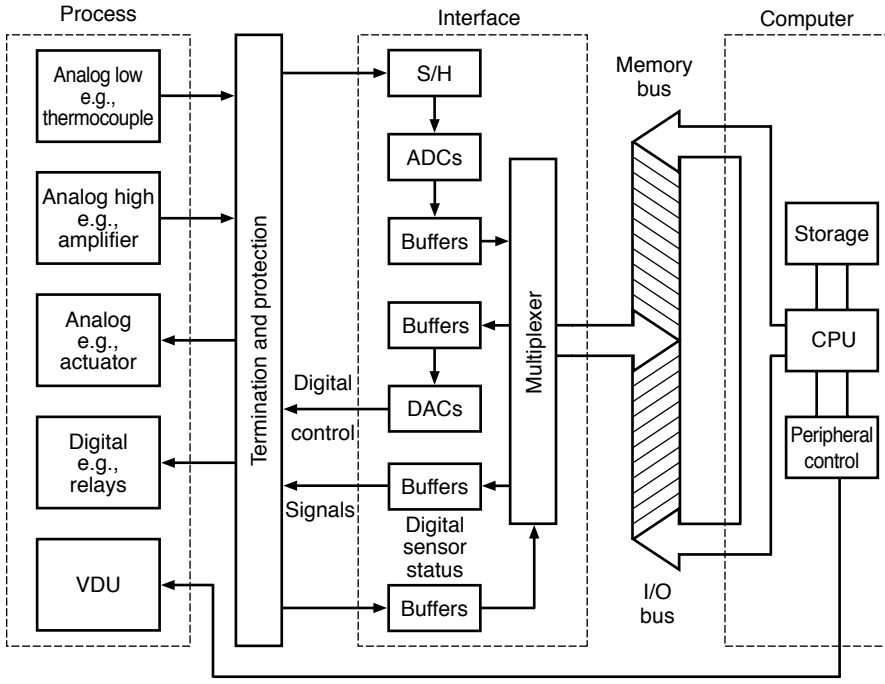

FIGURE 5.3
Block diagram of process–computer interface.

(5–30 V at 10 mA), and so on. These signals are often processed before interfacing between the plant and the computer. Some of the processing operations are as follows [1]:

1. Matching or termination for a standard signal type
2. Protection or barrier
3. Filtering
4. Conditioning
5. Manipulation such as linearization

5.5.1.1 Signal Matching

In a process control system the signals of various forms are transformed to a standard form of voltage or current. For example, optically transmitted signals are converted to electrical voltage signals by opto-electrical converters. In many industries pneumatic transducers transmit pneumatic signals. Such signals are converted to electrical signals by pneumatic to voltage or current converters. AC signals produced by some sensors are rectified to DC. In many cases, signals generated by high-impedance sensors are matched by using op-amp impedance matching modules.

5.5.1.2 Protection

The digital computers and the interfacing circuits operate at low voltage levels and these are always prone to accidental damage due to probable high current flowing from the plant side. Proper protection against this is incorporated by using a series of current-limiting resistors, circuit-breaking fuses, polarity protectors, opto-isolators, isolation transformers, and so on. Apart from protection, fault detectors are also used to detect faults like short circuits, open circuits in transducers, and so on.

5.5.1.3 Filtering

Low-level signals are corrupted with noise generated in the transducer itself or noise due to other electrical or electromagnetic interferences. Power line interference causes undulation to the transducer signals at power line frequency (50–60 Hz), which must be removed by RC or active high-pass filters. Similarly high-frequency noises generated by logic switching, microwave, radio waves, and so on can be filtered by low-pass filters.

5.5.1.4 Conditioning

Signals generated by the transducers and sensors are not always standard in terms of level or mode, and therefore, the signals are converted to standard voltage and current forms. There are two modes of standards: true-zero and live-zero. The standard current and voltage levels in true-zero modes are 0 to 5 mA, 0 to 10 mA, and 0 to 20 mA; and 0 to 20 V, 0 to 10 V, and 0 to 5 V,

respectively. The corresponding live-zero values are 4 to 20 mA and 10 to 50 mA; and 1 to 5 V and 0.4 to 2 V, respectively. The live-zero mode of signal manipulation is more popular for industrial applications because any fault in a transducer such as an open circuit can easily be detected when a 0 V signal appears at the computer side.

Another efficient mode of signal transmission is the frequency or pulse mode. This mode is effective when the distance from the plant to the computer is longer. This signal conversion is performed by a voltage-to-frequency converter. After transmitting the signal in frequency mode, the signal has to be reconverted to voltage or current mode to make it compatible with the digital computer.

5.5.1.5 Signal Manipulation

Linearization is an important signal manipulation needed when the transducer output is not linear to the physical signal. Many circuit level linearization techniques are available, but software-based linearization techniques are more efficient. Other signal manipulation methods are lead wire resistance compensation, offset nullification, logical operation, multiplication/division, integration, and so on.

5.5.2 Output Signal Processing

Similar to input signal processing, the signals generated by the computer are not always acceptable to the process; therefore, they might have to be converted to a level suitable for applying to the plant. The outputs of digital computers are mostly voltage or pulse. When pneumatic systems need to be operated, a voltage-to-pneumatic converter must be used. Actuators, like motors, need power circuits to get high current signals triggered by the voltages obtained from the computer. Digital pulses generated by a computer cannot drive a stepper motor directly, so a driver circuit is used to transform the low current pulses to high current pulses. Control valves are nonlinear devices, so a linear voltage signal cannot operate such devices efficiently. Linearization of such actuators can be achieved by special linearization circuitry.

Protection of the computer and other related circuitry from any high current that might flow from control components and actuators is also a part of the output signal processing. Relays and opto-coupled thyristors are solutions to such problems.

5.5.3 Interface Standards

When a set of transducers, sensors, and actuators are required to be interfaced between plant and computer several parameters must be matched: the interrupt structure, data timing and control, physical connections, signal levels, and programming. To provide a general guideline in respect to these points, several national or international signal interface standards are available such

as: the Computer Automated Measurement and Control (CAMAC), the British Standard Interface (BS4421:1969), the IEEE 488-1975 Instrumentation Standard Bus or General Purpose Bus Interface (GPIB), RS 232 Interface, and so on. However, all are not equally popular. Some proprietary interface standards are also available, like the Modular Electronic Digital Instrumentation Assemblies (MEDIA) developed by Imperial Chemical Industries (1975). The IEEE 488-1975 and RS 232 Interface standards are discussed here.

5.5.3.1 IEEE 488-1975 Instrumentation Standard

This standard was developed by Hewlett- Packard between 1972 and 1974, and it was adopted by the IEEE as a standard interface system. This bus can be a maximum length of 20 m and can connect up to 15 instruments at a maximum data rate of 500 Kbytes/sec. The code used for data transmission is US-ASCII and the bus width is 16 lines. Of these 16 lines, 8 lines are used for data, 3 lines for handshaking, and the remaining 5 lines are reserved for bus activity controls. The communication in the bus takes place between any two of the following:

- Listener: It receives data from other devices (e.g., printers).
- Talker: It transmits data to other devices (e.g., transducers).
- Controller: It sends addresses and commands to control the talk and listen operations (e.g., computer).

Figure 5.4 shows an IEEE 488 interface system and figure 5.5 shows the IEEE 488 interface connector.

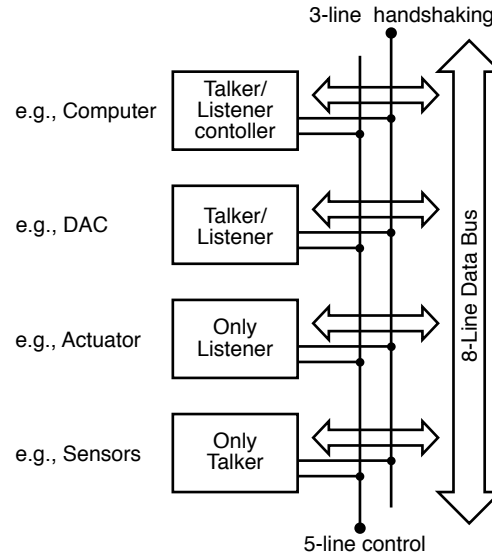

FIGURE 5.4
Block diagram of an IEEE 488 standard interface.

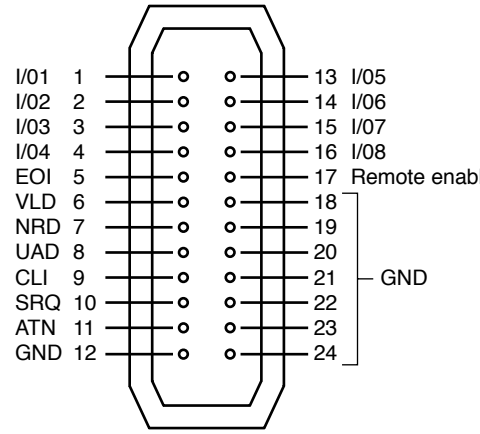

FIGURE 5.5
IEEE 488 bus connector.

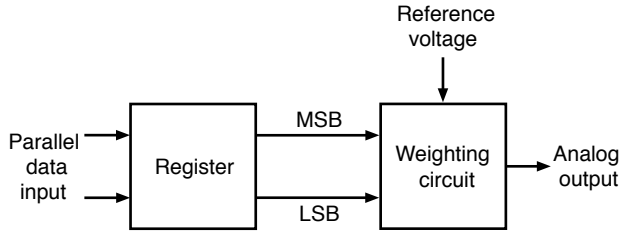

FIGURE 5.6
General structure of a DAC.

5.5.4 Analog and Digital Signal Conversion

The plant or process environment is always a combination of continuous and digital spectra, whereas the computer handles only digital or discrete spectra. The two-way communication between them is possible only by conversion of the analog signals to digital and the digital signals to analog form.

5.5.4.1 Digital to Analog Converter

A DAC works on a general principle of summing up a set of analog voltage generated by a switching circuit in proportion to the binary weightage to each bit of the binary number. Figure 5.6 shows the general structure of a DAC. The output voltage equation of the DAC in terms of the binary bits and the corresponding decimal weightage is given by

$$V_0 = \frac{V_{ref}}{2}\left[\frac{b_{n-1}}{2^0} + \frac{b_{n-2}}{2^1} + \cdots + \frac{b_0}{2^{n-1}}\right] \tag{5.1}$$

where b = a digital multiplier equal to analog zero for binary 0 and analog one for binary 1
V_{ref} = analog reference voltage
n = total number of digital bits

Let a DAC work on four binary bits $b_3\, b_2\, b_1\, b_0$ and at some instant the digital input is 1100. The equivalent analog value for this digital input will be

$$V_0 = \frac{V_{ref}}{2}\left[\frac{b_3}{2^0} + \frac{b_2}{2^1} + \frac{b_1}{2^2} + \frac{b_0}{2^3}\right]$$

$$= \frac{V_{ref}}{2}\left[\frac{b_3}{1} + \frac{b_2}{2} + \frac{b_1}{4} + \frac{b_0}{8}\right]$$

$$= \frac{V_{ref}}{2}\left[\frac{0}{1} + \frac{0}{2} + \frac{1}{4} + \frac{1}{8}\right]$$

$$= \frac{V_{ref}}{2}\left[0 + 0 + 0.25 + 0.125\right]$$

This expression is a summation of the four voltage components 0, 0, ¼, and ⅛ times V_{ref}. The value of the quantity in parentheses of equation 5.1 is equal to

$$\left[2 - \frac{1}{2^{n-1}}\right] = 2\left[1 - \frac{1}{2^n}\right]$$

The maximum value of output is

$$= \left[1 - \frac{1}{2^n}\right] V_{ref} \tag{5.2}$$

Here the smallest value of conversion (resolution) is

$$1\ \text{LSB} = \frac{1}{2^n} V_{ref}$$

This equation shows that the maximum analog output voltage is less than the reference voltage by a value of 1 LSB; that is, $(1/\ 2^n)V_{ref}$. This value is equivalent to the least significant bit (LSB) value. The summation operation of the output voltage given by equation 5.1 is performed by an op-amp summing amplifier circuit. In the summing amplifier the ratios between the feedback and input resistance are selected so that they become equal to the weightage values as

$$\frac{b_{n-1}}{2^0}, \frac{b_{n-2}}{2^1}, \ldots\ldots \frac{b_0}{2^{n-1}}$$

If V_{ref} = 10 V, 1 LSB is equal to 0.625 V then the analog output voltage corresponding to a digital input of 1111 is (10 – 0.625)V, or 9.325 V. This type of ADC where analog voltage changes from 0 to $+V_{ref}$ is called unipolar ADC. When the analog voltage changes from $-V_{ref}$ to $+V_{ref}$, the ADC is called a bipolar ADC. In a bipolar ADC, the most significant bit (MSB) is used to indicate the sign of the signal. Hence 1 LSB value for bipolar ADC is given by

$$1\,\text{LSB} = \frac{1}{2^{n-1}} V_{ref} \tag{5.3}$$

Therefore, for the same example of input as earlier, in unipolar ADC

$$1\,\text{LSB} = 1.25\ \text{V}$$

and $$V_{max} = (10 - 1.25)\ \text{V}$$
$$= 8.75\ \text{V}$$

The analog output for some specific inputs for a 4-bit ADC of both unipolar and bipolar modes can be shown as follows:

Unipolar mode	**Bipolar mode**
0000 = 0 V	0000 = –10.00 V
0001 = 0.625 V	0001 = –8.75 V
0100 = 2.500 V	0100 = –5.00V
0111 = 4.325 V	0111 = –2.50 V
1000 = 5.000V	1000 = 0 V
1001 = 5.625 V	1001 = +2.5 V
1100 = 7.500 V	1100 = +5.0 V
1111 = 9.325 V	1111 = +8.75 V

Based on the technique adopted by the weighting circuit, the two most typical DACs developed are adder and ladder types.

5.5.4.2 Analog to Digital Converter

An analog-to-digital conversion is conversion of analog or continuous signals to digital form. ADCs work on a general principle of generating parallel digital outputs by a counter that is converted to an analog form using a DAC. The analog output of the DAC is compared with the input analog signal using a comparator. When these two values become equal, the counter is stopped and the latest output of the counter is said to be the digital output. The most popular ADC types are counter type and successive approximation type. The difference between these two ADC types comes from the method of searching

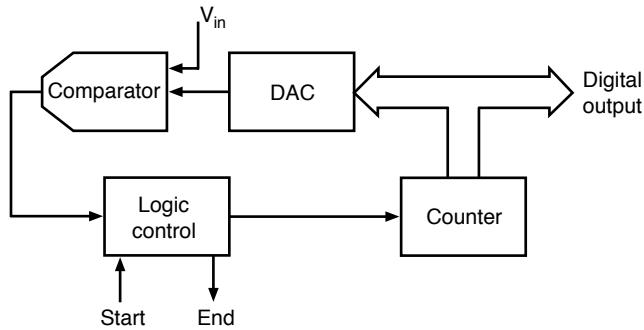

FIGURE 5.7
General structure of an ADC.

the exact digital output generated by the counter. Other forms of ADCs are incremental AD conversion, ramp AD conversion, subtracting AD conversion, and so on. The general structure of an ADC is shown in figure 5.7.

Problem 5.1.

The temperature of a dryer is measured by a thermocouple in the range of 0°C to 100°C. The output voltage obtained from the thermocouple is amplified by an amplifier to get the corresponding output voltage of 0 V to 5 V, which is again converted to digital format using an 8-bit unipolar ADC. Find:

1. the resolution of the measurement system
2. digital output corresponding to a temperature of 55°C
3. conversion error when the output voltage corresponding to 55°C is converted to digital form

SOLUTION:
Given $n = 10$
Temperature range = 100°C
ADC input voltage range = (5–0) V
Hence, $V_{ref} = 5$ V

1. The resolution is the same as the 1 LSB equivalent of temperature value

From equation 5.2:

$$1 \text{ LSB (unipolar)} = (1/2^n) \times V_{ref}$$
$$= (1/256) \times 5 \text{ V}$$
$$= 19.53 \text{ mV}$$

The corresponding temperature value = $100 \times 0.01953/5$

Resolution = 0.39°C

2. The analog voltage corresponding to 55°C

$$= 5 \times 55/100$$
$$= 2.75 \text{ V}$$

The decimal equivalent is

$$= 256 \times 2.75/\ 5$$
$$= 140.8$$

The comparator in the ADC will approximate this value to

$$\cong 141$$

Hence, the binary equivalent of 141 is

$$= 1000\ 1101$$

3. The voltage corresponding to binary 141

$$= 5 \times 141/256$$

$$= 2.753906 \text{ V}$$

The error in voltage $= (2.753906 - 2.75) = 3.906$ mV
The error in temperature $= (100 \times 0.003906)/\ 5$
$= 0.07812°C$

5.5.5 Interface Components

In the preceding sections, it has been discussed how the sensing or control signals are made compatible for interfacing between the computer and the plant. This section gives a brief overview of the devices available for such signal processing techniques. However, detailed coverage of these devices is available in other specialized texts.

Mention was made several times in chapter 2 and chapter 3 about the use of operational amplifiers as differential and summing amplifiers. Three other forms of operational amplifier are voltage amplifiers, current amplifiers, and instrumentation amplifiers. The amplifier modes are differential amplifier, inverting and noninverting signal sign relationship. A noninverting unity gain amplifier is used to match the impedance of the input and output devices. Although voltage-to-current and current-to-voltage converters are used to convert the form of signal only, because the device uses an operational amplifier, it functions like an amplifier in closed-loop mode.

For the purpose of measuring transducer outputs, an instrumentation amplifier is more popular. The circuit takes care of the common mode rejection ratio (CMRR), slew rate, offset and input/output impedance of the amplifier. The definitions of the features mentioned above are as follows [2]:

- *CMRR*. This is the ability of rejecting any change in input differential gain. Many transducers like strain gauges configured in Wheatstone

bridge produce a common mode signal along with the basic signal, which also gets amplified with the signal if not rejected. This makes calibration difficult. Operational amplifiers are designed with a high CMRR on the order of 100 dB to remove such common mode voltage components.

- *Slew rate.* When the input signal swings with a large leap the capacity of the amplifier to change the output with a maximum rate is called the slew rate. A typical value of the slew rate is 1 V/μs.
- *Offset voltage.* The output offset voltage of the range of 1 to 100 μV appears at the output even when the differential input voltage is zero. Similarly, input offset voltage is the voltage to be applied to the input to balance the amplifier. This value is typically 1 mV. Offset voltage is generated due to circuit parameter variations.
- *Impedance.* To transfer a maximum amount of power to a circuit, the output impedance of the amplifier should be sufficiently low. Similarly, to receive a maximum amount of power from the transducer without loading effect, the input impedance of the amplifier should be very high. Theoretically these impedance values of an op-amp are zero and infinite, respectively.
- *Offset voltage drift.* This is the drift of offset voltages due to temperature effect. Typical drift value is 1.0 μV/°C.

Another form of signal processing device is the voltage-to-frequency and frequency-to-voltage converter that is used to convert the mode of signal transmission. For long distances, signal transmission in frequency mode is more efficient. Digital computers and microprocessors can directly accept frequency-based signals or pulses. The use of such devices can be categorized as follows:

1. To convert pulses generated by transducers to voltage signals by an F/V converter
2. To convert transducer output voltages to pulses for transmitting the signal to a remotely located computer using a V/F converter
3. To convert pulse signals transmitted by transducer or transmitters to voltage signals before interfacing with computers by an F/V converter

Apart from amplifiers and signal converters, interface components like sample and hold circuits, data buffers, logic components, and so on play important roles in signal interfacing.

Sample and hold is used at the input of an ADC to hold a signal for a specified time before the ADC completes the conversion of the previous sample. This is important when the signal value changes at a rate faster than the conversion speed of the converter.

Data buffers are used to store the digital words produced by the ADC before interfacing with the computer. This is a temporary, intermediate storage

device to match the data generation rate of the input device with data reception rate of computers.

Logic components such as a data router or addresser, logic multiplexer, converter controller, and so on, are some of the additional interface components.

5.6 Examples of Computer-Based Measurement and Control in Food Processing

Application of computer-based data acquisition and control in food processing has been flourishing recently. Some examples of applications are discussed in the following sections.

5.6.1 Computer-Based Monitoring and Control of the Withering Process in the Tea Industry

A PC-based technique for on-line monitoring and control of withering percentage in the tea industry was developed by Bhuyan [3], the basic principle of which was already explained in section 3.3. The method includes on-line measurement of the weight of a representative section of the withering trough during withering using the load cell, interfacing the voltage signal representing the weight to the PC with a data acquisition card, data conversion, scaling, generating digital control signals, and finally implementing the equation of percentage of withering in software given by

$$Pw(t) = \frac{0.96W_W(t) \times 100}{W_g} \tag{5.4}$$

where $W_w(t)$ = instantaneous weight of withering in kg
W_g = initial weight of green tea leaf in kg

The primary hardware used in this technique is a data acquisition card that is directly plugged to the I/O slot of the PC bus. The card can accept up to 16 single-ended analog signals with the following magnitude of voltages:

0–0.5 V
0–1.0 V
0–2.5 V
0–5 V
0–10 V

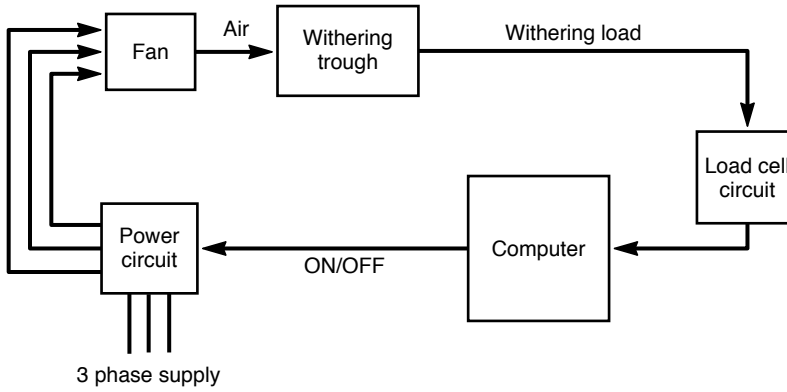

FIGURE 5.8
Schematic diagram of tea withering percentage control system.

The PCL card is set to 0–5 V in single-ended mode using the local settings of the card. There are two clock input frequencies to the 8254 programmable counter for triggering the ADC: 10 MHz and 1 MHz. The operation of the card can be controlled through the input and output ports. These ports are addressed using I/O port addresses from 300–30F (hex).

Figure 5.8 shows a diagram of the tea withering percentage monitoring and control system. Because the data acquisition card can accept 16 single-ended analog inputs, the device is intended for 16 withering troughs simultaneously. The analog signals from 16 numbers of load cells of the representative sections representing weight of the tea are first amplified at the site and the voltage signals are transmitted through sheathed and screened cable. The design of the load-cell-based instrumentation system was discussed in chapter 2. The bridge terminals of the load cells installed in the representative trough sections (16 numbers) are wired through screened cables to a central signal conditioner placed in the withering room equipped with 16 instrumentation amplifiers. The problem of noise is eliminated by using shielded cables. One added advantage of load cells, with respect to noise, is that due to its low impedance, noise is less severe than with high-impedance sensors. Moreover, multiple grounding both at the transducer site as well as the amplifier site is used to reduce noise.

In addition to monitoring of withering percentage of 16 withering troughs, on–off control of the withering fans is also included on the same PC. Finally, the withering fan speed reversal (see chapter 4) was performed as an integrated system. Because withering fan reversal control requires measurement of relative humidity of the withering room, the same PC performed relative humidity measurement using a second data acquisition card. This second card is dedicated only for withering fan speed reversal with 16 analog inputs for interfacing the depression temperatures. Therefore the PC workstation is able to integrate the following four operations:

1. Withering percentage monitoring
2. Withering on–off control
3. Relative humidity measurement
4. Withering fan speed reversal

The functions of the cards can be specified as follows:

- Card 1: Input—16 single-ended analog load signals
  - Output—16-bit digital outputs for on–off control of fans
- Card 2: Input—16 single-ended analog signals for humidity (depression temperature signals)
  - Output—16-bit digital outputs for forward and reverse control of fans

The digital outputs (D0–D15) of the first card are used to trigger the relays connected to the withering fan motors for on–off control. The data required to output a particular digital number D0 through D7 (low byte) and D8 through D15 (high byte) are applied through software. For example, for operating the troughs 1, 2, 3, 9, 10, and 16 in on state and rest in off state, the digital output requires the numbers 131 and 007 in decimal form for the low and high bytes, respectively. The low and high byte values for setting all the troughs in the on state are 255 and 255, and for the off state are 0 and 0, respectively.

The computer-based withering percentage measurement and on–off control of the fan includes the following steps:

1. Acquisition of 16 analog signals of weight of tea leaves
2. Conversion of signal to percentage of withering by using equation 5.4
3. Comparison of percentage of withering with target value
4. Digital output operation for on–off control

The computer-based speed reversal of the withering fan involves the following steps:

1. Acquisition of sixteen sets of depression temperatures
2. Conversion of signals to relative humidity using equation 3.33
3. Comparison of relative humidity with set-point values
4. Digital output operation for forward and reverse control of motors

5.6.1.1 The Control Scheme

Figure 5.9 shows a diagram of the measurement and control scheme. The device uses two controllers: an on–off controller for withering percentage

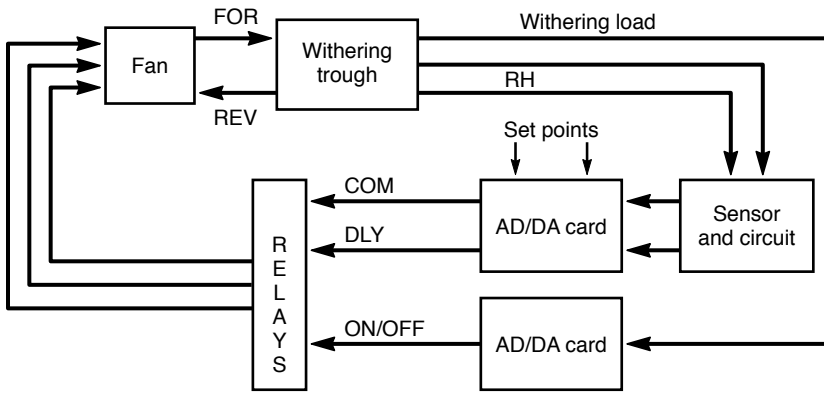

FIGURE 5.9
Schematic diagram of combined on–off and forward–reverse control in tea withering.

control and forward and reverse controller for speed reversal control. Implementation of both the controllers in electronic controller mode is discussed in chapter 4. The computer-based control integrates both the controllers using three data acquisition cards that generate digital control signals for both the controllers. For forward and reverse control of a single motor, three signals need to be generated:

TABLE 5.1

Share of Analog Inputs and Digital Output Ports of the Cards in Withering Control

Card No.	Analog Inputs	Digital Outputs
1	16 single-ended (SE) for withering percentage of 16 troughs	16 digital outputs for on–off control of 16 troughs
2	16 SE for dry- and wet-bulb temperatures in 8 troughs	16 digital outputs of COM output for 16 troughs
3	16 SE for dry- and wet-bulb temperature in 8 troughs	16 digital outputs of DLY output for 16 troughs

1. Command signal (COM) generated by the first card in response to the value of relative humidity and compared with signals against high and low set points.
2. A delay signal (DLY) generated by the second card in response to a similar comparison.
3. An on–off control signal generated by a third card.

Table 5.1 shows the share of analog inputs and digital outputs of the controllers. The format of COM and DLY signals is described as:

COM (Digital outputs) CD: CD_{15} …… CD_0

DLY (Digital outputs) DD: DD_{15} …… DD_0

The following example shows the method of generation of CD and DD signals. Let at *k*th instant the CD and DD values be

CD = 1100 1000 1111 0101 = 200 245
DD = 1111 1111 1111 1111 = 255 255

These values indicate that fan numbers 0, 2, 4, 5, 6, 7, 11, 14, and 15 are in forward direction and the rest are in reverse direction. All 16 fans are running because the DD bytes are 255 and 255. After comparison of relative humidity with high and low set point levels at (k +1)th instant, let the controller decide to reverse fans 2 and 7 and forward fan 1. Hence, the new values of the bytes are

CD = 1100 1000 0111 0011 = 200 115

Now, let the withering percentage controller decide to stop fans 7 and 11 after comparison of the withering percentage with target values. The new DD values will become

DD = 1111 0111 0111 1111 = 247 127

5.6.2 Computer-Based Sequential Timer for Tea Rollers

The electronic rolling timer was discussed in chapter 4. The same device was implemented in the computer by digital output operation to trigger indicators in a programmed manner for 16 rolling tables.

Here 16 analog inputs (AI_{15}–AI_0) are used to indicate the status of the rolling tables (i.e., on or off states of the motors). The state of the motors can be calibrated in terms of overloading or normal loading based on the current drawn by the motors. The current drawn by each rolling machine (only in one phase) driven by three-phase induction motors was converted to voltage signals. For example, in a typical 20 horsepower three-phase induction motor draws current given by the equation

$$I_L = \frac{P}{\sqrt{3} V_L \cos\phi} \tag{5.5}$$

where I_L = line current in A
V_L = line voltage in V
cos ϕ = power factor of the motor

From equation 5.5, taking the power factor as 0.8, the current is

$$= (20)(746) / \sqrt{3}(440)(0.8)$$

$$= 24.47 \text{ A} \cong 25 \text{ A}$$

On average, the overload current can be 4 to 6 times the normal current [4]. Taking overload current as 4 times the normal current, the maximum overload current of the motor is 100 A. Hence, the calibration of the current sensors can be done as:

0 A: 0 V
100 A: 5 V

Therefore a normal load current of 25 A will generate a voltage signal from the current sensor as

$$V_0 = (5)\ (25)/100 = 1.25 \text{ V}$$

When the analog input voltage from the roller machine is in the range of 0 V–1.25 V, the status can be termed normal loading and when it exceeds 1.25 V the status can be termed overload; in terms of percentages, say 100%, 200%, and so on. The roller table works on a certain load of tea leaves and the motor draws excessive currents when overloaded. When overloaded, this status should be indicated to the operator by a visual indication. These signals are collected by a combined circuit to bring the voltage levels to 5 V DC as explained previously.

5.6.2.1 Roller Charging Status

Charging of a roller is indicated by a red indicator and discharging by a green indicator. The digital output bits D15 through D0 are generated by the computer through a data acquisition card and are used for triggering the relays for green lights (G16–G1) of the rollers. Similarly digital bits D15 through D0 generated by a second card are used to trigger the red indicators R15 through R0 of the rollers. Table 5.2 shows the share of the signals to the cards used in the computer and table 5.3 shows the charging and discharging time of six rollers as per Program I of section 4.6.1. Table 5.4 and table 5.5 show the timing sequence of the roller green and red indicators.

TABLE 5.2

Share of Analog Inputs and Digital Output Ports of the Cards in Roller Timer

Card No.	Analog Inputs	Digital Outputs
1	16 SE signals for on–off status of 16 rollers	16 outputs for green indicators for 16 rollers
2	16 SE signals for loading status of 16 rollers	16 outputs for red indicators of 16 rollers

TABLE 5.3

Charging and Discharging Sequence of Rollers as per Program I

	Roller Charging Times (AM)															
Roller No.	**7:00**	**7:15**	**7:30**	**7:40**	**7:45**	**7:55**	**8:00**	**8:10**	**8:15**	**8:25**	**8:30**	**8:40**	**8:45**	**8:55**	**9:00**	**9:10**
1	1	1	0	0	1	1	1	1	0	0	1	1	1	1	0	0
2	0	1	1	1	0	0	1	1	1	1	0	0	1	1	1	1
3	0	1	1	1	1	0	0	1	1	1	1	0	0	0	1	1
4	0	0	0	1	1	1	1	0	0	1	1	1	1	0	0	0
5	0	0	0	0	0	1	1	1	1	0	0	1	1	1	0	0
6	0	1	0	0	0	0	0	0	1	1	1	1	0	0	1	1

Note: 1 = on; 0 = off.

TABLE 5.4

Timing Sequence of Roller Green Indicators

	Sequence/Slot															
Roller No.	**1/ 6T**	**2/ 3T**	**3/ 3T**	**4/ 2T**	**5/ T**	**6/ 2T**	**7/ T**	**8/ 2T**	**9/ T**	**10/ 2T**	**5/ T**	**6/ 2T**	**7/ T**	**8/ 2T**	**9/ T**	**10/ 2T**
1	0	1	0	0	0	1	1	0	0	0	0	1	1	0	0	0
2	0	0	1	0	0	0	0	1	1	0	0	0	0	1	1	0
3	0	0	0	1	1	0	0	0	0	1	1	0	0	0	0	1
4	0	0	0	0	1	1	0	0	0	0	1	1	0	0	0	0
5	0	0	0	0	0	0	1	1	0	0	0	0	1	1	0	0
6	0	0	0	0	0	0	0	0	1	1	0	0	0	0	1	1

Note: 1 = on; 0 = off; T =5 min.

TABLE 5.5

Timing Sequence of Roller Red Indicators

	Sequence/Slot															
Roller No.	**1/ 3T**	**2/ 3T**	**3/ 2T**	**4/ T**	**5/ 2T**	**6/ T**	**7/ 2T**	**8/ T**	**9/ 2T**	**10/ T**	**5/ 2T**	**6/ T**	**7/ 2T**	**8/ T**	**9/ 2T**	**10/ T**
1	1	1	0	0	1	1	1	1	0	0	1	1	1	1	0	0
2	0	1	1	1	0	0	1	1	1	1	0	0	1	1	1	1
3	0	0	1	1	1	1	0	0	1	1	1	1	0	0	1	1
4	0	0	0	1	1	1	1	0	0	1	1	1	1	0	0	1
5	0	0	0	0	1	1	1	1	0	0	1	1	1	1	0	0
6	0	0	0	0	0	0	1	1	1	1	0	0	1	1	1	1

Note: 1 = on; 0 = off; T =5 min.

The digital output byte corresponding to roller green indicators G6 through G1 is D6 through D0; the bits D15 through D7 are considered 0. Hence, the digital output byte (only low byte) for green indicators was triggered as per table 5.4.

Additionally a flashing operation of the green and red indicators for 3 min before starting and finishing was included. For example, in table 5.4 after 6T the green light of roller number 1 should flash for 3 min, so 3 min before 3T the digital output of the low byte of the card changes from 0000 0000 to 0000 0001; that is, the decimal value of the low byte is flashing from 0 to 1. In a similar manner, a flashing operation of 3 min of the red indicators before finishing is performed. Flashing of the green indicator makes the operator aware of the starting or loading of a roller and flashing of the red indicator informs the operator about finishing or unloading of the roller.

5.7 Conclusion

A computer can be used extensively for performing complex monitoring and control operations with the help of special hardware precisely at high speed. PC-based techniques can be made intelligent by programming in heuristic methods such as fuzzy logic and artificial neural networks.

A general overview of computer-based measurement and control including examples of process control in the tea industry was presented in this chapter.

Methods of interfacing transducer signals to the computer have improved significantly over the last decade. This has been made possible by the development of powerful interfacing modules supported by software. Today smart sensors can circumvent many problems that were insurmountable earlier. Linearization of sensor output is one such a problem that is still to be addressed sufficiently with computer-based techniques.

Techniques like machine vision and E-nose-based odor detection and classification using artificial intelligence are emerging fields that will gain importance in food processing in the years to come.

References

1. Barney, G. C. 1985. *Intelligent instrumentation: Microprocessor applications in measurement and control.* Englewood Cliffs, NJ : Prentice Hall International.
2. Millman, J., and Halkia, C. C. 1972. *Integrated electronics: Analog and digital circuits and systems.* New York: McGraw-Hill International.
3. Bhuyan, M. 1997. An integrated PC based tea process monitoring and control system. PhD Thesis, Department of Electronics, Gauhati University, India.

4. Del Toro, V. 1985. *Electric machines and power systems.* New Delhi: Prentice Hall of India.

Further Reading

1. Borbora, B. C. 1992. Techno-economic development of tea industry and role of electronic process controlled instruments. *Seminar on applications of electronics in tea industry.* Jorhat: Tea Research Association of India.
2. Moreira, R. G. 2001. *Automatic controls for food processing systems.* Gaithersburg, MD: Coultate TP.
3. Pinder, A. C., and Godfrey, G. 1993. *Food process monitoring systems*, London: Blackie Academic and Professional.
4. Cassel, D. A. 1983. *Microcomputers and modern control engineering.* Reston, VA: Reston.
5. Hunter, R. P. 1987. *Automated process control systems* (2nd ed.). Englewood, Cliffs, NJ: Prentice Hall.

Appendixes

APPENDIX A

SI Units

Quantity		Unit		
Symbol	**Definition**	**Name**	**Symbol**	**Definition**
Base units				
	Length	Meter	m	—
	Mass	Kilogram	kg	—
	Time	Second	sec	—
	Electric current	Ampere	A	—
	Thermodynamic temperature	Kelvin	K	—
	Amount of substance	Mole	mol	—
	Luminous intensity	Candela	cd	—
Supplementary units				
	Plane angle	Radian	rad	—
	Solid angle	Steradian	sr	—
Derived units				
ω	Angular velocity	Radian per second	rad/s	rad/sec
Q	Charge	Coulomb	C	A.sec
C	Capacity	Farad	$Fs^4.A^2/kg\text{-}m^2$	
G	Conductance	Siemen	S	χ^{-1}
W	Energy	Joule	J	$kg.m^2/sec^2$
f	Frequency	Hertz	Hz	s^{-1}
F	Force	Newton	N	$kg.m/sec^2$
E	Illuminance	Lux	lx	lm/m^2
L	Inductance	Henry	H	$kg/m^2/(sec^2.\ A^2)$
ϕ	Luminous flux	Lumen	lm	cd/sr
	Luminous efficacy	Lumen per watt	lm/W	lm/W
	Magnetic flux	Weber	Volt-sec	V.sec
p	Pressure	Pascal	Pa	N/m^2
P	Power	Watt	W	J/sec
R	Resistance	Ohm	Ω	$kg/m^2/(sec^3.\ A^2)$
S	Specific heat	Joule per kg-kelvin	J/kg.K	J/kg.K
λ	Thermal conductivity	Watt/meter-kelvin	W/m.K	W/m.K
V	Voltage	Volt	V	$A.\Omega$
Viscosity				
υ	Kinematic viscosity	Stokes	Square meter per sec	m^2/sec
μ	Absolute or dynamic viscosity	Poise	Pa.sec	$N.sec/m^2$

APPENDIX B

English System of Units

Quantity	English Unit	Conversion to SI
Length	Foot (ft)	1 ft = 30.48 cm
Area	Foot^2 (ft^2)	1 ft^2 = 929.0304 cm^2
Volume	Foot^3 (ft^3)	1 ft^3 = 28316.84 cm^3
Force	Pound (lb)	1 lb = 4.448 N
Mass	Pound (lb)	1 lb = 454 g
Energy	Foot-pound (ft-lb)	1 ft-lb = 1.356 J
Pressure	Pound/in.^{2} (Psi)	1 Psi = 6897 Pa
Power	Horsepower (hp)1 hp = 746 W	

APPENDIX C

CGS Systems of Units

Quantity	CGS Unit	Equivalent SI Unit
Length	Centimeter (cm)	100 cm = 1 m
Area	Centimeter^2 (cm^2)	10,000 cm^2 = 1 m^2
Volume	Centimeter^3 (cm^3)	1,000,000 cm^3 = 1 m^3
Force	Dyne	100,000 dyne = 1 N
Mass	Gram (g)	1,000 g = 1 kg
Energy	Erg	10,000,000 erg = 1 J
Pressure	Dyne/cm^2	10 dyne/cm^2 = 1 Pa

APPENDIX D

Standard Prefixes

Multiple	SI Prefix	Symbol
10^{12}	Tera	T
10^{9}	Giga	G
10^{6}	Mega	M
10^{3}	Kilo	k
10^{2}	Hecto	h
10	Deka	da
10^{-1}	Deci	d
10^{-2}	Centi	c
10^{-3}	Milli	m
10^{-6}	Micro	m
10^{-9}	Nano	n
10^{-12}	Pico	p
10^{-15}	Femto	f
10^{-18}	Atto	a

APPENDIX E

Piping and Instrumentation Drawing Sensor Designations

	First Letter	**Second Letter**
A	Analysis	Alarm
B	Burner	
C	Conductivity	Control
D	Density	
E	Voltage	Primary element
F	Flow	
G	Gaging	Glass (sight tube)
H	Hand	
I	Current (electric)	Indicate
J	Power	
K	Time	Control station
L	Level	Light
M	Moisture	
O		Orifice
P	Pressure	Point
Q	Quantity	
R	Radioactivity	Record
S	Speed	Switch
T	Temperature	Transmit
U	Multivariable	Multifunction
V	Viscosity	Valve
W	Weight	Well
Y		Relay
Z	Position	Drive

APPENDIX F

Standard Psychrometric Chart

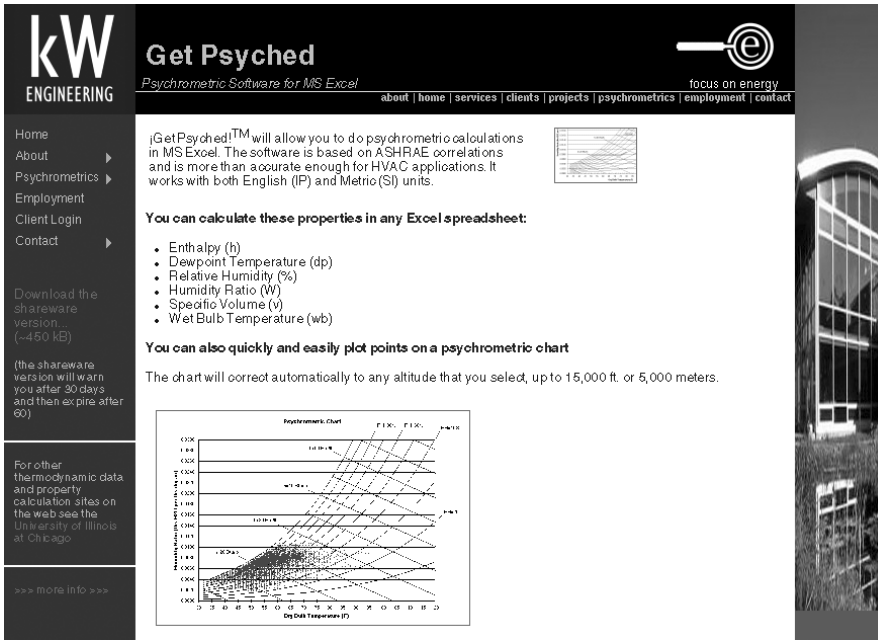

Reprinted with permission. Copyright © 2005 kW Engineering, Inc., 306 17th Street, Suite 100, Oakland, CA 94612., All rights reserved. www.kw-engineering.com

Index

Food Science

MEASUREMENT and CONTROL in FOOD PROCESSING

Manabendra Bhuyan

By the end of the twentieth century the growing reliance on computers had shifted food quality and safety activities from human inspection to automated, statistically driven monitoring systems. Information on instrumentation and control, conversion tables for measuring process parameters, and the use of the newer devices, though substantial, is spread over a multitude of specialized texts.

Measurement and Control in Food Processing presents a single common source for answering the cross-disciplinary questions that arise in today's food processing industry. The detailed text raises awareness of the current techniques of computerized measurement and process control, aids in the design of instruments and control schemes, and explains the applicability of these tools to enhance quality and productivity. Beginning with an illustrated introduction, followed by a detailed background in basic principles, the author lays a solid foundation for understanding the role of transducers and controllers, demonstrating the need for current practices by examining specific problems from his experience in the tea industry.

Integrating food processing and instrumentation engineering, ***Measurement and Control in Food Processing***—

- Examines digital processing, computer-based measurement, and advanced detection sensors such as electronic nose, biosensors, and fuzzy logic controls
- Addresses microcomputer-based monitoring by discussing the devices, standards, procedures, and suitable examples for process–computer interaction
- Demonstrates applied theory with case studies and examples
- Features photographs of commercial units and over 200 block, schematic, and circuit diagrams for instant visual reference
- Offers easy-reference tables to aid the instrumentation engineer in designing for new parameters

Bridging the gap between the food-processing engineer who may not know how to design a controller unit and the instrumentation engineer who may not understand the complex flavor components involved, ***Measurement and Control in Food Processing*** ensures that together they can consistently make a decent cup of tea.

7244

ISBN 0-8493-7244-5

90000

9 780849 372445

CRC

Taylor & Francis
Taylor & Francis Group
an informa business

A CRC PRESS BOOK
www.taylorandfrancisgroup.com

6000 Broken Sound Parkway, NW
Suite 300, Boca Raton, FL 33487

270 Madison Avenue
New York, NY 10016

2 Park Square, Milton Park
Abingdon, Oxon OX14 4RN, UK